THE UNIVERSITY *of* EDINBURGH

College of Medicine & Veterinary Medicine

An investigation into functional large-scale networks in individuals with schizophrenia using fMRI data and Dynamic Causal Modelling

Maria Dauvermann

Doctor of Philosophy
The University of Edinburgh
2014

Abstract

Schizophrenia is a complex and severe psychiatric disorder with positive symptoms, negative symptoms and cognitive deficits. Preclinical neurobiological studies showed that alterations of dopaminergic and glutamatergic neurotransmitter circuits involving the prefrontal cortex resulted in cognitive impairment such as working memory. Functional activation and functional connectivity findings of functional Magnetic Resonance Imaging (fMRI) data provided support for prefrontal dysfunction during fMRI working memory tasks in individuals with schizophrenia. However, these findings do not offer a neurobiological interpretation of the fMRI data.

Biophysical modelling of functional large-scale networks has been designed for the analysis of fMRI data, which can be interpreted in a mechanistic way. This approach may enable the interpretation of fMRI data in terms of altered synaptic plasticity processes found in schizophrenia. One such process is gating mechanism, which has been shown to be altered for the thalamo-cortical and meso-cortical connection in schizophrenia. The primary aim of the thesis was to investigate altered synaptic plasticity and gating mechanisms with Dynamic Causal Modelling (DCM) within functional large-scale networks during two fMRI tasks in individuals with schizophrenia.

Applying nonlinear DCM to the verbal fluency fMRI task of the Edinburgh High Risk Study, we showed that the connection strengths with nonlinear modulation for the thalamo-cortical connection was reduced in subjects at high familial risk of

schizophrenia when compared to healthy controls. These results suggest that nonlinear DCM enables the investigation of altered synaptic plasticity and gating mechanism from fMRI data.

For the Scottish Family Mental Health Study, we reported two different optimal linear models for individuals with established schizophrenia (EST) and healthy controls during working memory function. We suggested that this result may indicate that EST and healthy controls used different functional large-scale networks. The results of nonlinear DCM analyses may suggest that gating mechanism was intact in EST and healthy controls.

In conclusion, the results presented in this thesis give evidence for the role of synaptic plasticity processes as assessed in functional large-scale networks during cognitive tasks in individuals with schizophrenia.

Declaration

I declare that this thesis is my own work and has been composed by myself. The contribution to this thesis by others is clearly documented here and throughout the thesis where relevant. This work has not been submitted for any other degree or professional qualification.

Signed: _____

Dated: 06/07/2014_____

The work presented on the (i) Edinburgh High Risk Study and the (ii) Scottish Family Mental Health Study in this thesis are attributable to a number of past and present members of the Division of Psychiatry. My roles and contributions of others are clearly stated here and in the acknowledgements.

(i) Edinburgh High Risk Study

My primary role was the analysis of the Hayling Sentence Completion Task fMRI task in individuals at high genetic risk of schizophrenia and healthy controls with DCM. The effective connectivity analyses are theoretically and methodologically based on previously published findings of functional activation and functional connectivity of the Hayling Sentence Completion Task by Dr HC Whalley. Thus, the effective connectivity findings extend the functional activation and functional connectivity findings. Dr HC Whalley and Dr L Romaniuk provided methodological advice and support for the comparability between the previous findings and the effective connectivity findings.

(ii) Scottish Family Mental Health Study

My primary role for this study was the collection of multimodal neuroimaging data as part of the 'Neuroscience Grand Challenge Program' funded by Pfizer (formerly Wyeth) and the analysis of the working memory fMRI data. The multimodal neuroimaging data is comprised of five modalities: Structural MRI, Arterial Spin Labelling, Magnetic Resonance Spectroscopy (MRS), fMRI of two functional tasks (the "N-back" task for working memory and the "Hariri" task for emotional memory)

and Diffusion Tensor Imaging. The study populations are comprised of first-episode patients with schizophrenia, patients with established schizophrenia, patients with bipolar disorder, family members with and without the Disrupted-in-Schizophrenia-1 (DISC1) translocation and healthy controls (in total 135 study participants). Furthermore, I was involved in the development of scanning sequences for the study, which involved a MRS reproducibility study in eight healthy men.

Neuroimaging data acquisition included in this thesis span from June 2011 to January 2013 and is comprised of "N-back" fMRI data from 51 participants (26 individuals with established schizophrenia and 25 healthy controls). During this period Dr B Moorhead and/or I (Dr L Romaniuk helped occasionally) attended every scan and acquired the neuroimaging data. In particular, my role was to ensure the acquisition of the MRS data and to operate the equipment for the experimental functional imaging data. Therefore, I collected neuroimaging data from approximately 50% of all 135 scanned people. Due to recruitment difficulties, completion of the main study data collection was delayed and continued into April 2013.

Acknowledgements

First, I would like to offer special thanks to my primary supervisor, Dr B Moorhead, for his continued support and guidance throughout the PhD. I would also like to thank my supervisors Professors SM Lawrie and N Roberts for their advice and guidance. Special thanks are also due to the participants.

I would like to thank past and present members of the Division of Psychiatry, who have helped me during my time in the department for the (i) Edinburgh High Risk Study and the (ii) Scottish Family Mental Health Study.

(i) Edinburgh High Risk Study

I would like to give special thanks to Dr HC Whalley. My work on this project would not have been possible without her expertise and knowledge she shared generously with me. The opportunity of co-authoring on the review "Relationship between gyrification and functional connectivity of the prefrontal cortex in subjects at high genetic risk of schizophrenia" in Current Pharmaceutical Design provided the theoretical background for the development of the application of nonlinear Dynamic Causal Modelling for fMRI as part of the Edinburgh High Risk Study. Thanks go also to Dr L Romaniuk for support with scripting for the analyses. Lastly, I would like to acknowledge Professor EC Johnstone for valuable advice on the Edinburgh High Risk Study.

(ii) Scottish Family Mental Health Study

The Scottish Family Mental Health Study involves work and effort from a large number of people. I would like to acknowledge that the success of this study is attributable to great team effort. In particular, I would like to offer my thanks to those involved in participant recruitment (Professor DH Blackwood, Dr J McKirdy, B Duff, Dr A Watson, Dr KA Macritchie), clinical interviews (Dr A Watson, Dr KA Macritchie), neuropsychological assessments (B Duff, H Redpath) and technical assistance with the fMRI programming and set-up at the scanner (Dr L Romaniuk). Special thanks go to Dr B Moorhead, who shared his knowledge of every part of the study with me. Also I would like to thank the Scottish Mental Health Research Network for providing support for participant recruitment and neuropsychological assessments. Lastly, thanks go to the radiographers involved in the acquisition of the scans at the Clinical Research Imaging Centre at the Royal Infirmary Edinburgh.

I would like to give thanks to the Dr. Mortimer and Theresa Sackler Foundation for financial support of the PhD.

My thanks go to my friends and family, in particular to Vanja, Vincent, Cheryl, Stephen, Derek and Veronica.

My wonderful partner, Graham, who has supported me during me during all periods of the project.

Abbreviations

AC	Anterior cingulate
ACC	Anterior cingulate cortex
ACh	Acetylcholine
AMPA	Alpha-Amino-3-hydody-5-methyl-isoxazol-4-propioacid
ARMS	Subjects at-risk mental state
BMA	Bayesian Model Averaging
BMS	Bayesian Model Selection
BOLD	Blood Oxygen Level Dependent
CER	Cerebellum
CG	Cingulate gyrus
d'	Sensitivity index
D_1 receptors	D_1 subtype of the dopamine receptor
D_2 receptors	D_2 subtype of the dopamine receptor
D_4 receptors	D_4 subtype of the dopamine receptor
D_5 receptors	D_5 subtype of the dopamine receptor
DA	Dopamine
dACC	Dorsal anterior cingulate cortex
DCM	Dynamic Causal Modelling
DISC1	Disrupted-in-schizophrenia-1
DLPFC	Dorsolateral prefrontal cortex
DSM-IV-TR	Diagnostic and Statistical Manual of Mental Disorders, Fourth Edition, Text Revision
EC	Effective connectivity
EEG	Electroencephalogram
EHRS	Edinburgh High Risk Study
EST	People with established schizophrenia
FA	Functional activation
FAlarm	False alarms
FC	Functional connectivity
FEP	Subjects with first episode psychosis
FES	Subjects with first episode schizophrenia
FGA	First-generation antipsychotics
fMRI	Functional Magnetic Resonance Imaging
FWHM	Full width half maximum
GABA	γ-amino-butter-acid
GAF	Global Assessment of Functioning
GCM	Granger causal modelling
GLM	General linear model
Glu	Glutamate
HC	Healthy controls
HF	Hippocampal formation
HR	Subjects at high risk of schizophrenia
HRall	All subjects at high familial risk of schizophrenia (high risk subjects with psychotic symptoms and without psychotic symptoms)
HR+	Subjects at high familial risk of schizophrenia with psychotic symptoms
HR-	Subjects at high familial risk of schizophrenia without psychotic symptoms
HRF	Haemodynamic response function
HSCT	Hayling Sentence Completion Task

IFG	Inferior frontal gyrus
INS	Insula
IQ	Intelligence quotient
M1	Model 1
MD thalamus	Mediodorsal thalamus
MEG	Magnetoencephalography
MFG	Middle frontal gyrus
mGluR	Metabotropic Glu receptor
mPFC	Medial prefrontal cortex
MRI	Magnetic Resonance Imaging
MRS	Magnetic Resonance Spectroscopy
MTG	Middle temporal gyrus
NA	Noradrenaline
NART	National Adult Reading Test
NMDA	*N*-methyl-D-aspartate receptor
PANSS	Positive and Negative Syndrome Scale
PC	Parietal cortex
PCi	Posterior cingulate cortex
PET	Positron Emission Tomography
PFC	Prefrontal cortex
PHG	Parahippocampal gyrus
PPC	Posterior parietal cortex
PPI	Psychophysiological interaction
PSE	Present State Examination
rCBF	Regional cerebral blood flow
RT	Response time
SANS	Scale for Assessment of Negative Symptoms
SD	Standard deviation
SE	Standard error
SEM	Structural Equation Modelling
Serotonin	5-Hydroxytryptamin, 5-HT
SFG	Superior frontal gyrus
SGA	Second-generation antipsychotics
SMA	Supramarginal area
SN	Substantia nigra
SPECT	Single Photon Emission Computed Tomography
SPL	Superior parietal lobe
SPM	Statistical Parametric Mapping
STG	Superior temporal gyrus
UHR	Subjects at ultra high risk
VC	Visual cortex
V(l)PFC	Ventral (lateral) prefrontal cortex
VTA	Ventral tegmental area
Xp	Exceedance probability

Table of Contents

List of Tables

List of Figures

Appendix

Relevant publications based on the two introductory chapters and the Hayling Sentence Completion Task fMRI data of the Edinburgh High Risk Study contained within this thesis are presented.

Dauvermann MR, Whalley HC, Schmidt A, Lee GL, Romaniuk L, Roberts N, Johnstone EC, Lawrie SM, Moorhead TWJ. Computational neuropsychiatry – schizophrenia as a cognitive brain network disorder. Frontiers in Schizophrenia (2014). 5:30. eCollection 2014. doi: 10.3389/fpsyt.2014.00030. *The review of functional activation, functional connectivity and effective connectivity findings in verbal/numeric working memory in individuals with schizophrenia presented in chapters 1.3, 1.4, 1.5 and 2 formed the basis of this paper. Furthermore, the review of effective connectivity findings in verbal fluency in individuals at high risk of schizophrenia presented in chapter 3.3.2.3 formed an additional part of the paper. The paper is included in the appendix. The copyright is with the author.*

Dauvermann MR, Whalley HC, Romaniuk L, Valton V, Owens DGC, Johnstone EC, Lawrie SM, Moorhead TWJ. The Application of Nonlinear Dynamic Causal Modelling for fMRI in Subjects at High Genetic Risk of Schizophrenia. NeuroImage 2013; 73:16-29. doi: 10.1016/j.neuroimage.2013.01.063. *The data presented in chapter 3 forms the basis of this paper, which is included in the appendix. The copyright of the publisher has been requested.*

Dauvermann MR, Mukherjee P, Moorhead TWJ, Stanfield AC, Fusar-Poli P, Lawrie SM, Whalley HC. Relationship between gyrification and functional connectivity of the prefrontal cortex in subjects at high risk of schizophrenia. Curr Pharm Design 2012;18(4),434-442. *The conclusion of the review is cited in chapter 3.1. The abstract of the review is included in the appendix.*

Summary of organisation of thesis

This thesis considers the analysis of functional large-scale networks with effective connectivity to fMRI data in individuals with schizophrenia. Nonlinear DCM for fMRI has been applied to examine hypothesised differences in effective connectivity between (i) individuals at high genetic risk of schizophrenia and healthy controls (as part of the Edinburgh High Risk Study) and between (ii) individuals with established schizophrenia and healthy controls (as part of the Scottish Family Mental Health Study).

In chapter 1, functional activation and functional connectivity findings of working memory fMRI and Positron Emission Tomography studies in individuals with schizophrenia and healthy controls are summarised. These findings are discussed in context of the dopamine hypothesis of schizophrenia and the glutamate hypothesis of schizophrenia.

Effective connectivity findings of working memory fMRI studies in individuals with schizophrenia and healthy controls as assessed with DCM are discussed in chapter 2. It is considered to what extent effective connectivity findings may increase the interpretability of functional large-scale networks in comparison to functional connectivity findings.

In chapter 3, a protocol for the application of nonlinear DCM has been applied to the verbal fluency task in individuals at high genetic risk of schizophrenia and healthy controls as part of the Edinburgh High Risk Study. The main result was that effective

connectivity measures were significantly different of effective connectivity measures between high risk subjects and healthy controls, which may extend the previous functional connectivity findings.

For the Scottish Family Mental Health Study, the developed protocol for the application of nonlinear DCM was adapted for the working memory task in individuals with established schizophrenia and healthy controls (chapter 4). The main result was that individuals with established schizophrenia used a different functional network for the working memory function than healthy controls.

Finally, chapter 5 summarises and discusses the key findings to what extend these findings from the Edinburgh High Risk Study and the Scottish Family Mental Health Study may lead to a better insight into functional large-scale networks underlying cognitive function in individuals with schizophrenia.

1 Functional Magnetic Resonance Imaging studies in working memory in subjects with schizophrenia

1.1 General introduction to the thesis

Schizophrenia is a debilitating mental disorder, which is characterised by with positive symptoms, negative symptoms and cognitive deficits. Evidence from preclinical neurobiological studies showed that alterations of dopaminergic and glutamatergic neurotransmitter circuits involving the prefrontal cortex (PFC) resulted in cognitive deficits such as working memory. Functional activation (FA) and functional connectivity (FC) findings presented evidence for cortical impairment during fMRI working memory tasks in individuals with schizophrenia. However, these findings cannot be interpreted in neurobiological context.

Dynamic Causal Modelling (DCM) for fMRI has been developed for the biophysical modelling of functional large-scale networks of fMRI data. This method may enable the indirect assessment and interpretation of fMRI data in terms of altered synaptic plasticity processes (via learning during a specific experimental task). One neurobiological process, which has been proposed to underlie learning processes, is gating control or gating mechanism. In preclinical and computational studies is has been shown that gating mechanism is altered for the thalamo-cortical and/or meso-cortical connection in schizophrenia. The first overall aim of the thesis was to model connection strengths with nonlinear modulation, which may be interpreted as an indirect measure for gating mechanism during two fMRI tasks in individuals with schizophrenia. The second overall aim was to investigate, whether hypothesised altered cortical function or a compensation to impaired function may be found in individuals with schizophrenia when compared to healthy controls.

We applied nonlinear DCM to the Hayling sentence completion task (HSCT) fMRI task as part of the Edinburgh High Risk Study (EHRS). The HSCT is an established clinical tool for the assessment of PFC impairment (Burgess and Shallice et al., 1996). The application of DCM for the assessment of (nonlinear) effective connectivity (EC) measures to the HSCT task builds on previously published FA findings (Whalley et al., 2004) and FC (Whalley et al., 2005); thus, the DCM analyses can be seen as an extension to these findings. We focused on the investigation of connection strengths with nonlinear modulation of the thalamo-cortical connection.

We used nonlinear DCM to test hypothesised altered (nonlinear) EC measures during the "N-Back" working memory task in individuals with established schizophrenia (EST) and healthy controls as part of the (Scottish Family Mental Health Study, SFMHS). In this, we examined the connection strengths with nonlinear modulation of the meso-cortical connection.

We interpreted the findings of nonlinear EC measures of both studies in the context of (i) a possible indirect measure for gating mechanism; and (ii) an indication for altered cortical function or a compensatory process to impaired prefrontal function in individuals with schizophrenia when compared to healthy controls. In summary, the results presented in this PhD thesis suggest that synaptic plasticity processes (via learning processes) as indirectly assessed in functional large-scale networks during two cognitive tasks may be an underlying mechanism of prefrontal impairment or

compensatory mechanism in individuals with schizophrenia when compared to healthy controls.

1.1.1 Overall aims

There were two overall aims of the thesis, which applied to the modelling of functional large-scale networks with DCM for the EHRS and the SFMHS. The first aim was to assess nonlinear EC measures, which may be interpreted as an indirect measure for gating mechanism during two fMRI tasks in a given model in individuals with schizophrenia. The second overall aim was to examine possibly altered cortical function or compensation to impaired function during the two fMRI tasks in individuals with schizophrenia in contrast to healthy controls.

We present the main hypotheses separately for the EHRS and the SFMHS due to the different cognitive tasks modelled and different study populations of individuals with schizophrenia.

For the EHRS, we hypothesised that subjects at high familial risk of schizophrenia would show altered (nonlinear) EC measures between the mediodorsal (MD) thalamus and the inferior frontal gyrus (IFG) when compared to healthy controls, which may be an indirect indication of disrupted synaptic plasticity and gating mechanisms of the thalamo-cortical connection. This disruption of learning during the HSCT could be understood as a possible and indirect measure of a neurobiological process of altered prefrontal dysfunction during the HSCT, which applies specifically to the experimental task and brain function in the modelled networks.

For the SFMHS, we assumed that EST would display altered connection strengths with nonlinear modulation between the dorsolateral (DL)PFC and the ventral tegmental area (VTA) during the working memory "N-Back" task in contrast to healthy controls. Such an alteration during the "N-Back" task may indirectly resemble altered gating mechanism underlying prefrontal dysfunction or compensation to dysfunctional prefrontal function for the given experimental task and brain function in the modelled networks.

1.1.2 Dynamic Causal Modelling

DCM is a modelling framework for neuroimaging data (such as fMRI and electrophysiological data), which assesses neurobiophysiologically interpretable dynamic system models (Friston et al., 2003). In DCM for fMRI, these dynamic system models are fitted to fMRI data to provide estimates of connection strengths within a given model.

Nonlinear DCM as an extension has been devised to indirectly measure gating mechanisms at the neuronal level that provides a more precise estimation of how the rate of change of activity in one region influences the rate of change in other regions (Stephan et al., 2008). It has been proposed that gating mechanisms (i.e. nonlinear modulation of neuronal connections) originate from activity-dependent synaptic plasticity processes (Abbot et al., 1997; Salinas and Sejnowski, 2001) and may underlie cortical dysconnectivity in schizophrenia (thalamo-cortical connection, Negyessy and Goldman-Rakic, 2005; meso-cortical connection, Wang et al., 2010).

We selected DCM to measure EC in functional large-scale networks as part of the EHRS and the SMFHS in order to indirectly assess synaptic plasticity in a

hypothesis-driven way. In this, we devised a heuristic search protocol (chapter 3.4.5.2) to systematically assess EC measures and build the model space based on published research findings. Lastly, we selected DCM8 version (instead of newer DCM10 or DCM12 versions) to avoid the risk of unstable results.

It is noted that the assessment of synaptic plasticity processes via learning can only be considered indirect due to several factors and under certain conditions. For example, the limited temporal resolution of fMRI (Friston et al., 2003; Roiser et al., 2013) to measure biophysical mechanisms from EPI time series (Daunizeau et al., 2011a; Friston et al., 2012); and the lack of direct concentrations of dopamine (DA) or glutamate (Glu) do not allow the direct measurement of synaptic plasticity. Furthermore, the systematic testing of EC measures of task-dependent modulation can only be considered for the specific experimental task modelled and in a given model. We point out that EC findings cannot be interpreted as changes of neurotransmitter systems underlying the experimental task due to the lack of direct measurements of DA and Glu in the specific neuronal population. Thus, neuropsychological and neurocognitive interpretations must be considered in context of modelling of functional large-scale network findings.

1.1.3 Outline of the thesis

The PhD thesis considers the application of DCM for fMRI data in individuals with schizophrenia. Bilinear and nonlinear DCM has been used to investigate hypothesised alterations in EC measures between (i) individuals at high familial risk of schizophrenia and healthy controls (as part of the EHRS); and (ii) EST and healthy controls (as part of the SFMHS).

In chapter 1, FA and FC findings of working memory fMRI and Positron Emission Tomography (PET) studies in individuals with schizophrenia and healthy controls are summarised. These findings are discussed in context of the dopamine hypothesis of schizophrenia and the glutamate hypothesis of schizophrenia.

In chapter 2, different methods for the assessment of EC and advantages/disadvantages of DCM in specific are discussed. EC findings of working memory fMRI studies in individuals with schizophrenia and healthy controls as assessed with DCM are reviewed. We consider to what extent EC findings may increase the interpretability of functional large-scale networks in comparison to FC findings.

In chapter 3, a heuristic search protocol for the application of nonlinear DCM has been applied to the verbal fluency task in individuals at high genetic risk of schizophrenia and healthy controls (as part of the EHRS). The main result was that EC measures were significantly different between high risk subjects and healthy controls, which may extend the previous FC findings (Whalley et al., 2004).

In chapter 4, the devised heuristic search protocol for the application of nonlinear DCM was adapted for the working memory task in EST and healthy controls. The main result was that EST used a different functional network for the working memory function than healthy controls.

In chapter 5, a summary and discussion of the key findings from the EHRS and the SFMHS is presented in context of improved insight into functional large-scale networks underlying cognitive function in individuals with schizophrenia.

1.2 Introduction to chapter 1

It is widely established that schizophrenia is a brain disorder. This understanding has been formed by decades of research and it has been furthered through neurobiological and neuropsychopharmacological research. This research has revealed evidence of altered neurobiological mechanisms including brain molecular, cellular and chemical findings in schizophrenia. Furthermore, the notion of impaired working memory function in schizophrenia was originally based on research in animals and continues to provide novel knowledge of underlying neurobiological mechanisms (Goldman-Rakic and Selemon, 1997; Lewis and Moghaddam, 2006; Burgos-Gonzalez et al., 2010). One of the main findings for working memory impairment in schizophrenia was dysfunction of the PFC and alterations of neurotransmitter systems involving the PFC (Goldman-Rakic and Selemon, 1997; Goldman-Rakic et al., 1999). These findings have led to major neurobiological theories of schizophrenia such as the ‘dopamine hypothesis of schizophrenia’ and the ‘glutamate hypothesis of schizophrenia’. The strength of the hypotheses of schizophrenia lies in the opportunity of investigating neurobiological alterations in individuals with schizophrenia with the aim of gaining a better insight into the pathophysiological pathways of schizophrenia.

It is well known that individuals with schizophrenia have cognitive deficits in addition to clinical symptoms. The most common of such cognitive deficits is working memory impairment, which is apparent at every stage of the illness (Fusar-Poli et al., 2012; Seidman et al., 2010; Kim et al., 2011; Genevsky et al., 2010) and has been linked to the severity of clinical symptoms in schizophrenia (MacDonald and Schulz, 2009, Fusar-Poli et al., 2012). With the advent of clinical and cognitive neurosciences a plethora of functional Magnetic Resonance Imaging (fMRI) and positron emission tomography (PET) studies found that individuals with schizophrenia show altered DLPFC brain function in working memory in comparison to healthy controls (Goldberg and Weinberger, 1988; Goldman-Rakic 1994; Callicott et al., 2000; Callicott et al., 2003). In the later years, altered FC findings involving the (DL)PFC in individuals with schizophrenia were reported (Tan et al., 2006) with the aim of providing a better translational interpretation of human neuroimaging findings to preclinical findings.

In this chapter, we briefly describe the pathological and aetiological background of schizophrenia (chapter 1.2). We summarise neurobiological findings crucial for the understanding of schizophrenia as a brain disorder (chapter 1.3) by focusing on the description of the two main neurotransmitters and neurotransmitter systems implicated in schizophrenia: DA and Glu (chapter 1.3.1). Then we outline the main versions of the 'dopamine hypothesis of schizophrenia' and the 'glutamate hypothesis of schizophrenia', which were developed and revised based on the neurobiological findings (chapter 1.3.2). In the next step, we review clinical and cognitive neuroscientific findings of FA and FC findings from fMRI and PET studies

in working memory in individuals with schizophrenia and healthy subjects (chapter 1.4.2). In particular, we discuss if and to what extent the reviewed FA and FC findings can be interpreted in light of the dopamine and/or glutamate hypotheses of schizophrenia.

1.3 Schizophrenia – General overview

We briefly describe the criteria for the clinical diagnosis of schizophrenia based on the Diagnostic and Statistical Manual of Mental Disorders, Fourth Edition, Text Revision (DSM-IV-TR; American Psychiatric Association, 2000). The individuals with established schizophrenia (EST), who took part in this study, were diagnosed on the criteria of DSM-IV-TR.

1.3.1 Pathology

Schizophrenia is a severe psychiatric disorder, which is initially manifested through positive symptoms including delusions, hallucinations and disorganised thoughts. As the illness progresses, negative symptoms such as avolition, alogia and apathy may occur. Prior to diagnosis of the illness, cognitive deficits can occur and illness progression can also be associated with cognitive deficits (MacDonald and Schulz, 2009, Fusar-Poli et al., 2012).

Lifetime prevalence of schizophrenia is approximately 1%. The gender ratio between men and women is nearly 1:1, although men seem to have an earlier age onset than women (van Os and Kapur, 2009). The onset of the illness occurs

typically in late adolescence or early adulthood, however the range of onset can vary between childhood and late adulthood (Kumra et al., 2001).

The clinical symptoms are briefly described. Positive symptoms are characterized by delusions, hallucinations and formal thought disorders. Delusions are defined as unrealistic and dysfunctional beliefs. Hallucinations are pathological sensory sensations, mainly in the auditory modality without an objective basis for a stimulus. Formal thought disorders implicate a disruption of thought processes (Andreasen, 1995). Negative symptoms are characterized by a pathological deficit in activity and responsiveness. This deficit can be seen in impoverishment of verbal and nonverbal communication, social withdrawal, anhedonia and general reduction in emotion, psychomotor deceleration and a general apathic appearance (Andreasen, 1995).

It is widely established that cognitive deficits are considered a core symptom of schizophrenia (Elvevag and Goldberg, 2000, Kremen et al., 2000; Gold, 2004). These symptoms can encompass a range of executive functions such as impaired performance in attention, memory, planning, reasoning, language functions and social cognition. Working memory deficits are one of the main neurocognitive impairments found in subjects with first episode schizophrenia (FES) (Seidman et al., 2010; Kim et al., 2011) and EST (Genevsky et al., 2010). Similar deficits also occur in individuals at high risk of schizophrenia (HR; Fusar-Poli et al., 2012). Furthermore, recent evidence has been presented, which indicates a relationship between severity of working memory deficits and the severity of negative symptoms (Bora and Murray, 2013). The severity of working memory deficits that is

evident at the first episode of schizophrenia can predict the quality of life at the established stage of the illness (Seshadri et al., 2013; Kukla et al., 2013).

The pattern of clinical positive and negative symptoms leads to different subtypes as classified by DSM-IV-TR. The four different subtypes are: (i) paranoid, (ii) catatonic, (iii) hebephrenic (or disorganized) and (iv) simple deteriorative disorder. Here, we focus on the paranoid subtype since the patients, who participated in the SFMHS, received this diagnosis. Paranoid schizophrenia is characterized by delusions or auditory hallucinations, whereas thought disorder, disorganized behaviour or affective flattening are not present.

The course of schizophrenia is variable and can fluctuate. In some cases, individuals recover after the first psychotic episode, whereas in other cases, individuals fall chronically ill with the disorder.

Phases of the illness are commonly subdivided into three subgroups:

- High risk phase of the illness (also sometimes called prodrome);
- First episode schizophrenia, which is described by a maximum illness duration of approximately 18 months;
- Established phase of the illness, which is described by a minimum illness duration of approximately 18 months ranging to decades.

The high risk phase is further subgrouped into clinical high risk phase or familial high risk phase of adolescents and young adults, who are at enhanced risk of developing schizophrenia in the following years. Relevance of research on the

high risk phase and transition to the first-episode schizophrenia can be seen in the growing number of studies in this field and the new diagnosis category in DSM-V (Fusar-Poli et al., 2014).

For clinical risk of schizophrenia, it is thought that these people are at high risk because of the appearance of transient and partial psychotic symptoms (Fusar-Poli et al., 2012). Research on individuals at increased clinical risk can be summarised by the study populations of (i) subjects with an At-Risk Mental State (ARMS) and (ii) subjects at ultra-high risk (UHR). Individuals are considered to be at increased familial risk of developing schizophrenia when they have one first-degree relative with the illness (Johnstone et al., 2000).

Evidence has been presented that subjects at increased clinical risk and subjects at increased familial risk of schizophrenia show alterations in cognitive performance (clinical risk/familial risk, Bora et al., 2014), brain structure (clinical risk, Carletti et al. 2012; familial risk, Thermenos et al., 2013), brain function/connectivity (clinical risk, Pettersson-Yeo et al., 2011; familial risk, Thermenos et al., 2013), brain DA function (clinical risk, Egerton et al., 2013) and brain metabolite concentrations such as Glu (clinical risk, Egerton et al., 2014; familial risk, Tibbo et al., 2004).

1.3.2 Aetiology

The aetiology of the illness is still unknown. Several possible factors have been proposed, however, there is controversy about each factor and its possible inter-relationships with other factors. The primary factors and their interactions among

other risk factors are briefly summarised, which are believed to contribute to or mediate pathological mechanism(s) of schizophrenia:

(i) Heritability and risk genes

(ii) Environmental factors

(iii) Brain alterations

(i) First evidence of heritability of schizophrenia was published by twin studies (Gottesman and Shields, 1966; Shields and Gottesman, 1972). Similarly, susceptibility genes have been proposed to be involved in the pathophysiology of the illness (Harrison and Weinberger, 2005) but it has not been possible to prove this hypothesis. Twin and adoption studies suggested that rather an interaction between genetic and environmental factors may lead to schizophrenia than single genetic factors (Susser, 1985). Evidence has been presented which shows that multiple susceptibility and candidate genes may result in schizophrenia rather than a single gene (Mirnics et al., 2000; Schizophrenia Working Group of the Psychiatric Genomics Consortium, 2014).

(ii) Environmental factors have been suggested to play a role in the pathophysiology of the illness such as pregnancy and birth complications, neurological insults and life stressors (Heinz et al., 2013). Despite decades of research, it has not been able to prove this hypothesis as an aetiological cause of the illness. Thus, it is thought that genetic and environmental factors may interact and lead to a greater likelihood of the occurrence of the illness than genetic or environmental factors

individually (McDonald and Murray, 2000). An example of linking both state and trait markers in schizophrenia is research on endophenotypes (Braff et al., 2007; Glahn et al., 2014).

(iii) MRI studies reported evidence for brain alterations in brain structure, for example, enlarged third ventricles and grey matter loss in temporal regions (Raz and Raz, 1990; Tang et al., 2012) and brain function during cognitive tasks (for example, working during fMRI (Callicott et al., 2000; Callicott et al., 2003)). Neuroimaging studies showed not only alterations of brain structure and function but also possible interrelationships between brain alterations and genetic factors as well as environmental factors (Lenroot and Giedd, 2008).

1.3.3 Treatment

The most common treatment of individuals with schizophrenia is the prescription of antipsychotic medication. In some cases, patients may also undergo additional psychotherapy.

The antipsychotic drugs are subdivided into (i) 'first-generation antipsychotics' (FGA) or 'typical' antipsychotics and; (ii) 'second-generation antipsychotics' (SGA) or 'atypical' antipsychotics. Briefly, commonly prescribed FGA comprise haloperidol, fluphenazine and chlorpromazine. Examples of SGA are clozapine, olanzapine, risperidone, quetiapine, ziprasidone and aripriprazole. Despite the fact that antipsychotic treatment remains the main treatment of patients with schizophrenia, the exact details of the mode of actions of these drugs is not well understood (Howes et al., 2012).

1.4 Neurobiology of schizophrenia

1.4.1 Implicated neurotransmitters and neurotransmitter systems in schizophrenia

Preclinical research has provided a wealth of findings on alterations of neurotransmitter systems in schizophrenia with the focus on two main neurotransmitter systems of DA and Glu and their interactions. Furthermore, evidence suggest that alterations of DA and Glu involving the (DL)PFC and prefrontal circuits could underlie the pathophysiology of disrupted working memory function in schizophrenia (Moghaddam et al., 1997; Lewis and Moghaddam, 2006; Arnsten et al., 2012).

Besides DA and Glu, other neurotransmitters such as γ-amino-butter-acid (GABA), serotonin (5-hydroxytryptamine, 5-HT), acetylcholine (ACh) and noradrenaline (NA) are involved in the modulation of cognitive functions. In addition, alterations of GABA and 5-HT transmission are implicated in dopaminergic and/or glutamatergic circuits in schizophrenia (Carlsson et al., 1997; Lewis and Burgos-González, 2008; Lisman et al., 2008; Qi et al., 2010).

Risk genes and candidate genes are known to play a role in alterations of dopaminergic and glutamatergic modulation of the (DL)PFC, which could result in disruption of synaptic plasticity and therefore cognitive impairment in schizophrenia. Examples of suggested risk genes comprise the susceptibility gene Disrupted-in-schizophrenia-1 (DISC1) (Hayashi-Takagi et al., 2010; Ramsey et al., 2011), neuregulin and dysbindin (Harrison and Weinberger, 2005).

1.4.1.1 Dopamine

There are three main dopaminergic pathways, which are relevant for the innervation of motor and cognitive functions: (i) the nigro-striatal system; (ii) the meso-limbic system; and (iii) the meso-cortical system, of which the meso-limbic and meso-cortical circuits are pivotal for cognitive functions. Here, we focus on the meso-cortical DA system because of its relevant role in PFC neurotransmission and cognitive function such as working memory. The meso-cortical system modulates executive functions such as working memory from the VTA and to some extent from the substantia nigra (SN) to the PFC, in particular the DLPFC.

Findings from animal studies provided evidence for dopaminergic modulation of the (DL)PFC and working memory via meso-cortical D_1 receptor projection (D_1 receptor subtype of the DA receptor) to prefrontal pyramidal cells and GABAergic interneurons (Goldman-Rakic, 1996; Durstewitz et al., 1999; Durstewitz and Seamans, 2002). Alterations of meso-cortical D_1 receptor transmission of the (DL)PFC resulted in working memory impairment in schizophrenia (Durstewitz and Seamans, 2008; Goldman-Rakic, 1999). It is noted that findings have been reported that not only D_1 receptors but also D_2 receptors (D_2 subtype of the DA receptor) are involved in changes of *N*-methyl-D-aspartate (NMDA) receptor-dependent synaptic plasticity in the DLPFC, for example through imbalance of D_1/D_2 receptor expression (Tzschentke, 2001; Laruelle et al., 2005; Durstewitz and Seamans, 2008). Furthermore, D_4 and D_5 receptors (D_4 and D_5 subtypes of the DA receptors) have been proposed to be involved in interactions with glutamatergic and GABAergic neurons in the PFC (Cortés et al., 1989; Goldman-Rakic and Selemon, 1997).

1.4.1.2 Glutamate

Glu is the primary excitatory neurotransmitter in the PFC, which has cortico-mesal glutamatergic efferent projections to the VTA (Tzschentke, 2001) and excitatory glutamatergic afferents from cortical and subcortical regions, for example the MD thalamus (Leonard, 1969; Gioanni et al., 1999). Iontropic Glu receptors are divided into three groups: (i) NMDA receptors; (ii) Alpha-Amino-3-hydody-5-methyl-isoxazol-4-propioacid (AMPA) receptors; and (iii) kainate receptors.

Glu is implicated in cognitive functions such as working memory in interaction with DA (Arnsten et al., 2012). Ionotropic receptors modulate several basic physiological processes such as neuronal growth and synaptic plasticity, which are context-dependent or experience-dependent for the modulation of cognitive functions (Javitt, 2007; Newpher and Ehlers, 2008; Pinault, 2011).

1.4.1.3 Interactions between dopamine and glutamate

Both DA and Glu modulate cognitive function involving the DL(PFC) and aberrant dopaminergic and/or glutamatergic modulation can lead to cognitive impairment such as working memory via aberrant NMDA receptor function (Gonzalez-Burgos et al., 2010; Arnsten et al., 2012). Here we focus on the meso-cortical circuit (Gonzalez-Burgos et al., 2005; Wang, 2010), which plays a crucial role in the modulation of working memory in schizophrenia.

Dopaminergic and/or glutamatergic interactions have been first proposed after the observation of close proximity of both dopaminergic and glutamatergic terminals on same pyramidal cell in the PFC (Goldman-Rakic et al., 1989). Glutamatergic transmission from the PFC modulate dopaminergic neurons in the VTA (Jackson et

al., 2001; Sesack et al., 2002). These glutamatergic projections are mediated by NMDA receptor-dependent synaptic plasticity (Bonci et al., 1999; Overton et al., 1999). The efferent glutamatergic projections impact on dopaminergic neurons in the VTA, which project to the D_1 receptors in the DLPFC (Sesack et al., 2002, Carr et al., 2000; Gao and Wolf, 2007; Romanides et al., 1999). Based on these findings, it has been proposed that decreased glutamatergic projection from the PFC to the VTA results in reduced dopaminergic transmission via D_1 receptors from the VTA to the DLPFC (Lewis and Gonzalez-Burgos, 2006; Lewis and Gonzalez-Burgos, 2008).

These findings show that dopaminergic and glutamatergic projections activate cells and neurons reciprocally. They can be summarised by (i) DA – Glu interactions in the PFC and (ii) DA – Glu interactions in the VTA. Two examples for interactions in the PFC are (a) dopaminergic stimulation of the VTA leads to inhibition of prefrontal pyramidal cells and (b) glutamatergic regulation of prefrontal dopaminergic cells by ionotropic and/or metabotropic Glu receptors (mGluR) (Tzschentke, 2001). For DA – Glu interactions in the VTA, findings were reported of (a) Glu agonist/antagonist activity in dopaminergic neurons in the VTA, (b) midbrain glutamatergic regulation of different populations of DA neurons in the PFC and (c) prefrontal glutamatergic projections to the VTA generate dopaminergic burst activity in the VTA (Tzschentke, 2001).

It is noteworthy that other neurotransmitter and neuromodulators such as GABA, 5-HT, ACh, NA and nicotinic receptors (Tzschentke, 2001; Stephan et al., 2006; Stephan et al., 2009a) are involved in the meso-cortical-mesal circuit underlying working memory performance (Timofeeva and Levin, 2011), which are beyond the scope of this thesis.

1.4.1.4 Other implicated neurotransmitters and neurotransmitter systems

It has been reported that neurotransmitters such as GABA, 5-HT, ACh and NA are involved in modulation of cognitive function and these neurotransmissions are altered in schizophrenia. Furthermore, it has been shown that interactions between those and the dopaminergic and glutamatergic circuits exist. Here, we briefly summarise the effects of GABA on DLPFC circuitry and working memory in schizophrenia as the main researched area.

GABA is the primary inhibitory neurotransmitter and plays a major role in the DLPFC and prefrontal circuitries underlying working memory (Lewis and Gonzalez-Burgos, 2008; Timofeeva and Levin, 2011). Disruptions of GABAergic modulations such as reduced GABA synthesis and reuptake in DLPFC neurons in patients with schizophrenia have been reported (Lewis and Gonzalez-Burgos, 2008). Furthermore, it has shown that reductions of GABAergic receptors, specifically glutamic acid decarboxylase 67 and parvalbumin receptors, and genetic alteration involved in GABAergic transmission can lead to disruption of synaptic plasticity processes (Lewis and Gonzalez-Burgos, 2008) and therefore working memory impairments in schizophrenia (Gonzalez-Burgos et al., 2010; Timofeeva and Levin, 2011).

Evidence for interactions between glutamatergic and GABAergic projections, which could underlie cognitive functions such as working memory function in the (DL)PFC have been reported (Lewis and Gonzalez-Burgos, 2008). Prefrontal glutamatergic neurons project to the VTA and activate GABAergic neurons projecting to the

nucleus accumbens and may decrease meso-striatal projections (Sesack et al., 2002; Gao and Wolf, 2007).

1.4.2 Neurobiological theories of schizophrenia

DA and Glu circuits have been implicated in clinical and cognitive symptoms in subjects with schizophrenia. Evidence has been presented for alterations of DA, Glu and an alteration of the interaction between both neurotransmitters. The two main neurobiological hypotheses in schizophrenia are based on the theories of altered dopaminergic transmission ('dopamine hypothesis of schizophrenia') and altered glutamatergic transmission ('glutamate hypothesis of schizophrenia'). It is thought that both DA and Glu modulate the DLPFC and in schizophrenia alter the performance in cognitive processes such as in working memory (Tanaka, 2006; Tan et al., 2007; Anticevic et al., 2012).

Neurobiological research into alterations of dopaminergic and/or glutamatergic neurotransmission has paved the way for the understanding of schizophrenia as a disorder of the brain. The dopamine hypothesis posits that DA function is altered in schizophrenia and that this dysfunction may be the pathophysiological pathway leading to clinical and cognitive symptoms (Howes and Kapur, 2009; Qi et al., 2010). The glutamate hypothesis proposes that the altered dopaminergic dysfunction may be secondary to aberrant glutamatergic dysregulation, which may contribute to clinical and cognitive symptoms in schizophrenia (Coyle, 2012; Kantrowitz and Javitt, 2010).

1.4.2.1 Dopamine hypothesis of schizophrenia

The origin of the dopamine hypothesis of schizophrenia is based on the discovery of antipsychotic drugs by Delay et al., in 1952. Carlsson and Lindqvit reported the first findings of an effect of antipsychotic drugs on the metabolism of DA (Carlsson, 1978). The original dopamine hypothesis posits that alterations of dopaminergic receptors may underlie the clinical symptoms of schizophrenia (Emilien et al., 1999). Over last three decades, the dopamine hypothesis of schizophrenia has undergone reformulations in light of newly available preclinical and clinical findings. Here, we consider the three main hypotheses: (i) the 'dopamine receptor hypothesis', (ii) the 'modified dopamine hypothesis of schizophrenia', and (iii) the 'dopamine hypothesis: version III'.

1.4.2.1.1 'Dopamine receptor hypothesis'

The dopamine receptor hypothesis goes back to studies reporting clinical efficacy correlates with D_2 receptor affinity (Seeman and Lee, 1975; Creese et al., 1976; Seeman et al., 1976). Further evidence for the hypothesis was presented with increased synaptic monoamine levels during the induction of psychotic symptoms (Lieberman et al., 1987). The focus of this hypothesis rests on the excess of DA receptors. Thus, the clinical treatment is aimed at blocking the DA D_2 subtype of the DA receptors (Snyder, 1976).

1.4.2.1.2 'Modified dopamine hypothesis'

The modified dopamine hypothesis of schizophrenia has been formulated to integrate new findings (Davis et al., 1991). Preclinical and clinical studies (i.e. post-mortem,

metabolite and DA receptor neuroimaging studies) have advanced the understanding of relationships between affinity and occupancy of D_2 and D_1 subtypes of the DA receptors and regional specificity (Kapur and Seeman, 2001). Furthermore, it was assumed that findings of altered regional dopaminergic receptor function from preclinical and indirect clinical studies could be linked to clinical symptomatology in schizophrenia (Davis et al., 1991). The hypothesis suggests that 'hypofrontality', as measured with reduced regional cerebral blood flow (rCBF) in the PFC may indicate low DA levels in the PFC (Davis et al., 1991). Findings from preclinical lesion studies proposed that prefrontal 'hypodopaminergia' leads to striatal 'hyperdopaminergia' (Pycock et al., 1980; Scatton et al., 1982). In addition, it is hypothesised that prefrontal 'hypodopaminergia' could cause negative symptoms, whereas striatal 'hyperdopaminergia' could lead to positive symptoms (Davis et al., 1991).

1.4.2.1.3 'Dopamine hypothesis: version III'

The dopamine hypothesis: version III synthesises published findings on DA and its potential role in schizophrenia from the main fields into one unifying hypothesis. The hypothesis aims to provide a framework for findings from developments in clinical research into genetic (risk) factors, environmental risk factors, neurochemical and neuroimaging studies, and preclinical studies, which may be related to increased presynaptic striatal dopaminergic function in schizophrenia (Howes and Kapur, 2009). The authors outline four components for the hypothesis in their review article: (i) The interaction of "hits" such as fronto-temporal dysfunction, genes, stress and drugs may lead to striatal DA dysregulation (i.e. increased

presynaptic DA synthesis capacity) and therefore to psychosis. (ii) It is hypothesised that the primary dopaminergic dysfunction is located at the presynaptic dopaminergic level instead of the D_2 receptor level. (iii) The hypothesis assumes that the DA dysregulation combined with cultural and societal factors could lead to future clinical diagnosis of ‘‘psychosis’’ rather than schizophrenia. (iv) It has been proposed that the DA dysfunction could change the perception and judgment of stimuli (possibly through aberrant salience), which could result in cognitive deficits (Heinz, 2002; Kapur et al., 2003).

Recent meta-analyses, which examined markers of striatal DA alterations in schizophrenia, reported evidence of different types of elevated DA dysfunction. Supporting evidence for the dopamine hypothesis has been shown by increased striatal presynaptic dopaminergic function in medication-free or medication-naïve patients with schizophrenia contrasted to healthy controls (Howes et al., 2012) and increased striatal DA synthesis capacity (Fusar-Poli and Meyer-Lindenberg, 2013a). Furthermore, Fusar-Poli and Meyer-Lindenberg (2013b) found no difference in striatal DA active transporter density between patients with schizophrenia and healthy controls, which presents evidence for DA elevation in presynaptic terminals (Howes et al., 2012; Fusar-Poli and Meyer-Lindenberg, 2013a).

1.4.2.1.4 Summary

In summary, while both the dopamine receptor hypothesis and the modified dopamine hypothesis of schizophrenia have their origins in the neurobiological

investigation of the mode of action of antipsychotics, the dopamine hypothesis: version III aims at integrating advances in research of schizophrenia into one unifying dopamine hypothesis. The scope of understanding of dopaminergic dysregulation has become more defined, ranging from the whole brain perspective, via the perspective of regional specificity between (DL)PFC and striatum, to the current perspective of elevated presynaptic striatal dopaminergic function. The development of the dopamine hypothesis over the three versions has helped shape the understanding of schizophrenia as a brain disorder.

1.4.2.2 Glutamate hypothesis of schizophrenia

The origin of the glutamate hypothesis of schizophrenia was based on the discovery of psychotomimetic effects of ketamine and phencyclidine, which elicited psychotic symptoms in healthy people. Symptoms such as delusions and hallucinations experienced by healthy individuals were compared to positive symptoms seen in FES (Krystal et al., 1994; Abi-Saab et al., 1998). The glutamate hypothesis postulates a mechanistic process of altered interacting glutamatergic and/or dopaminergic neurotransmitter circuitries implicated in the pathophysiology of clinical and cognitive symptoms in schizophrenia (Luby et al., 1959; Carlsson et al., 2000; Farber et al., 2002; Javitt, 2007). In this review, we consider three models of the glutamate hypothesis with relevance to the investigation of altered working memory function in people with schizophrenia: (i) the NMDA receptor hypofunction model' of schizophrenia, (ii) the 'acute ketamine model', and (iii) the 'dysconnection hypothesis' of schizophrenia.

1.4.2.2.1 'N-Methyl-D-aspartate acid (NMDA) receptor hypofunction model'

The NMDA receptor hypofunction model of schizophrenia posits that the subtype of the Glu receptor is implicated in multiple pathological brain mechanisms of schizophrenia ranging across cellular, chemical and neuronal levels (Coyle, 2006; Coyle et al., 2010; Moghaddam and Krystal, 2012; Javitt et al., 2012). It has been proposed that NMDA receptor hypofunction could underlie the pathophysiology of negative and cognitive symptoms in schizophrenia (Carlsson et al., 1999; Coyle, 2006; Javitt, 2010; Goff and Coyle, 2001). Clinical trials with agents modulating the NMDA receptor in addition to treatment with FGA (such as chlorpromazine, haloperidol and perphenazine) and SGA (such as clozapine and olanzapine) presented supporting evidence for amelioration of negative and cognitive symptoms (Coyle, 2006; Heresco-Levy et al., 2002; Lane et al., 2005). Evidence for the involvement of NMDA receptor hypofunction through interactions among different neurotransmitters such as GABAergic interneurons (Coyle, 2006) and DA (Tzschentke, 2001; Sesack and Carr, 2002) has also been reported.

1.4.2.2.2 'Acute ketamine model'

Evidence for the glutamate hypothesis in humans is based on clinical studies with ketamine in healthy subjects. Results suggest that glutamatergic alterations could explain the pathophysiological mechanisms resulting in positive symptoms predominantly experienced by FES and those with first episode psychosis (FEP) (Krystal et al., 1994; Krystal et al., 1999). While findings from ketamine injection studies have aided the understanding of

glutamatergic signalling in the development of delusions and hallucinations, evidence for altered glutamatergic transmission in negative and cognitive symptoms is scarce. FMRI findings from ketamine studies in healthy subjects propose that altered glutamatergic signalling could be implicated in working memory (Krystal et al., 1994; Anticevic et al., 2012; Driesen et al., 2013). These findings are in keeping with evidence from glutamatergic animal models, which report aberrant working memory function after the inhibition of glutamatergic receptors (Moghaddam et al., 1997; Timofeeva and Levin, 2011; Fitzgerald, 2012; Arnsten et al., 2012).

1.4.2.2.3 'Dysconnection hypothesis'

The dysconnection hypothesis of schizophrenia posits that altered NMDA receptor-mediated synaptic plasticity may be the underlying pathophysiological mechanism in individuals with schizophrenia (Stephan et al., 2006; Stephan et al., 2009a). The authors propose that altered synaptic plasticity may explain both clinical symptoms and cognitive deficits in people with schizophrenia neurobiologically by altered NMDA receptor neuromodulation. It is thought that NMDA receptor transmission is modulated by multiple intracellular mechanisms and activation of specific D_1 and D_2 receptors, Glu receptor subtypes and GABA receptors on PFC pyramidal cells (Tseng and O'Donnell, 2004). The dysconnection hypothesis synthesises neurobiological findings (i.e. DA as one of the main neuromodulators leading to aberrant NMDA receptor function) with clinical and cognitive neuroscientific findings (i.e. cognitive impairment) in individuals with schizophrenia. The dysconnection hypothesis is based on the notion that schizophrenia can be considered

as a ‘disconnection syndrome’ (Friston and Frith, 1995) and extends the conceptual hypothesis of disrupted large-scale functional networks during cognitive tasks to aberrant synaptic plasticity. In the original review, Friston and Frith propose that schizophrenia can be considered as an illness, which relates aberrant FC during cognitive and sensorimotor function with positive symptomatology in individuals with schizophrenia. In addition to this conceptual notion, the dysconnection hypothesis offers a new approach of analysing altered synaptic plasticity, which allows a new interpretation of neurophysiological and neuroimaging data. This may be used to assist in the understanding of altered cognitive function in people with schizophrenia. For functional neuroimaging data, the biophysical modelling approach of DCM (Friston et al., 2003) has been proposed to infer biophysical processes (namely, NMDA receptor-dependent synaptic plasticity) underlying the Blood-Oxygen-Level Dependent (BOLD) responses. In addition, the authors provide arguments that the development of positive symptoms such as delusions can be explained by a ‘failure of self-monitoring mechanism’ or ‘corollary discharge’ (Stephan et al., 2009a). Abnormal EC findings from electroencephalogram (EEG) and fMRI studies across a range of cognitive tasks in subjects with schizophrenia in contrast to healthy controls have been reported (Dima et al., 2009; Dima et al., 2010; Wagner et al., 2013). These lead to a new insight into altered connectivity above those provided by FC studies, which are formulated under different theoretical frameworks. Specifically, DCM findings enable the inference of biophysical processes underlying neural responses (Friston et al., 2003; Friston and Dolan, 2010; Stephan and Friston, 2010).

1.4.2.2.4 Summary

In summary, the three hypotheses, the NMDA receptor hypofunction model, the acute ketamine model and the dysconnection hypothesis, have motivated researchers to investigate biophysical circuit processes implicated in glutamatergic and dopaminergic interactions in negative symptoms and cognitive function in schizophrenia. These circuit mechanisms are thought to underlie altered working memory function in schizophrenia. Research on the NMDA receptor hypofunction model has its roots in the pharmacological examination of antipsychotics, the development of new agents and its effects on clinical and cognitive symptoms in preclinical and clinical research in schizophrenia. The focus of researchers examining the acute ketamine model and the dysconnection hypothesis lies on elucidating proposed neurobiological processes of blockade of NMDA receptor underlying altered cognitive brain function in schizophrenia. The study designs of both versions differ in the investigation of (i) the pharmacological effect of ketamine on altered cognitive brain function and clinical symptomatology in healthy controls (the acute ketamine model) and (ii) altered synaptic plasticity during altered cognitive brain function in subjects with schizophrenia. Despite the different approaches, researchers of both versions of the glutamate hypothesis share the common aim of increasing our insight into schizophrenia by the translation of neurobiological knowledge from basic research to clinical research in schizophrenia. Furthermore, researchers share the common methodological approach of large-scale network analysis of fMRI data. Taken together, development over the three versions of the glutamate hypothesis of schizophrenia supports the notion of schizophrenia as a brain disorder.

1.5 Clinical and cognitive neuroscience of working memory in schizophrenia

Clinical and cognitive neuroscience studies have applied *in vivo* neuroimaging techniques of fMRI, PET and single-photon emission computed tomography (SPECT) to assess neurobiological processes that underlie working memory function in people with schizophrenia. Techniques such as PET and SPECT use injections of positron-emitting radionuclide as tracer (for PET) or gamma-emitting radionuclide as tracer (for SPECT) in the living brain. Although these nuclear medical imaging techniques are non-invasive they require the administration of tracers. FMRI provides non-invasive *in vivo* imaging, which measures brain function by means of the BOLD response (Ogawa et al., 1990).

1.5.1 Working memory

Working memory is thought to comprise executive functions such as attention, inhibition and planning (Baddeley, 1981, Hitch, 1984; Smith and Jonides, 1998; Smith and Jonides, 1999). Working memory is defined as the ability to briefly hold information in mind for manipulation or for long-term storage (Baddeley, 1996; Goldman-Rakic, 1996), which is necessary for the performance of cognitive tasks.

The computational approach of cognitive control by Braver and Cohen is similar to the construct of working memory (Braver et al., 1999; Cohen et al., 1992; Braver et al., 1997). However, two of the main novelties of the construct of cognitive control lie in: (i) the extension of the existing working memory definition; and (ii) the linkage between the psychological construct of working memory and the underlying neurobiological mechanism(s).

Braver et al., 1999 advanced the existing definition of working memory by the description of ‘context’ information as an element of working memory. The term ‘context’ indicates that relevant information is needed for the performance of the task (Braver et al., 1999; Cohen et al., 2002). Three specific processes within the construct of cognitive control have been described (Cohen et al., 2002) in order to define ‘context’. Furthermore, these hypothesised psychological processes have been related to known neurobiological findings.

The first process is active maintenance of representations, which is described as the ability to actively process relevant representations of the task's requirements, rules and aims. The second process of adaptive updating is the mechanism that ensures the continuous updating of previously maintained representations. This updating process encompasses two specific processes: (i) The detection of task-relevant stimuli and (ii) the detection of task-irrelevant stimuli, which are both essential for the successful performance of the cognitive task. Neurobiological findings support the hypothesis that updating is mediated by dopaminergic gating mechanisms via the VTA (Braver and Cohen, 1999; Cohen et al., 2002). The third process, conflict monitoring, is an attention process, which ensures the minimization of conflicts (i.e. errors such as false alarms or misses). It is thought that monitoring for potential conflicts can be measured as brain function in the anterior cingulate cortex (ACC; Cohen et al., 2002).

Different types of information can be manipulated, maintained, updated and stored during working memory performance:

- Verbal information, i.e. letters
- Numeric information, i.e. digits

- Visual images
- Auditory information, i.e. tones

Here, we focus on verbal and numeric working memory processes to ensure interpretability of BOLD responses between individuals with schizophrenia and healthy controls, which are not confounded by differences in domains of working memory stimuli. To further increase the interpretability among studies, FA and FC studies are reviewed that applied the verbal or numeric "N-back" task. The "N-back" task is considered to be as one of the most reliable experimental paradigms for the assessment of verbal/numeric working memory function in humans.

1.5.2 Findings of functional activation studies of verbal/numeric working memory in healthy subjects and subjects with schizophrenia

FMRI and PET findings of altered FA and FC during working memory have been reported in people with schizophrenia when they are compared to healthy controls (Kim et al., 2003; Honey and Fletcher, 2006). Furthermore, PET studies have presented evidence for indirect markers of altered DA transmission, which was correlated with working memory performance (Abi-Dargham et al., 2002; Fusar-Poli et al., 2010).

1.5.2.1 Functional magnetic resonance imaging studies

Working memory tasks were initially investigated with fMRI in healthy subjects (Cohen and Servan- Schreiber, 1992; Cohen et al., 1996; Smith and Jonides, 1999; Collette and Van der Linden, 2002). These initial studies used fMRI as a tool for

examining neurobiological markers that could be related to working memory performance. The examination of working memory function was extended to individuals with schizophrenia.

Reported findings of brain function during working memory (among several domains and components of working memory tasks) in healthy controls have led to the understanding that DA modulates working memory (Braver et al., 1999; Cohen et al., 2002; Cools et al., 2008). This evidence of dopaminergic involvement in working memory was extended by the findings of altered dopaminergic modulation in schizophrenia (Braver et al., 1999; Hazy et al., 2006). Subsequently, converging findings were reported that regions such as DLPFC, ACC and parietal cortex (PC) are activated in working memory in both healthy controls and in subjects with schizophrenia (Cole and Schneider, 2007; Lenartowicz and McIntosh, 2005; Woodward et al., 2006; Gazzaley and Nobre, 2012). However, in those with schizophrenia, these regions exhibit increased or reduced FAs and FC between prefrontal and parietal regions as well as between prefrontal and temporal regions in contrast to healthy controls. Alterations in FC occur at all stages of the illness (Broome et al., 2009; Liemburg et al., 2012): (i) in HR subjects (Rasetti et al., 2011); (ii) in FES and FEP (Barch et al., 2001) and (iii) in subjects with EST (Potkin et al., 2009).

Systematic reviews and meta-analyses of working memory fMRI studies in people with schizophrenia do not report consistent findings (Brown and Thompson, 2010; Manoach, 2003; Wager and Smith, 2003; Glahn et al., 2005). Some studies report increased activation of the DLPFC, commonly referred to as ‘hyperfrontality’, however other report decreased activation or ‘hypofrontality’. This picture of

differing FA in terms of the direction, extent and/or pattern of BOLD responses was attributed to the variation of domains and components of working memory tasks (Brown and Thompson, 2010; Manoach, 2003; Wager and Smith, 2003; Glahn et al., 2005). Also it was considered that methodological factors in the applied analyses (such as differences in behavioural performance at different working memory loads and their relationship with FA patterns) would contribute to these variations in FA (Manoach, 2003; van Snellenberg et al., 2006, Glahn et al., 2005). In addition, differences in medication could contribute to variation in the reported FA between studies.

Here, we review fMRI studies using the numeric or verbal "N-back" task to enable comparability among the studies (as outlined in chapter 1.4.1) in subjects with established schizophrenia (EST) and healthy controls, which reported FA findings (Table 1.1). The reviewed studies present group differences between subjects with schizophrenia and healthy controls.

In FA studies, evidence was reported for increased activation in DLPFC, PFC, ventral PFC (vPFC), medial frontal gyrus (MFG) and anterior cingulate (AC) during high working memory load in subjects with EST (Callicott et al., 2000; Callicott et al., 2003; Thermenos et al., 2005; Tan et al., 2006; Rasetti et al., 2011; Quidé et al., 2013). However, reduced activation in prefrontal regions, such as vPFC, DLPFC, AC and parietal regions was found during high working memory load in subjects with EST (Callicott et al., 2000; Perlstein et al., 2001; Callicott et al., 2003). One study in FES found a reduction activation in IFG, superior frontal gyrus (SFG) and AC during high working memory load (Guerrero-Pedraza et al., 2012). We note three factors, which contributed to difficulties in comparing the findings across the reviewed

studies: (i) missing information of phase of schizophrenia (Tan et al., 2006), (ii) heterogeneous groups of subjects with EST (Callicott et al., 2000; Guerrero-Pedraza et al., 2012; Quidé et al., 2013), and (iii) limited information on antipsychotic treatment (Callicott et al., 2000; Callicott et al., 2003; Thermenos et al., 2005; Tan et al., 2006; Rasetti et al., 2011; Guerrero-Pedraza et al., 2012; Quidé et al., 2013). Fundamentally, none of the FA findings was interpreted in context of the dopamine or glutamate hypothesis. The lack of a clear understanding in terms of neural activation and pathophysiological mechanism (with and without performance differences) suggests there is a need for studies examining wider prefrontal circuitry underlying working memory deficits in schizophrenia (Manoach, 2003; Glahn et al., 2005).

Table 1.1 Schizophrenia as a cognitive brain disorder - Summary of main FA findings in verbal/numeric working memory fMRI studies (Reproduced from Dauvermann et al., 2014).

Study	Subjects - Phase of Schizophrenia HC – HR, FES, EST	Medication	Experimental Paradigm	Main Finding(s)
Callicott et al., 2000	18 HC 13 EST[1]	Not reported	Numeric "2-back"	⬆ with increasing WM load in right DLPFC, left PFC, left AC; ⬇ with increasing WM load includ. right AC, right PCi, left vPFC.
Perlstein et al., 2001	16 HC 17 EST	17 EST, stable injectable FGA for two months	Verbal "2-back"	Main effect of group: ⬆ subgenual AC gyrus; Group X WM load interaction for high WM load: ⬇ in right DLPFC.
Callicott et al., 2003	14 HC 14 patients[2], subdivided into HP: 8 HC, 7 patients; LP: 6 HC, 7 patients	14 patients, 476.3 (291.7); 7 patients, 556.0 (157.0); 6 patients, 237.7 (96.4)	Numeric "2-back"	⬆ and ⬇ for high WM load in different subdivisions of the right and left DLPFC in 14 patients; Bilateral prefrontal areas of and ⬇ for high WM load in HP patients; Bilateral prefrontal areas of for high WM load in LP patients.
Thermenos et al., 2005	22 HC 14 EST	Not reported	Verbal "2-back"	⬆ for high WM load in right medial FG; ⬆ for hits during for high WM load in right medial FG.

⬆ Increased in subjects with schizophrenia in contrast to HC;
⬇ Decreased in subjects with schizophrenia in contrast to HC;
AC, anterior cingulate; DLPFC, dorsolateral prefrontal cortex; dPFC, dorsal prefrontal cortex; EST, subjects with established schizophrenia; FES, subjects with first episode schizophrenia; FG, frontal gyrus; FGA, First-generation antipsychotics; HC, healthy controls; HF, hippocampal formation; HP, high-performers; HR, Subjects at high risk of schizophrenia; IFG, inferior frontal gyrus; IPL, inferior parietal lobe; LP, low-performers; OFG, orbitofrontal gyrus; PCi, posterior cingulate; PHG, parahippocampal gyrus; ROI, region of interest; SGA, Second-generation antipsychotics; SFG, superior frontal gyrus; SPL, superior parietal lobule; vPFC, ventral prefrontal cortex; vlPFC, ventrolateral PFC; WM, working memory.
1 Patients with different schizophrenia subtypes, such as paranoid subtype, schizoaffective subtype, undifferentiated subtype;
2 Phase of illness, illness onset and illness duration not reported. Phase of illness based on symptoms scores;
3 Chlorpromazine equivalents in mg/day.

1.5.2.2 Positron emission tomography studies

PET and SPECT imaging in schizophrenia research are used to investigate indirect markers of DA measures such as $D_{2/3}$ receptors, presynaptic dopaminergic function, DA synthesis capacity, DA release and DA transporters. Three [$H_2{}^{15}O$] PET studies consistently reported reduced rCBF in DLPFC and posterior cingulate (PCi) in verbal/numeric "2-back" in subjects with EST in contrast to healthy controls (Carter et al., 1998; Meyer-Lindenberg et al., 2001; Meyer-Lindenberg et al., 2005) (Table 1.2).

Table 1.2 Schizophrenia as a cognitive brain disorder - Summary of main functional activation findings in verbal/numeric working memory PET studies.

Study	Subjects - Phase of Schizophrenia HC – HR, FES, EST	Medication	Experimental Paradigm	PET Technique/Method	Main Finding(s)
Carter et al., 1998	8 HC 8 EST[1]	EST medicated; No details of medication reported	Verbal "2-back"	rCBF measurement; Radioactive water [$H_2{}^{15}O$]	⬇ for high WM load in right DLPFC; ⬇ for high WM load in right PPC; ⬇ for low WM load in right DLPFC, but not in right PPC.
Meyer-Lindenberg et al., 2001	13 HC 13 patients[1,2]	13 patients not medicated for minimum 2 weeks; No details of medication reported	Numeric "2-back"	Multiple rCBF measurements; Administration of bolus injection of 10 mCi of radioactive water [$H_2{}^{15}O$] per scan;	Condition X group interaction (high WM load): ⬇ in bilateral DLPFC and bilateal IPL; Condition X group interaction (high WM load): ⬆ in medial FG, left STG, right PHG, right ICG.
Meyer-Lindenberg et al., 2005	22 HC 22 patients[2]	22 patients not medicated for minimum 2 weeks; No details of medication reported.	Numeric "2-back"	Multiple rCBF measurements; Administration of bolus injection of 10 mCi of radioactive water [$H_2{}^{15}O$] per scan	Group X task interaction (high WM load): ⬇ in right DLPFC and in left cerebellar region.

⬆ Increased in subjects with schizophrenia in contrast to HC; ⬇ Decreased in subjects with schizophrenia in contrast to HC;
DLPFC, dorsolateral prefrontal cortex; EST, subjects with established schizophrenia; FES, subjects with first episode schizophrenia; medial FG, frontal gyrus; HC, healthy controls; HR, Subjects at high risk of schizophrenia; ICG, inferior occipital gyrus; IPL, inferior parietal lobe; mCi, millicurie; PHG, parahippocampal gyrus; PET, positron emission tomography; PPC, posterior parietal cortex; rCBF, regional cerebral blood flow; STG, superior temporal gyrus; WM, working memory.
[1] Phase of illness, illness onset and illness duration not specified;
[2] Patients with paranoid subtype; schizoaffective subtype; undifferentiated subtype.

1.5.3 Functional connectivity studies of verbal/numeric working memory

FC studies mark the beginning of the notion of "disconnection" or "dysconnection" (Friston and Frith, 1995; Stephan et al., 2006; Stephan et al., 2009a) in investigating working memory deficits in people with schizophrenia. FC is defined as the statistical association or dependency among two or more anatomically distinct time-series (Friston and Frith, 1995). FC findings cannot be interpreted in terms of causal effects between connected regions and thus does not allow for a mechanistic inference of the BOLD responses.

1.5.3.1 Functional magnetic resonance imaging studies

FC studies applied voxel-based seed approaches to the BOLD response (Tan et al., 2006; Rasetti et al., 2011; Guerrero-Pedraza et al., 2012), with the exception of one study, which applied an ROI-to-ROI approach (Quidé et al., 2013) (Table 1.3). Despite the use of equivalent methodological approach of voxel-based seed correlation, the FC findings are not entirely comparable due to the use of different seed locations. Findings of reduced connectivity involving subregions of the PFC were found in FES and EST. Reduced FC findings in subjects with schizophrenia and EST were reported in the majority of studies: (i) Reduced prefrontal-parietal[1] FC in subjects with schizophrenia (Tan et al., 2006); (ii) Reduced prefrontal-hippocampal, prefrontal-striatal and within-PFC FC in EST (Rasetti et al., 2011) and (iii) Reduced parieto-prefrontal FC and between putamen and ventrolateral PFC (vlPFC) in EST (Quidé et al., 2013). Further evidence for reduced FC between MFG

[1] Reduced FC between the dorsal PFC and posterior PC.

and putamen was found in FES (Guerrero-Pedraza et al., 2012). In contrast to most studies that report reduced FC in the early and late phases of the illness, increased FC between the vPFC and posterior PC was shown in subjects with schizophrenia (Tan et al., 2006). The findings of both reduced and increased FC between subregions of the PFC and the posterior PC may be related to variations in behavioural response to task load for subjects with schizophrenia (Tan et al., 2006). Similar difficulties in comparing the FC findings among the studies are present as in the comparison of the FA studies due to unclear and missing information regarding the illness phase, diagnosis and medication treatment. Similarly, no reference is made to the dopamine or glutamate hypothesis in interpreting the FC findings.

Table 1.3 Schizophrenia as a cognitive brain disorder - Summary of main functional activation / functional connectivity findings in verbal/numeric working memory fMRI studies (Reproduced from Dauvermann et al., 2014).

Study	Subjects - Phase of Schizophrenia HC – HR, FES, EST	Medication	Experimental Paradigm	Functional Connectivity Method Seed regions/ROIs/VOIs Seed regions/ROIs/VOIs Definition Sphere size	Main Finding(s)
Tan et al., 2006	26 HC 15 patients[2], subdivided into HP: 14 HC, 8 patients; LP: 12 HC, 7 patients	15 patients, 501 (337.0)[3];	Numeric "2-back"	Seed-based cross-correlation Seed regions: right dPFC and left vPFC; Functional ROIs 10 mm sphere size	⬆FA with increasing WM load in bilateral vPFC in 15 patients; ⬆ FC between left vPFC and left SPL in 15 patients; ⬇FC between right dPFC and bilateral IPL in 15 patients.
Rasetti et al., 2011	153 HC 78 EST[2]	75 EST, FGA and SGA; 3 EST, data missing;	Numeric "2-back"	Seed-based cross-correlation[4] Seed regions: right DLPFC Functional ROIs 6 mm sphere size	⬆FA for high WM load in right DLPFC; ⬇FC between right DLPFC *and* bilateral HF; ⬇FC between right DLPFC and right IPL.
Guerrero-Pedraza et al., 2012	28 HC 30 FES[1]	Not reported	Numeric "2-back"	Seed-based cross-correlation Seed regions: left gyrus rectus, left IFG, left SFG, left AC, right PHG, right amygdala Functional ROIs Sphere size not reported	⬆FA for high WM load in left gyrus rectus, left IFG, left SFG, left AC, right PHG, right amygdala; ⬇ FC between medial FG and right precuneus; between medial FG and left OFG; between medial frontal gyrus and right precentral gyrus.

Quidé et al., 2013	28 HC 28 EST[1,2]	24 EST, 294.45 (316.36)[3];	Numeric "2-back"	ROI-to-ROI FC ROIs: bilateral DLPFC, vlPFC, putamen, caudate nuclei, IPL Functional ROIs Sphere size not reported	⬆ FA for high WM load in bilateral putamen, left DLPFC, OFC, cuneus and PC; ⬇FC between left putamen and right vlPFC; ⬇FC between left putamen and left vlPFC; between right IPL and right vlPFC.

⬆ Increased in subjects with schizophrenia in contrast to HC; ⬇ Decreased in subjects with schizophrenia in contrast to HC;
AC, anterior cingulate; DLPFC, dorsolateral prefrontal cortex; dPFC, dorsal prefrontal cortex; EST, subjects with established schizophrenia; FA, functional activation; FC, Functional connectivity; FES, subjects with first episode schizophrenia; FG, frontal gyrus; FGA, First-generation antipsychotics; HC, healthy controls; HF, hippocampal formation; HP, high-performers; HR, Subjects at high risk of schizophrenia; IFG, inferior frontal gyrus; IPL, inferior parietal lobe; LP, low-performers; OFG, orbitofrontal gyrus; PC, posterior cingulate; PHG, parahippocampal gyrus; ROI, region of interest; SGA, Second-generation antipsychotics; SFG, superior frontal gyrus; SPL, superior parietal lobule; vPFC, ventral prefrontal cortex; vlPFC, ventrolateral PFC; WM, working memory.

[1] Patients with different schizophrenia subtypes, such as paranoid subtype, schizoaffective subtype, undifferentiated subtype;

[2] Phase of illness, illness onset and illness duration not reported. Phase of illness based on symptoms scores.

[3] Chlorpromazine equivalents in mg/day

[4] Seed-based connectivity only reported here.

1.5.3.2 Positron emission tomography studies

In PET studies, reduced prefrontal-hippocampal FC findings in subjects with schizophrenia in contrast to healthy controls (Meyer-Lindenberg et al., 2001; Meyer-Lindenberg et al., 2005) confirmed the hypothesis of reduced functional connections in working memory (Table 1.4). Correlational PET studies provided indirect support for dopaminergic alterations during working memory function by significant correlations between rCBF and behavioural performance of the "2-back" task in subjects with schizophrenia (Abi-Dargham et al., 2002; Fusar-Poli et al., 2010).

Table 1.4 Schizophrenia as a cognitive brain disorder - Summary of main functional connectivity findings in verbal/numeric working memory PET studies.

Study	Subjects - Phase of Schizophrenia HC – HR, FES, EST	Medication	Experimental Paradigm	Functional Connectivity Method Seed regions/ROIs/VOIs Seed regions/ROIs/VOIs Definition Sphere size	Main Finding(s)
Meyer-Lindenberg et al., 2001	13 HC 13 patients[1,2]	13 patients not medicated for minimum 2 weeks; No details of medication reported	Numeric "2-back"	Canonical variates analysis; No further details reported.	Negative FC between ITL, HC and CER in patients; Positive FC between DLPFC and CG in HC;
Meyer-Lindenberg et al., 2005	22 HC 22 patients	22 patients not medicated for minimum 2 weeks; No details of medication reported.	Numeric "2-back"	Linear covariation approach; VOIs: HF (incl. ipsilateral temporal lobe) and medial frontal cortex (incl. AC); Anatomical VOIs; Sphere size not reported.	Positive correlation between left HF and right DLPFC for high WM load in patients. Negative correlation between left HF and right DLPFC for high working memory load in HC.

AC anterior cingulate; CER, cerebellum; CG, cingulate gyrus; DLPFC, dorsolateral prefrontal cortex; EST, subjects with established schizophrenia; FC, functional connectivity; FES, subjects with first episode schizophrenia; HC, healthy controls; HF, hippocampal formation; HR, Subjects at high risk of schizophrenia; ITL, inferior temporal lobe; WM, working memory.

[1] Phase of illness, illness onset and illness duration not specified;

[2] Patients with paranoid subtype; schizoaffective subtype; undifferentiated subtype.

In summary, findings presented by FC studies during the "N-back" task have paved the way for the understanding of large-scale functional networks in working memory. Furthermore, the insight of brain alterations in subjects with schizophrenia has advanced with FC from individually activated regions to connectivity between brain regions. The perspective of circuit-based neurobiology and cognitive brain function opens the doors for translational research from preclinical and clinical research in schizophrenia. However, FC is limited as the connection assessments are based upon regional correlations and this approach does not allow inferences of directions or causality between connected regions (Friston et al., 2003).

In summary, fMRI and PET studies in the field of clinical and cognitive neurosciences have been used to investigate brain function during working memory in people with schizophrenia. Both fMRI and PET findings have advanced the understanding of altered working memory performance, brain function and FC in subjects with schizophrenia by linking their findings to preclinical evidence and two versions of the dopamine hypothesis (i.e. the 'Modified dopamine hypothesis' (chapter 1.3.2.1.2) and the 'Dopamine hypothesis: version III' (chapter 1.3.2.1.2) as summarised in Figure 1.1. This has led to better insight into the interaction between altered working memory function and experimental/clinical factors (such as cognitive domains of working memory function, performance level, phases of illness, clinical symptomatology and effects of antipsychotic medication) in individuals with schizophrenia. We suggest that studies such as these reviewed here have contributed to shaping the understanding of schizophrenia as a cognitive brain disorder (Figure 1.1).

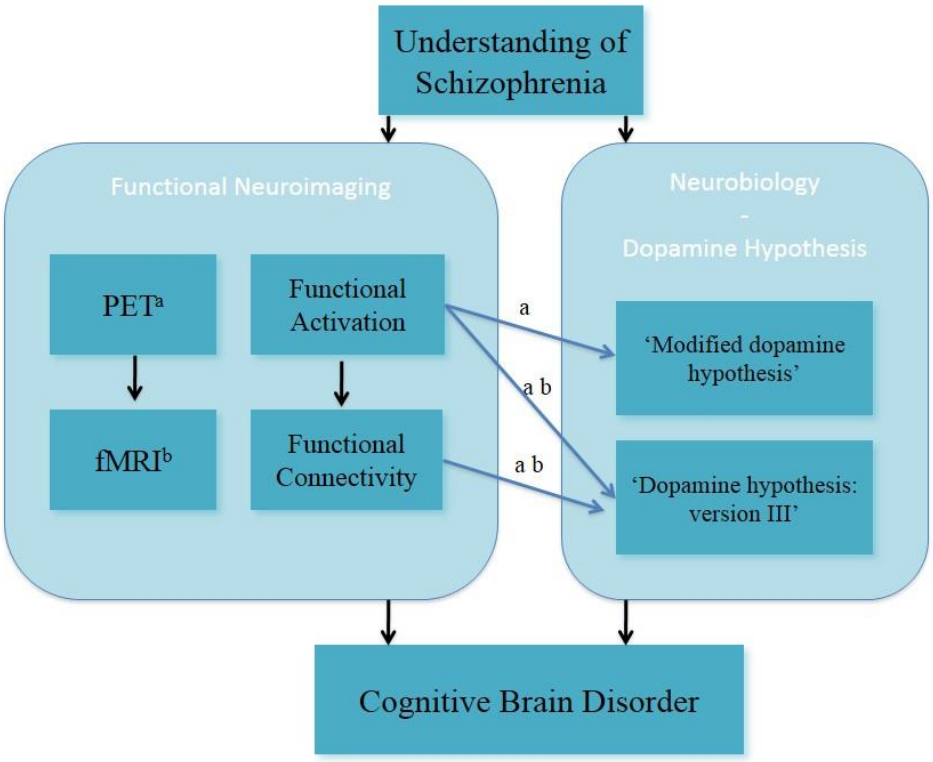

Figure 1.1 Understanding of schizophrenia as a cognitive brain disorder – Verbal/numeric "N-back" task (Reproduced from Dauvermann et al., 2014).

[a] fMRI;
[b] PET Positron emission tomography

1.6 Discussion

The two main neurobiological hypotheses of schizophrenia, the dopamine hypothesis and the glutamate hypothesis, have deeply influenced the understanding of schizophrenia as a brain disorder. More recently, those two hypotheses have introduced the notion of schizophrenia as a cognitive brain disorder, which has its basis from findings of altered dopaminergic and/or glutamatergic neurotransmission modulating and mediating working memory dysfunction in schizophrenia. Both the dopamine and the glutamate hypothesis have motivated clinical and cognitive

neuroscientists to examine the underlying neurobiological mechanisms of working memory impairment in individuals with schizophrenia with the potential of gaining a better insight into the pathophysiological pathway of working memory deficits.

Researchers in clinical and cognitive neurosciences have advanced the understanding of altered working memory function in subjects with schizophrenia. FMRI and PET studies in working memory among other neuroimaging and electrophysiological techniques, have reported on FA and FC findings in subjects with schizophrenia. The reviewed findings of FA and FC during the verbal/numeric "N-back" task revealed significantly reduced or increased BOLD responses or FC findings in subjects with schizophrenia in contrast to healthy subjects. These FC findings have introduced the notion of human large-scale networks underlying brain function during working memory and have formed the understanding of schizophrenia as a cognitive brain disorder.

In regard to the interpretability of FA and FC findings in context of the dopamine hypothesis and glutamate hypothesis we conclude that neither the FA nor the FC findings can fulfil this criterion due to the technical and methodological nature of the BOLD contrast (for the FA results) and the correlational analysis (for the FC results). For the FC findings, the correlational analyses do not allow for the inference of directions or weights of in functional connections. Thus, from FC findings it is not possible to draw inferences on causal processing.

Neurobiological hypotheses offer the potential for translational neuropsychiatry from preclinical to clinical data in schizophrenia. However, the challenge is to find equivalent techniques to interpret clinical neuroimaging data translationally to preclinical neurobiological data. One technique to possibly meet this aim is DCM for

fMRI, which has been introduced by Friston (Friston et al., 2003). By the means of DCM, mechanistic responses can be inferred from the computational modelling of cognitive brain function where the localised brain function is monitored through the BOLD response (Stephan and Mathys, 2014). This modelling approach may further our understanding of the neurobiological processes, which underlie altered working memory function in individuals with schizophrenia.

2 Modelling of functional large-scale networks from fMRI data in subjects with established schizophrenia

2.1 Introduction

Clinical and cognitive neurosciences have advanced the understanding of altered working memory function in subjects with schizophrenia through the use of neuroimaging. The notion of schizophrenia as a 'disconnection' and 'dysconnection disorder has been introduced, which has its beginnings in the idea of altered brain connectivity (Friston and Frith, 1995; Stephan et al., 2006; Stephan et al., 2009a) or altered functional large-scale networks.

Recent studies examining biophysical mechanisms underlying altered functional large-scale networks aim to bridge the gap between the human functional network activated in cognitive function such as working memory and preclinical neurobiological processes modulating cognitive function. Examples of such computational neuropsychiatric studies include EC of fMRI studies during working memory in subjects with schizophrenia among other modalities such as EEG and magnetoencephalography (MEG). The modelling of functional large-scale networks during working memory function could provide mechanistic explanations for altered brain function in individuals with schizophrenia. The advantage of modelling functional large-scale networks in terms of EC over FC is that inferences can be drawn on mechanistic processes based on probabilistic inference. We compare EC methods (i.e. Structural Equation Modelling (SEM), psychophysiological interaction (PPI), Granger causal modelling (GCM) and DCM) to analyse fMRI data before we focus on advantages and disadvantages in the application of DCM.

In our review of EC studies, we focus on DCM studies for fMRI investigating the numeric/verbal "N-back" task in subjects with schizophrenia and healthy controls and consider those studies in context of the dopamine and glutamate hypotheses of schizophrenia. DCM has been selected over other methods for assessing EC measures in working memory in subjects with schizophrenia such as SEM studies, Granger causality studies and PPI studies. DCM provides for the indirect measurement of altered synaptic plasticity processes via task-dependent changes in given models (Stephan et al., 2008; Stephan and Friston, 2010). Thus, it provides for the analysis of the numeric/verbal "N-back" task, which is sensitive to cognition impairments associated with schizophrenia. The potential of DCM research lies in the biophysical modelling of fMRI data in individuals with schizophrenia and this could result in development in the interpretability of clinical neuroimaging data in patients and may therefore lead to more effective treatments.

In this chapter, we summarise findings from studies modelling working memory function. In particular, evidence for modelling synaptic plasticity and gating mechanisms underlying the working memory function is considered. Furthermore, findings of disruptions of synaptic plasticity and gating processes in schizophrenia are presented (chapter 2.2.2). Evidence for these disruptions are presented for the thalamo-cortical and meso-cortical connection, which are known to be implicated in cognitive dysfunction and pathophysiology of schizophrenia. In the next step, DCM studies examining EC during working memory in people with schizophrenia compared to healthy controls are reviewed in consideration of their interpretability in

regard to the dopamine hypothesis and glutamate hypothesis of schizophrenia (chapter 2.2.4).

2.2 Computational modelling of working memory in schizophrenia

2.2.1 Computational neuroscience

New insights into the high-level computations of the brain such as working memory and its alterations in schizophrenia have been reported from computational modelling studies. These insights were enabled by the multi-disciplinary approach of computational neuroscience and preclinical neurobiology. The computational neuroscience approach has been influenced by Marr's theoretical framework for computational neuroscience research comprising three levels (Marr, 1976), which has paved the way for the computational implementation of preclinical neurobiological findings.

Modelling of neurobiological processes of synaptic plasticity and gating mechanisms lie at the basis of computational modelling approaches of learning and cognitive processes. These findings may lead to a better understanding of altered cognitive function such as working memory via altered functional large-scale networks in individuals with schizophrenia.

2.2.2 Computational modelling of synaptic plasticity and gating mechanism

Short-term synaptic modulation encompasses biophysical processes which are known to be highly relevant for cognitive tasks (Abbott and Regehr, 2004; Deng and Klyachko, 2011; Neher and Sakaba, 2008; Pan and Zucker, 2009). It has been reported that probabilistic computational modelling of short-term depression processes resembles gating mechanisms at the synaptic level (Pfister et al., 2010).

It is assumed that nonlinear effects originate from activity-dependent synaptic plasticity processes (Abbott et al., 1997; Rothman et al., 2009; Salinas and Sejnowski, 2001; Shu et al., 2003), which gate cognitive functions (Salinas and Sejnowski, 2001; Stephan et al., 2008) in a multiplicative nonlinear way. Gating processes show comparable nonlinear mechanisms (Abbott et al., 1997; Ardid et al., 2007; Berends et al., 2005; Chance et al., 2002; Freyer et al., 2011; Murphy and Miller, 2003; Rothman et al., 2009; Salinas and Sejnowski, 2001; Shu et al., 2003). This indicates that neurons from two or more sources integrate information for cognitive performance (Salinas and Sejnowski, 2001; Stephan et al., 2008).

It has been shown that gating at the synaptic level is mediated by glutamatergic neurotransmission (Berends et al., 2005; Neher and Sakaba, 2008; Pan and Zucker, 2009; Sun and Beierlein, 2011; Volman et al., 2010), which is modulated by excitatory (mainly glutamatergic) and inhibitory (inhibitory interneurons) inputs (Murphy and Miller, 2003; Salinas and Sejnowski, 2001; Salinas and Sejnowski, 2000; Wang, 2010).

There is evidence that alterations of glutamatergic neurotransmission may contribute to disrupted synaptic plasticity in schizophrenia (Balu and Coyle, 2012; Coyle, 2006). The glutamate hypothesis of schizophrenia proposes that altered glutamatergic modulation may underlie the pathophysiology of the disorder (Coyle, 2006; Coyle et al., 2010; Javitt, 2010). This suggests that Glu neurotransmission, specifically NMDA receptor-mediated transmission, may be disrupted in schizophrenia (Goff and Coyle, 2001; Goff et al., 1995; Javitt et al., 1994; Moghaddam et al., 1997). Despite the evidence for glutamatergic neurotransmission, it is thought that altered interactions between glutamatergic and dopaminergic neurotransmission may lead to the cortical dysconnectivity in schizophrenia (Alelú-Paz and Giménez-Amaya, 2008; Coyle, 2006; Javitt, 2010; Moghaddam et al., 1997). It is further known that other neurotransmitters such as GABA among others is implicated in neurotransmitter systems in prefrontal deficits (Thierry et al., 1988; Simpson et al., 1989; Akbarian et al., 1995; Lewis and Burgos-Gonzalez, 2008; Burgos-Gonzalez et al., 2010).

The majority of recent computational studies focused on the investigation of gating mechanisms on circumscribed connections between two brain regions, i.e. the thalamo-cortical connection and the meso-cortical connection. It is noted that the focus on these two connections is a simplification of a more complex circuit system, which has not been fully understood yet. Hypotheses and theories have been proposed, which posit a complex system consisting of interaction between several neurotransmitter systems (i.e. DA, Glu, GABA, 5-HT) and several brain regions (i.e. (DL)PFC, MD thalamus, VTA/SN area, hippocampus and striatum) (Mantz et al., 1990; Thierry et al., 1990; Tzschentke, 2001).

2.2.2.1 Thalamo-cortical connection

Thalamo-cortical synapses underlie nonlinear dynamic modulation (Chance et al., 2002; Deng and Klyachko, 2011; Destexhe, 2009; Negyessy and Goldman-Rakic, 2005), which indicates gating of the thalamo-cortical connection (Alelú-Paz and Giménez-Amaya, 2008; Chance et al., 2002; Deng and Klyachko, 2011; Destexhe, 2009; Kolluri et al., 2005; Negyessy and Goldman-Rakic, 2005). Gating mechanisms have also been shown to be implicated for the cortico-thalamic connection (Freyer et al., 2011; Shu et al., 2003).

Neurobiological studies examining neurotransmission underlying the thalamo-cortical connection in schizophrenia showed that this thalamo-cortical projection is primarily altered by excitatory glutamatergic neurotransmission (Balu and Coyle, 2012; Gray and Roth, 2007; McCormick and Bal, 1997; Romanides et al., 1999; Watis et al., 2008), which could be attributed to NMDA receptor dysfunction (Kiss et al., 2011; Santana et al., 2009), but also to thalamic inhibitory interneurons (Augustinaite and Heggelund, 2007; Crandall and Cox, 2012; Errington et al., 2010; Lewis and González-Burgos, 2008; Neher and Sakaba, 2008; Pan and Zucker, 2009), interneurons in the DLPFC (Wang, 2010); mGluR (Jones, 1997; Newpher and Ehlers, 2008; Pinault, 2011; Sodhi et al., 2011) and ionotropic receptors (Meador-Woodruff et al., 2003).

Findings from neurobiological preclinical studies suggest that altered gain control (i.e. nonlinear modulation of neuronal connections) of the thalamo-cortical connection could be one of the underlying factors for altered cortical dysconnectivity in schizophrenia (Andreasen et al., 1997; Negyessy and Goldman-Rakic, 2005).

In patients with schizophrenia, alterations of the thalamus, in particular the MD thalamus, have been associated with the pathology of schizophrenia (Clinton and Meador-Woodruff, 2004; Meador-Woodruff et al., 2003; Oh et al., 2009) because of its cortio-thalamo-cortico network (Briggs and Usray, 2008; Kantrowitz and Javitt, 2012; Oh et al., 2009). Alterations of cortical dysfunction and cognitive deficits have been reported in HR and patients with schizophrenia in verbal fluency tasks (Curtis et al., 1998; Fu et al., 2002; Fusar-Poli et al., 2011; Clinton and Meador-Woodruff, 2004; Jones, 1997; Meador-Woodruff et al., 2003). FC studies also demonstrated that the connection between the left MD thalamus and the DLPFC was disrupted, which emphasises the crucial role of the thalamo-cortical connection in schizophrenia (Hazlett et al., 2004; Krystal et al., 2003; Mitelman et al., 2005; Thermenos et al., 2004). These alterations of the thalamo-cortical connection may contribute to cortical dysfunction observed in schizophrenia (Balu and Coyle, 2012; Byne et al., 2009; Lewis and Lieberman, 2000; Pakkenberg et al., 2009; Sodhi et al., 2011; Watis et al., 2008).

2.2.2.2 Meso-cortical connection

Findings from preclinical and computational studies suggest that working memory could be gated at the level of microcircuits in the PFC (Salinas and Sejnowski, 2001; Deng and Klyachko, 2011; Barak et al., 2010; Mongillo et al., 2008; Pfister et al., 2010; Wang et al., 2010). It is thought that working memory as an executive function is centred on the (DL)PFC based on its role as a highly recurrent area (Goldman-Rakic, 1995; Deng and Klyachko, 2011; Brunel and Wang, 2001; Miller and Wang, 2006; Durstewitz et al., 1999) but also involving prefrontal-parietal regions and

prefrontal-midbrain regions (i.e. VTA (Levin et al., 1994; Romanides et al., 1999; Tzschentke, 2001; Wang et al., 2010).

The neurobiological neurotransmission of the meso-cortical connection in working memory is based on the same synaptic plasticity and gating mechanism processes as summarised for the thalamo-cortical connection (chapter 2.2.2). Evidence of neuromodulation of the gating mechanism of the meso-cortical connection has been shown to be mediated by DA (Durstewitz et al., 2000; Gao et al., 2003) and Glu (Tzschentke, 2001; Wang et al., 2010; Arnsten et al., 2010; Arnsten et al., 2012) such as AMPA receptors (Gao and Wolf, 2007; Sun et al., 2005) and NMDA receptors (Berends et al., 2005; Durstewitz, et al., 2000; Gao and Wolf, 2008; Tseng and O'Donnell, 2004).

In clinical fMRI studies, altered BOLD responses of the VTA/SN area in working memory in patients with schizophrenia in contrast to healthy controls have been reported (Braver et al., 1999; Braver and Cohen, 1999; Hazy et al., 2006). Furthermore, Braver and Cohen proposed the theory that altered midbrain activation could results from altered gating of the VTA (Braver et al., 1999; Braver and Cohen, 1999). Evidence from two recent studies provide support for altered VTA/SN activity during working memory in healthy controls, which has been interpreted as an indication of dopaminergic modulation of meso-cortical gating (Murty et al., 2011; D'Ardenne et al., 2012). Murty et al., (2011) examined FC from the VTA/SN area via the caudate to the DLPFC. D'Ardenne et al., (2012) suggested gain modulation between the VTA/SN and the DLPFC using a combined fMRI and transcranial magnetic stimulation study design. Both studies focused on the executive part of

working memory performance, which ensured the computation of signal changes of the VTA/SN area and the DLPFC. In summary, it has been suggested that gain control processes could be altered in people with schizophrenia, which could result in (DL)PFC dysfunction and working memory impairment in patients with schizophrenia when compared to healthy controls (Wang et al., 2010; Pettersson-Yeo et al., 2011; D'Ardenne et al., 2012).

2.2.3 Computational psychiatry and computational neuropsychiatry

Computational psychiatry is an emerging field within computational neuroscience. Computational psychiatry aims to provide an explanatory bridge between altered cognitive function and neurobiological mechanisms associated with the development of mental illness (Huys et al., 2011; Montague et al., 2012). Computational psychiatry in humans has been defined by outlining a set of components, which include biophysical modelling and computational modelling (Montague et al., 2012). Different types of computational models at different neural levels are used dependent on the study hypothesis (Huys et al., 2011).

Computational neuropsychiatry is a subfield of computational psychiatry, which is particularly concerned with the modelling of functional large-scale networks. Computational neuropsychiatry aims to provide an insight into neurobiological processes, which mediate altered cognitive function such as working memory function in individuals with schizophrenia.

Connectionist and neural network models in working memory/cognitive control in

subjects with schizophrenia have added to our understanding of both the brain function and the neurobiological mechanism underlying working memory (Cohen et al., 1996; Braver et al., 1999). The strength of these models are based on the translational link between human brain function (i.e. FA) and preclinical neurobiological evidence (namely, dopaminergic modulation) during working memory.

Following on from the work of Cohen and Braver, evidence for the understanding of schizophrenia as a cognitive network disorder has been presented by both preclinical studies (Tanaka et al., 2006; Lewis and Moghaddam, 2006; Lewis and Gonzalez-Burgos, 2008; Gonzalez-Burgos, 2010; Volk et al., 2010, Seshadri et al., 2013) and human FC studies in working memory (Tan et al., 2006; Rasetti et al., 2011; Guerrero-Pedraza et al., 2012; Quidé et al., 2013).

Recent studies examining biophysical mechanisms underlying altered functional large-scale networks aim to bridge the gap between the human functional network used in working memory and the preclinical neurobiological processes. Examples of such computational neuropsychiatric studies, including EC of working memory in subjects with schizophrenia, are reviewed. In this, we focus on DCM studies investigating the numeric/verbal "N-back" task in subjects with schizophrenia and healthy controls. These findings are considered in the context of the dopamine and glutamate hypotheses of schizophrenia.

2.2.4 Biophysical modelling of functional large-scale networks from fMRI data – Dynamic causal modelling for fMRI

2.2.4.1 Effective connectivity

EC has been introduced to provide insight into the notion of 'functional integration' during cognitive performance. 'Functional integration' has been advanced from the historic notion of 'functional specialization' (Friston, 2002) and is defined by context-dependent interactions among different brain regions (McIntosh, 2000; Friston et al., 2003).

Four methods for the EC assessment of fMRI data have been developed: (i) SEM; (ii) PPI; (iii) GCM; and (iv) DCM; the latter two are considered biophysical modelling methods. We provide an overview over those four methods before we outline the advantages and disadvantages in the application of DCM.

2.2.4.2 Methods for the assessment of effective connectivity of fMRI data

2.2.4.2.1 Psychophysiological interaction

The first EC analysis was published in 1995; this analysis was extended in the following years and was named PPI (Friston et al., 1997). PPIs were defined as interaction effects between the responses of one region, another region and experimental (i.e. task-related) variables (Friston et al., 1997). This PPI method is seen as the first application of EC and forms the basic concept for DCM, which was developed in 2003 (Friston et al., 2003) since the interaction terms introduce context-dependent interaction effects with experimental or 'psychological'effects.

2.2.4.2.2 Structural equation modelling

In clinical and cognitive neurosciences, SEM has been introduced to analyse EC for PET data (McIntosh et al., 1994) and fMRI data (Büchel and Friston, 1997). In the following years, SEM has been applied to a variety of higher cognitive functions such as verbal/numeric working memory fMRI data in healthy controls and/or individuals with schizophrenia (for example, Honey et al.; 2002; Schlösser et al., 2003a; Schlösser et al. 2003b) for the hypothesis-driven investigation of underlying functional large-scale networks.

The application for SEM for fMRI studies is based on the methodological framework of the 'measurement model' and the 'structural model' (Schlösser et al. 2006), which both describe relationships between measures and unobserved variables in the data set. SEM is a multivariate tool to examine a priori hypotheses about connections (and their directions) among specified regions in a network for a given fMRI data set. In SEM, EC can be defined 'within a path model as a system of linear equations' (Schlösser et al. 2006). The path coefficients are computed by the minimization of the difference between observed and estimated variables. Thus, EC is measured as the change of activation in one region ('target region') in dependence to the change of activation of another region ('source region') and covaried over all participants (of a population group) or over time.

A comparison between SEM and DCM for fMRI data has been published previously (Penny et al., 2004). There are two general commonalities, which SEM and DCM share: Firstly, the basic concept of both approaches is model comparison of fMRI data. Secondly, both SEM and DCM use model inversion for the assessment of EC

and EC changes due to a specific experimental task. At the same time, SEM and DCM can be differentiated by the generative models used to assess EC measures. In SEM, the assessment of changes in EC are linked to changes of haemodynamic changes underlying the observed BOLD signal. In contrast, in DCM, task-dependent changes in EC are measured at the neuronal level, which are compared with the observed haemodynamic signal by Bayesian inference (Buxton et al.; 1998). We selected the application of DCM over SEM to increase the biological interpretability of EC changes measured at the neuronal level.

2.2.4.2.3 Granger causal modelling

Granger causality was developed in the 1960s and has been widely used in economics since then (Granger, 1969). GCM rests on the concept Granger causality and the implementation of vector autoregressive models for fMRI data (Harrison et al., 2003), which forms the conceptual basis for the modelling approach for fMRI data (Goebel et al., 2003; Roebroeck et al., 2005). The development from vector regressive models to GCM is based on progress of Bayesian inference methods (such as haemodynamic models, model inversion and Bayesian model selection), which have contributed to the development of DCM (Stephan and Roebroeck, 2012).

The aim of Granger causality to fMRI data is to provide a description of (i) the structural and/or (ii) functional network underlying the given fMRI data, where the second case is part of GCM. For the structural network, indirect interactions and variables, which are unknown, are considered. For the functional network, EC is

understood as the combination between the network structure and the modulations of the functional task in relation to the network structure (Seth, 2005).

GCM has been applied to measure nonlinear connectivity (Marinazzo et al., 2011). Different nonlinear approaches have been proposed, which have used autoregressive and Kernel methods (Marinazzo et al., 2011). In particular, Kernel methods have received attention for the modelling of nonlinearity ('Kernel Granger Causality'). Reviews on the comparison of GCM and DCM for fMRI data (for example, Stephan and Roebroeck, 2012) and Kernel Granger Causality have been published (Marinazzo et al. 2011). GCM and DCM are both generic models that are based on the conceptual framework of the haemodynamic forward model to infer EC from fMRI data. Furthermore, both approaches share model inversion techniques for the model validation, which enables the assessment of changes in EC (Stephan and Roebroeck, 2012). The main differences between GCM and DCM lies in the applied approaches, which lead to potential problems of robustness of statistical analyses and biophysical interpretability of EC measures. GCM has been questioned for dealing with uncertainty of model parameters and neurobiophysical interpretability. DCM has been criticised for robustness of Bayesian inversion techniques (Stephan and Roebroeck, 2012). GCM and DCM are the only EC methods that have developed methods to assess nonlinear EC measures. In GCM, Kernel Granger Causality is based on Kernel methods to measure nonlinear effects in fMRI data (Marinazzo et al. 2011), whereas nonlinear DCM is based on the multiplicative computation of nonlinear modulation in DCM (Stephan et al., 2008). We selected DCM for the measurement of (nonlinear) EC over GCM because (i) DCM allows the assessment of task-dependent modulation; and (ii) the computation of nonlinear

modulation is similar to equations used for gating mechanism (Salinas and Sejnowski, 2001), which is not provided by GCM (Marinazzo et al. 2011).

2.2.4.2.4 Dynamic causal modelling for fMRI

DCM has been described as a biophysical modelling approach of neuronal dynamic processes (Friston et al., 2003; Friston and Dolan, 2010)[2], which can be used as a method for the computation of synaptic plasticity from fMRI task-based studies (Stephan et al., 2006, 2009a). Together biophysical modelling and Bayesian inference analysis form the framework for DCM (Daunizeau et al., 2011a; Daunizeau et al., 2011b; Stephan and Friston, 2010). Thus, DCM is a modelling approach, which combines defined network models (i.e. hypotheses) with Bayesian inversion methods (Friston and Dolan, 2010; Daunizeau et al., 2011a). Specifically, DCM assesses interregional EC through assessment of experimentally induced changes (Friston et al., 2003) and therefore allows for mechanistic inferences from neuronal function. Interregional EC is assessed by three modulations, which are defined in the model space: (i) Matrix *A* denotes endogenous connection strength between two regions in the absence of experimental manipulations ('intrinsic connections'); (ii) Matrix *B* reflects the experimental task modulation; and (iii) Matrix *C* denotes the connection strength of driving inputs, which represent extrinsic parameters that change the neuronal state of brain regions within the model (i.e. visual presentation of stimuli of the experimental task).

DCM for fMRI has been extended to nonlinear DCM to capture nonlinear interactions within the functional network (Stephan et al.; 2008). In nonlinear DCM,

[2] We consider DCM as the generative model approach as introduced in the seminal article by Friston (Friston et al., 2003).

the assessment of EC has been advanced to model connection strengths, which are modulated by the neural activity in one or more network regions (Matrix *D;* Stephan et al., 2008). The computation for the nonlinear modulation uses similar equations as previously reported in computational neuroscientific studies (Salinas and Sejnowski, 2001; Volman et al., 2010).

We summarise main advantages and disadvantages of DCM. The main advantages in the use of DCM over other EC methods are:

(i) The ability to model the experimental task modulation enables the investigation of task parameters. Thus, changes in connection strengths of the modulatory input (Matrix *B*) can be directly linked to the experimental condition of the task and therefore be interpreted in terms of learning.

(ii) The forward model of DCM, which lies at the basis of the conceptual framework of DCM for fMRI, in combination with Bayesian inference the haemodynamic "Balloon" model (Buxton et al.; 1998) has led to the implementation of DCM as the first generative model of fMRI data (Stephan and Roebroeck, 2012). DCM allows to infer EC at a neuronal level in contrast to the BOLD level in the other EC methods, which minimizes the interregional variance in BOLD responses (Stephan and Roebroeck, 2012).

(iii) Nonlinear DCM for fMRI enables the modelling of connection strength with nonlinear modulation, which has the potential to increase the biophysical plausibility of modelling fMRI data.

(iv) Developments in Bayesian inference methods for the use of DCM have enabled the systematic comparison of multiple models and different optimal

models in subjects, which may be relevant for clinical studies (Penny et al., 2010).

Not only advantages but also disadvantages in the application of DCM have been raised. The main disadvantages can be subdivided into (i) limitations of biophysical interpretability and (ii) robustness of statistical inference methods (Daunizeau et al., 2011a):

(i) DCM for fMRI has undergone developments to increase the biophysical plausibility despite the extension of nonlinear DCM for fMRI. One of the main criticism is based on the limited temporal resolution of fMRI (Friston et al., 2003; Roiser et al., 2013) to measure biophysical mechanisms from EPI time series (Daunizeau et al., 2011a; Friston et al., 2012). Thus, DCM can only be used as an indirect measure of synaptic plasticity when specific conditions are considered: Firstly, a principled investigation of assessment of connection strengths of task-dependent change in a given model space, which can be interpreted as synaptic plasticity (i.e. learning). Secondly, findings derived from DCM analyses cannot be solely interpreted as changes of neurotransmitter systems underlying the experimental task. Neuropsychological and neurocognitive interpretations should be considered in context of modelling of functional large-scale network findings.

(ii) The robustness of the statistical inference techniques used in DCM10 and DCM12 for all modalities in addition to fMRI has been discussed (Daunizeau et al., 2011a), which may result in the risk of unstable results over repeated runs of analyses (Daunizeau et al., 2009; Daunizeau et al., 2011a).

In summary, DCM is a useful tool for inferring EC underlying neural responses when DCM is applied in a principled and systematic way as a generic model when advantages and disadvantages are considered. Furthermore, the interpreted DCM findings in terms of neurobiological context (i.e. neurotransmitter systems) are complemented by neurocognitive interpretations.

2.2.4.3 Effective connectivity studies of verbal/numeric working memory in healthy subjects and subjects with schizophrenia

The first DCM studies in healthy controls described large-scale networks in working memory and a similar task (continuous performance test; Tana et al., 2010; Wang et al., 2009; Brázdil et al., 2007). A recent study in healthy controls built the linkage between EC results and underlying dopaminergic modulation of large-scale networks comprising of the DLPFC and PC during working memory performance (Tan et al., 2012).

To date four DCM studies have examined the verbal/numeric "N-back" task in subjects with schizophrenia using bilinear DCM (Crossley et al., 2009; Deserno et al., 2012; Schmidt et al., 2013; Zhang et al., 2013) (Table 2.1). These provide novel insights into reduced task-dependent EC and increased task-independent EC measures through modelling large-scale networks in schizophrenia.

In the first study, increased fronto-temporal intrinsic connectivity was found to be associated with increased FA of the superior temporal gyrus (STG) during the numeric "N-back" task in the subjects at the prodromal and at the acute psychotic stage of schizophrenia in contrast to the healthy controls. This finding was

suggested to be a potential marker for vulnerability to the disorder (Crossley et al., 2009). Furthermore, progressively decreased intrinsic connectivity between the STG and the MFG in ARMS and FES subjects in contrast to the healthy controls was reported. This finding suggested that FA may resemble increased task-independent EC between the PFC and the STG. However, the results of the study are not comparable to other DCM studies because (i) only one model was examined and (ii) the biological plausibility of the EC measures is not clearly accessible. No reference to the dopamine or glutamate hypotheses was made.

The second study investigated the working memory-dependent modulatory effect for the prefrontal-parietal connectivity in subjects with EST and healthy subjects during the numeric "N-back" task (Deserno et al., 2012). The large-scale networks included the right DLPFC, the PC and the visual cortex (VC) with bidirectional connections between all regions. The main finding was decreased task-dependent EC from the DLPFC to the PC in the subjects with EST in contrast to healthy controls. Thus, this finding could resemble evidence for the glutamate hypothesis of schizophrenia, specifically the NMDA receptor hypofunction model and the dysconnection hypothesis.

The third study examined possible vulnerability markers for psychosis from the verbal "N-back" task in ARMS subjects, FES subjects and healthy subjects (Schmidt et al., 2013). This study examined reduced task-dependent EC measures as well as relationships between connectivity parameters and antipsychotic medication received by subjects. In this study, EC in interhemispheric large-scale networks between the bilateral superior parietal lobes (SPL) and the bilateral MFG was assessed. This study reported novel findings of progressively decreased working

memory and induced modulation of connectivity between the MFG and the SPL (from healthy subjects to ARMS). Additionally, further decreased EC of modulatory effects were observed in non-medicated subjects with FEP contrasted to healthy controls. Evidence for amelioration of reduced EC between the MFG and the SPL in subjects with FES, who received SGA medication, could reflect alterations of dopaminergic regulation of NMDA receptor–dependent synaptic plasticity of fronto-parietal connections. However, this interpretation is limited by the lack of a control group of FES who are treated with different types of antipsychotic medication. These findings across different subpopulations of schizophrenia together with the effect of antipsychotic medication may reflect support for the NMDA receptor hypofunction model and the dysconnection hypothesis.

In the fourth study, Zhang et al (2013) explored EC measures in terms of possible neurobiological markers in groups of FES with high or low suicide risk and contrasted these with healthy controls during the verbal "N-back" task. The large-scale networks were defined by unidirectional and bidirectional connections between the two regions of the medial PFC and PC as well as working memory effects on these regions. This pilot study presented novel findings in FES at suicidal risk in terms of increased intrinsic connectivity from the PC to the MFG in both groups with FES (in comparison to healthy controls). This finding was interpreted as a possible association to schizophrenia, in which increased intrinsic connectivity from the MFG to the PC in the subjects with high risk of suicide could reflect vulnerability of suicide. However, the results are not directly comparable to the other DCM studies because of the study population, which focused on the issue of

suicide. The findings were also not interpreted in context of the dopamine or glutamate hypotheses.

Table 2.1 Schizophrenia as a cognitive brain network disorder - Summary of main findings in verbal/numeric working memory – Neuroimaging and biophysical modelling (Reproduced from Dauvermann et al., 2014).

Study	Subjects - Phase of Schizophrenia HC – HR, FES, EST	Medication	Experimental Paradigm	Networks – Model Space Number of models Regions	DCM Settings – DCM version Sphere size Inference technique(s)	Main Finding(s)
Crossley et al., 2009	13 HC 16 HR[1] 10 FES	HR, not medicated; 7 FES, risperidone or quetiapine 3 FES, not medicated	Numeric "2-back"	1 left hemispheric model; STG, SMA, MFG, INS, PPC	DCM in SPM5; Sphere sizes not reported; BMS not performed	Progressively⬆ IC of the prefrontal-temporal connection in HR and FES.
Deserno et al., 2012	42 HC 41 EST	35 EST, FGA; 5 EST, SGA 1EST, not medicated	Numeric "2-back"	48 intrahemispheric models; 3 model families; DLPFC, PC, VC	DCM10 in SPM8; 4 mm spheres; Random-effects BMS[5,6]; BMA	⬇EC (effect of task-modulation) from DLPFC to PC.
Schmidt et al., 2013	20 HC 17 HR[1] 21 FEP	HR, not medicated; 7 FEP, completely antipsychotic naïve; 6 FEP, antipsychotic naïve at the time of scanning; 8 FEP, SGA	Verbal "2-back"	12 intrahemispheric models; Bilateral SPL, bilateral MFG	DCM10 in SPM8; 12 mm spheres; Random-effects BMS[5]; BMA	Progressively⬇EC (effect of task-modulation) between MFG and SPL in HC, HR and FES. Ameliorated EC correlated with antipsychotic treatment.

Zhang et al., 2013	15 HC 14 FES[2] 19 FES[3]	FES[2], 254.76 (192.09)[4]; FES[3,] 325.88 (185.19)[4];	Verbal "2-back"	5 left hemispheric models; Medial PFC, PCC	DCM version not reported. SPM8; 6 mm spheres; BMS[5]; BMA	⬆ IC from PCC to medial PFC in both FES[5] and FES[6].

⬆ Increased in subjects with schizophrenia in contrast to HC;
⬇ Decreased in subjects with schizophrenia in contrast to HC;

BMA, Bayesian Model Averaging; BMS, Bayesian Model Selection; DLPFC, dorsolateral prefrontal cortex; EC, effective connectivity; EST, subjects with established schizophrenia; FES, subjects with first episode schizophrenia; FEP, subjects with first episode psychosis; FGA, first-generation antipsychotics; HC, healthy controls; HR, Subjects at high risk of schizophrenia; IC, Intrinsic connectivity; IFG, inferior frontal gyrus; INS, insula; MFG, middle frontal gyrus; PC, parietal cortex; PCC, posterior parietal cortex; PFC, prefrontal cortex; SGA, second-generation antipsychotics; SMA, supramarginal area; SPL, superior parietal lobe; SPM, Statistical Parametric Mapping; STG, superior temporal gyrus; VC, visual cortex.

[1] Subjects at high clinical risk of schizophrenia
[2] With high suicidal risk
[3] With low suicidal risk
[4] Chlorpromazine equivalents in mg/day
[5] BMS at the group-level
[6] BMS at the model family level.

We highlight main experimental and methodological limitations in the four DCM studies, which impede the comparability of findings (please see Table 2.1 for details). The main experimental limitation focuses on the discrepancies between the different patient subpopulations. Two studies analysed working memory fMRI data of subjects with ARMS and FES in comparison to healthy controls (Crossley et al., 2009; Schmidt et al., 2013), whereas one study modelled scans from subjects with EST (Deserno et al., 2012). Zhang et al., 2013 reported findings of a unique patient population of FES with high and low suicidal risk. In terms of methodological issues, one limitation lies in different definitions of model spaces for the large-scale networks, despite equivalence in the experimental tasks. Another limitation is that the reviewed DCM studies employed deterministic DCM for the comparison of the models. Deterministic models can predict processes perfectly if all inputs are known (Dayan and Abbot, 2000). However, at this early stage of employing biophysical modelling approaches to human brain function we do not have a full understanding of the brain responses to working memory. Future studies may employ stochastic DCM as an extension (Daunizeau et al., 2011a, Daunizeau et al., 2011b; Li et al., 2011). A further limitation is that different DCM versions were applied across the four studies, which impede the comparability of the findings. The priors are differently defined in the used DCM versions, which give rise to a variation in model evidence between the studies (Daunizeau et al., 2011a). Thus, it is possible that discrepancies in EC findings could be due to the prior definition and may not be solely due to differences in performance, brain function or clinical aspects of subjects with schizophrenia. Lastly, a general limitation of DCM for fMRI is that maximally ten regions within a large-scale

network can be modelled. This simplification results in difficulties of biophysical modelling of tasks, which are likely to encompass more than ten regions. Furthermore, not only the definition of different regions and different numbers of regions but also different modulatory inputs result in further extensions to the model space. Such model spaces are difficult to validate and analyse.

The four DCM studies presented evidence for increased task-dependent EC and increased task-*in*dependent EC findings during verbal/numeric working memory in subjects with schizophrenia. We discuss these EC findings in context of (i) the dopamine and glutamate hypothesis and (ii) FC findings during verbal/numeric working memory in subjects with schizophrenia.

(i) The four studies modelled large-scale networks during the "N-back" task in subjects with schizophrenia. However, only two out of these four studies consider their DCM results in the light of biophysical processes (Deserno et al., 2012 and Schmidt et al., 2013). The findings of reduced EC (namely, the effect of task-modulation) of the prefrontal-parietal connection in subjects with schizophrenia in contrast to healthy controls were interpreted biophysically and linked to the NMDA receptor hypofunction model and the dysconnection hypothesis (Deserno et al., 2012; Schmidt et al., 2013). Both studies reported reduced EC findings of the prefrontal-parietal connection during working memory, however, these findings need to be considered carefully due to different experimental designs (i.e. patient subpopulations, antipsychotic medication treatment of FGA and SGA) and methodological implementation (i.e. model space, DCM settings and inference techniques).

(ii) Three of the DCM studies reported altered EC findings of the prefrontal–parietal and parieto-prefrontal connections during the "N-back" task in subjects with schizophrenia in contrast to healthy controls. Deserno et al., (2012) and Schmidt et al., (2013) presented reduced EC (effect of task-modulation) of the prefrontal-parietal connection in subjects with schizophrenia in contrast to healthy controls, whereas Zhang et al., (2013) found increased EC (intrinsic connectivity) of the parietal-prefrontal connection. The reduced task-dependent EC findings are in keeping with reduced FC findings of these connections, although increased FC between a different prefrontal subregion and the PC was reported (Tan et al., 2006).

The study by Crossley et al., (2009) reported increased EC (intrinsic connectivity) of the prefrontal-temporal connection in subjects at HR and FES (in contrast to healthy controls). Reduced FC of the prefrontal-temporal connection during the "N-back" task in subjects with schizophrenia has been previously reported in PET studies (Meyer-Lindenberg et al., 2001; Meyer-Lindenberg et al., 2005). However, the regions within the PFC and temporal regions differ between the studies.

2.2.4.4 Summary

Evidence from brain function in working memory in subjects with schizophrenia at the level of functional large-scale networks (i.e. clinical and cognitive neurosciences) and neurobiological mechanisms in working memory in animal models of schizophrenia (i.e. preclinical neurobiological research) in combination with computational neuroscientific approaches has informed and enabled research in computational neuropsychiatry.

DCM studies using the verbal/numeric "N-Back" task in subjects with schizophrenia have reported both increased and reduced EC findings during cognition in subjects with schizophrenia in contrast to healthy controls. These studies applied DCM as a biophysical modelling approach to functional large-scale networks, which enabled the interpretation of EC findings on the basis of the glutamate hypothesis of schizophrenia, namely the NMDA receptor hypofunction model (chapter 1.3.2.2.1) and the dysconnection hypothesis (chapter 1.3.2.2.3) (Figure 2.1). We propose that DCM studies examining functional large-scale networks in combination with possible neurobiological mechanisms shape the understanding of schizophrenia as a cognitive brain network disorder (Figure 2.1).

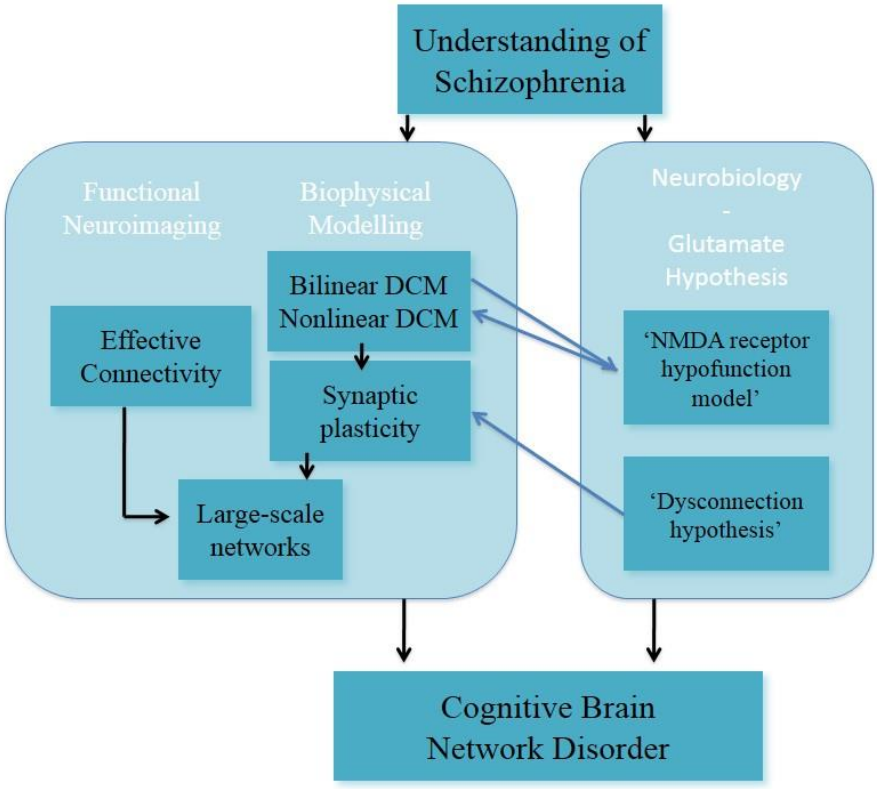

Figure 2.1 Understanding of schizophrenia as a cognitive brain network disorder – verbal/numeric "N-back" task (Reproduced from Dauvermann et al., 2014).

We emphasise that the findings support not only the glutamate hypothesis but also

the dopamine hypothesis. DA is a neuromodulator that may crucially affect Glu-induced synaptic plasticity. Synaptic plasticity may be involved in the regulation of DA synthesis and release via other neurotransmitter systems. Specifically for nonlinear effects, it has been shown that DA acts as a neuromodulator mediating postsynaptic gain (Braver and Cohen, 1999; Friston et al., 2012).

In a recent study, it has been reported that the combination of the DCM analysis of numerical "N-back" task in EST (Deserno et al., 2012) and generative embedding resulted in the dissection of three subgroups of EST based on the mechanistically-inferred DCM findings (Brodersen et al., 2013). This exemplary study showed that DCM can be applied as a generative model of large-scale networks in individuals with schizophrenia. In summary, DCM is a promising approach for modelling synaptic plasticity; nevertheless in its current form it cannot reflect the full complexity in the processing required for the implementation of tasks such as working memory.

2.3 Discussion

Preclinical neurobiological and computational findings reveal the relevance of synaptic plasticity and gating mechanism for learning and cognitive function. Furthermore, evidence of dopaminergic, glutamatergic and interactions between DA and Glu among other neurotransmitter systems for the modulation of synaptic plasticity, gating mechanism and therefore cognitive function such as working memory has been reported.

In schizophrenia research, it has been shown that alterations of dopaminergic and glutamatergic transmission could result in altered synaptic plasticity and gating

mechanism and consequently in cognitive deficits such as working memory deficits in individuals with schizophrenia. In other words, cognitive symptoms in individuals with schizophrenia could be explained by the alterations of dopaminergic and glutamatergic transmission and therefore by the dopamine hypothesis and glutamate hypothesis of schizophrenia.

FC findings of working memory in individuals with schizophrenia have advanced our knowledge of cognitive function in humans at the level of functional large-scale networks (chapter 1.4.3). However, it is not wholly understood what altered FC during cognition neurobiologically means in schizophrenia. EC findings from verbal/numeric working memory in people with schizophrenia, here specifically modelling functional large-scale networks with DCM, have shown indications of linkage between clinical network-based working memory (large-scale networks) and preclinical neurotransmitter modulation of cognitive function. A strength of DCM lies in interpretation of altered synaptic plasticity based on the inference of mechanistic information. We emphasise that the interpretation of altered neurotransmitter circuits should be considered carefully because DCM is likely to underestimate the processing complexity in neurobiological circuits.

We outline one main limitation of the reviewed DCM studies, which lies in the implementation of the bilinear approach of DCM for the assessment of activity-dependent synaptic plasticity underlying working memory function. One possible solution to this problem could be the application of nonlinear DCM (Stephan et al., 2008; Stephan and Friston, 2010).

Nonlinear DCM for fMRI is an advanced approach for increasing the biological plausibility of DCMs by the means of modelling ‘gain modulation’ (i.e. nonlinear

modulation of neuronal connections) (Friston and Dolan, 2010; Daunizeau et al., 2011a, Daunizeau et al., 2011b). In nonlinear DCM, the modulation of connection strengths by experimental inputs is supplemented by direct modulation of neural activity in one or more network regions (Friston et al., 2003; Stephan et al., 2008). The computations for gating in neural networks use the multiplicative computation of nonlinear modulation (Salinas and Sejnowski, 2001; Volman et al., 2010). Accordingly, nonlinear DCM can be used for inferring that the strength of a connection is modulated by activity of other neuronal populations (Stephan et al., 2007, Stephan et al., 2008).

Based on the preclinical neurobiological and computational evidence for altered synaptic plasticity and gating mechanism implicating cognitive symptoms in schizophrenia, we apply nonlinear DCM to two fMRI data sets in individuals with schizophrenia. In this, we focus on modelling the connection strengths of the thalamo-cortical connection during verbal fluency (chapter 3) and the meso-cortical connection during working memory (chapter 4).

3 Nonlinear Dynamic Causal Modelling for fMRI in subjects at high genetic risk of schizophrenia

3.1 Introduction

FA and FC measures during the fMRI HSCT were investigated in subjects at high genetic risk of schizophrenia as part of the EHRS study. Previous findings of FA (Whalley et al., 2004) and FC (Whalley et al., 2005) elucidated the state and trait effects in subjects at high familial risk of schizophrenia in contrast to healthy controls. These fMRI findings demonstrated significantly reduced activation of the MD thalamus in the HR subjects when compared to healthy controls (Whalley et al., 2004). This finding of reduced activation in HR subjects was further supported by reduced FC measures between the IFG and the MD thalamus only in the HR group (Whalley et al., 2005). These findings suggested that subjects at high familial risk of schizophrenia would be more vulnerable (due to the genetic loading) to develop schizophrenia than healthy controls. In addition, a following study considered the relationship between reduced FC in HR subjects and increased PFC folding (Harris et al., 2007), which was interpreted as a possible trait marker of the vulnerability of the illness (Dauvermann et al., 2012). These FC analyses in the EHRS cohort applied correlation based methods to analyse the fMRI data, which do not allow interpretations of causality or feedback mechanisms.

EC findings from cognitive tasks such as working memory in people with schizophrenia using DCM for fMRI (Friston et al., 2003) enable the modelling of functional large-scale networks. It has been proposed that these studies may lead to biophysical interpretations of altered FC findings (Dauvermann et al., 2014).

The DCM approach employed in the current research project was designed to investigate possible biophysical factors underlying the reduced FC between the IFG and the MD thalamus with linear and nonlinear DCM in subjects at high familial risk of schizophrenia. It was considered that altered connection strength between the IFG and the MD thalamus could lead to a better understanding of altered connectivity in schizophrenia (Krystal et al., 2003; Negyessy and Goldman-Rakic, 2005). Altered connection strength with nonlinear modulation of the thalamo-cortical connection during verbal fluency in HR subjects in contrast to healthy controls as assessed with nonlinear DCM may lead to a better understanding of schizophrenia.

At the beginning of this chapter, we summarise findings from fMRI studies during covert verbal fluency in individuals with schizophrenia and healthy controls, which are subdivided into FA, FC and EC findings (chapter 3.3.1). The reported FA and FC findings of the HSCT as part of the EHRS are described in detail to provide background to the DCM analyses, which extend the FA and FC findings (3.3.2). In the next step, the complete processing steps and results of the fMRI HSCT data including pre-processing, statistical analyses and DCM analyses are described (chapters 3.4.4 and 3.4.5). In particular, the heuristic search protocol for the application of bilinear and nonlinear DCM for the HSCT is presented (chapter 3.4.5.2). Finally, the results are discussed in context of possibly altered synaptic plasticity and gating mechanism in schizophrenia (chapter 3.6).

3.2 Overall aim

The main aim of the current study of the EHRS data was to investigate possible biophysical mechanisms underlying fMRI data in covert verbal fluency with DCM, which could explain reduced IFG and thalamic BOLD response (Whalley et al., 2004) and reduced FC between the IFG and the MD thalamus in the HR subjects in contrast to healthy controls (Whalley et al., 2005). Altered EC measures between the MD thalamus and the IFG may reflect disrupted synaptic plasticity and gating mechanisms of the thalamo-cortical connection (chapter 2.2.2.1).

DCM is a translational brain modelling framework with physiologically interpretable dynamic system models, which are fitted to the fMRI data to provide estimates of pathophysiological mechanisms of a neuronal group. Gating at the neuronal level that provides a more precise estimation of how the rate of change of activity in one region influences the rate of change in other regions (Friston, 2009; Friston et al., 2003; Stephan et al., 2008). The main advantage of nonlinear DCM over bilinear DCM is anchored in the differentiation between nonlinearities in the BOLD signal at the level of neuronal or haemodynamic mechanisms (Friston et al., 2003; Stephan et al., 2007; Stephan et al., 2008) by combining neuronal state equations with a haemodynamic feedforward network. Specifically, in nonlinear DCM (Stephan et al., 2008) inhibitions of a neuronal group or neuronal connection can be modelled. In addition, nonlinear DCM assesses selective changes in each region, which can be used to model effects exerted by neurotransmitters like Glu. In other words, the modelling of activity-dependent gating of connections may allow indirect estimations of excitatory glutamatergic subpopulations.

A heuristic search protocol was developed for the application of nonlinear DCM for fMRI data and applied to the EHRS data. This protocol was designed to examine hypothesised altered connection strengths of the thalamo-cortical and cortico-thalamic connections using nonlinear modulation and build upon previously reported HSCT findings (Whalley et al., 2004; Whalley et al., 2005).

3.3 Background

3.3.1 Theoretical background of functional magnetic resonance imaging studies and positron emission tomography studies of covert verbal fluency in healthy subjects and subjects with schizophrenia

The HSCT (Burgess and Shallice, 1996; Burgess and Shallice, 1997) is an established neuropsychological task in clinical and cognitive neurosciences to assess components of executive functions of the frontal lobes in healthy participants and patients with neurological syndromes (such as frontal lobe lesions) or individuals with schizophrenia (Chan et al. 2008). The HSCT consists of two parts - verbal response initiation (Part A) and verbal response suppression (Part B) – which capture different components of executive functions (Burgess and Shallice, 1996). Thus, Part A and Part B are considered to assess different psychological constructs (Siqueira et al. 2010). Part A is a verbal fluency-like test in which poor verbal fluency is understood as a sign of 'frontal initiation problems' (Burgess and Shallice, 1996). In contrast, Part B is designed to measure response suppression (or inhibition) and strategy development which are aspects of executive function and impaired in

patients with brain injuries (Burgess and Shallice, 1996). The combined application of Part A and Part B allow the comparison of two executive function components of initiation and suppression/inhibition in the same participants as a clinical tool. In clinical and cognitive neurosciences, studies have applied the HSCT in different variations such as (i) The original version as devised by Burgess and Shallice (Burgess and Shallice, 1996) to compare response initiation and response suppression/inhibition; (ii) Only Part A of the HSCT as a verbal fluency-like task; and (iii) Only Part B of the HSCT as a response suppression/inhibition task.

In Part A, participants are given sentences with the last word missing and they are required to complete the sentences meaningfully. Due to the task's constraint of measuring the search for words related to the activation of semantic networks by the presentation of the sentences (with the last word missing) (Chan et al. 2008), Part A is thought to be a verbal fluency-like neuropsychological task.

In Part B, participants are presented sentences with the last word missing which are comparable to the sentences in Part A. In this section of the HSCT, participants are requested to complete the sentences with words that do not make sense semantically. Part B measures the complex executive functions of response suppression/inhibition and strategy development because of the task's requirement to inhibit the spontaneous semantically meaningful completion of the task and the alternative work search (Chan et al. 2008).

Findings from fMRI and PET studies during the HSCT (Part A and/or Part B) and comparable covert verbal fluency tasks are summarised for FA/rCBF, FC and EC in healthy subjects and individuals with schizophrenia. We focus on studies, which

have used the HSCT and similar covert verbal fluency tasks in order to ensure the comparability of findings. For the FA findings, mostly PET studies are summarised, of which the majority examined rCBF in healthy controls only; one PET study investigated both EST and healthy controls. One fMRI study investigated BOLD response between HR subjects and healthy controls. FC findings from three fMRI studies, one in HR subjects, one in FES and one in EST are discussed. Finally, two DCM studies assessed EC measures during an overt version of the HSCT, one in healthy controls and one in ARMS subjects.

3.3.1.1 Findings of functional activation studies

The first PET studies on the HSCT have repeatedly reported robust left-hemispheric rCBF of the regions involved in the functional performance of response initiation and response suppression: the IFG, the MTG (Frith et al., 1991; Nathaniel-James and Frith, 2002), and the intraparietal gyrus/ IPS in healthy controls (Nathaniel-James et al., 1997; Collette et al., 2001). RCBF of the ACC was observed in addition to the previously mentioned regions by Nathaniel-James et al. (Nathaniel-James et al., 1997).

The seminal clinical PET study by Frith et al., 2005 showed no significant differences of rCBF between EST and healthy controls during the HSCT for the regions of the left DLPFC, ACC and the left STG (Frith et al., 1995). One fMRI study observed reduced BOLD response in the left IFG and left MD thalamus in HR subjects in contrast to healthy controls during the parametric contrast. Regions such as the ACC, left MTG and left IPS are activated during the task in both HR subjects and healthy controls (Whalley et al., 2004).

3.3.1.2 Findings of functional connectivity studies

Three clinical fMRI studies assessed FC during covert verbal fluency using different FC methods at the HR stage, first-episode stage and established stage of the illness. In the first study in HR subjects, the authors applied a seed-based cross-correlation analysis to the HSCT task which was run in two ways to investigate potential effects of task activation from the HSCT data: (i) With variance related to task effects removed from the data (denoted as 'removed variance'); and (ii) Without variance related to task effects modelled from the data (denoted as 'modelled variance') (Whalley et al., 2005). The first version of the connectivity analyses allowed the identification of regions without effects of task-related activation, whereas the second version comprises the task effects. Three sets of altered FC findings were observed: Firstly, reduced FC between right medial prefrontal regions and left cerebellar regions (with 'modelled variance' and 'removed variance') in HR subjects in contrast to healthy controls; secondly, increased FC between left parietal and left prefrontal regions (with 'modelled variance' and 'removed variance') in HR subjects in contrast to healthy controls; thirdly, reduced FC between the left IFG and the left MD thalamus (with 'modelled variance') in HR subjects only (Whalley et al., 2005).

Boksman et al., 2005 investigated the functional network of the PFC during a similar covert verbal fluency task to the HSCT in never-treated FES (Boksman et al., 2005). PPIs between the activity of voxels in the right AC and any regions with significant covariance with the activity of the right AC were run. Within-group PPI analyses revealed significant FC between the right AC and the left temporal lobe including the left ITG in healthy controls. In contrast, in individuals with FES a widespread functional network during the covert verbal fluency task was found including the

bilateral CG, bilateral SFG, left IFG and left STG. No significant between-group results between healthy controls and FES were reported.

The third study examined the hypothesis of disrupted fronto-temporal connectivity in schizophrenia during the HSCT in EST (Lawrie et al., 2002). A significantly lower correlation between the activity of left DLPFC and the activity of the left middle temporal cortex/superior temporal cortex was reported in EST in contrast to healthy controls. Furthermore, a significant association between the reduced FC measure and severity of auditory hallucinations were seen in EST (Lawrie et al., 2002).

3.3.1.3 Findings of effective connectivity studies

The first DCM study, which assessed EC measures during the HCST, employed bilinear DCM in healthy controls (Allen et al., 2008) and formed the basis for the following DCM study in ARMS subjects using the same experimental paradigm and DCM5[3] version (Allen et al., 2010; please see Table 3.1 for details). However, the Bayesian Model Selection (BMS) inference method is different between both studies. In the control DCM study, five models comprised of the left MTG and left MFG were compared among each other. The main finding was that the winning model was characterised by increased EC with task-dependent modulation (of response suppression in contrast to response initiation) for the connection from the left MTG to the left MFG (Allen et al., 2008).

Allen et al., (2010) investigated increased fronto-temporal EC (intrinsic connectivity) as a potential measure of vulnerability of developing schizophrenia in ARMS subjects. The specification of the models of this study was based on (i) the FA

[3] DCM5 version is implemented in SPM5 version. DCM5 and DCM8 methodology differ in terms of different model inversion techniques. In DCM8, model inversion is considered as a development from the previous DCM5 version.

findings between ARMS subjects and healthy controls and (ii) the control DCM findings (Allen et al 2008). Therefore, the region of the ACC was included in addition to the left-hemispheric MTG and MFG. In total, 14 different models were compared against each other. Two main findings were reported: Firstly, no significant effect of task-dependent modulation for the fronto-temporal connection between ARMS subjects and healthy controls was observed. Secondly, ARMS subjects displayed increased intrinsic connectivity between the ACC and the MTG in comparison to healthy controls. Furthermore, the BMS approach revealed that the same network was equally likely to explain the given HSCT fMRI data in both the ARMS subjects and the healthy controls.

Table 3.1 Summary of main findings of effective connectivity measures in verbal fluency (Partly reproduced from Dauvermann et al., 2014).

Study	Subjects – Phase of Schizophrenia HC – HR, FES, EST	Medication	Experimental Paradigm	Networks – Model Space Number of models Regions	DCM Settings – DCM version Sphere size Inference technique(s)	Main Finding(s)
Allen et al., 2008	13 HC	None	HSCT	5 left-hemispheric models; MFG, MTG	DCM in SPM5; 12 mm spheres; BMS as implemented in SPM5; Model evidence approximation of BIC and AIC	Winning model characterised by ⬆ EC with task-dependent modulation for connection MTG to MFG.
Allen et al., 2010	15 HC 15 HR[1]	2 HR risperidone and quetiapine[2]	HCST	14 left- hemispheric models; MFG, ACC, MTG	DCM in SPM5; 12 mm spheres; Random effects BMS[3]	⬆ IC between ACC and MTG. Same winning model in both groups.

⬆ Increased in subjects with schizophrenia in contrast to HC;
ACC, anterior cingulate cortex; AIC, Akaike Information Criteron; ARMS, Subjects with at risk mental state; BIC, Bayesian Information Criterion; BMS, Bayesian Model Selection; EC, effective connectivity; HC, healthy controls; HR, subjects at high risk of schizophrenia; HSCT, Hayling Sentence Completion Task; IC, intrinsic connectivity; MFG, middle frontal gyrus; MTG, middle temporal gyrus.
[1] Subjects at high clinical risk of schizophrenia/ARMS subjects
[2] At the time of scanning
[3] BMS at the group-level.

3.3.2 Background of the Edinburgh High Risk Study

The EHRS examined young adults at enhanced genetic risk of schizophrenia due to familial reasons over the period at which they are at greatest risk of becoming ill. Recruitment was conducted over the first five years of the study (1994-1999), details of which have been described previously (Hodges et al., 1999; Johnstone et al., 2000). Briefly, individuals with schizophrenia with a family history of schizophrenia and with unaffected relatives aged between 16-25 years were identified from psychiatric hospital case records in Scotland. Case-note diagnoses of schizophrenia were verified with the Operational Criteria Checklist (McGuffin et al., 1991). The unaffected relatives aged between 16 and 25 were then approached and invited to participate. These unaffected relatives provided the HR group for the EHRS study. The control subjects recruited for the study had no family history of schizophrenia. All subjects were well at recruitment and were antipsychotic naïve throughout the study. All subjects were supplied with detailed written information regarding the study and provided written informed consent. The study was approved by the Psychiatry and Clinical Psychology subcommittee of the Lothian research ethics committee.

Functional imaging was added to the protocol during the second phase of the study (1999-2004). Full details of the sample and the respective FA results for the HSCT (Whalley et al., 2004) and the results for the FC measures (Whalley et al., 2005) have been presented previously.

At the time of the scan, all HR subjects underwent the clinical interview, the Present State Examination (PSE; Wing et al., 1974). The results have been published previously (Whalley et al., 2004; Whalley et al., 2005). None of the subjects received the full diagnosis of psychosis. Twenty-seven HR subjects showed isolated transient or partial psychotic symptoms (HR+ subjects). Forty-two HR subjects did not report any psychotic symptoms (HR- subjects). None of the subjects were undergoing antipsychotic treatment, seeking professional support or saw themselves as unwell. Twenty-one healthy controls participated in the EHRS. Details on positive PANSS symptom measures (score > 2) for HR subjects, who participated in the HSCT fMRI task, have been reported previously (Whalley et al., 2007). Additionally, a detailed presentation of PSE scores at the time of the HSCT fMRI scan in the four subjects, who subsequently developed schizophrenia, and the mental state of these four individuals at the time of the diagnosis have been published (Whalley et al., 2006).

In demographics tests on the EHRS data, there were no statistically significant differences in age, gender, handedness or mean IQ between the healthy controls and the HR subjects. There were also no significant differences between HR+ subjects and HR- subjects (Table 3.2; Whalley et al., 2004; Whalley et al., 2005). Behavioural performance results showed that all participants performed the tasks appropriately in the scanner. There were no significant differences in word appropriateness scoring and reaction time between the groups (Whalley et al., 2004; Whalley et al., 2005).

Table 3.2 Demographic details of the previously published functional activation and functional connectivity findings from the EHRS (Reproduced from Whalley et al., 2004).

	Controls (n = 21)	High risk without symptoms (n = 42)	High risk with symptoms (n = 27)
Age (years) mean (SD)	26.8 (2.7)	26.8 (3.4)	25.1 (3.1)
Gender (male:female)	13:8	17:25	13:14
Mean NART IQ (SD)	97.95 (24.02)	99.56 (18.12)	97.86 (10.60)
Handedness (R:L:A)	19:2:0	39:2:1	21:4:2
Genetic liability (1^{st} degree; 2^{nd} degree)*	N/A	32:10	16:11

*First or second degree relatives with schizophrenia. N/A = not applicable; R = right; L = left; A = ambidextrous. NART, National Adult Reading Test.

3.3.2.1 Main fMRI findings from the second phase of the EHRS

The main fMRI findings on the HSCT in subjects at high familial risk of schizophrenia have been previously published (Whalley et al., 2004; Whalley et al., 2005) and are summarised in the following two subchapters for FA and FC results.

3.3.2.2 Functional activation findings

For the standard subtraction analysis (sentence completion versus rest) all groups displayed activation in regions commonly associated with self-generated word production tasks, i.e. dorsolateral and medial prefrontal regions (DLPFC and mPFC), MTG and the STG (Frith et al., 1995; Nathaniel-James et al., 1997; Lawrie et al., 2002). HR+ subjects showed increased activation of the left IPL in contrast to the HR- subjects and healthy controls. Furthermore, for the parametric contrast (i.e. increasing activations with increasing task difficulty across the four difficulty levels of the HSCT), greater activations of inferior frontal regions in HR subjects were in keeping with studies, which reported activation differences in lateral and medial

prefrontal regions in EST in contrast to healthy controls (Lawrie et al., 2002; Nathaniel-James and Frith, 2002). HR subjects showed reduced activation of the mPFC as well as the MD thalamus and cerebellar regions in comparison to healthy controls.

3.3.2.3 Functional connectivity findings

FC was assessed using a seed-based cross-correlation analysis approach as implemented in Statistical Parametric Mapping (SPM; The Wellcome Department of Cognitive Neurology and collaborators, Institute of Neurology, London, http//www.fil.ion.ucl.ac.uk/spm/). The results demonstrated that there were indications of negative correlations between medial prefrontal, thalamic and cerebellar regions in the HR+ and HR- subjects for seeds located both in the medial frontal gyrus and MD thalamus. Additionally, evidence of increased prefrontal-parietal FC in both the HR+ and the HR- subjects in comparison to healthy controls was reported. As mentioned in the introduction, these FC results were further examined and revealed a significant association between the reduced prefrontal-thalamic FC and increased prefrontal folding in HR subjects in comparison to the healthy controls (Dauvermann et al., 2012).

3.4 Methods

The analyses presented in this chapter pertain to the reported FC findings of the scans of 69 HR subjects and 19 healthy controls (Whalley et al., 2005). The pre-processing, first and second level analyses of these subjects were reprocessed in SPM8 (update revision number 3684). The EC analyses were processed in DCM8.

For the current DCM study, the EPI processing of the HSCT data was redone to ensure compliance with the DCM analysis methodology. The DCM required settings for spatial smoothing and oversampling of voxel size have been applied (Dauvermann et al., 2013). In keeping with the previous analyses we applied established SPM first level and second level between group analyses employing the settings used in our previous analyses (Whalley et al., 2004). There were no differences noted between the previously reported results by Whalley et al., 2004 and the new second level results.

3.4.1 Study populations

The recruitment of the subjects for the EHRS has been reported previously (Whalley et al., 2004; Whalley et al., 2005; Johnstone et al., 2003).

The subject inclusion for the current DCM study was initially based on the main FC study by Whalley et al., (2005). DCM has stringent requirements for subject inclusion (please see below). Two healthy controls and 23 HR subjects did not meet the requirements of sufficient BOLD response in all regions that were included in the models and were excluded. Full details on the final inclusion of subjects as well as demographic and clinical details of the groups were summarised in Table 3.3. Based on the PSE and the initial subject inclusion by Whalley et al., 2005, 20 subjects were allocated to the HR+ group and 26 subjects to the HR- group. The PSE measures were converted to PANSS measures using the rescaled PANSS system (Kay et al., 1987; Johnstone et al., 2003).

Table 3.3 Demographic and clinical details (Reproduced from Dauvermann et al., 2013).

	Healthy Controls	HR-	HR+	Four ill	Test	*p*-Value
Number	19	26	20	4	-	-
Mean Age (SD)	26.9 (3.5)	25.8 (3.2)	26.1 (3.1)	22.8 (4.50)	$F = .518^{a}$	.598
Gender (M:F)	12:7	12:14	9:11	3:1	$x^2 = 2.56^{b}$	.345
Mean NART IQ (SD)	99.94 (9.50)	96.74 (8.90)	98.58 (10.00)	97.95 (16.33)	$F = 1.175$	.211
Handedness (R:L)	16:3	23:3	18:2	4:0	$x^2 = 4.36^{c}$	.099
PSE Score[d] (0/1:2:3)	19:0:0	26:0:0	0:16:4	0:0:4	-	-

HR-, high risk subjects without psychotic symptoms; HR+, high risk subjects with psychotic symptoms, Four ill, four HR subjects who became subsequently ill; NART, National Adult Reading Test; IQ, intelligence quotient; ANOVA, analysis of variance; PSE, Present State Examination; SD, Standard Deviation.

[a] ANOVA

[b] Pearson's chi-square

[c] Kruskal-Wallis Test

[d] Simplified PSE scoring system, see text. No subject received a score of 4 at the baseline interview.

3.4.2 Functional experimental details

A summary of the results from the previous analyses applied to the HSCT data are detailed in chapter 3.3.2.1. Full details of these analyses and the experimental details have been previously reported (Whalley et al., 2004; Whalley et al., 2005).

The response initiation condition (Part A) of the HSCT (Burgess and Shallice, 1996) was used as the experimental verbal fluency task in the scanner. Subjects were shown sentences with the last word missing and were asked to silently think of an appropriate word to complete the sentence reasonably, and press a button when they had done so. Sentences were used from the sentence completion norms by Bloom and Fischler (Bloom and Fischler, 1980). Based on the sentence completion context, four difficulty levels were defined to adapt the initiation section of the HSCT for application of an fMRI task. Examples of each difficulty level have been presented previously (Whalley et al., 2004). The functional experimental design was a block

design alternating rest conditions with task conditions, where the task conditions reflected the four levels of difficulty. Those task conditions enabled the statistical analysis of differences in activation over parametric manipulations of task difficulty in sentence completion blocks. The participants received standardized instructions of the HSCT before they entered the scanner.

Participants were presented with the same sequence of sentences as given in the scanner and were asked to remember the word they first thought of in the scanner immediately after the scanning session. Behavioural performance was assessed by means scores for word appropriateness score and RT for each difficulty level. Word appropriate scores were defined by the word frequency list of sentence completion norms (Bloom and Fischler, 1980). The detailed scoring system has been published previously (Whalley et al., 2004).

3.4.3 Functional scanning procedure

Details of the functional scanning procedure for the HSCT have been reported previously (Whalley et al., 2004; Whalley et al., 2005). The acquisition of the HSCT functional imaging data was carried out at the Brain Imaging Research Centre for Scotland (Edinburgh, Scotland, UK) on a GE 1.5 T Signa scanner (GE Medical, Milwaukee, USA). An EPI sequence was used to acquire the functional scans. The following parameters were used: axial orientation TR/TE=4000/40 ms; matrix 64×128; FOV 22×44 cm 2 ; 38 slices; 5 mm slice thickness; no gap. A total of 204 volumes were acquired. Visual stimuli were presented using a screen (IFIS, MRI Devices, Waukesha, WI, USA) placed in the bore of the magnet; corrective lenses were used where necessary.

3.4.4 Scan pre-processing and statistical analysis

The DCM scan pre-processing including first and second level analysis stages for (voxel-wise) functional response comparisons were performed using SPM8 running in Matlab (version 7.1; The MathWorks, Natick, MA, USA). The DCM analysis was performed under DCM8. It should be noted at the time of the DCM analysis for this study DCM10 was available. However, the DCM10 release from the SPM group was undergoing updates and not considered as a stable release.

DCM has technical requirements for the haemodynamic response model, which lies at the conceptual basis of DCM (Friston et al., 2003; Stephan et al., 2007; Stephan et al., 2008). The haemodynamic model minimally adjusts differences between the predicted and measured BOLD series (Friston et al., 2003; Stephan et al., 2007; Stephan et al., 2008). In DCM8, slice timing has been incorporated into the model specification step to enable the use of DCM with longer TRs than 1000 ms (Kiebel et al., 2007). Parameters for spatial smoothing and oversampling the voxel size of the acquisition parameters from the functional scanning procedure have been applied. All other settings were kept as applied in the previous analyses (Whalley et al., 2004).

3.4.4.1 Spatial pre-processing

Following the previous analyses (Whalley et al., 2004), the first four volumes were discarded to ensure that no noise at the beginning of the magnetisation could distort the quality of the scans.

3.4.4.1.1 Realignment

The realignment processing step registers the EPI time series for each single subject to the first volume in the acquisition series to remove movement artefacts and create the mean image. The process is the estimation of 6 parameters of the rigid-body affine transformations in 3D resulting in the minimisation of the sum of squared differences between each volume and the reference image. In the following co-registration, these created transformations are applied to the images which corrects for the degree of movement during the scan acquisition corresponding to the translation and rotation in the x-axis, y-axis and z-axis.

3.4.4.1.2 Normalisation

The normalisation algorithms are based on the least squares approach and the linear combination of the template image to the ends of (i) the acquisition of averages from within/inter subject comparisons in stereotactic normalisation and (ii) accurate matching of FA and structural anatomy. A mean image taken from the realignment processing step was used as the subject image for the normalisation of each subject's scan set into the standardised MNI space. The MNI standard space was defined by the SPM8 EPI template. The normalization used linear affine regularisation with nonlinear deformations and oversampled with sinc interpolation to voxels sized 1 x 1 x 1 mm^3.

3.4.4.1.3 Spatial Smoothing

This processing step minimises noise and artefacts from the distribution of residuals within the subject. The normalised images were spatially convolved with an 8 x 8 x 8

mm^3 full width half maximum (FWHM) Gaussian filter. This step is relevant for the first level statistical analysis, from which the parametric contrast based on the progressive difficulty level was extracted.

3.4.4.1.4 Visual Inspection

The images were visually inspected at two time points during the pre-processing to ensure good image quality and correctly run pre-processing. The first time point was at the alignment step by inspection of the movement parameters smaller than 3 mm. The second inspection was based on noise in the scans after the smoothing step. Following previous subject exclusion (Whalley et al., 2004), five subjects due to image noise in the scans were excluded on the basis of these qualitative tests.

3.4.4.2 Statistical analysis

We applied the established first and second level analyses employing settings used in the previous analyses (Whalley et al., 2004; Whalley et al., 2005). From the second level analysis we generated statistical parametric maps of the *T* statistics at each voxel SPM (1), which characterised differences in increased activation of regions with increasing task difficulty (i.e. the four difficulty levels of the HSCT).

3.4.4.2.1 First level analysis

The statistical first level analysis was performed using the general linear model (GLM) approach which is implemented in SPM8 based on this general equation Eq. [3.1]:

$$Y = \beta X + \varepsilon \quad [3.1]$$

Y = observed response, i.e. EPI time series data
β = regression weights or parameters to be estimated for each of the explanatory variables in the design matrix
X = linear combination of explanatory variables (i.e. covariates or regressors)
ε = residual error

Each SPM column in the design matrix resembles the effects specified in the model. In this study, at the single subject level the data was modelled with five conditions (the four difficulty levels and the rest condition). Each of these conditions was modelled by a boxcar convolution with the haemodynamic response function (HRF) as implemented in SPM8. The HRF convolution enables the smooth and delayed transition between the conditions. The individual's set of movement estimates created in the realignment pre-processing step was also entered in the GLM to fit the subject's movement as possible 'covariates of no interest'.

The settings applied for the estimation of the design matrix followed the previously published settings (Whalley et al., 2004; Whalley et al., 2005):

- Single subject filtering in the time domain:
- Low pass filter (Gaussian kernel, 4 s (FWHM))
- High pass filter (400 s cut-off)
- Mask image

A standard brain mask image applied to the first level analysis.

The main aim for the statistical analysis was the examination of areas showing increased activation with increased sentence completion difficulty level because this parametric contrast lies at the basis of the DCM analyses. The settings for the parametric contrast were [-3 -1 1 3 0].

Furthermore, the standard subtraction contrast analysis for all four sentence completion conditions versus rest condition was set [1 1 1 1 -4].

3.4.4.2.2 Second level analysis

Contrast images of parameter estimates encoding condition-specific effects were entered into second level random effects analyses. ANOVA was used to determine group differences. For the second level random effects analyses we repeated the between group analyses for the current DCM study. As described previously, one of the main interests of the initial hypotheses of the EHRS was to investigate 'trait' effects and 'state' effects between healthy controls and the HR subjects as a group and within the HRall subjects subdivided into HR+ subjects and HR- subjects (Whalley et al., 2004; Whalley et al., 2005). 'Trait' effects were defined as differences between the healthy controls and all HR subjects. In contrast, 'state' effects resembled differences within the HR group comparing HR- subjects and HR+ subjects. The groups were matched on demographic measures. Thus, these measures were not included as possible confounders in the estimation of the model.

For all second level analyses, the statistical maps were thresholded at the level of p = .001 uncorrected. We report regions that survive cluster-level correction for multiple comparisons across the whole brain at $p < .05$. All reported P - values in this thesis are at the corrected cluster level and the co-ordinates were converted from MNI to Talairach co-ordinates. The identification of regions was run using a combination of the Talairach Daemon (Lancaster et al., 1997; Lancaster et al., 2000) in combination with the Talairach brain atlas (Talairach and Tournoux; 1988). The results reported by Whalley et al., (2004) were also found in this analysis.

3.4.5 Functional integration – Bilinear and nonlinear Dynamic Causal Modelling for fMRI data

The examination of underlying causality for the reduced FC between the IFG and the MD thalamus in HRall subjects in contrast to the healthy controls was the primary objective of this DCM study. To this end, the thalamo-cortical and cortico-thalamic connection strengths with nonlinear modulation were assessed using bilinear and nonlinear DCM for fMRI.

The primary objective was to consider in what ways the HSCT task would indicate how subjects at high familial risk of schizophrenia would exhibit vulnerability to the development of the disorder that was not evident in healthy controls. Support for this hypothesis has been given by the previously reported findings of reduced FC measures between the IFG and the MD thalamus in the HR group in contrast to the healthy controls (Whalley et al., 2005). This 'trait' effect of high genetic risk of developing the disorder has been further supported by measures of increased PFC folding (Harris et al., 2007) and by the significant correlation between the reduced FC measures and increased prefrontal cortical folding in the same cohort (Dauvermann et al., 2012). These findings motivated the current the DCM study to the end of investigating the causal factors, which may underlie these findings by applying nonlinear DCM to the HSCT fMRI data of the EHRS.

Methodological issues for the application for the DCM approach were considered regarding the employment of the DCM8 version run for the current DCM study. The DCM analyses for bilinear and nonlinear DCM were run in DCM8 as implemented in SPM8. The main reasons for the employment of DCM8 for the current study and the DCM study on working memory fMRI data (chapter 4) were based on both

theoretical and pragmatic grounds: Firstly, the definition of prior densities and parameterisation of the models for fMRI used in DCM8 in the version 3684 and therefore the mechanistic interpretation of the underlying distributed neuronal mechanisms is widely accepted in the research community. Secondly, the initial DCM analyses for the current DCM study were performed using DCM8. Thus, all analyses were completed using the DCM8 approach in SPM8 version, including the DCM analyses for the fMRI working memory data in subjects with established schizophrenia and healthy controls (chapter 4).

In the following chapter 3.4.5, we describe the methods applied for the EHRS DCM study. In subchapter 3.4.5.1, the subject and ROI selection as the standard procedure for the preparation for the DCM is described. Chapter 3.4.5.2 gives the devised heuristic search protocol for the application of nonlinear DCM for fMRI data is introduced and explained. Then in chapter 3.4.5.3, we describe the post-hoc analysis performed for the connection strengths with nonlinear modulation and psychotic symptoms.

3.4.5.1 Subject and ROI selection

In this DCM study of the EHRS cohort, a different subgroup of HR subjects were examined than those noted in the previously published EHRS papers on FC measures (Whalley et al., 2005; Dauvermann et al., 2012). This was necessary because DCM has stringent requirements for the subject and region selection. In addition to the selection of the fMRI scans (Whalley et al., 2004), the condition of activation in each ROI comprised in the models examined must be met (Dauvermann et al., 2013).

In detail, the second level analysis in the initial sample of 21 healthy controls and 69 HR subjects identified robust left-lateralized activations in the IPS, IFG, MTG, ACC and the MD thalamus as previously reported (Whalley et al., 2004). ROIs located in all five regions were selected for the DCM analyses. The selection of the IPS, IFG, MTG and the ACC ROIs is consistent with other functional imaging studies of the HSCT in studies in healthy controls (Allen et al., 2008; Collette et al., 2001; Frith et al., 1991; 1995; Nathaniel-James and Frith, 2002; Nathaniel-James et al., 1997) and in a study of HR subjects (Allen et al., 2010). Our previous reports demonstrated deficits in FC between the MD thalamus and the IFG in HR subjects when they were compared to healthy controls (Whalley et al., 2005; Dauvermann et al., 2012). Thus, we included the MD thalamus in the large-scale network used for our DCM study. Also it has been established that altered synaptic plasticity of the connection from the MD thalamus to the PFC may underlie cortical dysfunction in schizophrenia (Negyessy and Goldman-Rakic, 2005).

The five ROIs were defined by extracting the eigenvectors (i.e. time series) from each subject's individual activation map thresholded at $p < .05$ uncorrected at the closest maxima within a distance of 8 mm of the group peak voxel (for the IPS, IFG and MTG) and within 6 mm of the group peak voxel respectively (for the ACC and MD thalamus). This rationale ensured that the functional regions included in the DCM models were consistent across subjects (Stephan et al., 2007). In cases where the subject did not show activation in all five ROIs that satisfied the criteria, data from these subjects were excluded (2 healthy controls and 23 HR subjects). The final subject selection included 19 healthy controls and 46 high risk subjects. This selection included the four subjects who subsequently developed schizophrenia

(Dauvermann et al., 2013). The ROI locations detailed in Table 3.4 are given in accordance with the standard Talairach and Tournoux atlas (Talairach and Tournoux, 1988) which was used by Whalley et al., (2005). The co-ordinates were in keeping with the previously reported co-ordinates (Whalley et al., 2005).

Table 3.4 Coordinates of the five ROIs (Reproduced from Dauvermann et al., 2013).

	Coordinates in Talairach Space
IPS, BA40	-42 -48, 48
IFG, BA47	-50, 18, -4
MTG BA21	-50, -37, -5
ACC, BA32	0, 22, 34
MD Thal	-8, -13, 6

ACC, anterior cingulate cortex; IFG, inferior frontal gyrus; IPS, intra parietal sulcus; MD Thal, mediodorsal thalamus; MTG, middle temporal gyrus.

3.4.5.2 Heuristic study protocol for bilinear and nonlinear Dynamic Causal Modelling

We adopted an approach that would allow us to model nonlinear biological responses expected for the HCST by the means of nonlinear DCM for fMRI, specifically for the bidirectional connection between the IFG and the MD thalamus.

In order to ensure that the established DCM methods for determining whether linear and nonlinear modelling could be applied to the EHRS data in a structured process, we developed a heuristic search protocol to optimise the DCM architecture. We used this protocol to test DCM methods on the experimental groupings that had been previously employed in the analyses of the EHRS data and to evaluate group differences in the EHRS study. The heuristic protocol splits the DCM processing into three separate phases:

(i) In phase 1, bilinear DCM was used in order to test the structure for the HSCT across all subjects;

(ii) In phase 2, nonlinear DCM was applied to model the nonlinear mechanisms of the thalamo-cortical and cortico-thalamic connections; and

(iii) In phase 3, connection strengths with nonlinear modulation within the winning models were assessed.

A flow diagram for our DCM protocol is given in Figure 3.1.

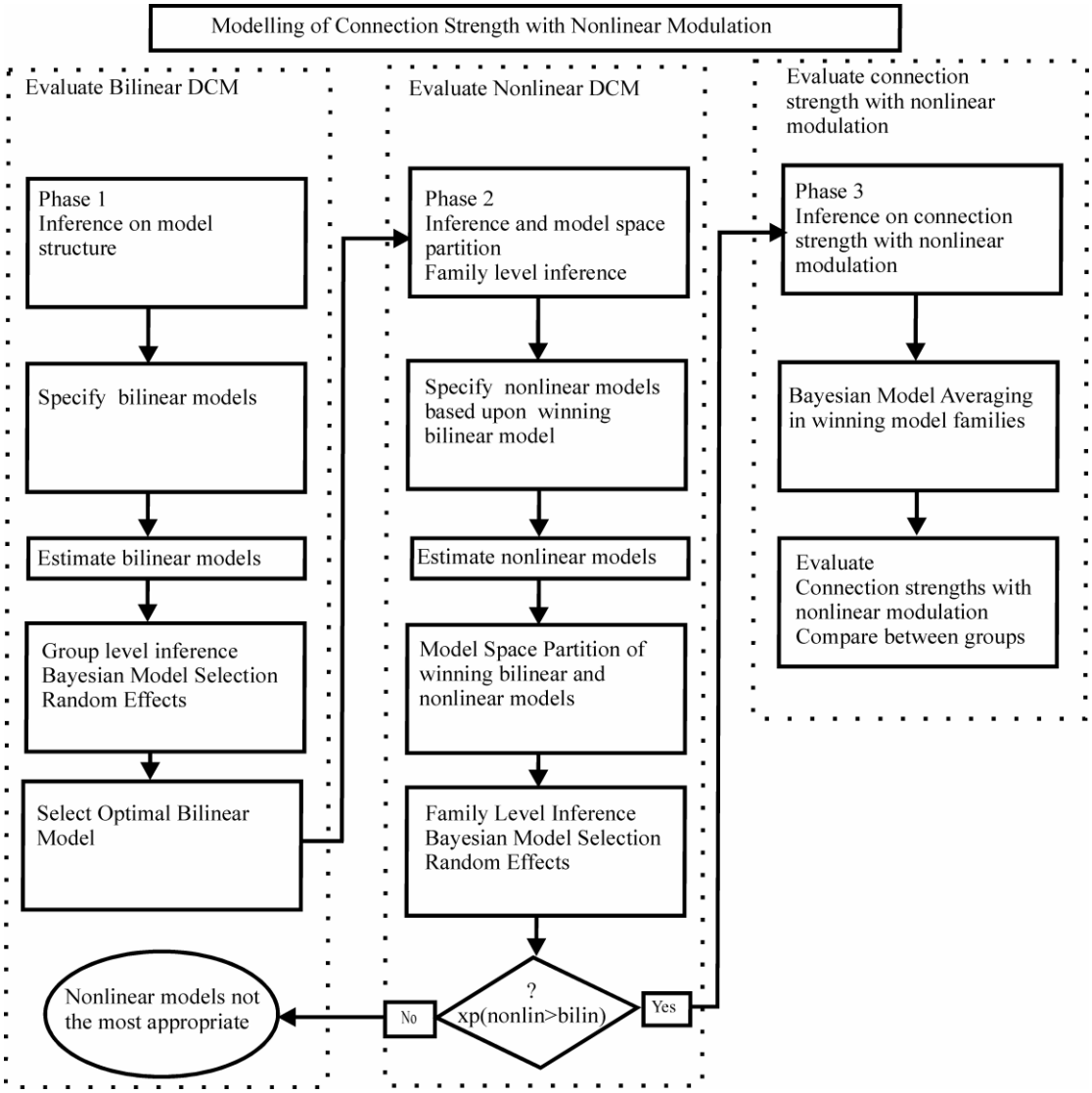

Figure 3.1. Protocol for the application of Nonlinear DCM for fMRI (Reproduced from Dauvermann et al., 2013).

This protocol is subdivided into three phases which allow the modelling of connection strength with nonlinear modulation. The protocol was run for each grouping: (i) Healthy controls and all high risk subjects, (ii) Healthy controls, high risk subjects without psychotic symptoms and high risk subjects with psychotic symptoms, (iii) Healthy controls, high risk subjects without psychotic symptoms, high risk subjects with psychotic symptoms and four ill subjects who subsequently developed schizophrenia.

To ensure that the DCM based analyses were consistent across the contrast groupings we ran the phased protocol on three separate groupings of the EHRS data. In the first

grouping, the DCM analyses were applied to healthy controls (n=19) and HRall subjects (n=46). In the second grouping, the DCM analyses were applied to healthy controls (n=19), HR− (n=26) and HR+ (n=20). In the third grouping, the DCM analyses were applied to healthy controls (n=19), HR− (n=25), HR+ (n=17) and the four ill HR subjects (n=4), i.e. those subjects who subsequent to scanning developed schizophrenia.

1) In phase 1, bilinear DCM was used in order to select the structure for the HSCT large-scale network across all subjects. This analysis contained modulations for the activity-dependent neuronal interactions between the five regions of the network. The analysis steps are depicted in the protocol (column 1; Figure 3.1). The optimal model of this analysis was entered into phase 2.

2) In phase 2, nonlinear DCM was applied to model the connection strengths with activity-dependent modulation of the reciprocal neuronal projection between the MD thalamus and the IFG. In order to ensure the modelling of the gating (i.e. nonlinear models), two preconditions were met:

   (i) The specification of the nonlinear models was based on the optimal bilinear model. Therefore, the bilinear model and the nonlinear models differed only in the single parameter of nonlinearity from each other.

   (ii) The implementation of Model Space Partitioning (MPS) and Family Inference was used to compare the bilinear and nonlinear models, which indicated that the chosen nonlinear model family outperformed the best of the bilinear models. The analysis steps are depicted in the

protocol (column 2, Figure 3.1). The winning models of the BMS analysis entered the third phase.

3) In phase 3, the connection strengths with nonlinear modulation within the winning model family were assessed using the posterior densities over connection strengths as assessed with Bayesian Model Averaging (BMA). This step allowed inference of the connection strengths with nonlinear modulation of the bidirectional projection between the IFG and the MD thalamus. The analysis steps are depicted in the protocol (column 3, Figure 3.1).

The theoretical implementations of bilinear DCM (Friston et al., 2003), nonlinear DCM (Stephan et al., 2008) and Family Level Inference (e.g. MSP, BMS at the model family level and BMA; Penny et al., 2010) have been reported previously. The application of bilinear DCM, MSP, Family Inference and BMA has been shown to produce reliable results (Seghier et al., 2011).

Theoretically, the inference computations (i.e. Inference on nonlinear DCM, Inference Level at the family level with BMS allow for the testing of an infinite number of models (Penny et al., 2010)). However, we considered a limited but plausible model space that was comprised of eight bilinear models and four nonlinear variants of the winning bilinear model.

3.4.5.2.1 Phase 1: Bilinear Dynamic Causal Modelling

3.4.5.2.1.1 Theoretical background

The SPM based DCM application has been designed for the assessment of interregional EC and the modulation of this connectivity by experimentally induced changes (Friston et al., 2003). DCM allows one to infer neuronal function mechanistically by the means of estimation of how the neural activity in one region changes the neural activity in another region. The ensuing responses are then entered into a biophysical model of haemodynamic responses at each region or voxel (Friston, 2009; Friston et al., 2003). Hidden neural dynamics are described by coupled differential equations and linked to predicted BOLD responses. The bilinear neuronal state equation Eq. [3.2] describes the timing and the place of the onset of the inputs as well as the modulation of the neuronal states and endogenous connectivity changes, given m known inputs (Friston et al., 2003; Stephan et al., 2007):

$$f(x,u) = f(0,0) + \frac{\partial f}{\partial x}x + \frac{\partial f}{\partial u}u + \frac{\partial^2 f}{\partial x \partial u}xu : \qquad [3.2]$$
$$f(x,u) = \frac{dx}{xt} = \left(A + \sum_{i=1}^{m} uB^{(j)}\right)x + Cu$$

x = neuronal state
m = number of inputs
u_i = ith input
A = matrix A
B = matrix B
C = matrix C

In DCM the neuronal states, which represent the neuronal population activity of the modelled brain regions, change in accordance with the system's connectivity and experimentally controlled inputs. In Eq. [3.2], matrix A represents the endogenous strength with the connections in the absence of experimental manipulations; matrix B

denotes the modulation of those connections by the experimental manipulation (here, the measured changes in EC induced by the four difficulty levels of the HSCT); matrix *C* reflects driving inputs, which represent extrinsic parameters that change the neuronal state of brain regions within the model (here, visual presentation of the sentences with the last word missing). The bilinear effects were driven by box car stimulus functions encoding task difficulty, whereas the driving inputs were driven by box car stimulus functions encoding the main effect of task (Dauvermann et al., 2013).

3.4.5.2.1.2 Model space of bilinear models

The original objective of DCM was to enable generative biophysical modelling. In order to meet this aim, the models examined must meet stringent neurobiological and neurocellular evidence, which enables the biophysical interpretation of the modelling approach. Thus, the details for the DCMs are derived from preclinical and clinical (i.e. subjects at high risk of schizophrenia and subjects with schizophrenia) biological, cellular, chemical and imaging studies.

There are four conditions defined for the current DCM study of the EHRS data:

(i) Each region within the large-scale network must have been reported in PET and fMRI studies during the covert verbal fluency task in healthy controls and in subjects with schizophrenia (chapter 3.3.1).

(ii) Each connection between the regions of the network must have been established in the functional involvement during the performance of the covert verbal fluency task in healthy controls and in subjects with schizophrenia (chapter 3.3.6.2.1.2).

(iii) The experimental conditions of the covert verbal fluency task must be known to be involved in the performance of the covert verbal fluency task in healthy controls and in subjects with schizophrenia (chapter 3.3.1).

(iv) Evidence for gating mechanisms for the thalamo-cortical and cortico-thalamic connection in schizophrenia must exist in the literature (chapter 2.2.2.1).

In the EHRS DCM analyses we employed eight linear models, which were based upon a review of published findings. Details of this review are given below and this review is the basis of the specification of the EHRS model space. Evidence for the bidirectional connections between the MD thalamus and IFG (matrix *A*) was based on (Abitz et al., 2007; Kolluri et al., 2005; Lewis and Lieberman, 2000; Onn and Wang, 2005), and for the bidirectional connections between the MD thalamus and the ACC (matrix *A*) we considered findings from (Lee et al., 2007; Lewis and Lieberman, 2000; Onn and Wang, 2005; Welsh et al., 2010). For modelling the experimental manipulations, well established PET studies and fMRI in healthy subjects performing the HSCT were used (Collette et al., 2001; Frith et al., 1991, 1995; Nathaniel-James and Frith, 2002; Nathaniel-James et al., 1997) as well as FC results in HR subjects of schizophrenia (Whalley et al., 2005). Specifically, two previous DCM studies on the task in healthy subjects (Allen et al., 2008) and HR subjects of schizophrenia (Allen et al., 2010) enabled the modelling of the matrices *B* and *C*.

In phase 1, eight linear DCMs were modelled for each subject. Firstly, the models differed in their unidirectional and bidirectional connections between the five regions

(matrix *A*). Specifically, the eight models are subdivided into two groups: (i) Endogenous connection from the IPS to the IFG (Figure 3.2; Models 1–4) and (ii) endogenous connection from the IPS to the MTG (Figure 3.2; Models 5–8).

The models are specified in terms of the bilinear effect of the parametric (difficulty) of the task. Thirdly, the processing of visual stimuli was modelled by the driving input that corresponded to the main effect of task (relative to rest).

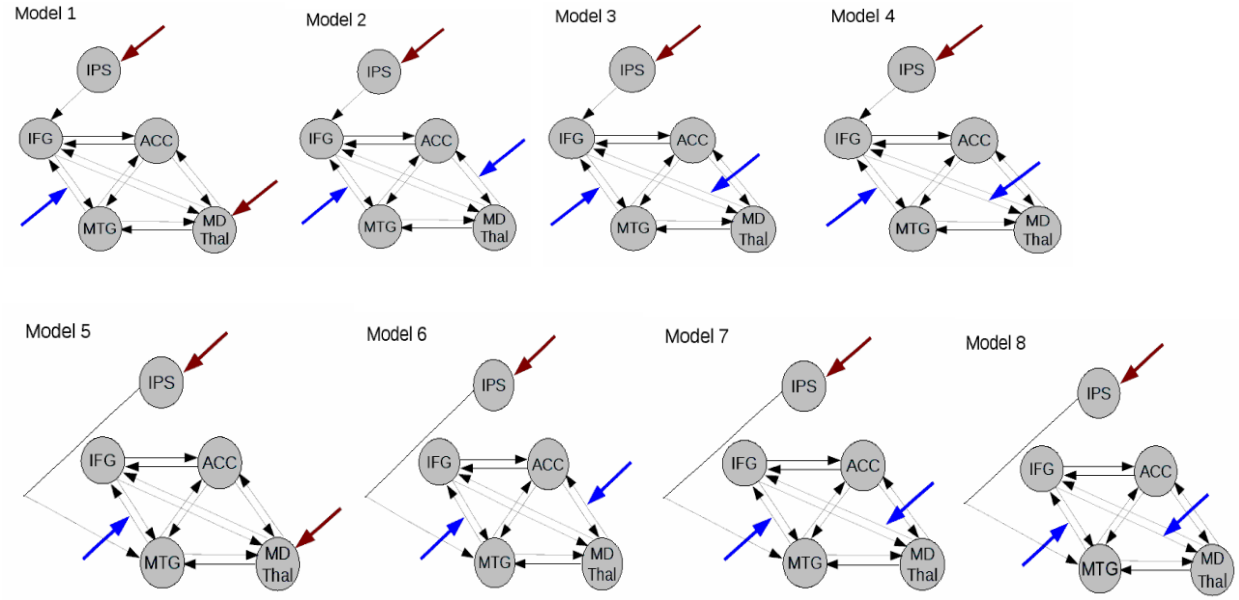

Figure 3.2. Model space of linear models (Reproduced from Dauvermann et al., 2013).

Models 1 to 4 are characterised by the endogenous connections from IPS to IFG.
Model 1 is specified by driving inputs into the IPS and the MD Thal and modulatory input onto the connection from the MTG to the IFG.
Model 2 is specified by driving input into the IPS and modulatory inputs onto the connection from the MTG to the IFG and from the MD Thal to the ACC.
Model 3 is specified by driving input into the IPS and modulatory inputs onto the connection from the MTG to the IFG and from the MD Thal to the IFG.
Model 4 is specified by driving input into the IPS and modulatory inputs onto the connection from the MTG to the IFG and from the IFG to the MD Thal.

Models 5 to 8 are denoted by the endogenous connection from IPS to MTG.
Model 5 is specified by driving inputs into the IPS and the MD Thal and modulatory input onto the connection from the MTG to the IFG.
Model 6 is specified by driving input into the IPS and modulatory inputs onto the connection from the MTG to the IFG and from the MD Thal to the ACC.
Model 7 is specified by driving input into the IPS and modulatory inputs onto the connection from the MTG to the IFG and from the MD Thal to the IFG.
Model 8 is specified by driving input into the IPS and modulatory inputs onto the connection from the MTG to the IFG and from the IFG to the MD Thal.

3.4.5.2.1.3 Random effects Bayesian Model Selection

The phase 1 structure of the heuristic protocol Figure 3.1 is setup to identify the model that provides the most probable explanation of the fMRI data using the random effects BMS process as implemented in SPM8. We estimated the model evidence with the negative free energy (Stephan et al., 2009b). This measure takes into account not only the relative fit of competing models but also their relative complexity (cf. number of free parameters) (Stephan et al., 2009b). After the estimation of the model evidence, we computed the model evidence at the group level (Penny et al., 2004) by applying a hierarchical Bayesian approach (Stephan et al., 2009b) in order to correct for outliers. The application of the posterior exceedance probability estimates the criterion for the conditional likelihood of the model given the data at random (Stephan et al., 2009b). In Eq. [3.3], the exceedance probability (φ_k) is the likelihood that model *k* is more likely than any other model (of the *K* models tested), given the group data.

$$\exists k \in \{1...k\}, \forall j \in \{1...k \mid j \neq k\}: \quad \varphi_k = p(r_k > r_j \mid y; a) \qquad [3.3]$$

φ_k = exceedance probabilities (*Xp); sum to one over all models tested*

3.4.5.2.2 Phase 2: Nonlinear Dynamic Causal Modelling

3.4.5.2.2.1 Theoretical background

Bilinear DCM allows for the inference of dynamic biophysical processes at the neuronal level that translate neuronal activity of regions into predicted BOLD measurements (Stephan et al., 2008). Nonlinear DCM represents an extension of bilinear DCM, where the modulation of connection strengths by experimental inputs is supplemented by direct modulation with neural activity in one or more regions

(Friston et al., 2003; Stephan et al., 2008). In other words, nonlinear DCM allows for the modelling of the interaction between two regions through a third region. Thus, nonlinear DCM is more representative of how biological systems work. This corresponds to an activity-dependent modulation of synaptic efficacy, which models the short-term plasticity we are interested in. The well-established computations for gating in neural networks is the multiplicative computation of nonlinear modulation (Salinas and Sejnowski, 2001; Volman et al., 2010). Nonlinear DCM (Stephan et al., 2007, 2008) can be used to examine whether the connection strength of a connection is modulated by activity of other neuronal populations. To model nonlinear interactions within the network, the bilinear state equation Eq. [3.2] extends the Taylor series to set matrix *D* to be second order in the neuronal states (Stephan et al., 2008; Eq. [3.4]).

$$f(x,u) = f(0,0) + \frac{\partial f}{\partial x}x + \frac{\partial f}{\partial u}u + \frac{\partial^2 f}{\partial x \partial u}xu + \frac{1}{2}\frac{\partial^2 f}{\partial x^2}\frac{x^2}{2}$$

$$D^{(j)} = \Theta\,|\,\frac{1}{2}\frac{\partial^2 f}{\partial x_j^2}\,|\,u = 0\left(1 \le j \le n\right): \qquad [3.4]$$

$$f(x,u) = \frac{dx}{dt} = \left(A + \sum_{i=1}^{m} uB^{(j)} + \sum_{j=1}^{n} x_j D^{(j)}\right)x + Cu$$

x_j = jth neuronal state
u_i = ith input
A = matrix *A*
B = matrix *B*
C = matrix *C*
D = matrix *D*

Matrices *A*, *B* and *C* were modelled as described in bilinear DCM (see section 3.3.6.2.1.2) on Model space of bilinear models). Matrix *D* resembles the gating of a connection between two regions by the activity of a third region. Therefore, nonlinear DCM enables us to consider whether the strength of a connection (here, the

connections of interest are the connection from the IFG to the MD thalamus and the connection from the MD thalamus to the IFG) depends on the activity of other neuronal populations (here, the focus of the study was on the MD thalamus and the IFG; Alelú-Paz and Giménez-Amaya, 2008; Kolluri et al., 2005). Thus, the nonlinear modulation of the network interactions can be allocated to an explicit neuronal population (Stephan et al., 2007; Stephan et al., 2008).

3.4.5.2.2.2 Model space of nonlinear models

The constraints used in phase 2 for the nonlinear DCM were established in the bilinear modelling conducted in phase 1. The constraints on the *A*, *B* and *C* matrices were recovered from the optimal Model 7 from the bilinear DCM analyses. This model served as the "basic" structure of the nonlinear models. In phase 2, our primary aim was to model the connectivity with nonlinear modulation of the reciprocal neuronal projection between the MD thalamus and the IFG. The nonlinear DCMs were specified on the basis of neurobiological evidence for nonlinear mechanisms in neuronal functions, including cognitive tasks for evidence on altered cortico-thalamic and thalamo-cortical connections (Alelú-Paz and Giménez-Amaya, 2008; Kolluri et al., 2005) in schizophrenia. Figure 3.3 shows the four different nonlinear models that were used to identify the gating of the bidirectional endogenous connection between the IFG and the MD thalamus. Two out of the four nonlinear models were specified by the nonlinear modulation from the MD thalamus onto both endogenous connections between the IFG and the MD thalamus. The other two further models were specified by the nonlinear modulation from the IFG onto both endogenous connections between the IFG and the MD thalamus (Figure 3.3).

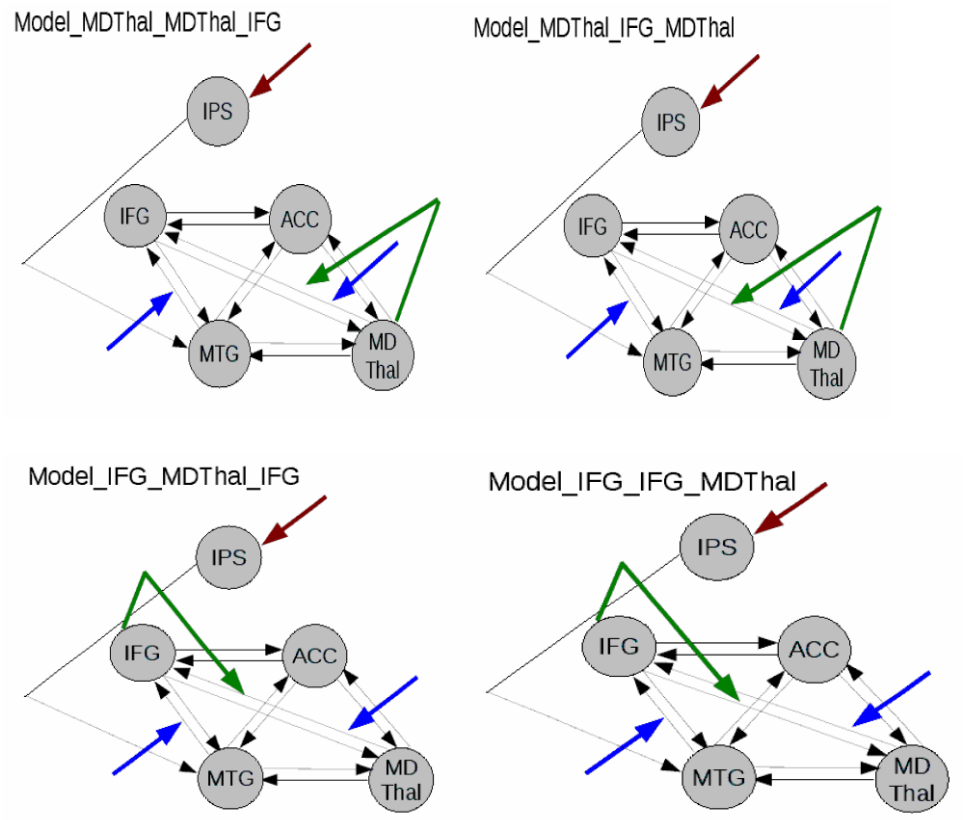

Figure 3.3. Model space of nonlinear models (Reproduced from Dauvermann et al., 2013).

Model_MDThal_MDThal_IFG and Model_MDThal_IFG_MDThal are characterised by the nonlinear modulation from the MD Thal onto the bidirectional connection between the MD Thal and the IFG. Both models are specified upon the winning bilinear model and form model family 2.

Model_MDThal_MDThal_IFG is specified by the nonlinear modulation from the MD Thal onto the connection from the MD Thal to the IFG.

Model_MDThal_IFG_MDThal is specified by the nonlinear modulation from the MD Thal onto the connection from the IFG to the MD Thal.

Model_IFG_MDThal_IFG and Model_IFG_IFG_MDThal are characterised by the nonlinear modulation from the IFG onto the bidirectional connection between the MD Thal and the IFG. Both models are specified upon the winning bilinear model and form model family 3.

Model_IFG_MDThal_IFG is specified by the nonlinear modulation from the IFG onto the connection from the MD Thal to the IFG.

Model_IFG_IFG_MDThal is specified by the nonlinear modulation from the IFG onto the connection from the IFG to the MD Thal.

3.4.5.2.2.3 Model Space Partitioning – Family Level Inference - Random effects Bayesian Model Selection

In phase 2, we applied the established Bayesian inference approach of Family Level Inference and BMA (Penny et al., 2010). Family Level Inference allows the comparison of models of different characteristics (i.e. bilinear and nonlinear models) at the family level. Family Level Inference removes uncertainty about aspects of model characteristics by focusing on the criterion of interest (Penny et al., 2010). To this end, the models differed from each other in the nonlinear aspect.

Here, the model space was partitioned into three model families:

(i) Model Family 1: bilinear model

Model Family 1 contained the optimal bilinear model (Figure 3.2; Model 7).

(ii) Model Family 2: nonlinear models — MD thalamus

Model Family 2 contained the two nonlinear models with nonlinear modulation from the MD thalamus (Figure 3.3; Model_MDThal_MDThal_IFG and Model_MDThal_IFG_MDThal).

(iii) Model Family 3: nonlinear models — IFG

Model Family 3 contained the two nonlinear models with nonlinear modulation from the IFG (Figures 3.3; Model_IFG_MDThal_IFG and Model_IFG_IFG_MDThal).

It is hypothesised that the for the EHRS study that different subject groups use different coping strategies to solve the HSCT. Family Level Inference provides an approach for random effects analyses (Penny et al., 2010) that can account for these different coping strategies. Additionally, this inference method deals with model

families that contain different number of models (Penny et al., 2010). Random effect BMS at the family level uses a Gibbs sampling method (with 1,000,000 samples) and a Dirichlet distribution to compute the family frequencies of each model family in the population and defining a prior over these likelihoods and the exceedance probabilities. In Eq. (3), the exceedance probability (φk) is the likelihood that a model family k represents the analysed time sequences (of K families compared), for the given the fMRI task (Penny et al., 2010). It has been previously shown that this approach is reliable (Seghier et al., 2011).

3.4.5.2.3 Phase 3: Bayesian Model Averaging – Theoretical background

In phase 3, we applied BMA over the winning models identified from the BMS at the family level in the phase 2 processing. BMA assesses the full posterior density on parameters by weighting the evidence to the contribution of each model to the mean effect (Penny et al., 2010). Posterior density means that models with the highest evidence maximize their contribution to the evidence, while models with weak evidence minimize their contribution to the evidence. These results can be computed for posterior means of connectivity on single subject level.

The significance of connection strength with nonlinear modulation for the four nonlinear DCMs (Figure 3.3) was computed by the fraction of samples in the posterior density that differed from zero. Significant effects are reported at a posterior probability level of 0.95. This approach has been shown to produce reliable results (Seghier et al., 2011). In short, we used BMA to assess the posterior density

over the bidirectional connections between the MD thalamus and the IFG by pooling evidence from different groups of subjects, in a way that accounts for uncertainty about the particular model generating the data.

Apart from the examination of the connection strength with nonlinear modulation, the connection strengths for endogenous connections, connections with modulatory inputs and connections of direct inputs were assessed with the same procedure.

3.4.5.3 Correlations between clinical measures and parameter estimates of connection strengths with nonlinear modulation

The final component of the heuristic protocol evaluates the individual posterior densities of the connection strengths. The connection strengths with nonlinear modulation are entered into a statistical analysis where within-group correlations between the connection strengths with nonlinear modulation and the clinical symptoms assessed using the individual rescaled PANSS scores as an explorative approach. The correlations were run on the individual symptoms as assessed with PANSS in three separate analyses: (i) Positive symptoms (P1 – P7); (ii) negative symptoms (N1 – N7); and (iii) general symptoms (G1 – G16) (Kay et al., 1987). In order to estimate the sampling error of the original subpopulations, bivariate Pearson correlation with Bootstrapping and Confidence Intervals of 95% were constructed (Cohen, 1988; Efron and Tibshirani, 1993). Furthermore, the correlations were corrected for multiple comparisons. These analyses were run in the healthy controls, HRall and HR+ but not in the four ill subjects because of the small number of this group. The statistical analyses were conducted in SPSS (SPSS BMI 19.0).

3.5 Results

3.5.1 Demographic and clinical details

There were no significant differences in mean age, gender, mean intelligence quotient (NART IQ) or handedness between the groups (Table 3.3).

3.5.2 Functional activation

The localisation results are presented as between group results for the parametric contrast and the sentence completion versus baseline contrast for both the main 'trait' effect and 'state' effect in order to ensure that the processed EPI scans in SPM8 reproduced the previously reported between group differences (Whalley et al., 2004).

3.5.2.1 Main 'trait' effect

For the examination of the 'trait' effect, healthy controls were compared with HRall subjects. The between group results for the parametric contrast are displayed in Table 3.5.

3.5.2.1.1 Parametric contrast

The results for the between group differences for the parametric contrast revealed increased activation with increasing task difficulty in healthy controls compared to all HR subjects together in the following regions (Table 3.5):

Table 3.5 Main 'Trait' Effect: Between-group random effects analysis – Parametric contrast.

P value	Extent	Peak height coordinates	Region	*Z* score
Parametric Contrast: Healthy Controls (n=21) < HRall subjects (n=69)				
n/s				
Parametric Contrast: Healthy Controls (n=21) > HRall subjects (n=69)				
.0033	156	18, 43, 2 1, 60, 56	R frontal: medial frontal gyrus, BA10	4.34
.0007	245	-3, -73, -8 -10, -73, -11 -18, -76, -14	L cerebellum: posterior lobe, declive	3.98
>0.001	294	8, -13, 6 -8, -17, 11 16 -12 8	R/L sub-lobar: thalamus	3.90

Reported *p* values are thresholded at $p < .05$ FWE corrected cluster level, extent threshold = 50 voxels. Coordinates represent the three maxima within the same cluster.

3.5.2.1.2 Sentence completion versus rest

For the sentence completion versus rest contrast, no statistically significant group differences were observed between the healthy controls and all HR subjects.

3.5.2.2 'State' effects

For the 'state' effects, healthy controls and HR- subjects in one group versus HR+ subjects were compared. The between group results for the sentence completion versus rest contrast are displayed in Table 3.6.

3.5.2.2.1 Parametric Contrast

No significant group differences between healthy controls/HR- subjects and HR+ subjects were observed.

3.5.2.2.2 Sentence completion versus rest

Increased activation in the left parietal lobe was observed in HR+ subjects versus HR subjects and healthy controls. There were significant results for the opposite contrast.

Table 3.6 Between-group random effects analysis – sentence completion versus rest contrast.

P value	Extent	Peak height coordinates	Region	*Z* score
Sentence completion versus rest: Healthy Controls and HR- subjects < HR+ subjects				
0.001	387	-42, -48, -48 -45, -39, 60 -37 -43, 30	L parietal: inferior parietal lobule, BA 40	4.46
Sentence completion versus rest: Healthy Controls and HR- subjects > HR+ subjects				
n/s				

Reported *p* values are thresholded at $p < .05$ FWE corrected cluster level, extent threshold = 50 voxels. Coordinates represent the three maxima within the same cluster.

3.5.3 Functional integration – Dynamic Causal Modelling

The DCM results for the grouped analyses follow the three phases of the DCM protocol given in Figure 3.1. In the first phase, the optimal model for the HSCT identified the general structure of the network. In the second phase, this structure was further interrogated to reveal the model families that best explain the expected group separation in our cohort. In the third phase, the nonlinear modulation was assessed within the two winning model families resulting from the analyses in phase 2. The findings of each phase are compared between the three groupings.

3.5.3.1 Bilinear Dynamic Causal Modelling and Bayesian Model Selection at the group level

The application of phase 1 processing in the DCM protocol provided the exceedance probabilities of the eight linear models labelled M1 to M8 across the three subject groupings are presented Figure 3.4. In Figure 3.4a, the BMS results are shown for the first grouping of healthy controls and all HR. In Figure 3.4b, the BMS results are shown for the second grouping of healthy controls, HR− and HR+. In Figure 3.4c, the BMS results are shown for the third grouping of healthy controls, HR−, HR+ and the four ill subjects who subsequently developed schizophrenia. This random effects BMS analyses showed that Model 7 (M7) outperformed all other models for the tested groupings. Model 7 demonstrated *Xp* of 0.63 in healthy controls and *Xp*=0.52 in HRall (Figure 3.4a); *Xp*=0.59 in HR− and *Xp*=0.63 in HR+ (Figure 3.4b); and *Xp*=0.63 in the four ill subjects (Figure 3.4c). The likelihood of Model 7 is three times the probability of the closest likely Model 6 or Model 8.

a 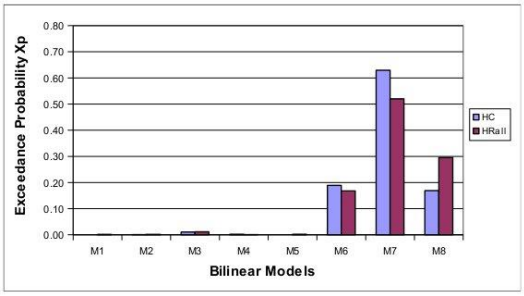

b 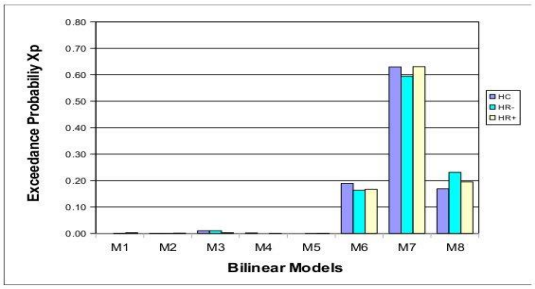

c 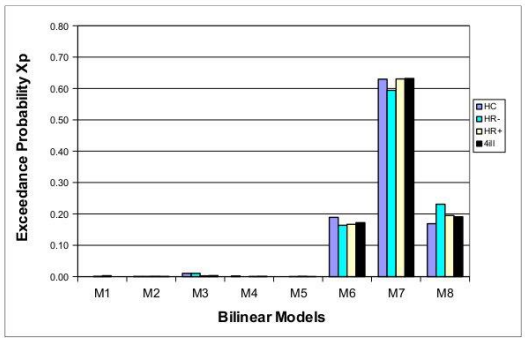

Figure 3.4 Bayesian Model Selection at the Group Level for Bilinear Models (Reproduced from Dauvermann et al., 2013).

Figure 3.4a. Bayesian Model Selection at the group level for healthy controls and all high risk subjects
First grouping of the BMS analysis for healthy controls and HRall. Model 7 is the optimal model in both healthy controls and HRall.
Figure 3.4b. Bayesian Model Selection at the group level for healthy controls, high risk subjects without psychotic symptoms and high risk subjects with psychotic symptoms.
Second grouping of the BMS analysis for healthy controls, HR- and HR+. Model 7 is the optimal model in healthy controls, HR- and HR+.
Figure 3.4c. Bayesian Model Selection at the group level for healthy controls, high risk subjects without psychotic symptoms, high risk subjects with psychotic symptoms and the four ill subjects
Third grouping of BMS analysis for healthy controls, HR-, HR+ and four ill subjects. Model 7 is the optimal model in healthy controls, HR-, HR+ and the four ill subjects.
BMS, Bayesian Model Selection; HC, healthy controls; HR-, high risk subjects without psychotic symptoms; HR+, high risk subjects with psychotic symptoms; Four ill subjects, four HR subjects who became subsequently ill; eight bilinear models (Figure 3.2) are labelled M1 to M8; M7, Model 7 (Figure 3.2); *Xp*, exceedance probability.

Model 7 is illustrated in Figure 3.2. It contains one unidirectional connection from the IPS to the MTG and reciprocal endogenous connections between all the other regions. The BMS results from Model 5 to Model 8 demonstrate that the unidirectional connection from the IPS to the MTG is more likely than the connection from the IPS to the IFG. Furthermore, the exceedance probabilities from

Model 3 and particularly Model 7 show that the task-dependent modulation was optimal for the forward connection between the MTG and the IFG and the forward connection between the MD thalamus and the IFG. Model 7 is similarly structured to the optimal model found in the HSCT study reported by Allen et al., (2010) although this study did not include the MD thalamus.

We note that the exceedance probability in the implementation of Model 7 is consistent across the tested groups. The exceedance probabilities for Model 7 vary from a minimum of 0.58 to a maximum of 0.63 across all subject groupings. We also note similar consistency in exceedance probabilities for the other tested bilinear models. This consistency in BMS exceedance probabilities in healthy controls and HR subjects was also reported by Allen et al., (2010).

3.5.3.2 Nonlinear Dynamic Causal Modelling and Bayesian Model Selection at the model family level

The results of phase 2 are presented for the repeated grouping analyses. Three model families were compared against each other. The partitioning of the model space was the same for each grouping (see section on Model Space Partitioning – Family Level Inference – Bayesian Model Averaging). We compared the different model families using the random effects BMS approach at the family level to reveal the optimal model family across the three groupings in healthy controls and the high risk subjects.

The BMS analysis over the model families resulted in different *Xp* values being recorded between the healthy controls and the HR subjects (Figure 3.5). The main findings of this phase are structured following the structure of Figure 3.5, which

summarises and compares the three groupings. The exceedance probabilities for the two winning Model Families 2 and 3 were summarised (for a similar approach see Penny et al., 2010; Seghier et al., 2011).

(i) The two winning model families 2 and 3 outperform the model family 1 in every group. In other words, both model families 2 and 3 are more likely than model family 1 to explain the HSCT fMRI data.

(ii) Model families 2 and 3 accounted for a total of Xp=0.95 in healthy controls and Xp=0.99 in HRall in the first run (Figure 3.5a).

(iii) Model families 2 and 3 accounted for a total of Xp=0.95 in healthy controls, Xp=0.99 in HR− and Xp=0.99 in HR+ in the second run (Figure 3.5b).

(iv) Model families 2 and 3 accounted for a total of Xp=0.95 in healthy controls, Xp=0.95 in HR−, Xp=0.99 in HR+ and Xp=0.86 in the four ill subjects in the third run (Figure 3.5c).

a

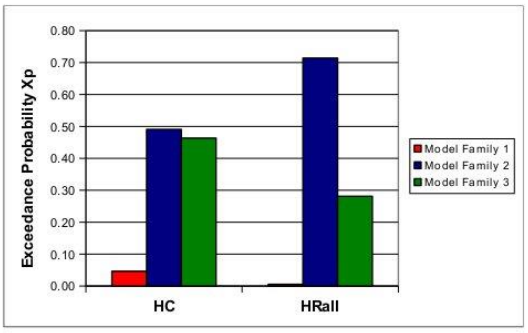

b

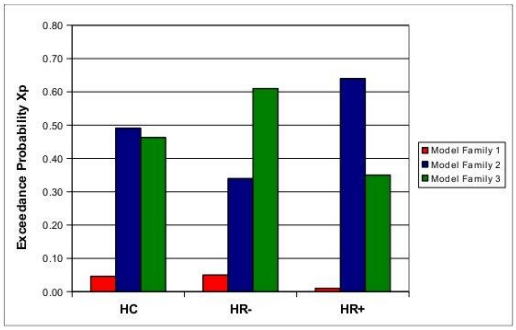

c

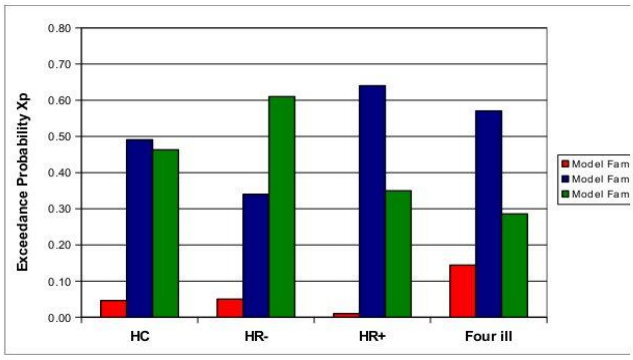

Figure 3.5. Bayesian Model Selection at the Model Family Level (Reproduced from Dauvermann et al., 2013).

Figure 3.5a. Bayesian Model Selection at the model family level for healthy controls and all high risk subjects
First grouping of the BMS analysis for healthy controls and HR all. The winning model families are Model Families 2 and 3 in both healthy controls and HRall.
Figure 3.5b. Bayesian Model Selection at the model family level for healthy controls, high risk subjects without psychotic symptoms and high risk subjects with psychotic symptoms
Second grouping of the BMS analysis for healthy controls, HR- and HR+. The winning model families are Model Families 2 and 3 in healthy controls, HR- and HR+.
Figure 3.5c. Bayesian Model Selection at the model family level for healthy controls, high risk subjects without psychotic symptoms, high risk subjects with psychotic symptoms and the four ill subjects.
Third grouping of the BMS analysis for healthy controls, HR-, HR+ and four ill subjects. The winning model families are Model Families 2 and 3 healthy controls, HR-, HR+ and the four ill subjects.
BMS, Bayesian Model Selection; HC, healthy controls; HR-, high risk subjects without psychotic symptoms; HR+, high risk subjects with psychotic symptoms; Four ill subjects, four HR subjects who became subsequently ill; Xp, exceedance probability. Red Column: Model Family 1 - Bilinear Model 7; Blue Column: Model Family 2 - Nonlinear Models with nonlinear modulation from MD Thalamus: Green Column: Model Family 3 - Nonlinear Models with nonlinear modulations from IFG.

In both model families 2 and 3, the nonlinear modulations onto both reciprocal connections between the MD thalamus and the IFG reveal the optimal modelling.

The results of the three groupings demonstrated that the distribution of likelihoods of the model families 2 and 3 differentiated between the groupings of HR subjects. In the first grouping, the HRall showed a different distribution of exceedance probabilities to healthy controls. In the second run, the finding revealed that the distribution of the HR+ seemed to resemble the distribution of the HRall. In the third run, the additional subgroup of four ill subjects demonstrated that the pattern of greater likelihood of model family 2 than model family 3 as it was observed in HR+ was repeated in the four ill subjects.

3.5.3.3 Bayesian Model Averaging – Posterior densities of connection strengths

The results for the posterior densities of connection strengths follow the outlined structure: Firstly, the connection strengths with nonlinear modulation are presented before endogenous connection strengths, connection strengths for modulatory inputs are reported.

3.5.3.3.1 Connection strength with nonlinear modulation

The result of the significant connection strengths with nonlinear modulation for the Model MDThal_MDThal_IFG (Figure 3.3) demonstrated reduced connection strengths with nonlinear modulation in HR+ and the four ill subjects but not in HRall.

In order to investigate the posterior probabilities of the connectivity with nonlinear modulation, we assessed the connection strengths from model family 2, nonlinear models — MD thalamus (Figure 3.3) in every grouping. The BMA analysis within

the two winning models resulted in different posterior probabilities of the nonlinear modulation in the Model MDThal_MDThal_IFG (Figure 3.3; Figure 3.6).

(i) The connection strength with nonlinear modulation was reduced in HRall, HR+ and the four ill subjects across the three groups; this parameter was significantly lower in the HR+ and the four ill HR subjects in contrast to the healthy controls (posterior probability 0.95).

(ii) The connection strength with nonlinear modulation was not significantly different between the healthy controls and the HRall (Figure 3.6a).

(iii) The connection strength with nonlinear modulation was significantly reduced in the HR+ in contrast to healthy controls (posterior probability 0.95; Figure Table 3.6b).

(iv) The connection strength with nonlinear modulation was significantly reduced in the four ill subjects in comparison to healthy controls (posterior probability 0.95; Table 3.5c).

a

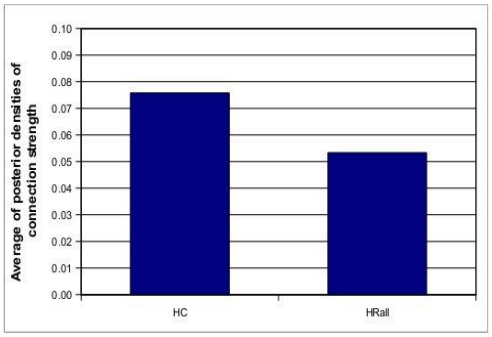

b

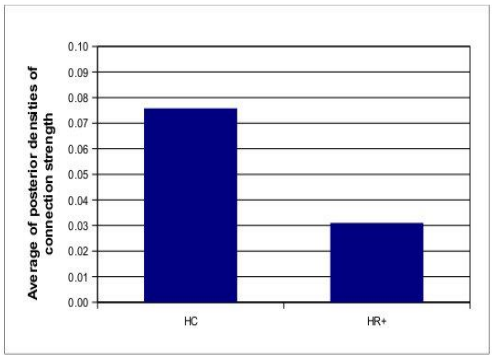

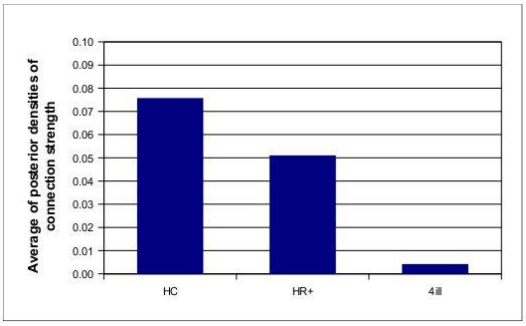

c

Figure 3.6. Bayesian Model Averaging Results for the Thalamo-cortical Connection with Nonlinear Modulation from the MD Thalamus - Model_MDThal_MDThal_IFG (Reproduced from Dauvermann et al., 2013).

Figure 3.6a. Average of posterior densities of connection strength with nonlinear modulation for healthy controls and all high risk subjects
First grouping of the BMA analysis for healthy controls and all high risk subjects. The connection strength with nonlinear modulation was not significantly different.
Figure 3.6b. Average of posterior densities of connection strength with nonlinear modulation for healthy controls and high risk subjects with psychotic symptoms.
Second grouping of the BMA analysis for healthy controls and HR+. The connection strength with nonlinear modulation was significantly reduced in HR+ in contrast to healthy controls.
Figure 3.6c. Average of posterior densities of connection strength with nonlinear modulation for healthy controls, high risk subjects with psychotic symptoms and the four ill subjects.
Third grouping of the BMA analysis for healthy controls, HR+ and four ill subjects. The connection strength with nonlinear modulation was four ill subjects in contrast to the healthy controls.
Average of posterior densities of connection strength with nonlinear modulation (in Hertz), (all significant at posterior probability threshold $p > .95$). BMA, Bayesian model averaging; HC, healthy controls; HR+, High Risk subjects with psychotic symptoms; four ill subjects, 4 subjects who subsequently became ill.

3.5.3.3.2 Endogenous connection strength

The average of the posterior densities of the endogenous connection strengths from all three groupings are summarised in Table 3.7. There were no significant differences found.

Table 3.7 Average of posterior densities of endogenous connection strength (in Hertz).

Model MDThal_MDThal_IFG	HC	HR- subjects	HR+ subjects	Four ill subjects
IPS -> MTG	0.22 (0.25)	0.19 (0.23)	0.24 (0.22)	0.20 (0.25)
IFG -> ACC	0.02 (0.08)	0.02 (0.10)	0.04 (0.13)	0.03 (0.16)
ACC -> IFG	0.02 (0.09)	0.02 (0.11)	0.04 (0.12)	0.03 (0.14)
IFG -> MTG	0.05 (0.15)	0.08 (0.08)	0.08 (0.13)	0.03 (0.13)
MTG -> IFG	0.05 (0.11)	0.09 (0.06)	0.04 (0.13)	0.11 (0.15)
IFG -> MDThal	0.01 (0.10)	0.01 (0.09)	0.04 (0.10)	0.03 (0.12)
MDThal -> IFG	0.01 (0.09)	0.01 (0.08)	0.04 (0.10)	0.03 (0.23)
ACC -> MTG	0.10 (0.10)	0.09 (0.06)	0.11 (0.14)	0.01 (0.12)
MTG -> ACC	0.03 (0.05)	0.12 (0.05)	0.11 (0.11)	0.06 (0.11)
ACC -> MDThal	0.00 (0.04)	0.03 (0.05)	0.03 (0.07)	0.02 (0.09)
MDThal -> ACC	0.12 (0.15)	0.06 (0.05)	0.05 (0.10)	0.02 (0.11)
MTG -> MDThal	0.03 (0.04)	0.10 (0.11)	0.13 (0.08)	0.08 (0.13)
MDThal -> MTG	0.08 (0.12)	0.08 (0.11)	0.00 (0.12)	0.01 (0.14)

Mean (SE)
HC, healthy controls; HR-, high risk subjects without psychotic symptoms; HR+, high risk subjects with psychotic symptoms; Four ill subjects, four HR subjects who became subsequently ill.

3.5.3.3.3 Connection strength with modulatory inputs

The averages and standard deviations of the posterior densities of connection strengths with modulatory inputs across the three groupings are presented in Table 3.8. There were no significant differences between the groups.

Table 3.8 Average of posterior densities of connection strength of modulatory inputs (in Hertz).

Model MDThal_MDThal_IFG		HC		HR- subjects		HR+ subjects		Four ill subjects	
"Low difficulty level"									
MTG ->IFG	MDThal -> IFG	0.05 (0.10)	0.04 (0.13)	0.06 (0.12)	0.06 (0.14)	0.02 (0.10)	0.08 (0.15)	0.03 (0.16)	0.01 (0.15)
"Low medium difficulty level"									
MTG ->IFG	MDThal -> IFG	0.04 (0.09)	0.01 (0.15)	0.06 (0.10)	0.05 (0.14)	0.07 (0.12)	0.06 (0.14)	0.04 (0.14)	0.01 (0.14)
"High medium difficulty level"									
MTG ->IFG	MDThal -> IFG	0.06 (0.15)	0.07 (0.16)	0.06 (0.13)	0.06 (0.15)	0.04 (0.15)	0.03 (0.10)	0.04 (0.11)	0.01 (0.11)
"High difficulty level"									
MTG ->IFG	MDThal -> IFG	0.07 (0.16)	0.02 (0.08)	0.03 (0.12)	0.06 (0.15)	0.04 (0.12)	0.02 (0.17)	0.02 (0.14)	0.01 (0.13)

Mean (SE)
HC, healthy controls; HR-, high risk subjects without psychotic symptoms; HR+, high risk subjects with psychotic symptoms; Four ill subjects, four HR subjects who became subsequently ill.

3.5.3.4 Correlations between clinical measures and posterior densities of connection strength with nonlinear modulation

In the post-hoc analysis of symptom correlations, we examined whether the finding of reduced EC could underlie the clinical symptoms as assessed with the individual symptoms of the rescaled PANSS in the HR+. A significant correlation was found between the individual connection strength with nonlinear modulation of Model_MDThal_MDThal_IFG (Figure 3.2a) and the individual rescaled PANSS symptom 'delusion' (P1; Kay et al., 1987) in HR+ ($r = -.246$; $p = .041$; 95 % CI (−0.543; −0.024)). This finding met significance with corrections for multiple comparisons. The significant association in HR+ supported the more pronounced reduction of this connection strength with nonlinear modulation in the four subjects (Table 3.5c), who showed delusions at the time of transition to the illness. Furthermore, the correlation in HR+ in addition to the significant relationship in HRall (r=−.201; p=0.05; 95% CI (−0.446; 0.02); significant with corrections for multiple comparisons) confirms the BMS results on the model family level (Figure 3.5a in HRall and Figure 3.5b in HR+). The distribution of the likelihood of the model families 2 and 3 between HRall, HR− and HR+ (Figure 3.5a and Figure 3.5b) can therefore be explained by the lower connection strength with nonlinear modulation (in the Model MDThal_MDThal_IFG) as a state-marker in the HRall and HR+ groups.

There were no significant associations between the individual PANSS symptom 'hallucination' (P3; hallucinatory behaviour; Kay et al., 1987) and the connection strength with nonlinear modulation in HR+ or HRall. Furthermore, we did not observe any significant relationships between other individual PANSS symptoms

(positive, negative and general symptoms; Kay et al., 1987) and nonlinear EC measures in HR+ or HRall. Lastly, we do not report the correlation results for the healthy controls due to the inadequately small number of healthy controls for the correlation analyses, who showed positive, negative and general symptoms as assessed with PANSS.

3.6 Discussion

We applied nonlinear DCM to fMRI data for the HSCT in subjects at high familial risk of schizophrenia. For the HSCT, nonlinear DCM allowed us to model connection strength with nonlinear modulation and assess the interactions between neuronal populations in the MD thalamus and the IFG. Our results demonstrate that the connection strength with nonlinear modulation of the thalamo-cortical connection is reduced in HR+. This could result in reduced prefrontal-thalamic FC and cortical dysconnectivity and both is in keeping with and extends our previous findings of FC on this cohort (Whalley et al., 2005). In addition, we see further reductions of connection strength with nonlinear modulation in the four subjects who subsequently developed schizophrenia in our HR cohort although this should be considered preliminary given the small subject number in this group. Furthermore, we found significant negative correlations between connection strength with nonlinear modulation and the PANSS symptom severity of delusion in HR+ and the HRall. This indicates that the presence of active symptomatology in HR+ (and to a lesser extent in the HRall) may be a factor for the state-related differences between HR− and HR+. None of the subjects reported the presence of psychotic symptoms at more than a subclinical level at the time of scanning and indeed regarded themselves as

well. None were on antipsychotic medication. Thus, our findings are not confounded by the effect of medication.

Our results of reduced connection strength with nonlinear modulation in the HR+ and four ill HR subjects are in keeping with studies, which propose that nonlinear models can resemble reduced gating and provide a better explanation to the fMRI data than linear models. The finding of reduced connection strength with the thalamo-cortical projection via the MD thalamus in the HR+ and the four ill subjects supports the hypothesis of disrupted synaptic plasticity, which is gated by nonlinear biophysical processes (Chance et al., 2002; Deng and Klyachko, 2011; Destexhe, 2009; Negyessy and Goldman-Rakic, 2005). Our results support previous findings of disrupted synaptic plasticity of the thalamo-cortical connection (Krystal et al., 2003; Negyessy and Goldman-Rakic, 2005) resulting in cortical dysconnectivity in schizophrenia (Balu and Coyle, 2012; Byne et al., 2009; Goff and Coyle, 2001; Lewis and Lieberman, 2000; Pakkenberg et al., 2009; Sodhi et al., 2011; Watis et al., 2008).

Consistent with previous FC and EC studies using verbal fluency tasks, functional connections between the left IPS and left prefrontal regions, left IFG and left thalamus (Whalley et al., 2005), left IFG and ACC, left STG/MTG and ACC (Boksman et al., 2005; Allen et al., 2008; Allen et al., 2010) and left MFG and left MTG (Allen et al., 2008; Allen et al., 2010). In FC studies, altered functional connections between the left IFG and left thalamus, left parietal and left prefrontal regions in HR subjects in contrast to healthy controls (Whalley et al., 2005), task-

dependent functional coupling between the right AC and left IFG as well as left STG in FES (Boksman et al., 2005) and negative correlations between the left DLPFC and left middle temporal cortex/superior temporal cortex in EST in contrast to healthy controls (Lawrie et al., 2002). Furthermore, supporting evidence for task-dependent modulation (of response suppression in contrast to response initiation of the HSCT) from the left MTG to the left MFG in healthy controls (Allen et al., 2008) and from the left MFG to the left MTG in ARMS subjects and healthy controls (Allen et al., 2010) was reported from two DCM studies. Lastly, intrinsic connection strength was increased in ARMS subjects in contrast to healthy controls (Allen et al., 2010).

For the bilinear models, the optimal model 7 in this study was similarly specified to the winning model in healthy controls and ARMS subjects and resulted in no significant group differences as previously reported (Allen et al., 2010). These findings suggest that (i) the task-dependent modulation from the MTG to MFG may reflect successful response initiation of the HSCT in all participants and (ii) in comparable cognitive coping of the HSCT in ARMS subjects and HR subjects despite significant group differences in FA (Whalley et al., 2004; Allen et al., 2010), FC between IFG and thalamus (Whalley et al., 2010) and EC between MTG and ACC (Allen et al., 2010). Given comparable behavioural performances between the study populations, we propose that the previously reported group differences at the FA and FC level may reflect altered cortical function (Schlösser et al., 2008) or a compensation to impaired function (Tan et al., 2006). We speculate that the lack of significant group differences in task-dependent modulation at the level of bilinear models may be due to the complex structure of the networks consisting of five regions in the EHRS networks (in comparison to three regions in Allen et al., 2010)

in addition to the endogenous connections, connections with modulatory input and driving inputs. This finding may reflect one of the limitations of deterministic DCM, which does not account for unknown variables in the models. In terms of the main result of nonlinear models, we propose that the modelling of the nonlinear modulation in addition to the 'structure' of the bilinear models may have provided additional information, which led to greater probabilities in explaining the given fMRI data. On the neurocognitive level, we speculate that the reduced connection strengths with nonlinear modulation in HR+ subjects and four ill subjects may reflect a compensatory mechanisms, which is related to the severity of the transient 'delusion' symptom. Currently, the knowledge of neurocognitive mechanisms underlying gating mechanisms in cognitive processes in humans is limited and clearly needs further research.

It has been proposed that cortical dysfunction in verbal fluency tasks could be mediated by thalamic glutamatergic disruption (Fusar-Poli et al., 2011) and/or alterations of the thalamo-cortical neuronal projection (Byne et al., 2009; Lewis and Lieberman, 2000; Pakkenberg et al., 2009; Sodhi et al., 2011; Watis et al., 2008). In more detail, supporting evidence for increased BOLD response of the right DLPFC in ARMS/UHR subjects in contrast to healthy controls in the HSCT[4] was reported, which was negatively related with lower thalamic Glu levels in ARMS subjects (ARMS, Fusar-Poli et al., 2011; UHR, Allen et al., 2014). Furthermore, it was shown that not only Glu concentrations from the thalamus in UHR subjects were reduced in contrast to healthy controls but also that thalamic Glu concentrations were negatively

[4] This version of the HSCT involved response initiation (Part A) and response suppression/inhibition (Part B).

associated with the severity of total positive symptoms in UHR in non-remission in contrast to UHR subjects in remission after 18 months (Egerton et al., 2014). In subjects at enhanced familial risk of schizophrenia, no significant group differences in thalamic Glu concentrations were reported (Yoo et al., 2009), however, increased Glx/Cr concentrations in the right medial frontal lobe in subjects at enhanced familial risk when compared to healthy controls have been found (Tibbo et al., 2004). Additional MRS studies in familial risk of schizophrenia did not find significant group differences in Glu/Glu-related levels in the left DLPFC/AC/left thalamus between HR subjects at familial risk and healthy controls (Yoo et al., 2009; Lutkenhoff et al., 2010).

Furthermore, alterations of glutamatergic neurotransmission leading to the pathophysiology of schizophrenia as part of the glutamate hypothesis of schizophrenia have been suggested (Coyle, 2006; Coyle et al., 2010; Javitt, 2010). In terms of glutamatergic neurotransmission, NMDA receptor-dependent modulation of the thalamo-cortical connection may be disrupted in schizophrenia (Balu and Coyle, 2012; Gray and Roth, 2007; McCormick and Bal, 1997; Romanides et al., 1999; Watis et al., 2008). It is noted that not only glutamatergic alterations are involved but alterations of interactions between DA and Glu among other implicated neurotransmitters are implicated (Cronenwett and Csernansky, 2010). One example of indirect relationship between cortical dysconnectivity and dopaminergic alterations has been presented by increased BOLD response of the bilateral PFC and greater PFC-midbrain FC in UHR, who subsequently developed schizophrenia in contrast to UHR, who did not subsequently develop schizophrenia (Allen et al., 2014). We consider that our indications of lower connection strengths with nonlinear

modulation of the thalamo-cortical connection during the HSCT suggest that altered glutamatergic and/or dopaminergic transmission of the MD thalamus could underlie the reduced gating of the task. We speculate that the difference in connection strengths with nonlinear modulation may be linked to clinical symptoms in HR+ subjects rather than behavioural performance since only clinical symptoms were significantly different between the groups. However, we acknowledge the lack of measures of Glu and DA concentration in the MD thalamus in this study.

There are general limitations of bilinear and nonlinear DCM and specific limitations of this study. The temporal resolution of fMRI is limited, which leads to an inability to consider conduction delays in inputs and interregional interactions (Friston et al., 2003) in contrast to DCM for EEG/MEG (Daunizeau et al., 2011a; Stephan and Friston, 2010; Friston and Dolan, 2010). DCM requires strict subject and ROI inclusion criteria (Stephan et al., 2007), which results in exclusion of more subjects compared to the usual fMRI analyses, leading to a smaller sample size for this study than for our previous analyses (Whalley et al., 2005; Whalley et al., 2004). Also DCM8 does not allow a direct assessment of alterations of excitatory glutamatergic subpopulations (Marreiros et al., 2008) in the models or an explicit neuronal population (Daunizeau et al., 2009). Thus, we cannot definitely state that glutamatergic neurotransmission is implicated in the lower connection strength with the gating in the high risk subjects. It is noted that underestimation of processing complexity of neurobiological networks is likely not only with bilinear DCM but also with nonlinear DCM (Dauvermann et al., 2014). The nonlinear dynamical systems were estimated by deterministic inference methods, and these do not fully

represent the random or stochastic noise of neuronal activity (Saarinen et al., 2008) and hidden neuronal and physiological processes (Li et al., 2011). Our DCM analyses of subjects who subsequently develop schizophrenia were limited to four individuals. Because of the small size in this group in the DCM analysis it is not possible to consider the DCM results to have predictive validity although the four individuals can be treated as single-subject results (Stephan et al., 2007). For predictive studies using DCM results, the DCM-based generative embedding approach using support vector machines (Brodersen et al., 2011; Brodersen et al., 2013) is an additional approach. Finally, the DCM analyses in this study were run in DCM8 limiting us to deterministic and one-state DCM.

3.7 Conclusion

Our results show that gating mechanism at the neuronal population level of the MD thalamus could be altered and may contribute to or be an underlying cause for the development of psychotic symptoms. This study suggests that nonlinear DCM could further our understanding of altered connectivity in subjects at high familial risk stage of schizophrenia.

The methodological approach of this study has been adopted for the investigation of possibly altered gating mechanism in working memory in subjects with established schizophrenia contrasted to healthy controls (chapter 4).

4 Dynamic Causal Modelling for fMRI in working memory in individuals with established schizophrenia

4.1 Introduction

Findings from FC studies during verbal/numeric working memory in individuals with schizophrenia have increased insight into altered large-scale networks underlying working memory deficits (chapter 1.4.3). EC studies have reported altered connection strengths during cognitive tasks in people with schizophrenia when contrasted to healthy controls. These results may offer a biophysical interpretation of altered large-scale networks and possibly altered neurotransmission in schizophrenia (chapter 2.2.4.3). However, it is possible that the complexity of neurobiological networks is underestimated in DCM in its current implementation.

Findings from the application of nonlinear DCM of the EHRS study showed that the connection strengths with nonlinear modulation of the thalamo-cortical connection during verbal fluency was significantly reduced in subjects at high familial risk of schizophrenia in comparison to healthy controls. These findings were interpreted as a possible marker of disrupted synaptic plasticity and glutamatergic transmission at the high risk stage of schizophrenia (chapter 3.6).

In this study, we assessed the connection strength of nonlinear modulation of the bidirectional connection between the DLPFC and the VTA/SN area during verbal working memory in healthy controls and EST. The role of the VTA/SN area and the meso-cortical connection in dopaminergic neurotransmission and working memory has received extensive evidence from preclinical research (chapter 1.3.1, chapter 1.3.2) and computational modelling of preclinical findings (chapter 2.2.2.2). The dopamine hypothesis (chapter 1.3.2.1) and the glutamate hypothesis (chapter 1.3.2.2)

have been partly formulated on the basis of the findings on dopaminergic alterations of the VTA and the meso-cortical connection in animal models of schizophrenia. In humans, research on the functional role of the VTA in working memory is rare due to technical difficulties of neuroimaging techniques such as fMRI/PET (such as field strength for fMRI; Tomasi et al., 2007) and ethical reasons of invasive *in vivo* investigation of neuronal and cellular mechanisms in humans. With improvement of technical aspects (such as higher field strength of MRI scanners, improved EPI sequences; improved DA transporter ligands for PET) and modelling of parametric working memory loads/high working memory loads, recent fMRI studies provided evidence for the implication of the VTA/SN area in working memory and/or dopaminergic modulation in healthy controls (fMRI, Murty et al., 2011; D'Ardenne et al., 2012; Xu et al., 2013; Yu et al., 2013; PET, Mehta et al., 2008) and in EST (fMRI, D'Aiuto et al., 2014). We applied the heuristic search protocol for nonlinear DCM for fMRI (chapter 3.4.5.2) to the verbal "N-back" task in healthy controls and EST.

The theoretical background for this study is based on the reviewed FA, FC and EC findings (of the DLPFC, IPS and ACC) during the verbal/numeric "N-Back" task in individuals with schizophrenia and healthy controls (chapters 1.4.2, 1.4.3 and 2.2.4.3), the established functional role of the VTA in working memory and dopaminergic modulation in basic neuroscience (chapter 1.3.1, chapter 1.3.2 and chapter 2.2.2.2) and novel findings of the functional role of the VTA in working memory in humans by findings of FA, FC (fMRI, Murty et al., 2011; D'Ardenne et al., 2012; Xu et al., 2013; Yu et al., 2013; D'Aiuto et al., 2014) and pharmacological

occupancy in clinical and cognitive neurosciences (PET, Mehta et al., 2008). The heuristic search protocol for the application of nonlinear DCM for fMRI (chapter 3.4.5.2) was applied to the "N-Back" task of this study. Therefore, the chapters referring to the DCM scan processing and results (chapter 4.3.7 and chapter 4.4.4) follow the outline as given in the appropriate methods and results from chapter 3 (chapter 3.4.5 and chapter 3.5.3). Lastly, the findings are discussed in context of possibly altered synaptic plasticity and gating mechanism in schizophrenia (chapter 4.5).

4.2 Overall aim

The aim of the current study was to examine potentially altered neurobiological mechanisms underlying verbal working memory in fMRI data with nonlinear DCM for EST and healthy controls. Altered EC measures from nonlinear modulation may resemble disrupted synaptic plasticity and gating mechanisms of the meso-cortical connection during verbal working memory in schizophrenia (chapter 2.2.2.2). For the current study, it was hypothesised that EST would show altered connection strength with nonlinear modulation of the meso-cortical connection and/or cortico-mesal connection during the verbal "N-back" task compared to healthy controls.

In chapter 3, we presented the application of nonlinear DCM to the EHRS study. We found evidence for altered activity-dependent synaptic plasticity processes, which are thought to be of nonlinear nature. These nonlinear processes or gain modulations (Abbot et al., 2007; Rothman et al., 2009; Salinas and Sejnowski, 2001; Shu et al., 2003) have been suggested as being involved in working memory processes (Salinas

and Abbot, 1996; Salinas and Sejnowski, 2001). Furthermore, it has been proposed that gating processes during working memory may be altered in schizophrenia (Wang et al., 2010).

As described in the previous chapter of the DCM EHRS study, nonlinear DCM for fMRI assesses inhibitions of a neuronal connection and provides a means to model nonlinearities in fMRI tasks (Stephan and Friston, 2010; Stephan et al., 2008). Thus, the heuristic search protocol from the DCM EHRS study was applied to the "N-back" task. The DCM specification followed the same guidelines as outlined in chapter 3.4.5.1 and 3.4.5.2. Therefore, the model space was defined on the basis of the between-group FA results during the "N-Back" task. The bidirectional connection between the DLPFC and the ipsilateral VTA/SN area was modelled with connection strength with nonlinear modulation based on neurobiological findings of gating mechanism during working memory in schizophrenia (chapter 2.2.2.2).

4.3 Methods

For this study, verbal working memory fMRI data from EST and matched healthy controls were analysed with DCM for fMRI. These subjects were drawn from a large study, the SFMHS, which encompassed family members with the DISC1 translocation (Blackwood et al., 2001), family members without the translocation, EST, patients with bipolar disorder, FEP and healthy controls. The SFMHS is a multimodal imaging study, which is funded through a Pfizer Grand Challenge Fund project.

Recruitment for the DISC1 family encompassed areas of the Borders, Galloway, Dumfries, Glasgow and North Lanarkshire. EST and healthy volunteers were recruited from Edinburgh and Midlothian. The study was approved by the local Research Ethics Committee and institutional review board. All participants provided written informed consent.

The EST and healthy controls subject selection for the DCM study was determined by the behavioural performance during the fMRI verbal "N-back" task. The level of task performance was assessed using the sensitivity index *d'* as part of the signal detection theory (MacMillan and Creelman, 1991). The statistical analyses of the demographic, clinical and behavioural measures were conducted in SPSS (SPSS BMI 19.0).

The scan pre-processing, statistical analysis for the FA and the DCM analyses were run in SPM8 (update revision number 3684) running in Matlab (version 7.1; The MathWorks, Natick, MA, USA). The DCM analyses were run using DCM8.

Standard SPM processing was performed for the scan pre-processing and the statistical analyses. For the pre-processing, the same settings were applied as detailed in chapter 3.4.4.1. The methodological approach of the bilinear and nonlinear DCM analyses as described in chapter 3.4.5 was applied to the "N-Back" fMRI data. The model space was limited to interhemispheric models to account for: (i) Drop-out of EST and HC based on the lack of BOLD response of the VTA/SN area; and (ii) Enabling the modelling of connection strengths with nonlinear modulation in the "N-Back" task.

(i) Given the 'novel' role of the VTA/SN area in working memory in humans, it was possible that not every participant could be included for the DCM analyses with stringent requirement for subject and ROI selection (see chapter 3.4.5.1). In particular, it was not possible to foresee how many participants would show BOLD response of the VTA/SN area at the required threshold level.

(ii) Nonlinear DCM for fMRI has not been applied to the "N-Back" task previously. Thus, we focused on the systematic investigation of the connection strengths with nonlinear modulation in inter-hemispheric models.

4.3.1 Study populations

EST and matched healthy controls were recruited as part of the SFMHS from spring 2011 to winter 2013. Potential EST were identified through the research register of the Scottish Mental Health Research Register (http://www.smhrn.org.uk/), mental health services in Edinburgh, by contacting consultant psychiatrists throughout NHS in Edinburgh or hospital medical notes. Healthy participants were recruited through the Research Register as well through the social network of the patients and matched to the EST. The healthy volunteers had no family history of schizophrenia or any other major psychiatric illness. Exclusion criteria included history of severe brain injury, dependency or harmful use of alcohol or drugs for the last 12 months. MRI scanning safety was ensured. The study was approved by the South East Scotland Research Ethics Committee of the University of Edinburgh. All subjects provided written informed consent.

In this chapter, DCM findings are presented from 18 healthy controls and 13 EST for the left hemisphere and 16 healthy controls and 15 EST for the right hemisphere. The different inclusion numbers of healthy controls and EST for the left and right hemispheres are based on the fact that no every healthy control or EST showed activation of the bilateral VTA/SN area or bilateral IPS (details are presented in chapter 4.3.7.1). Full details of demographic and clinical details of the included participants for the DCM analyses are displayed in Table 4.2. FMRI scans from a total number of 25 healthy controls and 26 EST were considered for the study. Two HC and eight EST were excluded because of poor behavioural performance during the "N-back" task. The cut-off for poor behavioural performance was set at $d' < 1.93$ which equals a hit rate < 85% and a FAlarm > 20%. "N-back" fMRI data from 21 healthy controls and 16 EST were statistically analysed, after scans of two healthy controls and two EST were discarded due to movement or poor scan quality. For the DCM analyses in the left hemisphere, three healthy controls and three EST were excluded, whereas five healthy controls and one EST were excluded for the right hemisphere due to lack of required activation of the bilateral VTA/SN area or bilateral IPS (details are presented in chapter 4.3.7.1).

At the time of scan (or within a week of the scan) all subjects, both EST and healthy controls, underwent the clinical PANSS interview (Kay et al., 1987), the Scale for Assessment of Negative Symptoms (SANS (Andreasen, 1989) and the Global Assessment of Functioning (GAF; Hall, 1995). The rescaled PANSS scoring system and the standard scoring system for the SANS were used. A clinical diagnosis of established schizophrenia in accordance with DSM-IV-TR (American Psychiatric Association, 2000) and full psychiatric mental records were assessed by two

experienced clinicians. At the time of the scan, none of the EST had acute psychotic symptoms. All EST were on antipsychotic medication (Table 4.3).

4.3.2 Functional experimental details

EST and healthy controls performed the verbal "N-back" task (Kirchner, 1958) in the scanner. After pilot scans with healthy controls, who were naïve to the "N-back" task, it was considered that the "3-back" task was too difficult to perform for healthy volunteers and EST. Thus, the "2-back" task was chosen, which is in keeping with reported FA, FC and EC findings of the "N-back" task in schizophrenia studies. These studies repeatedly showed robust DLPFC BOLD responses in healthy controls and individuals with schizophrenia.

Task instructions were given before entering the scanner and in the scanner. An instruction for each block was displayed at the beginning of the next condition. Stimuli were presented visually on a screen, which the subjects could see through goggles mounted on the head coil. The goggles contained corrective lenses, which could be adjusted when necessary. The subjects received both a left-hand and a right-hand push button unit, which was synced with the experimental programme Presentation® provided by Neurobehavioural Systems (operating system Microsoft Windows http://www.neurobs.com/). The subjects were instructed to press their right index finger for target stimuli and their left index finger for non-target stimuli.

The experimental paradigm was a block design (Broome et al., 2009), which consisted of three conditions: (i) Baseline condition ("0-back"), (ii) Low working memory load ("1-back"), and (iii) High working memory load ("2-back"). The subjects were presented with a sequence of single capital letters appearing one at a

time on the centre of the screen. For the "0-back" condition, subjects were instructed to press the right button when the letter "X" was presented and the left button for all other letters. For the "1-back" condition, the target stimulus was defined as the identical match between the current letter and the letter one turn back. For the "2-back" condition, subjects were supposed to detect the target stimulus which was the same letter as the letter two turns back. The subjects were asked to respond as quickly as possible.

The block conditions were ordered by increasing working memory load from "0-back" (A) to "1-back" (B) to "2-back" (C). This block sequence was presented in three trials (A B C A B C A B C). During each block, stimuli were presented for 1000 ms and each stimulus was preceded by 2000 ms of instructions. There were 14 letters in each block with four target stimuli. The task lasted for 7.21 min.

The block design enabled to analyses the fMRI data with a parametric contrast of increasing activation with increasing working memory load ("0-Back" versus "2-Back") and the standard subtraction analyses for (i) "0-back" versus "1-back" and (ii) "1-back" versus "2-back".

4.3.3 Scanning procedure

Brain imaging was carried out at the Clinical Research Imaging Centre (CRIC) at the Queen's Medical Research Institute (Edinburgh, UK) on a Siemens 3 Tesla whole-body MRI Verio scanner (Siemens Medical Systems, Erlangen, Germany) using the matrix head coil with 12 elements.

An initial localizer scan was performed to measure the interhemispheric angle and the anterior commissure – posterior commissure (AC-PC) line. The structural images

were acquired using T_1-weighted, magnetisation prepared rapid acquisition gradient echo (MP-RAGE) images prescribed parallel to the AC-PC line, providing 160 sagittal slices of 1.0 mm thickness, 256 x 256mm^2 FOV, matrix size 256 x 256 mm^2. Further scan parameters were TR = 2300 ms, TE = 2.98 ms, TI = 900 ms and a flip angle = 9°.

EPI scans for the "N-back" task were acquired continuously during the experimental task (TR/TE = 1560/26 ms, matrix size of 256 x 256 mm^2; FOV 256 x 256 mm^2). Twenty six interleaved slices with 4 mm slice thickness were acquired within each TR period. Each EPI sequence encompassed 293 volumes of which the first 6 volumes were discarded.

4.3.4 Behavioural data

During the scanning, the behavioural performance in terms of response times (RTs) and accuracy were recorded in logfiles written in Presentation. RTs and accuracy were assessed separately for the hemispheres because a different number of participants entered in the DCM analyses for both hemispheres.

RTs were computed separately for the baseline condition "0-back", both working memory conditions "1-back" and "2-back" and for the overall performance across all conditions. Then, the RTs entered a GLM with group and sex as fixed factors and age and IQ as covariates.

Accuracy of the behavioural performance was analysed with the sensitivity index *d'* as part of the signal detection theory using the formula (MacMillan and Creelman, 1991; Eq. [4.1]):

$$d' = z(Hits) - z(FAlarm) \quad [4.1]$$

z = statistical Z value

FAlarm = False alarm

Hits and false alarm (FAlarm) rates of zero and one were adjusted as previously described (MacMillan and Kaplan, 1985). The task performance was separately calculated for the "1-back", the "2-back" condition and the overall performance across all conditions. A higher d' value denotes a higher accuracy in performance. The *d'* values entered a GLM with group and sex as fixed factors and age and IQ as covariates.

4.3.6 Scan pre-processing and statistical analysis

The scan pre-processing, statistical analysis for the FA and the DCM analyses were run in SPM8. The DCM analyses were run using DCM8.

Standard processing was performed for the scan pre-processing and the statistical analyses. For the pre-processing, the settings described in chapter 3.3.4 were applied with appropriate adjustments for the specific scanning in this data set. The DCM requirements for the pre-processing as detailed in chapter 3.4.4.1 for the parameters for spatial smoothing and oversampling the voxel size have been adopted for this study. The pre-processing was run using batch scripts to ensure the identical processing for each individual.

For the current study, specific requirements have been defined in addition to the standard conditions of good scan quality and movement within 3 mm to ensure the

application of nonlinear DCM and to allow the interpretation of the EC results. The three requirements were:

(i) Subject selection for the scan processing and DCM analyses based on the behavioural performance;

(ii) Error condition in the GLM for the statistical scan analyses;

(iii) Two pre-conditions for bilinear and nonlinear DCM analyses as part of the application of the heuristic protocol as outlined in chapter 3.4.5.2.

(i) Subjects with comparable high behavioural performance between healthy controls and EST were selected. The criterion for inclusion was d' value > 1.93, which was congruent with a hit rate > 85% and a FAlarm rate of < 20% (see chapter 4.3.1). Therefore, the interpretation of the hypothesised altered connection strengths with nonlinear modulation will not be confounded by differences in task performance.

(ii) FAlarm as identified during the behavioural analysis were modelled separately in each subject. This condition ensured the identification of the VTA/SN area in the parametric contrast (increased activation with increased working memory load; "0-Back" versus "2-Back").

(iii) The modelling of the error condition from the statistical analyses ensured the examination of the two pre-conditions for the DCM analyses: (i) The connection strength with driving inputs into the VTA/SN area could be modelled and assessed and (ii) the connection strength with nonlinear modulation of the bidirectional connection between the DLPFC and the VTA/SN area could be modelled and assessed.

4.3.6.1 Spatial pre-processing

The first six acquisitions were discarded to ensure that the steady state of the magnetisation was fulfilled before the experimental paradigm started.

4.3.6.1.1 Realignment

The change in TR (1560 ms) and number of acquisitions (n = 293) in the EPI acquisition for the "N-back" task had been accordingly amended for the pre-processing of the scans.

The EPI time series for each single subject were registered to the mean in the series to remove movement artefacts and the mean image was created. The maximum level of movement for each individual was assessed based on the graphical output and the movement regressors written for the three orthogonal imaging planes.

4.3.6.1.2 Normalisation

The same settings from the EHRS were applied to the working memory data. The mean image was determined for the definition of the parameters. The images were normalised to an SPM8 EPI template and resampled using sinc interpolation to cubic sized voxels of 1 x 1 x 1 mm^3 (please see chapter 3.4.4.1.2).

4.3.6.1.3 Spatial smoothing

Following the pre-processing protocol from the EHRS, the normalised scans were spatially smoothed with a 8 x 8 x 8 mm^3 FWHM Gaussian filter to ensure the conditions needed for the parametric analyses (please see chapter 3.4.4.1.3).

4.3.6.1.4 Visual inspection

The same procedure for the visual inspection was performed as described in chapter 3.4.4.1.4. Two healthy controls were excluded at this stage because of poor image quality (assumed to result from excessive scanner noise) as reported in the chapter 4.3.1. Two EST were excluded at this stage of the analysis because of significant movement artefact of > 3 mm peak to peak.

4.3.6.2 Statistical analysis

The first level statistical analyses were run using batch scripts. The scripts were devised from the basis of SPM scripts.

4.3.6.2.1 First level analysis

In this study, at the single subject level the data was modelled with three "N-Back" conditions ("0-back", "1-back" and "2-back") in the first three columns. The fourth and fifth column correspond to the behavioural correct responses (hits) and incorrect responses (FAlarm). As previously described (chapter 3.4.4.2.1, each condition was modelled by a boxcar convolution with the hrf as implemented in SPM8. Similarly, the movement regressor for each individual was entered as 'covariates of no interest' within the GLM.

The settings applied for the estimation of the design matrix followed the settings in chapter 3.4.4.2.1:

- Single subject filtering in the time domain:
- Low pass filter (Gaussian kernel, 4 s (FWHM))
- High pass filter (400 s cut-off)

Three contrasts were constructed to test areas of activation:

(i) Parametric contrast/"0-Back" versus "2-Back": Increasing activation with increasing working memory load under the assumption of linear memory load from "0-Back" to "2-Back": ([-1 0 1]);

(ii) Standard subtraction analysis: "0-back" versus "1-Back" ([-1 1 0]);

(iii) Standard subtraction analysis: "1-back" versus "2-back" ([0 -1 1]).

4.3.6.2.2 Second level analysis

The contrast images of each individual for the parametric contrast ("0-back" versus "2-back") and the conditions for low working memory load ("0-back" versus "1-back") and high working memory load ("1-back" versus "2-back") were entered into a second level random effects analysis in order to infer on differential activations between the EST and the healthy controls. A one sample t-test was run to define the areas of activation within each of the group before a two sample t-test was used to determine differences in activation between the two groups.

For both the within-group and the between-group analyses, statistical parametric maps were thresholded at the level of $p = .001$, uncorrected. Regions are reported that survived cluster-level correction for multiple comparisons across the whole brain at $p < .05$. Previous reports on FA of the VTA/SN area applied a threshold of $p < .05$ FDR to the statistical maps (Genovese et al., 2002). We followed these settings for the VTA/SN area. The coordinates were converted and identified as previously described in chapter 3.4.4.2.2.

4.3.6.2.2.1 Parametric contrast

The main interest was to examine group differences of increasing activation with increasing working memory load ("0-back" versus "2-back").

Both groups were matched on age and gender (chapter 4.4.1). Nonetheless, for confidence reasons, these two factors were entered as covariates in the second level random effects for the within-group and between-group analyses. IQ has not been entered following the common approach in clinical studies. However, IQ has indirectly been corrected for when EST were selected based on the behavioural performance level in the "N-Back" task.

4.3.6.2.2.2 Standard subtraction analyses

For completion, the two subtraction contrasts for low and high working memory loads were tested for group differences in FA. Both EST and healthy controls were matched on age, gender and movement measures. As reported in chapter 4.3.6.2.1 these factors were defined as covariates in the second level random effects analyses. IQ has not been entered.

4.3.7 Functional Integration – Bilinear and nonlinear Dynamic Causal Modelling for fMRI data

The bidirectional connections between the DLPFC and the VTA/SN area were modelled to investigate the possibility of altered connection strength with nonlinear modulation during verbal working memory between EST and healthy controls.

Evidence from preclinical studies suggests that the meso-cortical connection and/or the cortico-mesal connection are gated by neuronal regions in the VTA and the

DLPFC in schizophrenia (chapter 2.2.2.2). Thus, the heuristic search protocol for the application of nonlinear DCM for fMRI (chapter 3.4.5.2; Figure 3.1; Dauvermann et al., 2013) was applied to the fMRI "N-Back" task to assess connection strength with nonlinear modulation of this bidirectional connection.

The bilinear and nonlinear DCM analyses of the "N-Back" task were performed using DCM8 as implemented in SPM8 which was the identical version used for the DCM analyses and followed the previously presented outline of chapter 3.4.5. Specific changes in the application of the DCM methods in contrast to the EHRS DCM study are outlined specifically in the following subchapters:

- Subject and ROI selection (chapter 4.3.7.1)
- Model Space for the DCM analyses (chapter 4.3.7.2)
    - Model Space for Bilinear Models (chapter 4.3.7.2.1)
    - Model Space for Nonlinear Models (chapter 4.3.7.2.2.1)
    - Model Space Partitioning – Family Level Inference (chapter 4.3.7.2.2.2).

The DCM analyses were run separately for the groups and for the hemispheres.

4.3.7.1 Subject and ROI selection

The main finding from FA results for the between-group analysis for the parametric contrast was that EST showed significantly reduced activation of the DLPFC (BA9/BA46), the IPS (BA40), the dorsal ACC (dACC; BA32) and the VTA/SN area in contrast to the healthy controls (chapter 4.4.3.2.1). The VTA/SN area was included in the models in addition to the established regions of the DLPFC, IPS and

ACC in working memory in humans to model the functional involvement of the midbrain region in working memory/dopaminergic modulation as widely accepted evidence in preclinical research (chapter 1.3.1, chapter 1.3.2 and chapter 2.2.2.2). The inclusion of the VTA/SN area further received support from recent fMRI and PET studies in humans that reported on the functional role of the VTA/SN area in working memory in healthy controls (Murty et al., 2011; D'Ardenne et al., 2012; Xu et al., 2013; Yu et al., 2013) and EST (D'Aiuto et al., 2014). The coordinates of the VTA/SN area are in keeping with previous studies on the VTA/SN area in working memory (Tomasi et al. 2007; Murty et al. 2011; D'Ardenne et al. 2012; Yu et al. 2013; D'Aiuto et al. 2014).

The time series of these four regions were extracted. The coordinates of the four ROIs are given in Table 4.1 according to the standard Talairach and Tournoux atlas (Talairach and Tournoux, 1988).

The ROI selection followed the same procedure of the time series extraction as reported in chapter 3.4.5.1 (Dauvermann et al., 2013). Briefly, the four ROIs were selected by extracting the time series from the individual's activation map of the parametric contrast thresholded at $p < .05$ uncorrected at the closest maxima within a standard distance of 8 mm of the group peak level for the IPS and DLPFC and adjusted distance of 6mm of the group peak level for the dACC and the VTA/SN area. These time series extraction rationales ensured the consistent selection of functional regions to be included for the DCM analyses across all subjects (Stephan et al., 2007).

The subjects were selected on the basis of the requirement of activation in all four ROIs in the left or the right hemisphere. This process led to the exclusion of three

healthy controls and three EST, who did not show activation of the left VTA/SN area or the left IPS. For the right hemisphere, five healthy controls and three EST were excluded because of lack of BOLD response of the right VTA/SN area. Demographic details of the included subjects for the DCM analyses of each hemisphere are given in Table 4.2. Clinical details of the participants for both hemispheres are presented in Table 4.3.

Table 4.1 Coordinates of the four ROIs for the DCM analyses.

	Coordinates in Talairach Space (L/R)	
IPS, BA40	-44, -46, 42	49, -47, 30
DLPFC, BA9/BA46	-46, 25, 31	41, 29, 17
dACC, BA32	3, 36, 26	
VTA/SN area	-9, -17, -6	7, -17, -3

dACC, dorsal anterior cingulate cortex, DLPFC, dorsolateral prefrontal cortex, IPS, intra parietal sulcus, VTA/SN area, ventral tegmental area/substantia nigra area.

4.3.7.2 Heuristic study protocol for bilinear and nonlinear Dynamic Causal Modelling

The hypothesis of this study was that EST would show altered connection strengths with nonlinear modulation of the connection between the DLPFC and the VTA/SN area. To this end, we used the heuristic study protocol from the EHRS DCM study (chapter 3.4.5.2; Dauvermann et al., 2013) and applied it to the "N-Back" task of the SFMHS. The logic of the current DCM study was drawn from the EHRS DCM study.

Briefly, the three phases of the protocol are outlined for the current DCM study on the fMRI "N-Back" task in healthy controls and EST:

(i) In phase 1, bilinear DCM was run to test the structure of the "N-back" task for healthy controls and EST separately (chapter 4.3.7.2.1);

(ii) In phase 2, nonlinear DCM was used to model the connection strengths with nonlinear modulation between the DLPFC and the VTA/SN (chapter 4.3.7.2.2);

(iii) In phase 3, the connection strengths with the nonlinear modulation for the bidirectional connection between the DLPFC and VTA/SN area within the winning models were assessed with BMA (chapter 4.3.7.2.3).

The three phases of the DCM analyses were run separately for the left and right hemispheres.

4.3.7.2.1 Phase 1: Bilinear Dynamic Causal Modelling

The four conditions for biophysical modelling with DCM have been outlined in chapter 3.4.4. Those conditions were applied to the fMRI "N-Back" scans of this study.

4.3.7.2.1.1 Model space of bilinear models

Findings from preclinical neurobiological and clinical neuroimaging studies provide the basis of the specification for regions, connections and modulations for the linear DCMs. In total, the model space of bilinear models was comprised of nine DCMs.

The involvement of the four regions of the DLPFC, IPS, AC (coordinates in Table 4.1) for the "N-back" task in individuals with schizophrenia are well established. Clinical fMRI and PET studies during the "N-back" task repeatedly reported on the involvement of the DLPFC, IPS and AC in terms of FA, FC and EC measures during the "N-back" task in EST and healthy controls (chapters 1.4.2, 1.4.3, 2.2.4.3). For FA findings, both increased and reduced BOLD responses of the DLPFC, IPS and AC

for the low and high working memory load were observed in EST when compared to healthy controls (chapter 1.4.2). FC studies provided further support for reductions in FC measures between (i) the DLPFC and IPS and (ii) the DLPFC and AC in EST in contrast to healthy controls (1.4.3). Altered EC measures during the verbal/numeric "N-back" task presented evidence for decreased EC (effect of task modulation) from the DLPFC to the PC in EST in contrast to healthy controls (2.2.4.3).

The inclusion of the AC in the DCMs was based on the findings of its role in error monitoring and error conflict (Becerril et al., 2011; Wang et al., 2010; Brázdil et al., 2007; Krawitz et al., 2011), which is implicated in working memory processes (Botvinick et al., 2001; Kerns et al., 2004).

The VTA/SN area as the fourth region in the models was selected due its known functional role in working memory from preclinical (chapter 1.3.1, chapter 1.3.2) and computational modelling studies (chapter 2.2.2.2). Such studies reported evidence for dopaminergic alterations of the meso-cortical connection, glutamatergic alterations of the cortico-mesal connection and interactions between dopaminergic and glutamatergic alterations of the DLPFC – VTA/SN area – circuits.

In recent years, clinical and cognitive neuroscientific studies showed that the VTA/SN area is functionally implicated in working memory function in healthy controls (FA, Tomasi et al. 2007; Murty et al., 2011; D'Ardenne et al., 2012; Yu et al., 2013) and EST (D'Aiuto et al., 2014) as well as functional networks in healthy controls (FC, Xu et al. 2013).

The specification of the endogenous connections (matrix *A*), connections with modulatory input (matrix *B*) and effects of driving inputs (matrix *C*) follows evidence provided by preclinical neurobiological and clinical neuroimaging studies. Endogenous connections between the regions were specified by neurotransmitter projections such as dopaminergic projections from the VTA/SN area to the DLPFC (Au-Young et al., 1999; D'Ardenne et al., 2012; Gao and Wolf, 2007; Takahata and Moghaddam, 1998; Girault and Greengard, 2004) and glutamatergic projection from the DLPFC to the VTA/SN area. The bidirectional connection between the ACC and the VTA/SN area was defined on the basis of known dopaminergic projections (Onn and Wang, 2005). FC and EC findings were used to specify functional connections between the IPS and the DLPFC (FC, Tan et al., 2006; Rasetti et al., 2011; Quidé et al., 2013; EC, Deserno et al., 2012; Schmidt et al., 2013; Zhang et al., 2013), the IPS and ACC (FC, Meyer-Lindenberg et al., 2001; EC during a similar task, Brázdil et al., 2007) and the DLPFC and the ACC (Brázdil et al., 2007).

Connections with modulatory input were defined by the experimental manipulation of the "N-back" task, namely the parametric modulation of the task ("0-back" versus "2-back"). Evidence for (parametric) working memory load effect and interactions effects with working memory load has been provided by fMRI studies during the "N-back" task in healthy subjects and subjects with schizophrenia for (i) FA results of bilateral subregions of the PFC (including the DLFC), bilateral IPL, AC (fMRI studies, Callicott et al., 2000; Perlstein et al., 2001; Callicott et al., 2003; Thermenos et al., 2005; Tan et al., 2006; Rasetti et al., 2011; Guerrero-Pedraza et al., 2012; Quidé et al., 2013; (ii) FC measures of bilateral subregions of the PFC (including the

DLFC) and bilateral IPL (Tan et al., 2006; Rasetti et al., 2011; Quidé et al., 2013) and (iii) EC measures of bilateral subregions of the PFC (including the DLFC) and bilateral IPL (Deserno et al., 2012; Schmidt et al., 2013; Zhang et al., 2013). Based on these clinical findings, the connection from the IPS to the DLPFC was specified by the parametric modulatory experimental input.

Driving input or matrix *C* was defined by DCM studies, which reported evidence of effects of visual presentation of stimuli to the IPS (during a similar task, Brázdil et al., 2007; Wang et al., 2010). The role of the VTA/SN area in working memory has been reported previously (D'Ardenne et al., 2012).

The nine DCMs differed in their unidirectional and bidirectional connections between the four regions (defined by matrix *A*). The specifications of the matrices *B* and *C* across the nine DCMs were identical. The nine DCMs are displayed in Figure 4.1.

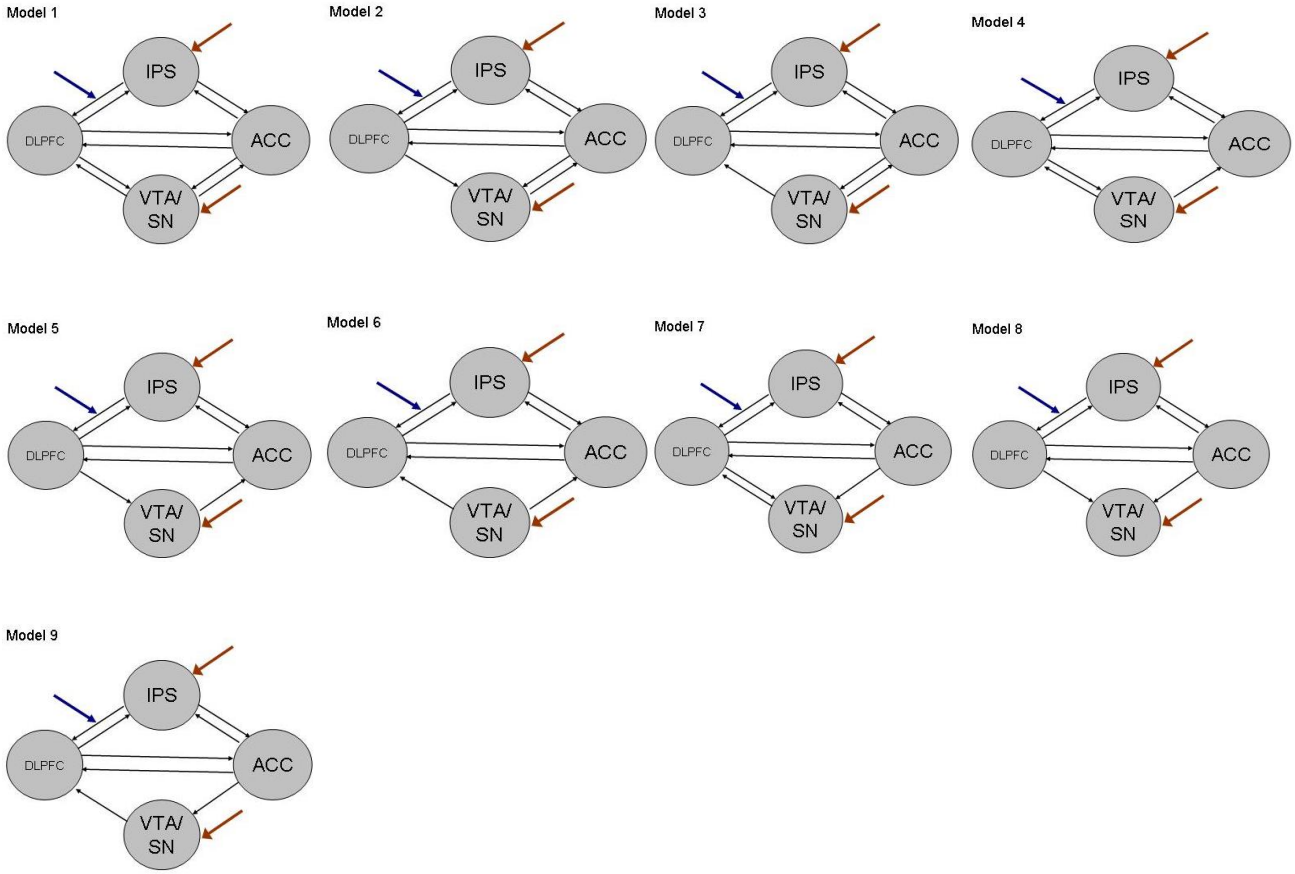

Figure 4.1 Model space of linear models.

All nine models are characterised by bidirectional endogenous connections between the IPS and DLPFC, IPS and ACC and DLPFC and ACC. Furthermore, all models are defined by a modulatory input on the connection from the IPS to the DLPFC. All models receive driving two inputs: One driving input (presented visual stimuli, i.e. single letters) enters the IPS; and one driving input (FA) enters the VTA/SN area.

The nine models differ in the specification of unidirectional or bidirectional endogenous connections: (i) Between the DLPFC and the VTA/SN area and (ii) between the ACC and VTA/SN area.
Model 1 is specified by a bidirectional endogenous connection (i) between DLPFC and VTA/SN area and (ii) ACC and VTA/SN area.
Model 2 is specified by a unidirectional endogenous connection from DLPFC to VTA/SN area and a bidirectional endogenous connection between ACC and VTA/SN area.
Model 3 is specified by a unidirectional endogenous connection from VTA/SN area to DLPFC and a bidirectional endogenous connection between ACC and VTA/SN area.
Model 4 is specified by a bidirectional endogenous connection between DLPFC and VTA/SN area and a unidirectional endogenous connection from VTA/SN area to ACC.
Model 5 is specified by a unidirectional endogenous connection from DLPFC to VTA/SN area and a unidirectional endogenous connection from VTA/SN area to ACC.
Model 6 is specified by a unidirectional endogenous connection from VTA/SN area to DLPFC and a unidirectional endogenous connection from VTA/SN area to ACC.
Model 7 is specified by a bidirectional endogenous connection between DLPFC and VTA/SN area and a unidirectional endogenous connection from ACC to VTA/SN area.
Model 8 is specified by a unidirectional endogenous connection from DLPFC to VTA/SN area and a unidirectional endogenous connection from ACC to VTA/SN area.
Model 9 is specified by a unidirectional endogenous connection from VTA/SN area to DLPFC and a unidirectional endogenous connection from ACC to VTA/SN area.

4.3.7.2.1.2 Random effects Bayesian Model Selection

BMS at the group level has been applied to models of both hemispheres in EST and healthy controls separately as outlined in chapter 3.4.5.2.1.3.

4.3.7.2.2 Phase 2: Nonlinear Dynamic Causal Modelling

The theoretical argumentation for the modelling of the connection strengths with nonlinear modulation follows the logic of the EHRS DCM study based on hypothesised altered connection strengths with nonlinear modulation in a parametric fMRI task. Thus, the definition of the model space of the nonlinear DCMs has been applied according to the protocol as outlined in chapter 3.4.5.2.2.2 (chapter 4.3.7.2.2.1). Necessary changes concerning the partition of the model space into model family are presented.

4.3.7.2.2.1 Model space of nonlinear models

The model space of nonlinear models was comprised of four nonlinear models in congruence with chapter 3.4.5.2.2.2. In keeping with the BMS approach at the group level as outlined in phase 1 of the protocol (column 1; Figure 3.1), the optimal bilinear model for the EST and the healthy controls functions as the "basic" structure of the nonlinear DCMs.

For both hemispheres, the winning linear model for EST was Model 1; whereas as Model 7 was the optimal model for healthy controls.[5] Therefore, the nonlinear

[5] For the right hemisphere in the healthy subjects, Model 7 was chosen to enter this phase of the DCM analyses instead of Model 8. As displayed in Table 4.15, the *Xp* of Model 8 (*Xp* = 0.23) was greater than the *Xp* for Model 7 (*Xp* = 0.16) or Model 2 (*Xp* = 0.18). Models 8 and 2 are characterised by a unidirectional endogenous connection from the DLPFC to the VTA/SN area, whereas Model 7 (Figure 4.1) is defined by a bidirectional connection between the DLPFC and the VTA/SN area.

models were defined separately for EST and healthy controls. However, the aim of modelling the bidirectional connection between the DLPFC and the VTA/SN area with nonlinear modulation remained the common goal for both groups.

For EST, two nonlinear models were constructed on the structure of the winning Model 1 with the nonlinear modulation from the DLPFC to both connections between the DLPFC and the VTA/SN area (i.e. nonlinear models – DLPFC). Two further models were defined on the basis of Model 1 by connecting the nonlinear modulation from the VTA/SN area to the connections between the DLPFC and the VTA/SN (i.e. nonlinear models – VTA/SN; Figure 4.2).

Model 7 was selected instead of Model 8 in order to enable the modelling of the bidirectional connection between the DLPFC and the VTA/SN area.

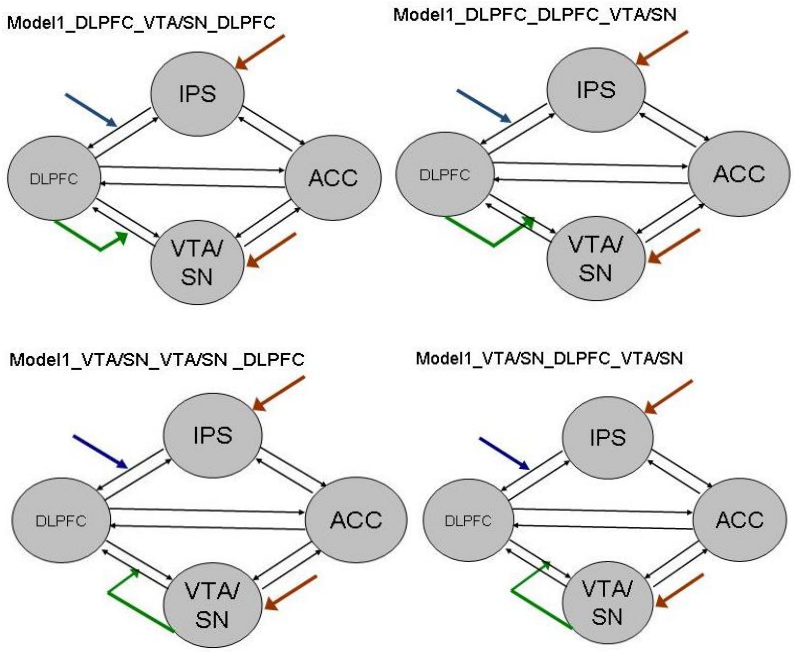

Figure 4.2 Four nonlinear models for subjects with established schizophrenia.

The nonlinear models are specified on the basis of the winning Model 1 in EST. The endogenous connections, modulatory input and driving inputs are defined as in Model 1 (Figure 4.1).
Model 1_DLPFC_VTA/SN_DLPFC and Model 1_DLPFC_DLPFC_VTA/SN are characterised by the nonlinear modulation from the DLPFC on the bidirectional connection between VTA/SN area and DLPFC. Both models are specified upon the winning bilinear model and form model family 2.
Model 1_DLPFC_VTA/SN_DLPFC is specified by the nonlinear modulation from DLPFC to the connection from VTA/SN area to DLPFC.
Model 1_DLPFC _DLPFC_VTA/SN is specified by the nonlinear modulation from DLPFC to the connection from VTA/SN area to DLPFC.
Model 1_VTA/SN_VTA/SN_DLPFC and Model 1_VTA/SN_DLPFC_VTA/SN are characterised by the nonlinear modulation from the VTA/SN area on the bidirectional connection between VTA/SN area and DLPFC. Both models are specified upon the winning bilinear model and form model family 3.
Model 1_VTA/SN_VTA/SN_DLPFC is specified by the nonlinear modulation from VTA/SN area to the connection from DLPFC to VTA/SN area.
Model 1_VTA/SN_DLPFC_VTA/SN is specified by the nonlinear modulation from VTA/SN area to the connection from VTA/SN area to DLPFC.

For healthy controls, two nonlinear models were constructed on the basis of winning Model 7 with the nonlinear modulation from the DLPFC to the connections between the DLPFC and the VTA/SN area (i.e. nonlinear models – DLPFC). Two further models were defined on the basis of Model7 with nonlinear modulation from the VTA/SN area to the connections between the DLPFC and the VTA/SN area (i.e. nonlinear models – VTA/SN area; Figure 4.3).

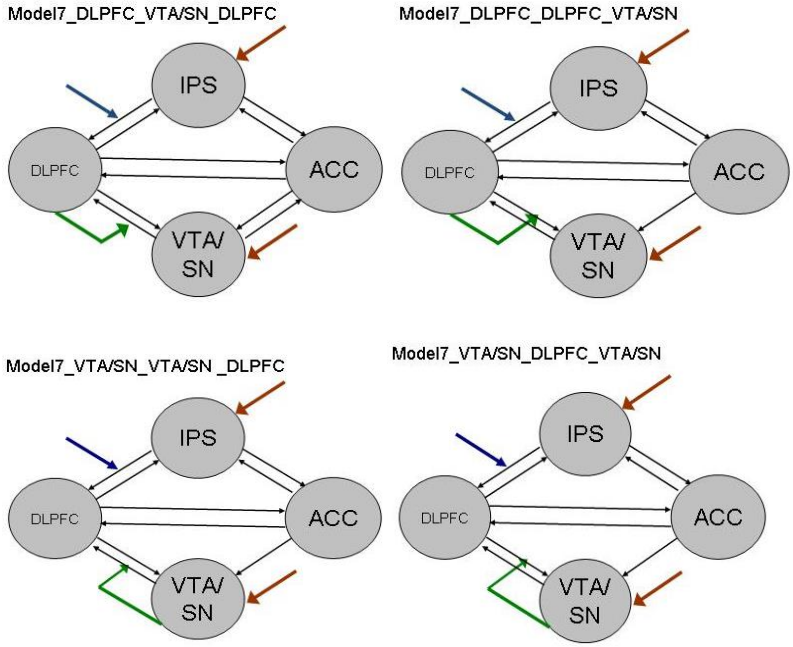

Figure 4.3 Four nonlinear models for healthy controls.

The nonlinear models are specified on the basis of the winning Model7 in healthy controls. The endogenous connections, modulatory input and driving inputs are defined as in Model 7 (Figure 4.1).

Model 7_DLPFC_VTA/SN_DLPFC and Model 7_DLPFC_DLPFC_VTA/SN are characterised by the nonlinear modulation from the DLPFC on the bidirectional connection between VTA/SN area and DLPFC.

Model 7_DLPFC_VTA/SN_DLPFC is specified by the nonlinear modulation from DLPFC to the connection from VTA/SN area to DLPFC.

Model 7_DLPFC _DLPFC_VTA/SN is specified by the nonlinear modulation from DLPFC to the connection from VTA/SN area to DLPFC.

Model 7_VTA/SN_DLPFC_VTA/SN and Model 7_VTA/SN_VTA/SN_DLPFC are characterised by the nonlinear modulation from the VTA/SN area on the bidirectional connection between VTA/SN area and DLPFC. Both models are specified upon the winning bilinear model and form model family 3.

Model 7_VTA/SN_DLPFC_VTA/SN is specified by the nonlinear modulation from VTA/SN area to the connection from VTA/SN area to DLPFC.

Model 7_VTA/SN_VTA/SN_DLPFC is specified by the nonlinear modulation from VTA/SN area to the connection from DLPFC to VTA/SN area.

4.3.7.2.2.2 Model Space Partitioning – Family Level Inference – Random effects Bayesian Model Selection

The previously described BMS inference approach at the model family level phase 2 of the protocol (column 2, Figure 3.1) has been applied to the current data set. The BMS analysis was separately run for both groups and each hemisphere. An example is shown for EST:

(i) Model Family 1: bilinear model

Model Family 1 contained the optimal bilinear model (Figure 4.1).

(ii) Model Family 2: nonlinear models – DLPFC

Model Family 2 contained the two nonlinear models with nonlinear modulation from the DLPFC (Figure 4.2).

(iii) Model Family 3: nonlinear models – VTA/SN area

Model Family 3 contained the two nonlinear models with nonlinear modulation from the VTA/SN area (Figure 4.2).

The exceedance probabilities for the two winning model families 2 and 3 were summarised as described in chapter 3.4.5.2.2.3.

4.3.7.2.3 Phase 3: Bayesian Model Averaging

The objective of the BMA analysis was to assess posterior densities of the connection strength with nonlinear modulation for the meso-cortical and cortico-mesal connection in the winning models from the previous step of the BMS approach. BMA has been applied to the winning models from the BMS analysis at the model family level for both groups.

4.4 Results

The results of demographic and clinical details, behavioural performance and EC analyses are presented separately for the left and right hemispheres because different numbers of participants were included for the analyses in each hemisphere. For the left hemisphere, 18 healthy controls and 13 EST entered the DCM analyses, whereas 16 healthy controls and 15 EST were included for analyses in the right hemisphere.

4.4.1 Demographic and clinical details

The demographic details (Table 4.2) and clinical details (Table 4.3) are given for the final subject inclusion for the DCM analyses. Those DCM analyses were performed separately for the left and the right hemispheres. The results of significance levels are comparable between the two hemispheres.

In summary for both hemispheres, both EST and healthy controls did not differ from each other in mean age, sex or handedness (Table 4.2). There was a significant difference for IQ between the groups (left hemisphere: t = 2.234, df 16, p = .034; right hemisphere: t = .043, df 16, p = .007). Healthy controls showed a significantly greater IQ than EST.

All EST were treated with a range of FGA and SGA with varying doses. Three EST received secondary antipsychotic medication and ten EST took additional medication such as antidepressants, mood stabilisers and anticholinergics.

Table 4.2 Demographic details for subjects included in the DCM analyses.

	Healthy controls (L/R)		EST (L/R)		Test (L/R)		*p* – Value (L/R)	
Number	18	16	13	15	_	_	_	_
Mean age (SD)	35.00 (14.96)	34.31 (13.90)	36.46 (8.36)	37.07 (9.95)	t = -.346	t = -.637	p = .732	p = .529
Gender (M:F)	13:5	12:4	11:2	13:2	x^2= .663	x^2 = .675	p = .416	p = .411
Mean IQ (SD)	120.00 (7.81)	120.94 (7.29)	108.77 (16.12)	107.53 (15.53)	t = 2.324	t = .043	p = .034	p = .007
Handedness (R:L)	16:1[1]	15:0[1]	8:3[1]	10:3[1]	U = 82.500	U = 75.00	p = .394	p = .316
Level of Education (0:1: 2)[2]	(3:0:13)[1]	(1:0:13)[1]	(1:3:9)	(1:3:11)	x^2= 4.465	x^2 = 3.136	p = .107	p = .208

[1] Data missing.

[2] 0, Compulsory; 1, More than compulsory; 2, Post-Secondary.

Table 4.3 Clinical details for subjects included in the DCM analyses.

	Healthy controls (L/R)		EST (L/R)		Test (L/R)		*p* – Value (L/R)	
Number	18	16	13	15	-	-	-	-
Illness Onset (in years; mean (SD)	N/A	N/A	19.92 (3.10)	21.47 (6.14)	-	-	-	-
Illness Duration (in months; min – max (>99))	N/A	N/A	min 80 to max > 99	min 60 to max > 99	-	-	-	-
Total PANSS Score[1], mean (SD)	1.89 (5.16)	2.13 (5.44)	19.23 (14.27)	21.53 (14.56)	t = -3.84	t = -3.71	p < .001	p < .001
Total Positive Score, mean (SD)	0.39 (0.98)	0.44 (1.03)	5.46 (4.14)	6.00 (4.09)	t = -3.65	t = -3.77	p = .001	p < .001
Total Negative Score, mean (SD)	0.11 (0.32)	0.13 (0.34)	5.85 (5.00)	6.47 (4.94)	t = -3.83	t = -4.16	p = .001	p < .001
Total General Score, mean (SD)	1.39 (4.95)	1.56 (5.24)	10.54 (7.85)	9.20 (8.08)	t = -3.45	t = -2.91	p = .001	p = .004
Total SANS Score, mean (SD)	0.78 (2.37)	0.88 (2.50)	17.77 (15.78)	17.33 (15.09)	t = -4.13	t = -4.43	p = .01	p < .001
GAF Score, mean (SD)	Missing	Missing	48.00 (22.55)	49.93 (21.52)	-	-	-	-
Chlorpromazine equivalent dose[2], Mean (SD)	N/A	N/A	515.00 (410.06)	475.00 (400.55)	-	-	-	-
Antipsychotic medication[3]	N/A	N/A	(b) 5; (c) 1; (d) 4; (e) 3	(a) 1; (b) 5; (c) 1; (d) 5; (e) 3	-	-	-	-
Antipsychotic medication additional[4]	N/A	N/A	(a) 2; (b) 1	(a) 2; (b) 1	-	-	-	-
Other medication[5]	N/A	N/A	(a) 7; (b) 1; (c) 2	(a) 7; (b) 1; (c) 2	-	-	-	-

GAF, Global Assessment of Functioning
[1] Rescaled total PANSS scores.
[2] to 100 mg CPZ.
[3] (a) Aripiprazole, (b) Clozapine, (c) Depixol (depot), (d) Olanzapine, (e) Risperidone/Risperidone Consta depot.
[4] (a) Amilsulpride, (b) Chlorpromazine.
[5] (a) Antidepressant, (b) Mood Stabiliser, (c) Anticholinergics.

4.4.2 Behavioural performance

The results of RTs (Table 4.4) and behavioural accuracy (Table 4.5) for healthy controls and EST are given. The results are briefly summarised for both hemispheres. RTs were longer with increasing working memory load for both EST and healthy controls. However, there were no statistically significant differences between the two groups for the three experimental conditions nor across all conditions ("2-back" for the left hemisphere: F =1.527, df 25, p = .228; "2-back" for the right hemisphere: F =2.195, df 25, p = .151). There were no significant main effects for group and sex or for the interaction effect between group and sex.

Table 4.4 Response times during the "N-back" task in the scanner.

	Healthy controls (L/R)		EST (L/R)		Test (L/R)		p – Value (L/R)	
Number	18	16	13	15	_	_	_	_
RT overall (mean, SD)	3.77 (0.75)	3.68 (0.66)	3.86 (0.46)	3.88 (0.43)	F = .337	F = 1.118	p = .567	p = .300
RT "0-back" (mean, SD)	3.58 (0.53)	3.53 (0.49)	3.59 (0.48)	3.62 (0.45)	F = .095	F = .367	p = .761	p = .550
RT "1-back" (mean, SD)	4.09 (0.86)	4.05 (0.81)	4.17 (0.67)	4.18 (0.63)	F = .349	F = .507	p = .560	p = .483
RT "2-back" (mean, SD)	4.63 (1.18)	4.56 (1.13)	5.18 (0.74)	5.12 (0.70)	F = 1.527	F = 2.195	p = .228	p = .151

RT, response time.

The sensitivity indices did not reveal a significant difference across the task conditions between the two groups ("2-back" for the left hemisphere: F =1.527, df 25, p = .228; "2-back" for the right hemisphere: F =2.195, df 25, p = .151). There were no significant main effects for group and sex or for the interaction effect between group and sex. However, there was a significant effect of IQ (for the left hemisphere: F =9.717, df 1, p = .005; for the right hemisphere: F =10.623, df 1, p =

.003) and a significant effect of age (for the left hemisphere: F =4.718, df 1, p = .040; for the right hemisphere: F =4.437, df 1, p = .045).

Table 4.5 Task accuracy of behavioural performance during the "N-back" task in the scanner.

	Healthy controls (L/R)		EST (L/R)		Test (L/R)		p – Value (L/R)	
Number	18	16	13	15	_	_	_	_
d' values overall (mean, SD)	3.71 (0.38)	3.72 (0.40)	3.31 (0.39)	3.28 (0.37)	F = 3.018	F = 2.714	p = .095	p = .112
d' values "1-back" (mean, SD)	3.52 (1.37)	3.55 (1.46)	2.98 (0.25)	3.01 (0.24)	F = .916	F = .935	p = .348	p = .343
d' values "2-back" (mean, SD)	3.54 (2.00)	3.67 (2.10)	2.82 (0.31)	2.78 (0.30)	F = 1.322	F = 2.008	p = .261	p = .169

d', sensitivity index.

4.4.3 Functional activation

The results for the within-group and between-group analyses are subdivided into the parametric contrast ("0-back" versus "2-back") as the main contrast of interest for the following DCM analyses. For completeness, the findings of the two standard subtraction analyses for the low working memory load and the high working memory load are presented.

4.4.3.1 Within - group results

4.4.3.1.1 Parametric contrast

Both groups displayed two main regions of increasing activation with working memory load (i) the DLPFC (BA46/BA9) (bilateral for healthy controls; here left, x = -47, y = 33, z =26) and right hemisphere for EST; x = 33, y = 30, z = 34) and (ii) IPS (BA40) (bilateral for healthy controls; here right, x = 47, y = -40, z = 43 and left

hemisphere for EST; x = -43, y = -40, z = 43). Further details are contained in Table 4.6 for healthy subjects and Table 4.7 for EST. The BOLD responses of the DLPFC (BA46/BA9) for healthy subjects are given in Figure 4.4 and for EST in Figure 4.5.

Table 4.6 Parametric Contrast for healthy controls (*n* = 21).

P value	Extent	Peak height coordinates	Region	*Z* score
< .001[1]	3388	-47, 33, 26 30, -50, 56 46, 37, 23	L frontal: middle frontal gyrus, BA46	6.37
< .001[1]	3357	47, -40, 43 32, -62, 36 33, -64, 47	R parietal: inferior parietal lobule, BA40	5.98
< .001[1]	1735	32, -56, 38 -35, -71, -30 -12, -80, -21	R parietal: superior parietal lobule, BA7	5.38
< .001[1]	5061	57, -29, -8 47, -24, -12 59, -45, -11	R temporal: middle temporal gyrus, BA21	5.27
.029[2]	605	-31, -51, 65 -11, -61, 66 -20, -61, 66	L parietal: superior parietal lobe, BA7	4.36

[1]Reported *p* values are thresholded at 0.001FWE corrected cluster level, extent threshold = 200 voxels. Coordinates represent the three maxima within the same cluster.
[2] Reported *p* values are thresholded at 0.001 uncorrected cluster level, extent threshold = 200 voxels. Coordinates represent the three maxima within the same cluster.

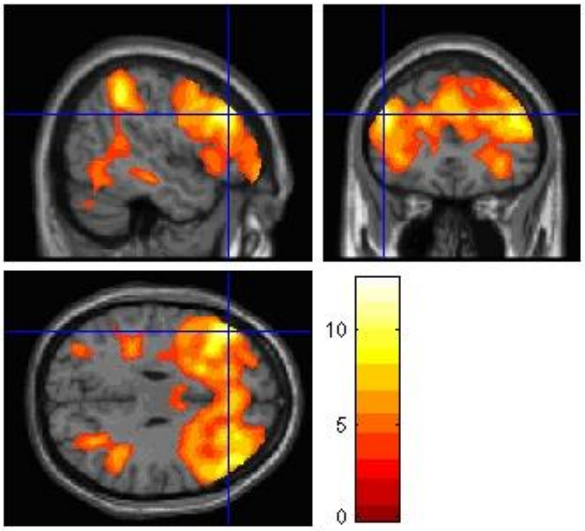

Figure 4.4 Parametric Contrast for healthy controls (*n* = 21). Left middle frontal gyrus, BA46.

Reported *p* values are thresholded at 0.001 FWE corrected cluster level, extent threshold = 200 voxels. Coordinates represent the three maxima within the same cluster.

Table 4.7 Parametric Contrast for EST (*n* = 16).

P value	Extent	Peak height coordinates	Region	*Z* score
< .001[1]	1153	33, 30, 34 26, 10, 50	R frontal: middle frontal gyrus, BA9	5.59
< .001[1]	1112	-43, -40, 43 -12, -56, 55 -35, -38, 62	L parietal: inferior parietal lobule, BA40	5.48
< .001[1]	1842	49, -41, 44 41, -40, 44	R parietal: inferior parietal lobule, BA40	5.05
.006[2]	650	-45, -68, 1	L occipital: middle occipital gyrus, BA37	3.78
.052[2]	293	-13, -7, 1	L sub-lobar: lentiform nucleus	3.73

[1]Reported *p* values are thresholded at 0.001FWE corrected cluster level, extent threshold = 200 voxels. Coordinates represent the three maxima within the same cluster.
[2] Reported *p* values are thresholded at 0.001 uncorrected cluster level, extent threshold = 200 voxels. Coordinates represent the three maxima within the same cluster.

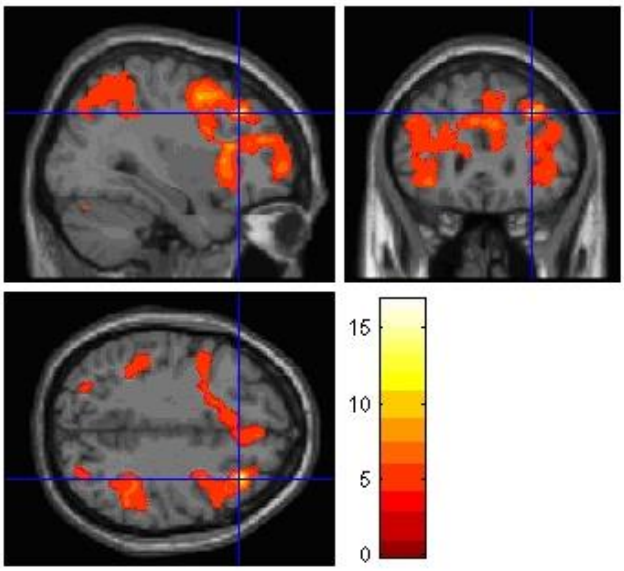

Figure 4.5 Parametric Contrast for EST (*n* = 16). Right middle frontal gyrus, BA9.
Reported *p* values are thresholded at 0.001FWE corrected cluster level, extent threshold = 200 voxels. Coordinates represent the three maxima within the same cluster.

4.4.3.1.2 Summary of standard subtraction analyses

For completeness, the within-group results for the low working memory load ("0-back" versus "1-back"; (Table 4.8; Table 4.9) and the high working memory load ("1-back" versus "2-back"; (Table 4.10 and Table 4.11) are presented. We report selected results which are thresholded to at $p < .001$ FWE corrected cluster level with extent threshold = 600 voxels and $z > 6$. BOLD responses of the regions such as the DLPFC and IPL overlap with the within-group results of the parametric contrast ("0-back" versus "2-back").

For the low working memory load, both groups demonstrated activations in regions commonly reported for this task condition as shown for the DLPFC (BA46) (left hemisphere for healthy controls; x = -44, y = 34, z = 19; and right hemisphere for EST; ; x = 46, y = 18, z = 24) (Table 4.8 and Table 4.9).

Table 4.8 Selection of results for the low working memory load for healthy controls (*n* = 21).

P value	Extent	Peak height coordinates	Region	*Z* score
< .001	1790	44, -42, 58 47, -41, 42 39, -43, 45	R parietal: inferior parietal lobule, BA40	6.19
< .001	2815	-44, 34, 19 -36, 54, -4 -27, 5, 34	L frontal: middle frontal gyrus, BA46	5.38
< .001	2004	24, 50, -6 41, 44, 17 44, 34, 23	R frontal: superior frontal gyrus, BA10	5.12
.036	966	57, -34, -13 49, -24, -14	R temporal: middle temporal gyrus, BA21	4.98

Reported *p* values are thresholded at 0.001FWE corrected cluster level, extent threshold = 200 voxels. Coordinates represent the three maxima within the same cluster.

Table 4.9 Selection of results for the low working memory load for EST (*n* = 16).

P value	Extent	Peak height coordinates	Region	*Z* score
< .001	7865	-37, 44, 35 -35, -55, 55 -39, -45, 42	L frontal: superior frontal gyrus, BA9	5.04
< .001	5254	-39, 6, 32 -36, 16, 16 -39, 32, 28	L frontal: precentral gyrus, BA9	4.57
< .001	5221	46, 18, 24 46, 31, 15 45, 12, 33	R frontal: middle frontal gyrus, BA46	4.41
< .001	1436	-50, -63, -5 -47, -68, -1 -44, -72, 7	L occipital: middle occipital gyrus, BA19	4.37

Reported *p* values are thresholded at 0.001 FWE corrected cluster level, extent threshold = 200 voxels. Coordinates represent the three maxima within the same cluster.

For the high working memory load, both healthy controls and EST displayed the activated region of the MFG/SFG (BA8) (right hemisphere for healthy controls; x = 27, y = 14, z = 47; right hemisphere for EST; x = 2, y = 34, z = 46) (Table 4.10 and Table 4.11).

Table 4.10 Selection of results for the high working memory load for healthy controls (*n* = 21).

P value	Extent	Peak height coordinates	Region	*Z* score
< .001	2869	27, 14, 47 24, 38, 28 -24, 2, 39	R frontal: middle frontal gyrus, BA8	7.12
< .001	8562	30, -52, 39 -44, -38, 42 47, -39, 42	R parietal: superior parietal lobule, BA7	6.15
.009	1670	52, -55, -2 57, -44, -10 45, -53, -5	R temporal: middle temporal gyrus, BA37	4.20
.015	1508	-2, -24, 29 6, -28, -22	L limbic: cingulate gyrus, BA24	4.06

Reported *p* values are thresholded at 0.001FWE corrected cluster level, extent threshold = 200 voxels. Coordinates represent the three maxima within the same cluster.

Table 4.11 Selection of results for the high working memory load for EST (*n* = 16).

P value	Extent	Peak height coordinates	Region	*Z* score
< .001[1]	3144	-17, -58, 51 36, -58, 54 -28, -51, 62	L parietal: precuneus	5.51
< .001[1]	5326	2, 34, 46 -36, 8, 24 -22, 14, 48	R frontal: superior frontal gyrus, BA8	5.23
< .001[1]	4342	26, 19, 7 55, 17, -2 49, 25, -2	R sub-lobar: putamen	5.06
.015[2]	516	-14, -8, 0 -10, -8, 0	L sub-lobar: lentiform nucleus	4.53
.004[1]	1517	-20, 59, 3 -24, 53, -3 -21, 46, -6	L frontal: superior frontal gyrus, BA10	4.17
.006[2]	695	27, 30, 33 26, 389, 34	R frontal: middle frontal gyrus, BA9	4.15

[1]Reported *p* values are thresholded at 0.001FWE corrected cluster level, extent threshold = 200 voxels. Coordinates represent the three maxima within the same cluster.
[2] Reported *p* values are thresholded at 0.001 uncorrected cluster level, extent threshold = 200 voxels. Coordinates represent the three maxima within the same cluster.

4.4.3.2 Between - group results

4.4.3.2.1 Parametric contrast

Results of the group differences for the parametric contrast ("0-back" versus "2-back") showed greater increased activation with increasing working memory load in the healthy controls compared to the EST in the regions involving the bilateral DLPFC (BA9/46) (x = -46, y = 25, z = 31; p = .036; x = 41, y = 29, z = 17; p = .044 (Figure 4.6; both at p < .001, FWE corrected cluster level. Other regions included the IPS (BA40) (x = 49, y = -47, z =30; p = .022; at p < .01 uncorrected cluster level) and the ACC (BA32) (x = 3, y = 36, z = 26; p = .0243; at p < .01 uncorrected cluster level; (Table 4.12). The bilateral midbrain region VTA/SN was significantly activated in healthy controls in contrast to the EST (left hemisphere, x = -9, y = -17, z = -6; p = .047 (Figure 4.7; right hemisphere, x = 7, y = -17, z = -3; p = .049; both at p < .05 FDR corrected cluster level).

There were no group differences for increased activation for EST in contrast to healthy controls. Not all of these regions were noted for the within-group results, however those activated regions were evident at a lower threshold of p = .005. As expected from the sensitivity index d' results (chapter 4.4.2), no interaction effects between group and task performance were observed.

Table 4.12 Between-group random effects analysis for the parametric contrast.

P value	Extent	Peak height coordinates	Region	*Z* score
Healthy Controls < EST				
n/s				
Healthy Controls > EST				
.006[1]	1097	-52, -22, -12 -60, -17, -12	L temporal: middle temporal gyrus, BA21	4.27
.036[1]	580	-46, 25, 31	L frontal: middle frontal gyrus, BA9	3.83
.044[1]	345	41, 29, 17	R frontal: middle frontal gyrus, BA46	3.66
.022[2]	1344	49, -47, 30	R parietal: inferior parietal lobule, BA40	3.56
.043[2]	685	3, 36, 26	R limbic: anterior cingulate, BA32	3.53
.004[3]	1836	-13, -2, 8 -13, -7, 4	L sub-lobar: thalamus	3.50
.047[4]	267	-9, -17, -6	L midbrain: substantia nigra/ventral tegmental area	3.32
.049[4]	204	7, -17, -3	R midbrain: substantia nigra/ventral tegmental area	3.03

[1] Reported *p* values are thresholded at $p < .001$ FWE corrected cluster level, extent threshold = 200 voxels. Coordinates represent the three maxima within the same cluster.
[2] Reported *p* values are thresholded at $p < .01$ uncorrected cluster level, extent threshold = 200 voxels. Coordinates represent the three maxima within the same cluster.
[3] Reported *p* values are thresholded at $p < .05$ FWE corrected cluster level, extent threshold = 200 voxels. Coordinates represent the three maxima within the same cluster.
[4] Reported *p* values are thresholded at $p < .05$ FDR corrected cluster level, extent threshold = 200 voxels. Coordinates represent the three maxima within the same cluster.

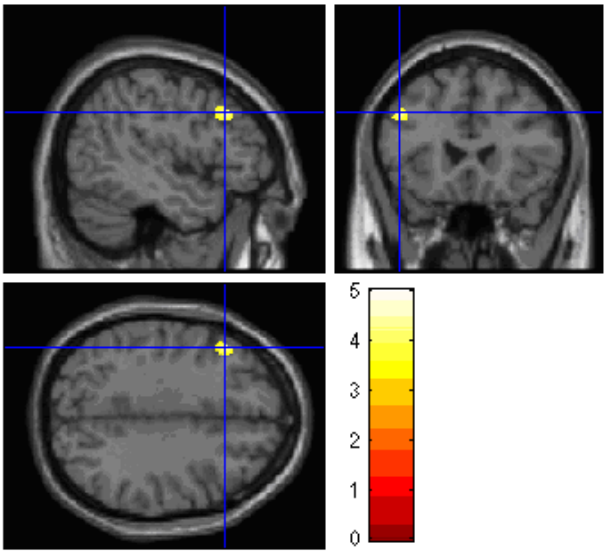

Figure 4.6 Between-group random effects analysis for the parametric contrast. Left MFG, BA9.

Reported *p* values are thresholded at *p* < .001FWE corrected cluster level, extent threshold = 200 voxels. Coordinates represent the three maxima within the same cluster.

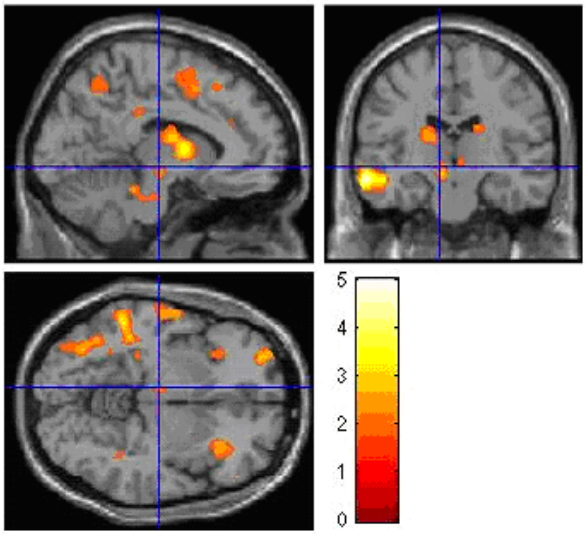

Figure 4.7 Between-group random effects analysis for the parametric contrast. Left Midbrain, VTA/SN.

Reported *p* values are thresholded at *p* < .05 FDR corrected cluster level, extent threshold = 200 voxels. Coordinates represent the three maxima within the same cluster.

In summary, increased activations with increased working memory load were found in healthy controls in contrast to EST in regions consistently reported during the "N-back" task: (i) DLPFC (left, Callicott et al., 2000; bilateral, Tan et al., 2006), (ii) IPS (right, Callicott et al., 2000) and (iii) AC (right, Callicott et al., 2000). Other fMRI studies during working memory reported significant differences between healthy subject and patients with schizophrenia of the dACC (BA32; Becerril et al., 2011; Wang et al., 2010; Brázdil et al., 2007). Furthermore, healthy controls compared to EST displayed significantly greater working memory load related to increased activation in the bilateral VTA/SN area. This finding replicates previously reported BOLD responses for the midbrain region during working memory in healthy subjects (D'Ardenne et al., 2012; Düzel et al., 2008; Murty et al., 2011).

4.4.3.2.2 Summary of standard subtraction analyses

For the low working memory load, healthy controls showed increased activation in the left MTG (BA21) in comparison to EST (Table 4.13). There were no other significant group differences.

Table 4.13 Between-group random effects analysis for the low working memory load.

P value	Extent	Peak height coordinates	Region	*Z* score
Healthy Controls < EST				
n/s				
Healthy Controls > EST				
.014*	1755	-66, -22, -15 -57, -19, -14 -59, -17, -8	L temporal: middle temporal gyrus, BA21	4.48

*Reported *p* values are thresholded at $p < .01$ uncorrected cluster level, extent threshold = 200 voxels. Coordinates represent the three maxima within the same cluster.

Healthy subjects displayed increased activation of the left precuneus and the left ACC in contrast to EST (Table 4.14). No other group differences were observed.

Table 4.14 Between-group random effects analysis for the high working memory load.

P value	Extent	Peak height coordinates	Region	*Z* score
Healthy Controls < EST				
n/s				
Healthy Controls > EST				
.028[1]	1879	-5, -55, 49 -11, -50, 45 -14, -58, 44	L parietal: precuneus	3.77
< 0.001[2]	5683	-7, -7, 30 21, 24, 31 -42, 28, 25	L limbic: cingulate gyrus, BA24	3.17

[1]Reported *p* values are thresholded at 0.01 uncorrected cluster level, extent threshold = 200 voxels. Coordinates represent the three maxima within the same cluster.
[2] Reported *p* values are thresholded at $p < .05$ FWE corrected cluster level, extent threshold = 200 voxels. Coordinates represent the three maxima within the same cluster.

4.4.4 Functional integration – Dynamic Causal Modelling

The results of the bilinear and nonlinear DCM analyses are given separately for the findings for the left and right hemispheres following the phased protocol in Figure 3.1. The outline of this results section is in keeping with the outline of the methods section. In the first step, the winning model for the "N-back" task for bilinear DCM is presented. Then the optimal bilinear model and four nonlinear models entered the next phase of determining the likelihood of linear and nonlinear models before the connection strength of the nonlinear modulation was assessed and compared between the healthy controls and the EST.

4.4.4.1 Bilinear Dynamic Causal Modelling and Bayesian Model Selection at the group level

For the left hemisphere, the optimal model for the healthy controls was Model 7 (*Xp* = 0.24) whereas Model 1 was the winning model for the EST (*Xp* = 0.23) (Table 4.15; Figure 4.8).

Model 1 (see Figure 4.1) is characterised by bidirectional endogenous connections between (i) IPS and DLPFC, (ii) IPS and dACC, (iii) DLPFC and dACC, (iv) DLPFC and the VTA/SN area and (v) ACC and the VTA/SN area. Experimental manipulations are modelled by the connection from the IPS to the DLPFC, whereas the visual presentation of the stimuli and the individual errors during the working memory tasks are set on the IPS and the VTA/SN area, respectively. Model 7 (Figure 4.1) differs from Model 1 only in the unidirectional connection from the ACC to the VTA/SN area instead of the bidirectional connection in comparison to Model 1.

The *Xps* of the Models 1, 2, 7 and 8 ranged between *Xp* = 0.14 – 0.24 for the healthy controls and *Xp* = 0.13 – 0.23 for the EST, respectively. In more detail, Models 1 and 2 were more likely to explain the given fMRI data in EST than in the healthy controls. In contrast, Models 7 and 8 displayed a higher probability in the healthy controls than in the EST. The main difference between the two pairs of DCMs are the specification of a bidirectional endogenous connection between the ACC and the VTA/SN area (Models 1 and 2; Figure 4.1) and a unidirectional endogenous connection between the ACC and the VTA/SN area (Models 7 and 8; Figure 4.1).

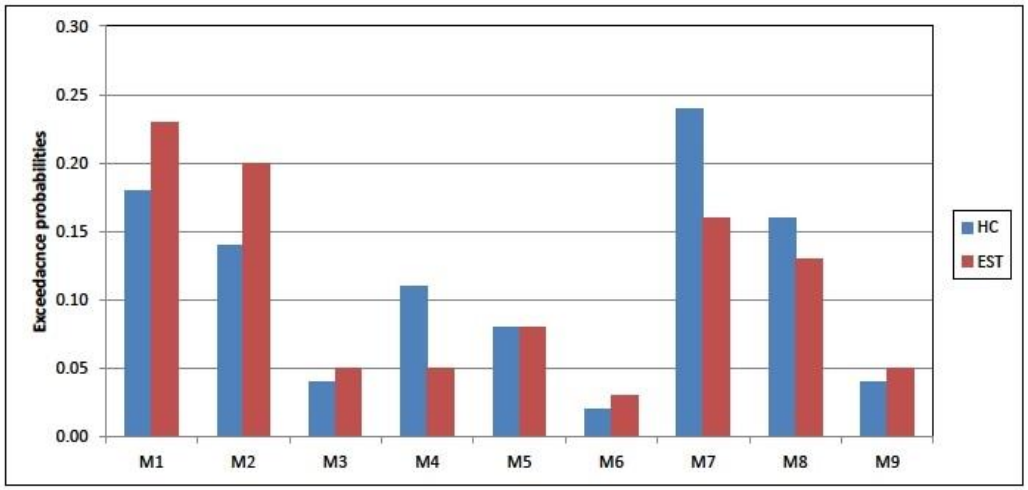

Figure 4.8 Exceedance probabilities for the linear models in healthy controls and EST – Left hemisphere.

Results for HC are based on Model 7 and results for EST are based on Model 1 (Figure 4.1). HC, healthy controls; EST; *Xp,* Exceedance probability. M1, Model 1; M7, Model.

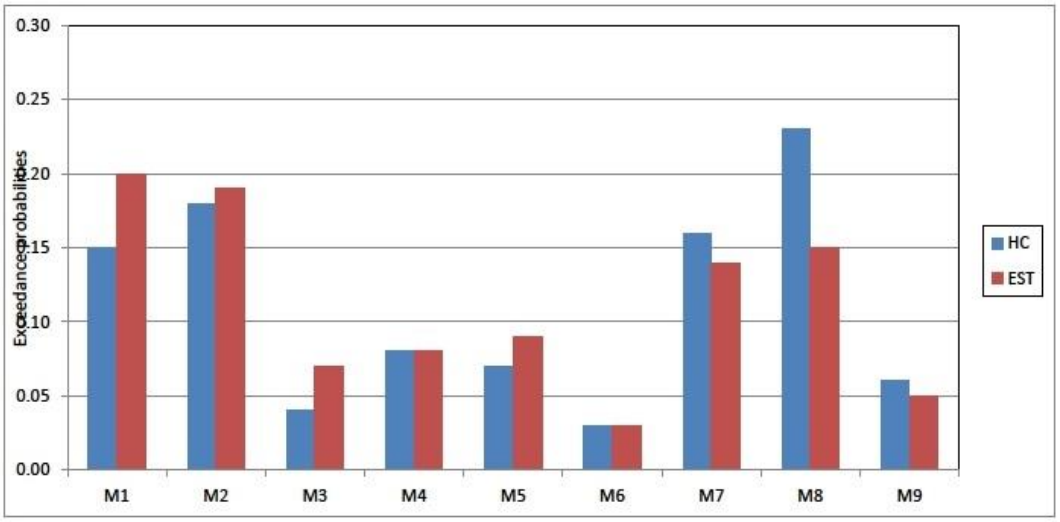

Figure 4.9 Exceedance probabilities for the linear models in healthy controls and EST – Right hemisphere.

Results for HC are based on Model 7 and results for EST are based on Model 1 (Figure 4.1). HC, healthy controls; EST; *Xp,* Exceedance probability. M1, Model; M7, Model.

For the right hemisphere, Model 8 is the optimal model in the healthy controls (*Xp* = 0.23) with Model 7 displaying the third greatest likelihood of *Xp* = 0.16, whereas Model 1 is the optimal model for the EST (*Xp* = 0.20) (Figure 4.9). Models 1, 7 and 8 showed similar probabilities and were more likely to explain the given fMRI data

in healthy controls than in EST. In comparison, Models 1 and 2 outperformed Models 7 and 8 and were more likely to explain the fMRI data in EST than in healthy controls. The structure of Model 1 (optimal model in EST) and Model 8 (optimal model in healthy controls) are differently characterised by endogenous connections: Model1 is defined by bidirectional endogenous connections between (i) the DLPFC and the VTA/SN area and (ii) the ACC and VTA/SN area. In contrast, Model 8 is described by unidirectional endogenous connections from (i) the DLPFC to the VTA/SN area and (ii) from the ACC to the VTA/SN area.

Table 4.15 Exceedance probabilities for the linear models in healthy controls and EST.

	Healthy controls – Left hemisphere	Healthy controls –Right hemisphere	EST – Left hemisphere	EST –Right hemisphere
Model 1	0.18	0.15	0.23*	0.20*
Model 2	0.14	0.18	0.20	0.19
Model 3	0.04	0.04	0.05	0.07
Model 4	0.10	0.08	0.06	0.08
Model 5	0.08	0.07	0.08	0.09
Model 6	0.02	0.03	0.03	0.03
Model 7	0.24*	0.16	0.16	0.14
Model 8	0.16	0.23*	0.13	0.15
Model 9	0.04	0.06	0.05	0.06

* Model 7 is the winning model in healthy subjects in the left hemisphere.
* Model 8 is the winning model in healthy controls in the right hemisphere.
* Model 1 is the winning model in EST in both hemispheres.

In summary for both the left and the right hemispheres, the results of both hemispheres across the healthy controls and EST reflected a similar pattern. Models 1, 2, 7 and 8 displayed the greatest likelihoods for both healthy controls and EST in

both hemispheres with *Xp* values in comparable ranges. Furthermore, the likelihoods of the optimal models were comparable between both hemispheres within each group and between the groups. Despite these similarities, Models 7 and 8 showed greater *Xp* values for healthy controls for both hemispheres, whereas Models 1 and 2 showed greater likelihood for EST for both hemispheres.

4.4.4.2 Nonlinear Dynamic Causal Modelling and Bayesian Model Selection at the model family level

We report three main results for the BMS results at the model family level: (i) outperformance of nonlinear models over bilinear model, (ii) winning model family for the left hemisphere in healthy controls and EST and (iii) winning model family for the right hemisphere in health controls and EST. However, it is noted that the findings cannot be directly compared between the healthy controls and EST due to two different model structures used for the BMS analyses. Bilinear Model7 was modelled for the nonlinear models for healthy controls; in contrast, bilinear Model 1 was the basis for the nonlinear models in EST.

(i) For both the left and right hemispheres, the nonlinear model families outperformed the linear model family in healthy controls and EST (Figure 4.10 and Figure 4.11; Table 4.16). Therefore, the pre-condition of greater likelihood of the nonlinear models over the linear model was met as previously defined in the heuristic search protocol (column 2, Figure 3.1).

For healthy controls, nonlinear model family 2 (nonlinear models – DLPFC) and nonlinear model family 3 (nonlinear models – VTA/SN) (left hemisphere, Xp = 0.90; right hemisphere, Xp = 0.89) outperformed the linear model family 1 (bilinear model) (left hemisphere, Xp = 0.10; right hemisphere, Xp = 0.11) (Figure 4.10 and Figure 4.11; Table 4.16).

A similar picture was observed in EST. Nonlinear model family 2 (nonlinear models – DLPFC) and nonlinear model family 3 (nonlinear models – VTA/SN) displayed greater likelihoods (left hemisphere, Xp = 0.82; right hemisphere, Xp = 0.90) than the bilinear model family 1 (left hemisphere, Xp = 0.18; right hemisphere, Xp = 0.10) (Figure 4.10 and Figure 4.11; Table 4.16).

(ii) The winning model family for the left hemisphere was model family 2 in healthy controls and EST with comparable likelihoods of Xp = 0.46 for healthy controls and Xp = 0.44 for the EST. Model family 3 was the second winning model family in both groups (Xp = 0.44 for the healthy controls and Xp = 0.38 for the EST; (Figure 4.10; Table 4.16). The likelihoods of model families 2 and 3 were only slightly different in both healthy controls and EST.

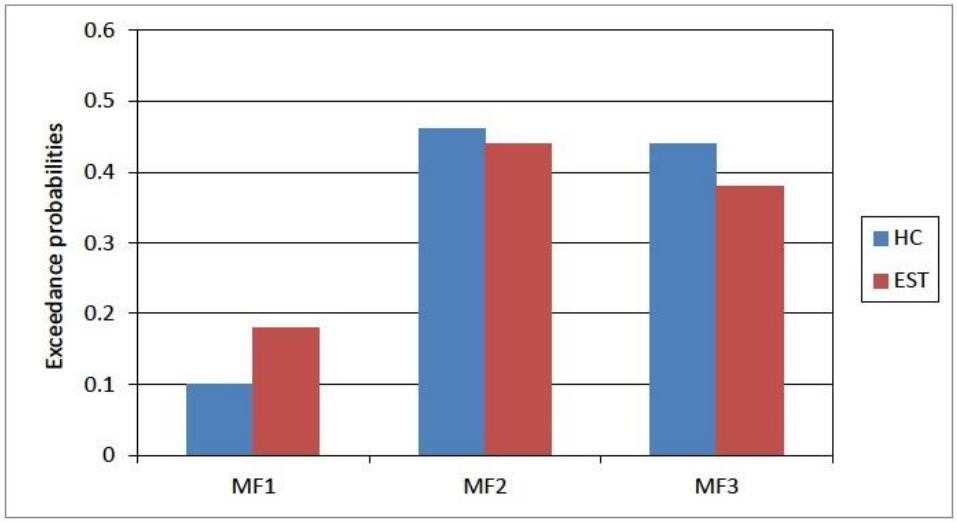

Figure 4.10 Bayesian Model Selection results at the model family level for the left hemisphere.

Results for HC are based on Model 7 and results for EST are based on Model 1 (Figure 4.1).
HC, healthy controls; EST; *Xp,* Exceedance probability.
MF1, Model family 1, bilinear model
MF2, Model family 2, nonlinear models – DLPFC
MF3, Model family 3, nonlinear models – VTA/SN

(iii) For the right hemisphere, healthy controls and EST showed the same winning model family 2 as the most likely model family for the given fMRI data (*Xp* = 0.45 for healthy controls, *Xp* = 0.56 for EST). Model family 3 was the second winning model family with in both groups with *Xp* = 0.44 for healthy controls, *Xp* = 0.34 for EST). The difference in probabilities between the model families 2 and 3 was marginally different in healthy subjects. However, model family 2 was more likely than model family 3 in EST (Figure 4.11).

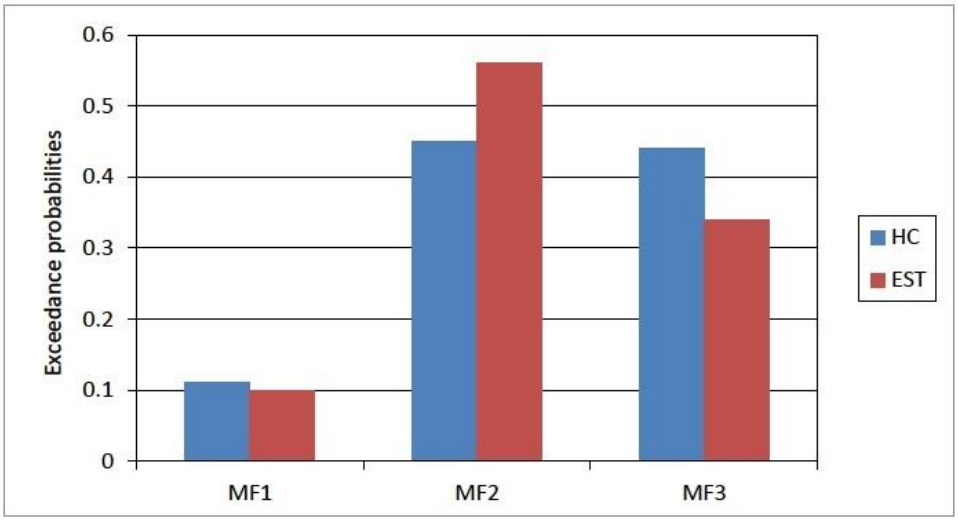

Figure 4.11 Bayesian Model Selection results at the model family level for the right hemisphere.

Results for HC are based on Model 7 and results for EST are based on Model 1 (Figure 4.1).
HC, healthy controls; EST; *Xp,* Exceedance probability.
MF1, Model family 1, bilinear model
MF2, Model family 2, nonlinear models – DLPFC
MF3, Model family 3, nonlinear models – VTA/SN

Table 4.16 Bayesian Model Selection results at the model family level for both hemispheres.

	Healthy controls Model 7 – Left hemisphere	Healthy controls Model 7 –Right hemisphere	EST Model 1 – Left hemisphere	EST Model 1 –Right hemisphere
Model family 1	0.10	0.11	0.18	0.10
Model family 2	0.46*	0.45*	0.44*	0.56*
Model family 3	0.44	0.44	0.38	0.34

* Denotes the winning model family.
Results for HC are based on Model 7 and results for EST are based on Model 1 (Figure 4.1).
Model family 1, bilinear model.
Model family 2, nonlinear models – DLPFC
Model family 3, nonlinear models – VTA/SN

In summary, the *Xp*s of model families 2 and 3 in healthy subjects were similar for the right and the left hemispheres (Table 4.16). This finding is in keeping with the previous DCM results for nonlinear DCM in healthy controls on the verbal fluency task where the likelihoods between both nonlinear model families were similar (see

chapter 3.4.3.2; Dauvermann et al., 2013). In contrast, in EST the *Xp*s for model families 2 and 3 differed between the hemispheres (Table 4.16). Notably, the difference in likelihood of model family 2 in contrast to model family 3 for the right hemisphere was greater than for the left hemisphere.

4.4.4.3 Bayesian Model Averaging – Posterior densities of connection strengths

The findings of the posterior densities of connection strengths are presented separately for healthy controls and EST for the winning models of model family 2 and both hemispheres. Connection strengths with nonlinear modulation, endogenous connection strengths and connection strengths with modulatory inputs are given.

The results for the connection strengths cannot be directly compared between the groups because two different model structures underlie the BMS and BMA findings: Bilinear Model7 entered the BMS and BMA analyses for healthy controls, whereas bilinear Model1 was the optimal linear model for EST.

4.4.4.3.1 Connection strength with nonlinear modulation

The average connection strengths with nonlinear modulation for the connections between the DLPFC and the VTA/SN area are presented.

The posterior densities of connection strengths with nonlinear modulation for the connection from the DLPFC to the VTA/SN area for the right and left hemispheres between healthy controls and EST were comparable (Figure 4.12). A similar picture was observed for the connection from the VTA/SN area to the DLPFC between the groups although negative values of connection strengths with nonlinear modulation were found for the right hemisphere in both healthy controls and EST. For the left

hemisphere, negative values for the connection strengths with nonlinear modulation were observed only in EST (Figure 4.12).

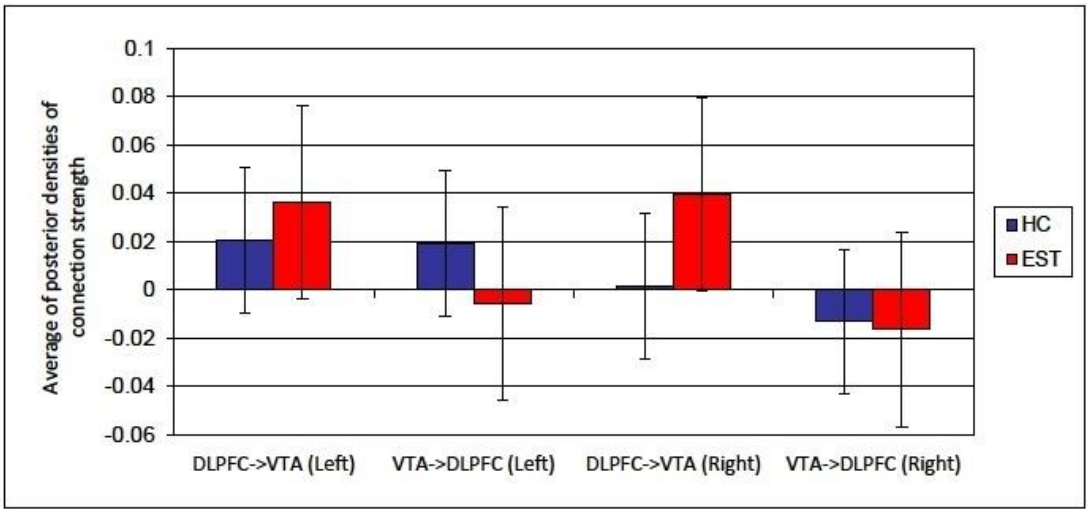

Figure 4.12 Average of posterior densities of connection strength with nonlinear modulation.

Results for HC are based on Model 7_DLPFC_VTA/SN_DLPFC (Figure 4.3) and results for EST are based on Model 1_DLPFC_VTA/SN_DLPFC (Figure 4.2).

4.4.4.3.2 Endogenous connection strength

For healthy controls, the averages of posterior densities of endogenous connection strengths were similar between the left and right hemispheres. A similar pattern was observed for both hemispheres in EST (Table 4.17). However, a direct comparison is not possible due to different model structures.

Table 4.17 Average of posterior densities of endogenous connection strength (in Hertz).

Model DLPFC_VTA_DLPFC	Healthy controls Model 7 – Left hemisphere	Healthy controls Model 7 –Right hemisphere	EST Model 1 – Left hemisphere	EST Model 1 –Right hemisphere
IPS -> DLPFC	0.34 (0.05)	0.28 (0.13)	0.25 (0.12)	0.22 (0.12)
IPS -> ACC	0.27 (0.09)	0.26 (0.11)	0.25 (0.12)	0.25 (0.12)
DLPFC -> IPS	-0.05 (0.07)	-0.04 (0.09)	0.04 (0.12)	0.04 (0.12)
DLPFC -> ACC	0.15 (0.05)	0.12 (0.08)	0.16 (0.13)	0.14 (0.10)
DLPFC -> VTA/SN	0.15 (0.11)	0.14 (0.09)	0.14 (0.13)	0.12 (0.13)
ACC -> IPS	0.05 (0.04)	-0.04 (0.10)	0.03 (0.10)	0.02 (0.10)
ACC- > DLPFC	0.10 (0.03)	0.06 (0.12)	0.10 (0.10)	0.08 (0.17)
ACC -> VTA/SN	0.10 (0.12)	0.10 (0.06)	0.12 (0.12)	0.11 (0.10)
VTA/SN -> DLPFC	0.01 (0.05)	0 (0.05)	0.04 (0.06)	0.04 (0.07)
VTA/SN -> ACC	n/a	n/a	0.07 (0.08)	0.06 (0.08)

Mean (SE)
Results for HC are based on Model 7_DLPFC_VTA/SN_DLPFC (Figure 4.3) and results for EST are based on Model 1_DLPFC_VTA/SN_DLPFC (Figure 4.2).

4.4.4.3.3 Connection strength with modulatory inputs

The averages of posterior estimates of connection strengths with modulatory inputs lied in similar ranges between healthy controls and EST as well as between both hemispheres (Table 4.18). A comparison of connection strengths between the groups is not allowed based on different model structures.

Table 4.18 Average of posterior densities of connection strengths with modulatory inputs (in Hertz).

Model DLPFC_VTA_DLPFC	Healthy controls Model 7 – Left hemisphere	Healthy controls Model 7 –Right hemisphere	EST Model 1 – Left hemisphere	EST Model 1 –Right hemisphere
"0-back"	0.18 (0.06)	0.16 (0.09)	0.12 (0.10)	0.10 (0.11)
"1-back"	0.04 (0.01)	0.02 (0.07)	0.17 (0.03)	0.05 (0.06)
"2-back"	0.17 (0.04)	0.14 (0.04)	0.08 (0.09)	0.10 (0.11)

Mean (SE)
Results for HC are based on Model 7_DLPFC_VTA/SN_DLPFC (Figure 4.3) and results for EST are based on Model 1_DLPFC_VTA/SN_DLPFC (Figure 4.2).

4.5 Discussion

We applied bilinear and nonlinear DCM to fMRI data for the "N-back" task in EST and healthy controls. The main result of nonlinear DCM analyses was that the nonlinear models outperformed the linear models in healthy controls and EST separately. This finding was apparent in both groups and in both hemispheres despite two different functional networks in healthy controls and EST. Notably, the two nonlinear model families were equally likely between both hemispheres in healthy controls, whereas the probabilities of the two nonlinear model families varied between the two hemispheres in EST. The outperformance of nonlinear models over linear models suggests that the meso-cortical and/or cortico-mesal connection is gated in healthy controls and EST independently. This findings may support preclinical and computational findings of gated synaptic plasticity processes during working memory (chapter 2.2.2.2). We further propose that the gating mechanism may be intact in EST based on the similar averages of connection strengths.

Currently, it is not understood what the neurocognitive and neuropsychological processes of gating or what their effects are in working memory. We speculate that

gating as assessed with nonlinear DCM for fMRI may lead to successful performance of working memory given the comparable performance levels in this study based on recent neuroimaging studies employing EEG reported findings on the relevance of intact sensory gating during working memory tasks (Lijffijtet al., 2009; Shimi and Astle et al. 2013; Huang et al., 2013). However, more research is needed to shed light on possible neurocognitive mechanisms of gating in working memory and its potentially altered effect in individuals with schizophrenia. We note that the reported group differences of the parametric contrast ("0-Back" versus "2-Back") may reflect altered cortical function (Schlösser et al., 2008) or a compensatory mechanism to impaired cognitive function (Tan et al., 2006) in EST in keeping with previous FA studies (Callicott et al., 2000; Tan et al., 2006; Deserno et al., 2012).

The main result of the bilinear DCM analyses was that there were two different winning bilinear models for healthy controls and EST during the "N-back" task for both hemispheres due to the adaptation of the heuristic search protocol from the EHRS. We interpreted this finding as a possible indication for different underlying functional networks for the performance of working memory in EST and healthy controls. From a cognitive neuroscience perspective, the different functional networks may be an indication for altered functional connections between prefrontal and midbrain regions or a compensatory mechanism of these regions in EST. However, we cannot rule out that clinical symptoms or antipsychotic medication may have changed the functional networks. Controversial results of both ameliorating and worsening effects of antipsychotics on FA findings (da Silva Alves et al., 2008; Honey et al., 1999; Menzies et al., 2007; Ettinger et al., 2011), FC findings (Nejad et

al., 2012) and EC findings (Schlösser et al., 2003; Schmidt et al., 2013) during working memory performance in individuals with schizophrenia were reported. We cannot interpret the EC findings in terms of potential pharmacological effects since this study was not designed for such an investigation. In addition, EST in this study were treated with a variety of antipsychotic medications (FGA and SGA).

It has been proposed that alterations of dopaminergic and glutamatergic neurotransmission could lead to the pathophysiology of schizophrenia as part of the glutamate hypothesis of schizophrenia (Coyle, 2006; Coyle et al., 2011; Javitt, 2010). In particular, interactions between dopaminergic and glutamatergic modulation via AMPA and NMDA receptors of the meso-cortical connection may be disrupted in schizophrenia (chapter 2.2.2.2). Due to the impossibility of comparing the connection strengths with nonlinear modulation between healthy controls and EST, we cannot interpret potentially altered neurotransmission in EST.

A direct comparison of bilinear and nonlinear findings with previous DCM studies is limited because of differing functional networks being employed to assess the N-back task. Additional factors that limit a comparison of bilinear DCM findings with three clinical DCM studies in "N-back" are the use of differing DCM versions (DCM10, Deserno et al., 2012; Schmidt et al., 2013; not reported DCM version, Zhang et al., 2013) and differently defined model space as discussed in chapter 2.2.4.3.

Specific methodological limitations are given for the DCM analyses of this study, which have not been previously discussed (chapter 2.2.4.3; chapter 3.6). Firstly, one limitation of the bilinear DCM analysis lies in the limited linear model space investigated in the current study. The number of models and the variability among the models was limited in contrast to previously tested model spaces of the "N-back" task in individuals with schizophrenia (Deserno et al., 2012; Schmidt et al., 2013). Furthermore, the models were limited to intrahemispheric DCMs only, whereas it can be assumed that working memory function happens interhemispherically. Secondly, only models containing the exact same regions within a model and the exact number of regions can enter a model comparison. Thus, currently implemented model comparison and Bayesian inference approaches in DCM (across all DCM versions) does not allow the comparison of different models between two groups. Thirdly, it is possible that the BOLD response of the VTA/SN area was not great enough to assess connection strengths with nonlinear modulation given the small VOI sphere of 6 mm in addition to the small numbers of the two population groups. This limitation of the lack of robustness of the VTA/SN area in this sample set is reflected in the number of healthy controls and EST due to lack of sufficiently activated bilateral VTA/SN region (and the bilateral IPS) and the intrahemispheric models. Greater BOLD response in the bilateral VTA/SN area would have allowed the extension of the model space to interhemispheric models and therefore more biologically plausible model space. Nonetheless, we note that the number of excluded participants for this DCM analysis is comparable to other clinical DCM studies.

Future DCM analyses of working fMRI data in individuals with schizophrenia could be improved in several ways. Firstly, interhemispheric DCMs should be specified in the model space since FA, FC and EC findings report evidence for altered BOLD responses, FC and EC between healthy controls and EST in both hemispheres. Therefore, it can be assumed that functional networks underlying working memory may function interhemispherically and thus in a more complex way than it was hypothesised in this study. Secondly, potential pharmacological effects of antipsychotics in EST and their effects on connection strengths (with nonlinear modulation) could be investigated, for example by comparing different subgroups defined by type of antipsychotic medication (i.e. FGA or SGA), dose of medication, duration of antipsychotic treatment, mode of action of medication and possible additional medication treatment. Thirdly, DCM settings should be chosen to allow a comparison among several DCM studies including the same DCM version and comparable model space. Fourthly, for better temporal resolution in investigations of gating processes underlying functional networks, DCM for fMRI and EEG analyses could be combined.

4.6 Conclusion

Our results of different optimal model structures for healthy controls and EST may indicate different functional networks for the performance of the verbal "N-Back" task. The investigation of possibly altered functional large-sale networks before the onset of schizophrenia may lead to a better insight into the pathophysiology of cognitive deficits in individuals with schizophrenia.

5 General discussion

5.1 Introduction

The main objective of the work on the EHRS and SFMHS cohorts was the modelling of synaptic plasticity and gating mechanisms, which are thought to be implicated in cognitive tasks in schizophrenia: The connections considered in the modelling work included the thalamo-cortical connection and the meso-cortical connection. For the EHRS, the connection strength with nonlinear modulation of the thalamo-cortical connection during verbal fluency in subjects at high familial risk of schizophrenia and healthy controls was assessed with nonlinear DCM for fMRI. For the SFMHS, the meso-cortical connection during working memory in EST and healthy controls was analysed with nonlinear DCM.

In this chapter, key DCM findings of the EHRS and the SFMHS are summarised and discussed in context of methodological aspects and future directions. Finally, concluding remarks of modelling fMRI data for long-term goals of development of diagnostic tools and treatment for individuals with schizophrenia are given.

5.2 Key findings

For the EHRS, the application of nonlinear DCM to verbal fluency fMRI data revealed that the connection strength with nonlinear modulation of the thalamo-cortical connection was reduced in HR+ in contrast to healthy controls (chapter 3.5.3.3.1). This finding was supported by significantly negative correlations between connection strength with nonlinear modulation and severity of the ‘delusion’ symptom in HR+ and HRall (chapter 3.5.3.4). We proposed that the findings of reduced connection strength with nonlinear modulation may resemble findings from

preclinical and computational studies of reduced gating of the thalamo-cortical connection. Furthermore, we suggested that the altered connection strengths with nonlinear modulation in HR+ in contrast to healthy controls may provide a mechanistic explanation of the previously reported reduced BOLD response of the DLPFC in HR when compared to healthy controls (Whalley et al., 2004) and reduced prefrontal-thalamic FC in HR (Whalley et al., 2005). The reduced connection strengths with nonlinear modulation were interpreted as indications of thalamic glutamatergic alteration in context of the glutamate hypothesis of schizophrenia (chapter 3.6). In summary, we assessed altered synaptic plasticity and altered gating mechanism of the thalamo-cortical connection in HR when compared to healthy controls by the means of connection strengths with nonlinear modulation.

The work in this thesis is the first study to assess connection strengths with nonlinear modulation of fMRI data. The methodology and logic of the application of nonlinear DCM for fMRI from the EHRS was adapted for the investigation of hypothesised altered synaptic plasticity and gating mechanism of the meso-cortical connection during working memory in EST and healthy controls for the SFMHS. In contrast to the EHRS in which HR and HC showed the same optimal model, EST and HC were found to use two different optimal models in the SFMHS.

For the bilinear DCM analyses of the working memory fMRI data of the SFMHS, two different optimal linear models were found for EST and healthy controls (chapter 4.4.4.1). We proposed that this finding may indicate that EST used a different functional large-scale network for the functional performance of the

working memory task than healthy controls. As a consequence of this main result at the group level, the connection strengths at the model family level could not be compared between EST and healthy controls. Therefore, the hypothesis of altered connection strength with nonlinear modulation of the meso-cortical connection between the two groups was not possible (chapter 4.4.4.2). However, we speculated that the gating mechanism during working memory was intact in EST based on comparable averages of posterior densities of connection strengths with nonlinear modulation between the two groups. Taken together, we reported findings of possibly different functional large-scale networks underlying the functional performance of working memory between EST and healthy controls.

5.3 Methodological considerations and future directions

5.3.1 Suitability of Dynamic Causal Modelling for fMRI for modelling synaptic plasticity and gating mechanisms in individuals with schizophrenia

Originally, DCM was invented for the analysis of fMRI data to assess EC measures (Friston et al., 2003) with the objective of increasing interpretability of connectivity measures. In the following years, it has been proposed that DCM could be a tool to assess synaptic plasticity processes underlying the neural responses (Stephan et al., 2006; Stephan et al., 2009a). This assumption has been specifically phrased for the investigation of possibly altered synaptic plasticity processes in individuals with

schizophrenia when compared to healthy controls as hypothesised by the dysconnection hypothesis of schizophrenia (Stephan et al., 2006; Stephan et al., 2009a).

Since the original design of bilinear DCM for fMRI, nonlinear DCM (Stephan et al., 2008) and two-state DCM (Marreiros et al., 2008) have been developed to account for greater biophysical plausibility. In nonlinear DCM, one can assess the strengths of a connection by activity of other neuronal populations (Stephan et al., 2007, Stephan et al., 2008). Two-state DCM offers to infer intrinsic connectivity of two neuronal states, i.e. neuronal populations, in one region within the network (Marreiros et al., 2008). Here, we focus on nonlinear DCM.

The main characteristic of nonlinear DCM is the implementation of second-order derivatives for the assessment of connection strengths with nonlinear modulation (Stephan et al., 2008; Stephan and Friston, 2010), which are comparable to equations used in preclinical and computational studies to assess altered synaptic plasticity processes such as gating mechanisms (Abbott et al., 1997; Chance et al., 2002; Salinas and Sejnowski, 2001). Further support for the computation of second-order differential equations comes from DCM for EEG/MEG. In the state equation for DCM for EEG/MEG, comparable second-order derivatives are applied to infer neuronal interactions of inhibitory and excitatory subpopulations (Kiebel et al., 2006; Chen et al., 2008; Kiebel, 2012).

Criticism towards limited biophysical plausibility of DCM for fMRI remains despite the support for the second-order derivatives in assessing connection strengths with

nonlinear modulation of fMRI data, which is based on the limited temporal resolution of fMRI (Friston et al., 2003; Roiser et al., 2013) to measure biophysical mechanisms from EPI time series (Moran et al., 2011; Friston and Dolan, 2010; Daunizeau et al., 2011a; Friston et al., 2012).

A second limitation of DCM was considered in a review of the robustness of the statistical inference techniques used in DCM10 and DCM12[6] for all modalities (i.e. fMRI, EEG, MEG, steady-state responses, local field potentials) (Daunizeau et al., 2011a). Criticism has been raised towards the use of the free energy principle for the derivation of approximate Bayesian inference, which results in the risk of unpredictable results of model evidence and posterior densities of connection strengths over repeated runs of analyses (Daunizeau et al., 2009; Daunizeau et al., 2011a). Two aspects of the free energy optimization procedure, which may affect unstable model evidence and posterior densities of connection strengths have been discussed: (i) The construct of "global maximum level" of free energy (Daunizeau et al., 2011a) and (ii) the use of the mean-field/Laplace approximation as part of the variational Bayesian scheme for inference (Daunizeau et al., 2009; Daunizeau et al., 2011a). The investigation of minimising the risks for the unstable results and possible solutions for more reproducible findings is ongoing.

In summary, DCM is a useful tool for inferring synaptic plasticity processes, which may underlie neural responses when the robustness of the statistical inference is

[6] DCM8 is considered stable.

ensured. We propose to combine DCM for fMRI and DCM for EEG/MEG to further increase the biological plausibility in addition to the application of nonlinear DCM.

5.3.2 Investigating functional large-scale networks of fMRI data in context of the dopamine hypothesis and glutamate hypothesis of schizophrenia

In a recent review, it has been proposed that DCM studies that modelled cognitive function in subjects with schizophrenia may be able to interpret EC findings on the basis of the dopamine hypothesis and glutamate hypothesis of schizophrenia (Dauvermann et al., 2014; numeric/verbal working memory, Deserno et al., 2012; Schmidt et al., 2013; verbal fluency, Dauvermann et al., 2013).

These exemplary studies used DCM as a biophysical modelling approach to functional large-scale networks to report altered EC findings during a cognitive task in individuals with schizophrenia in contrast to healthy controls. The findings were interpreted in terms of altered synaptic plasticity processes and dopaminergic/glutamatergic transmission in individuals with schizophrenia when compared to healthy controls supporting the disconnection hypothesis of schizophrenia (Stephan et al., 2006; Stephan et al., 2009a). Thus, these results may show indications of linkage between clinical large-scale networks and preclinical neurotransmitter modulation of cognitive function. Altered synaptic plasticity during cognitive function (such as working memory and verbal fluency) can be interpreted with dopaminergic and glutamatergic mechanisms. We emphasise that the interpretation of altered neurotransmitter circuits should be considered carefully because DCM is likely to underestimate the processing complexity in neurobiological

circuits.

The main finding of the SFMHS was that EST and healthy control showed different functional large-scale networks during the "N-Back" task, which may reflect compensatory mechanisms in EST given the comparably high performance. Thus, different functional networks may be interpreted as different learning strategies between EST and healthy controls und therefore different synaptic plasticity. We discuss possible methodological aspects of the SFMHS, which may offer an explanation for the reported findings. Firstly, the comparison of connection strengths (with nonlinear modulation) between EST and healthy controls was not possible due to the application of the heuristic search protocol from the EHRS. The robust nature of the protocol developed for the EHRS showed that EST and healthy controls of the SFMHS resolved the working memory task by using different functional networks. Secondly, although the connection strengths could not be compared among the two groups we speculate that synaptic plasticity processes could be altered between the groups based on the two different functional networks. In general, the inference of connection strength as assessed with DCM is based on the premise that each specified model entering the model comparison may resemble a model of regions and connections known to be implicated during the examined brain function. Therefore, it can be assumed that different structures of functional networks may point at the possibility of different neurobiological networks between EST and healthy controls. Currently, DCM does not allow the comparison of different models among two groups. Lastly, EST were treated with antipsychotic medication, which may have ameliorated the connection strengths (Schmidt et al., 2013) although the mode of actions of

antipsychotic medication is unclear.

5.3.3 Understanding of schizophrenia as a cognitive brain network disorder

Our understanding of schizophrenia is in continuous development. Translation between preclinical and clinical research plays a crucial role in forming the notion of schizophrenia.

The understanding of schizophrenia as a brain disorder has developed by observations of effects of antipsychotic treatment in patients with schizophrenia. In addition, preclinical systematic research of pharmacological effects on brain processes has revealed evidence of alterations of cellular, chemical and molecular mechanisms:

(i) Findings of dopaminergic and glutamatergic transmission in animal models of schizophrenia contributed to the understanding of schizophrenia as a brain disorder.

(ii) Findings of neurotransmitter circuits, mainly dopaminergic and glutamatergic circuits, were found to modulate working memory in animal models of schizophrenia in combination with computational studies (Durstewitz and Seamans, 2008). Such evidence contributed to shape the understanding of schizophrenia as a cognitive network disorder.

However, the understanding of schizophrenia has not only been shaped by preclinical research but also by clinical research in individuals with schizophrenia, which has been and continues to be illuminated by preclinical neurobiological and computational work. The field of clinical and cognitive neurosciences has

contributed to forming our understanding of schizophrenia as a cognitive brain disorder. In addition, biophysical modelling of fMRI scans has led to the progress in our understanding of schizophrenia as a cognitive brain network disorder.

For future research, we propose the combination of biophysical modelling of functional large-scale networks and other computational neuropsychiatric aspects, which are able to detect critical neurobiological processes and which are of clinical relevance for individuals with schizophrenia. Long-term objectives of predicting and improving clinical treatment in patients with schizophrenia may be met by considering investigation of the following neuropsychiatric factors:

- Neurotransmitter systems
- Behaviour
- Clinical symptoms
- Effects of antipsychotic medication
- Clinical outcome.

Research on these combined analyses in individuals at different phases of schizophrenia in comparison to healthy controls may lead to better insight into the nature or development of functional large-scale networks from the high risk stage over the course of schizophrenia. It is conceivable that altered functional large-scale networks are already apparent at the high risk stage before the onset of schizophrenia. Alternatively, functional large-scale networks could change after the onset of the illness based on altered neurobiological processes.

Finally, we suggest study designs, which may lead to better insight into the development of clinical treatment for subjects with schizophrenia by combining

neuroimaging techniques or modelling approaches of neuropsychiatric factors, for example:

(i) Combination of biophysical modelling of functional large-scale networks with computation, for example:
    a. Brain function and brain circuit model (Anticevic et al., 2012);
    b. Brain function and behaviour (Murray et al., 2012);
    c. Brain function and effect of antipsychotic medication:

(ii) Combination of biophysical modelling of functional large-scale networks with multimodal neuroimaging study designs, for example:
    a. FMRI and EEG/MEG study designs;
    b. FMRI and TMS study designs (D'Ardenne et al., 2012);
    c. FMRI and MRS study designs;
    d. FMRI and PET study designs;

(iii) Combination of biophysical modelling of functional large-scale networks with models of sensory learning (a), reinforcement learning (b) and classification algorithms (c), for example:
    a. Sensory learning (den Ouden et al., 2009; den Ouden et al., 2010);
    b. Reinforcement learning (Montague et al., 2012);
    c. Machine learning approach (Brodersen et al., 2011; Brodersen et al., 2013).

Here, we discuss a possible future DCM for fMRI and MRS study design, which falls into the category of (ii) 'Combination of biophysical modelling of functional large-scale networks with multimodal neuroimaging study designs'. This study design

can be seen as an additional study design to the existent DCM study in working memory in EST and healthy controls as part of the SFMHS (chapter 4).

In the DCM part of the SFMHS, we assessed EC measures of functional large-scale networks during working memory in EST and healthy controls. In particular, we measured the connection strengths with nonlinear modulation of the meso-cortical connection. The main result was that EST and HC showed two different optimal models for the working memory task, which we interpreted as an indication for a compensatory mechanism and/or 'learning' strategy. However, due to the lack of a Glu measure in the participants, we could not comment on possible glutamatergic alterations and their effect on differing synaptic plasticity underlying the functional large-scale networks.

Here, we suggest the following study design to investigate possible relationships between glutamatergic levels in prefrontal regions and connectivity measures in working memory in EST and HC. The study design consists of three parts, of which the second and third part supplement the first part (i.e. chapter 4):

(i) Application of DCM for fMRI to "N-Back task" in EST and healthy controls;

(ii) *In vivo* resting Glu level measurement by the means of Single-Voxel Spectroscopy/MRS in the same participants and the same scanning session in prefrontal regions such as the bilateral DLPFC and ACC, which are known to be implicated in working memory function. Furthermore, the regions of the DLPFC and ACC are specified as regions in the functional networks.

(iii) Post-hoc analysis of relationships between (nonlinear) connection strengths and Glu concentrations.

The combination of modelling functional large-scale networks with assessment of glutamatergic concentrations in the same participants may lead to a better understanding of working memory and possibly related glutamatergic involvement in individuals with schizophrenia.

5.4 Concluding remarks

We have conducted modelling of functional large-scale networks and considered how they contribute to our understanding of schizophrenia as a cognitive brain network disorder. The DCM findings of the EHRS and the SFMHS enabled us to investigate functional networks during the performance of a cognitive task and to interpret the findings in context of neurobiological hypotheses of schizophrenia. For the EHRS, we reported findings of altered synaptic plasticity during verbal fluency between subjects at high familial risk of schizophrenia and healthy controls. For the SFMHS, we showed that EST and healthy controls used different functional networks during working memory. For future research, the combination of modelling fMRI scans and other neuropsychiatric factors can bring researchers closer to the common long-term objectives of developing imaging based diagnostic tools with the potential of improving treatment for individuals with schizophrenia.

6 Bibliography

Abbott LF, Regehr WG (2004) Synaptic computation. Nature 431:796-803.

Abbott LF, Varela JA, Sen K, Nelson SB (1997) Synaptic depression and cortical gain control. Science 275:220-224.

Abi-Dargham A, Mawlawi O, Lombardo I, Gil R, Martinez D, Huang Y, Hwang DR, Keilp J, Kochan L, Van Heertum R, Gorman JM, Laruelle M (2002) Prefrontal dopamine D1 receptors and working memory in schizophrenia. J Neurosci 22:3708-3719.

Abi-Saab WM, D'Souza DC, Moghaddam B, Krystal JH (1998) The NMDA antagonist model for schizophrenia: promise and pitfalls. Pharmacopsychiatry 31 Suppl 2:104-109.

Abitz M, Nielsen RD, Jones EG, Laursen H, Graem N, Pakkenberg B (2007) Excess of neurons in the human newborn mediodorsal thalamus compared with that of the adult. Cereb Cortex 17:2573-2578.

Akbarian S, Kim JJ, Potkin SG, Hagman JO, Tafazzoli A, Bunney WE, Jr., Jones EG (1995) Gene expression for glutamic acid decarboxylase is reduced without loss of neurons in prefrontal cortex of schizophrenics. Arch Gen Psychiatry 52:258-266.

Alelu-Paz R, Gimenez-Amaya JM (2008) The mediodorsal thalamic nucleus and schizophrenia. Journal of psychiatry & neuroscience : JPN 33:489-498.

Allen P, Chaddock CA, Egerton A, Howes OD, Barker G, Bonoldi I, Fusar-Poli P, Murray R, McGuire P (2014) Functional Outcome in People at High Risk for Psychosis Predicted by Thalamic Glutamate Levels and Prefronto-Striatal Activation. Schizophrenia bulletin. pii: sbu115. [Epub ahead of print].

Allen P, Stephan KE, Mechelli A, Day F, Ward N, Dalton J, Williams SC, McGuire P (2010) Cingulate activity and fronto-temporal connectivity in people with prodromal signs of psychosis. Neuroimage 49:947-955.

Allen P, Mechelli A, Stephan KE, Day F, Dalton J, Williams S, McGuire PK (2008) Fronto-temporal interactions during overt verbal initiation and suppression. J Cogn Neurosci 20:1656-1669.

Andreasen NC (1997) Improvement of negative symptoms: Concepts, definition and assessment. International clinical psychopharmacology 12 Suppl 2:S7-10.

Andreasen NC (1989) The Scale for the Assessment of Negative Symptoms (SANS): conceptual and theoretical foundations. Br J Psychiatry Suppl 49-58.

Anticevic A, Gancsos M, Murray JD, Repovs G, Driesen NR, Ennis DJ, Niciu MJ, Morgan PT, Surti TS, Bloch MH, Ramani R, Smith MA, Wang XJ, Krystal JH, Corlett PR (2012) NMDA receptor function in large-scale anticorrelated neural systems with implications for cognition and schizophrenia. Proc Natl Acad Sci U S A 109:16720-16725.

Ardid S, Wang XJ, Compte A (2007) An integrated microcircuit model of attentional processing in the neocortex. J Neurosci 27:8486-8495.

Arnsten AF, Wang MJ, Paspalas CD (2012) Neuromodulation of thought: flexibilities and vulnerabilities in prefrontal cortical network synapses. Neuron 76:223-239.

Arnsten AF, Paspalas CD, Gamo NJ, Yang Y, Wang M (2010) Dynamic Network Connectivity: A new form of neuroplasticity. Trends Cogn Sci 14:365-375.

American Psychiatric Association (2000) Diagnostic and Statistical Manual of Mental Disorders, Fourth Edition: DSM-IV-TR: American Psychiatric Pub.

Augustinaite S, Heggelund P (2007) Changes in firing pattern of lateral geniculate neurons caused by membrane potential dependent modulation of retinal input through NMDA receptors. The Journal of physiology 582:297-315.

Au-Young SM, Shen H, Yang CR (1999) Medial prefrontal cortical output neurons to the ventral tegmental area (VTA) and their responses to burst-patterned stimulation of the VTA: neuroanatomical and in vivo electrophysiological analyses. Synapse 34:245-255.

Baddeley A (1996) The fractionation of working memory. Proc Natl Acad Sci U S A 93:13468-13472.

Baddeley A (1981) The concept of working memory: a view of its current state and probable future development. Cognition 10:17-23.

Balu DT, Coyle JT (2011) Neuroplasticity signaling pathways linked to the pathophysiology of schizophrenia. Neurosci Biobehav Rev 35:848-870.

Barak O, Tsodyks M, Romo R (2010) Neuronal population coding of parametric working memory. J Neurosci 30:9424-9430.

Barch DM, Carter CS, Braver TS, Sabb FW, MacDonald A, 3rd, Noll DC, Cohen JD (2001) Selective deficits in prefrontal cortex function in medication-naive patients with schizophrenia. Arch Gen Psychiatry 58:280-288.

Becerril KE, Repovs G, Barch DM (2011) Error processing network dynamics in schizophrenia. Neuroimage 54:1495-1505.

Berends M, Maex R, De Schutter E (2005) The effect of NMDA receptors on gain modulation. Neural computation 17:2531-2547.

Blackwood DH, Fordyce A, Walker MT, St Clair DM, Porteous DJ, Muir WJ (2001) Schizophrenia and affective disorders--cosegregation with a translocation at chromosome 1q42 that directly disrupts brain-expressed genes: clinical and P300 findings in a family. American journal of human genetics 69:428-433.

Bloom PA, Fischler I (1980) Completion norms for 329 sentence contexts. Mem Cognit 8:631:642.

Boksman K, Theberge J, Williamson P, Drost DJ, Malla A, Densmore M, Takhar J, Pavlosky W, Menon RS, Neufeld RW (2005) A 4.0-T fMRI study of brain connectivity during word fluency in first-episode schizophrenia. Schizophr Res 75:247-263.

Bonci A, Malenka RC (1999) Properties and plasticity of excitatory synapses on dopaminergic and GABAergic cells in the ventral tegmental area. J Neurosci 19:3723-3730.

Bora E, Lin A, Wood SJ, Yung AR, McGorry PD, Pantelis C (2014) Cognitive deficits in youth with familial and clinical high risk to psychosis: a systematic review and meta-analysis. Acta psychiatrica Scandinavica 130:1-15.

Bora E, Murray RM (2013) Meta-analysis of Cognitive Deficits in Ultra-high Risk to Psychosis and First-Episode Psychosis: Do the Cognitive Deficits Progress Over, or After, the Onset of Psychosis? Schizophr Bull.

Botvinick MM, Braver TS, Barch DM, Carter CS, Cohen JD (2001) Conflict monitoring and cognitive control. Psychol Rev 108:624-652.

Braff D, Schork NJ, Gottesman, II (2007) Endophenotyping schizophrenia. Am J Psychiatry 164:705-707.

Braver TS, Barch DM, Cohen JD (1999) Cognition and control in schizophrenia: a computational model of dopamine and prefrontal function. Biol Psychiatry 46:312-328.

Braver TS, Cohen JD (1999) Dopamine, cognitive control, and schizophrenia: the gating model. Prog Brain Res 121:327-349.

Braver TS, Cohen JD, Nystrom LE, Jonides J, Smith EE, Noll DC (1997) A parametric study of prefrontal cortex involvement in human working memory. Neuroimage 5:49-62.

Brázdil M, Mikl M, Marecek R, Krupa P, Rektor I (2007) Effective connectivity in target stimulus processing: a dynamic causal modeling study of visual oddball task. Neuroimage 35:827-835.

Briggs F, Usrey WM (2008) Emerging views of corticothalamic function. Curr Opin Neurobiol 18:403-407.

Brodersen KH, Deserno L, Schlagenhauf F, Lin Z, Penny WD, Buhmann JM, Stephan KE (2013) Dissecting psychiatric spectrum disorders by generative embedding. Neuroimage Clin 4:98-111.

Brodersen KH, Schofield TM, Leff AP, Ong CS, Lomakina EI, Buhmann JM, Stephan KE (2011) Generative embedding for model-based classification of fMRI data. PLoS computational biology 7:e1002079.

Broome MR, Matthiasson P, Fusar-Poli P, Woolley JB, Johns LC, Tabraham P, Bramon E, Valmaggia L, Williams SC, Brammer MJ, Chitnis X, McGuire PK (2009) Neural correlates of executive function and working memory in the 'at-risk mental state'. Br J Psychiatry 194:25-33.

Brown GG, Thompson WK (2010) Functional brain imaging in schizophrenia: selected results and methods. Curr Top Behav Neurosci 4:181-214.

Brunel N, Wang XJ (2001) Effects of neuromodulation in a cortical network model of object working memory dominated by recurrent inhibition. Journal of computational neuroscience 11:63-85.

Bryson G, Bell M, Greig T, Kaplan E (1999) Internal consistency, temporal stability and neuropsychological correlates of three cognitive components of the Positive and Negative Syndrome Scale (PANSS). Schizophr Res 38:27-35.

Büchel C, Friston KJ (1997) Modulation of connectivity in visual pathways by attention: cortical interactions evaluated with structural equation modelling and fMRI. Cerebral cortex 7:768-778.

Burgess PW, Shallice T (1997) The Hayling and Brixton Tests. Bury St Edmunds (UK). Thames Valley Test Company.

Burgess PW, Shallice T (1996) Response suppression, initiation and strategy use following frontal lobe lesions. Neuropsychologia 34(4):263-272.

Byne W, Hazlett EA, Buchsbaum MS, Kemether E (2009) The thalamus and schizophrenia: current status of research. Acta neuropathologica 117:347-368.

Callicott JH, Mattay VS, Verchinski BA, Marenco S, Egan MF, Weinberger DR (2003) Complexity of prefrontal cortical dysfunction in schizophrenia: more than up or down. Am J Psychiatry 160:2209-2215.

Callicott JH, Bertolino A, Mattay VS, Langheim FJ, Duyn J, Coppola R, Goldberg TE, Weinberger DR (2000) Physiological dysfunction of the dorsolateral prefrontal cortex in schizophrenia revisited. Cereb Cortex 10:1078-1092.

Carletti F, Woolley JB, Bhattacharyya S, Perez-Iglesias R, Fusar Poli P, Valmaggia L, Broome MR, Bramon E, Johns L, Giampietro V, Williams SC, Barker GJ, McGuire PK (2012) Alterations in white matter evident before the onset of psychosis. Schizophrenia bulletin 38:1170-1179.

Carlsson A (1978) Does dopamine have a role in schizophrenia? Biol Psychiatry 13:3-21.

Carlsson A, Waters N, Waters S, Carlsson ML (2000) Network interactions in schizophrenia - therapeutic implications. Brain Res Brain Res Rev 31:342-349.

Carlsson A, Hansson LO, Waters N, Carlsson ML (1999) A glutamatergic deficiency model of schizophrenia. Br J Psychiatry Suppl 2-6.

Carlsson A, Hansson LO, Waters N, Carlsson ML (1997) Neurotransmitter aberrations in schizophrenia: new perspectives and therapeutic implications. Life Sci 61:75-94.

Carr DB, Sesack SR (2000) Projections from the rat prefrontal cortex to the ventral tegmental area: target specificity in the synaptic associations with mesoaccumbens and mesocortical neurons. J Neurosci 20:3864-3873.

Carter CS, Perlstein W, Ganguli R, Brar J, Mintun M, Cohen JD (1998) Functional hypofrontality and working memory dysfunction in schizophrenia. Am J Psychiatry 155:1285-1287.

Chan RCK, Shum D, Toulopoulou T, Chen EYH (2008) Assessment of executive functions: Review of instruments and identification of critical issues. Arch Clin Neuropsychol 23(2):201-216.

Chance FS, Abbott LF, Reyes AD (2002) Gain modulation from background synaptic input. Neuron 35:773-782.

Chen CC, Kiebel SJ, Friston KJ (2008) Dynamic causal modelling of induced responses. Neuroimage 41:1293-1312.

Clinton SM, Meador-Woodruff JH (2004) Thalamic dysfunction in schizophrenia: neurochemical, neuropathological, and in vivo imaging abnormalities. Schizophr Res 69:237-253.

Cohen J (1988) Statistical Power Analysis for the Behavioral Sciences. Hillsdale, New Yersey: Lawrence Erlbaum Associates.

Cohen JD, Braver TS, Brown JW (2002) Computational perspectives on dopamine function in prefrontal cortex. Curr Opin Neurobiol 12:223-229.

Cohen JD, Braver TS, O'Reilly RC (1996) A computational approach to prefrontal cortex, cognitive control and schizophrenia: recent developments and current challenges. Philos Trans R Soc Lond B Biol Sci 351:1515-1527.

Cohen JD, Servan-Schreiber D (1992) Context, cortex, and dopamine: a connectionist approach to behavior and biology in schizophrenia. Psychol Rev 99:45-77.

Cole MW, Schneider W (2007) The cognitive control network: Integrated cortical regions with dissociable functions. Neuroimage 37:343-360.

Collette F, Van der Linden M (2002) Brain imaging of the central executive component of working memory. Neurosci Biobehav Rev 26:105-125.

Collette F, Van der Linden M, Delfiore G, Degueldre C, Luxen A, Salmon E (2001) The functional anatomy of inhibition processes investigated with the Hayling task. Neuroimage 14:258-267.

Cools R, Gibbs SE, Miyakawa A, Jagust W, D'Esposito M (2008) Working memory capacity predicts dopamine synthesis capacity in the human striatum. J Neurosci 28:1208-1212.

Cortes R, Camps M, Gueye B, Probst A, Palacios JM (1989) Dopamine receptors in human brain: autoradiographic distribution of D1 and D2 sites in Parkinson syndrome of different etiology. Brain Res 483:30-38.

Coyle JT, Basu A, Benneyworth M, Balu D, Konopaske G (2012) Glutamatergic synaptic dysregulation in schizophrenia: therapeutic implications. Handbook of experimental pharmacology 267-295.

Coyle JT (2012) NMDA receptor and schizophrenia: a brief history. Schizophr Bull 38:920-926.

Coyle JT, Balu D, Benneyworth M, Basu A, Roseman A (2010) Beyond the dopamine receptor: novel therapeutic targets for treating schizophrenia. Dialogues Clin Neurosci 12:359-382.

Coyle JT (2006) Glutamate and schizophrenia: beyond the dopamine hypothesis. Cell Mol Neurobiol 26:365-384.

Crandall SR, Cox CL (2012) Local dendrodendritic inhibition regulates fast synaptic transmission in visual thalamus. J Neurosci 32:2513-2522.

Creese I, Burt DR, Snyder SH (1976) Dopamine receptor binding predicts clinical and pharmacological potencies of antischizophrenic drugs. Science 192:481-483.

Cronenwett WJ, Csernansky J. (2010) Thalamic pathology in schizophrenia. Curr Top Behav Neurosci 4:509-28.

Crossley NA, Mechelli A, Fusar-Poli P, Broome MR, Matthiasson P, Johns LC, Bramon E, Valmaggia L, Williams SC, McGuire PK (2009) Superior temporal lobe dysfunction and frontotemporal dysconnectivity in subjects at risk of psychosis and in first-episode psychosis. Hum Brain Mapp 30:4129-4137.

Curtis VA, Bullmore ET, Brammer MJ, Wright IC, Williams SC, Morris RG, Sharma TS, Murray RM, McGuire PK (1998) Attenuated frontal activation during a verbal fluency task in patients with schizophrenia. Am J Psychiatry 155:1056-1063.

da Silva Alves F, Figee M, van Amelsvoort T, Veltman D, de Haan L (2008) The revised dopamine hypothesis of schizophrenia: evidence from pharmacological MRI studies with atypical antipsychotic medication. Psychopharmacology bulletin 41:121-132.

D'Aiuto L, Prasad KM, Upton CH, Viggiano L, Milosevic J, Raimondi G, McClain L, Chowdari K, Tischfield J, Sheldon M, Moore JC, Yolken RH, Kinchington PR, Nimgaonkar VL (2014) Persistent infection by HSV-1 is associated with changes in functional architecture of iPSC-derived neurons and brain activation patterns underlying working memory performance. Schizophr Bull doi:10.1093/schbul/sbu032 [Epub ahead of print].

D'Ardenne K, Eshel N, Luka J, Lenartowicz A, Nystrom LE, Cohen JD (2012) Role of prefrontal cortex and the midbrain dopamine system in working memory updating. Proc Natl Acad Sci U S A 109:19900-19909.

Daunizeau J, David O, Stephan KE (2011a) Dynamic causal modelling: a critical review of the biophysical and statistical foundations. Neuroimage 58:312-322.

Daunizeau J, Preuschoff K, Friston K, Stephan K (2011b) Optimizing experimental design for comparing models of brain function. PLoS computational biology 7:e1002280.

Daunizeau J, Kiebel SJ, Friston KJ (2009) Dynamic causal modelling of distributed electromagnetic responses. Neuroimage 47:590-601.

Dauvermann MR, Whalley HC, Schmidt A, Lee GL, Romaniuk L, Roberts N, Johnstone EC, Lawrie SM, Moorhead TW (2014) Computational Neuropsychiatry - Schizophrenia as a Cognitive Brain Network Disorder. Front Psychiatry 5:30.

Dauvermann MR, Whalley HC, Romaniuk L, Valton V, Owens DG, Johnstone EC, Lawrie SM, Moorhead TW (2013) The application of nonlinear Dynamic Causal Modelling for fMRI in subjects at high genetic risk of schizophrenia. Neuroimage 73:16-29.

Dauvermann MR, Mukherjee P, Moorhead WT, Stanfield AC, Fusar-Poli P, Lawrie SM, Whalley HC (2012) Relationship between gyrification and functional connectivity of the prefrontal cortex in subjects at high genetic risk of schizophrenia. Current pharmaceutical design 18:434-442.

Davis KL, Kahn RS, Ko G, Davidson M (1991) Dopamine in schizophrenia: a review and reconceptualization. Am J Psychiatry 148:1474-1486.

Dayan PA, L.F. (2000) Theoretical Neuroscience: Computational and Mathematical Modeling of Neural Systems. Cambridge, MA: The MIT Press.

Delay J, Deniker P, Harl JM (1952) [Therapeutic use in psychiatry of phenothiazine of central elective action (4560 RP)]. Ann Med Psychol (Paris) 110:112-117.

den Ouden HE, Daunizeau J, Roiser J, Friston KJ, Stephan KE (2010) Striatal prediction error modulates cortical coupling. J Neurosci 30:3210-3219.

den Ouden HE, Friston KJ, Daw ND, McIntosh AR, Stephan KE (2009) A dual role for prediction error in associative learning. Cereb Cortex 19:1175-1185.

Deng PY, Klyachko VA (2011) The diverse functions of short-term plasticity components in synaptic computations. Communicative & integrative biology 4:543-548.

Deserno L, Sterzer P, Wustenberg T, Heinz A, Schlagenhauf F (2012) Reduced prefrontal-parietal effective connectivity and working memory deficits in schizophrenia. J Neurosci 32:12-20.

Destexhe A (2009) Self-sustained asynchronous irregular states and Up-Down states in thalamic, cortical and thalamocortical networks of nonlinear integrate-and-fire neurons. Journal of computational neuroscience 27:493-506.

Dima D, Dietrich DE, Dillo W, Emrich HM (2010) Impaired top-down processes in schizophrenia: a DCM study of ERPs. Neuroimage 52:824-832.

Dima D, Roiser JP, Dietrich DE, Bonnemann C, Lanfermann H, Emrich HM, Dillo W (2009) Understanding why patients with schizophrenia do not perceive the hollow-mask illusion using dynamic causal modelling. Neuroimage 46:1180-1186.

Driesen NR, McCarthy G, Bhagwagar Z, Bloch MH, Calhoun VD, D'Souza DC, Gueorguieva R, He G, Leung HC, Ramani R, Anticevic A, Suckow RF, Morgan PT, Krystal JH (2013) The impact of NMDA receptor blockade on human working memory-related prefrontal function and connectivity. Neuropsychopharmacology 38:2613-2622.

Durstewitz D, Seamans JK (2008) The dual-state theory of prefrontal cortex dopamine function with relevance to catechol-o-methyltransferase genotypes and schizophrenia. Biol Psychiatry 64:739-749.

Durstewitz D, Seamans JK, Sejnowski TJ (2000) Dopamine-mediated stabilization of delay-period activity in a network model of prefrontal cortex. J Neurophysiol 83:1733-1750.

Durstewitz D, Seamans JK (2002) The computational role of dopamine D1 receptors in working memory. Neural Netw 15:561-572.

Durstewitz D, Kelc M, Güntürkün O (1999) A neurocomputational theory of the dopaminergic modulation of working memory functions. J Neurosci 19:2807-2822.

Düzel S, Schutze H, Stallforth S, Kaufmann J, Bodammer N, Bunzeck N, Munte TF, Lindenberger U, Heinze HJ, Düzel E (2008) A close relationship between verbal memory and SN/VTA integrity in young and older adults. Neuropsychologia 46:3042-3052.

Efron B, Tibshirani, R.J. (1993) An Introduction to the Bootstrap. New York: Chapman and Hall.

Egerton A, Stone JM, Chaddock CA, Barker GJ, Bonoldi I, Howard RM, Merritt K, Allen P, Howes OD, Murray RM, McLean MA, Lythgoe DJ, O'Gorman RL, McGuire PK (2014) Relationship Between Brain Glutamate Levels and Clinical Outcome in Individuals at Ultra High Risk of Psychosis. Neuropsychopharmacology : official publication of the American College of Neuropsychopharmacology.

Egerton A, Chaddock CA, Winton-Brown TT, Bloomfield MA, Bhattacharyya S, Allen P, McGuire PK, Howes OD (2013) Presynaptic striatal dopamine dysfunction in people at ultra-high risk for psychosis: findings in a second cohort. Biological psychiatry 74:106-112.

Elvevag B, Goldberg TE (2000) Cognitive impairment in schizophrenia is the core of the disorder. Critical reviews in neurobiology 14:1-21.

Emilien G, Maloteaux JM, Geurts M, Owen MJ (1999) Dopamine receptors and schizophrenia: contribution of molecular genetics and clinical neuropsychology. Int J Neuropsychopharmacol 2:197-227.

Errington AC, Renger JJ, Uebele VN, Crunelli V (2010) State-dependent firing determines intrinsic dendritic Ca2+ signaling in thalamocortical neurons. J Neurosci 30:14843-14853.

Ettinger U, Williams SC, Fannon D, Premkumar P, Kuipers E, Moller HJ, Kumari V (2011) Functional magnetic resonance imaging of a parametric working memory task in schizophrenia: relationship with performance and effects of antipsychotic treatment. Psychopharmacology (Berl) 216:17-27.

Farber NB, Kim SH, Dikranian K, Jiang XP, Heinkel C (2002) Receptor mechanisms and circuitry underlying NMDA antagonist neurotoxicity. Mol Psychiatry 7:32-43.

Fitzgerald PJ (2012) The NMDA receptor may participate in widespread suppression of circuit level neural activity, in addition to a similarly prominent role in circuit level activation. Behav Brain Res 230:291-298.

Freyer F, Roberts JA, Becker R, Robinson PA, Ritter P, Breakspear M (2011) Biophysical mechanisms of multistability in resting-state cortical rhythms. J Neurosci 31:6353-6361.

Friston KJ, Shiner T, FitzGerald T, Galea JM, Adams R, Brown H, Dolan RJ, Moran R, Stephan KE, Bestmann S (2012) Dopamine, affordance and active inference. PLoS computational biology 8:e1002327.

Friston KJ, Dolan RJ (2010) Computational and dynamic models in neuroimaging. Neuroimage 52:752-765.

Friston K (2009) Causal modelling and brain connectivity in functional magnetic resonance imaging. PLoS biology 7:e33.

Friston KJ, Harrison L, Penny W (2003) Dynamic causal modelling. Neuroimage 19:1273-1302.

Friston KJ (2002) Dysfunctional connectivity in schizophrenia. World psychiatry: official journal of the World Psychiatric Association 1:66-71.

Friston KJ, Buechel C, Fink GR, Morris J, Rolls E, Dolan RJ (1997) Psychophysiological and modulatory interactions in neuroimaging. NeuroImage 6:218-229.

Friston KJ, Frith CD (1995) Schizophrenia: a disconnection syndrome? Clin Neurosci 3:89-97.

Frith CD, Friston KJ, Herold S, Silbersweig D, Fletcher P, Cahill C, Dolan RJ, Frackowiak RS, Liddle PF (1995) Regional brain activity in chronic schizophrenic patients during the performance of a verbal fluency task. Br J Psychiatry 167:343-349.

Frith CD, Friston KJ, Liddle PF, Frackowiak RS (1991) A PET study of word finding. Neuropsychologia 29:1137-1148.

Fu CH, Morgan K, Suckling J, Williams SC, Andrew C, Vythelingum GN, McGuire PK (2002) A functional magnetic resonance imaging study of overt letter verbal fluency using a clustered acquisition sequence: greater anterior cingulate activation with increased task demand. Neuroimage 17:871-879.

Fusar-Poli P, Nelson B, Valmaggia L, Yung AR, McGuire PK (2014) Comorbid depressive and anxiety disorders in 509 individuals with an at-risk mental state: impact on psychopathology and transition to psychosis. Schizophrenia bulletin 40:120-131.

Fusar-Poli P, Meyer-Lindenberg A (2013a) Striatal presynaptic dopamine in schizophrenia, Part I: meta-analysis of dopamine active transporter (DAT) density. Schizophr Bull 39:22-32.

Fusar-Poli P, Meyer-Lindenberg A (2013b) Striatal presynaptic dopamine in schizophrenia, part II: meta-analysis of [(18)F/(11)C]-DOPA PET studies. Schizophr Bull 39:33-42.

Fusar-Poli P, Bonoldi I, Yung AR, Borgwardt S, Kempton MJ, Valmaggia L, Barale F, Caverzasi E, McGuire P (2012) Predicting psychosis: meta-analysis of transition outcomes in individuals at high clinical risk. Arch Gen Psychiatry 69:220-229.

Fusar-Poli P, Stone JM, Broome MR, Valli I, Mechelli A, McLean MA, Lythgoe DJ, O'Gorman RL, Barker GJ, McGuire PK (2011) Thalamic glutamate levels as a predictor of cortical response during executive functioning in subjects at high risk for psychosis. Arch Gen Psychiatry 68:881-890.

Fusar-Poli P, Howes OD, Allen P, Broome M, Valli I, Asselin MC, Grasby PM, McGuire PK (2010) Abnormal frontostriatal interactions in people with prodromal signs of psychosis: a multimodal imaging study. Arch Gen Psychiatry 67:683-691.

Gao C, Wolf ME (2008) Dopamine receptors regulate NMDA receptor surface expression in prefrontal cortex neurons. Journal of neurochemistry 106:2489-2501.

Gao C, Wolf ME (2007) Dopamine alters AMPA receptor synaptic expression and subunit composition in dopamine neurons of the ventral tegmental area cultured with prefrontal cortex neurons. J Neurosci 27:14275-14285.

Gao M, Liu CL, Yang S, Jin GZ, Bunney BS, Shi WX (2007) Functional coupling between the prefrontal cortex and dopamine neurons in the ventral tegmental area. J Neurosci 27:5414-5421.

Gao WJ, Wang Y, Goldman-Rakic PS (2003) Dopamine modulation of perisomatic and peridendritic inhibition in prefrontal cortex. J Neurosci 23:1622-1630.

Gazzaley A, Nobre AC (2012) Top-down modulation: bridging selective attention and working memory. Trends Cogn Sci 16:129-135.

Genevsky A, Garrett CT, Alexander PP, Vinogradov S (2010) Cognitive training in schizophrenia: a neuroscience-based approach. Dialogues Clin Neurosci 12:416-421.

Genovese CR, Lazar NA, Nichols T (2002) Thresholding of statistical maps in functional neuroimaging using the false discovery rate. Neuroimage 15:870-878.

Gioanni Y, Rougeot C, Clarke PB, Lepouse C, Thierry AM, Vidal C (1999) Nicotinic receptors in the rat prefrontal cortex: increase in glutamate release and facilitation of mediodorsal thalamo-cortical transmission. The European journal of neuroscience 11:18-30.

Girault JA, Greengard P (2004) The neurobiology of dopamine signaling. Arch Neurol 61:641-644.

Glahn DC, Knowles EE, McKay DR, Sprooten E, Raventos H, Blangero J, Gottesman, II, Almasy L (2014) Arguments for the sake of endophenotypes: examining common misconceptions about the use of endophenotypes in psychiatric genetics. American journal of medical genetics Part B, Neuropsychiatric genetics : the official publication of the International Society of Psychiatric Genetics 165B:122-130.

Glahn DC, Ragland JD, Abramoff A, Barrett J, Laird AR, Bearden CE, Velligan DI (2005) Beyond hypofrontality: a quantitative meta-analysis of functional neuroimaging studies of working memory in schizophrenia. Hum Brain Mapp 25:60-69.

Goebel R, Roebroeck A, Kim DS, Formisano E (2003) Investigating directed cortical interactions in time-resolved fMRI data using vector autoregressive modeling and Granger causality mapping. Magnetic resonance imaging 21:1251-1261.

Goff DC, Coyle JT (2001) The emerging role of glutamate in the pathophysiology and treatment of schizophrenia. Am J Psychiatry 158:1367-1377.

Goff DC, Tsai G, Manoach DS, Coyle JT (1995) Dose-finding trial of D-cycloserine added to neuroleptics for negative symptoms in schizophrenia. Am J Psychiatry 152:1213-1215.

Gold JM (2004) Cognitive deficits as treatment targets in schizophrenia. Schizophr Res 72:21-28.

Goldman-Rakic PS (1999) The physiological approach: functional architecture of working memory and disordered cognition in schizophrenia. Biol Psychiatry 46:650-661.

Goldman-Rakic PS, Selemon LD (1997) Functional and anatomical aspects of prefrontal pathology in schizophrenia. Schizophr Bull 23:437-458.

Goldman-Rakic PS (1996) Regional and cellular fractionation of working memory. Proc Natl Acad Sci U S A 93:13473-13480.

Goldman-Rakic PS (1995) Cellular basis of working memory. Neuron 14:477-485.

Goldman-Rakic PS, Leranth C, Williams SM, Mons N, Geffard M (1989) Dopamine synaptic complex with pyramidal neurons in primate cerebral cortex. Proc Natl Acad Sci U S A 86:9015-9019.

Gonzalez-Burgos G, Hashimoto T, Lewis DA (2010) Alterations of cortical GABA neurons and network oscillations in schizophrenia. Curr Psychiatry Rep 12:335-344.

Gonzalez-Burgos G, Kroener S, Seamans JK, Lewis DA, Barrionuevo G (2005) Dopaminergic modulation of short-term synaptic plasticity in fast-spiking interneurons of primate dorsolateral prefrontal cortex. J Neurophysiol 94:4168-4177.

Gottesman, II, Shields J (1966) Contributions of twin studies to perspectives on schizophrenia. Progress in experimental personality research 3:1-84.

Granger CWJ (1969) Investigating causal relations by econometric models and cross-spectral methods. Econometrica 37:424-438.

Gray JA, Roth BL (2007) Molecular targets for treating cognitive dysfunction in schizophrenia. Schizophr Bull 33:1100-1119.

Guerrero-Pedraza A, McKenna PJ, Gomar JJ, Sarro S, Salvador R, Amann B, Carrion MI, Landin-Romero R, Blanch J, Pomarol-Clotet E (2012) First-episode psychosis is characterized by failure of deactivation but not by hypo- or hyperfrontality. Psychol Med 42:73-84.

Hall RC (1995) Global assessment of functioning. A modified scale. Psychosomatics 36:267-275.

Harris JM, Moorhead TW, Miller P, McIntosh AM, Bonnici HM, Owens DG, Johnstone EC, Lawrie SM (2007) Increased prefrontal gyrification in a large high-risk cohort characterizes those who develop schizophrenia and reflects abnormal prefrontal development. Biol Psychiatry 62:722-729.

Harrison PJ, Weinberger DR (2005) Schizophrenia genes, gene expression, and neuropathology: on the matter of their convergence. Mol Psychiatry 10:40-68; image 45.

Harrison L, Penny WD, Friston K (2003) Multivariate autoregressive modeling of fMRI time series. NeuroImage 19:1477-1491.

Hayashi-Takagi A, Takaki M, Graziane N, Seshadri S, Murdoch H, Dunlop AJ, Makino Y, Seshadri AJ, Ishizuka K, Srivastava DP, Xie Z, Baraban JM, Houslay MD, Tomoda T, Brandon NJ, Kamiya A, Yan Z, Penzes P, Sawa A (2010) Disrupted-in-Schizophrenia 1 (DISC1) regulates spines of the glutamate synapse via Rac1. Nature neuroscience 13:327-332.

Hazlett EA, Buchsbaum MS, Kemether E, Bloom R, Platholi J, Brickman AM, Shihabuddin L, Tang C, Byne W (2004) Abnormal glucose metabolism in the mediodorsal nucleus of the thalamus in schizophrenia. Am J Psychiatry 161:305-314.

Hazy TE, Frank MJ, O'Reilly RC (2006) Banishing the homunculus: making working memory work. Neuroscience 139:105-118.

Heinz A, Deserno L, Reininghaus U (2013) Urbanicity, social adversity and psychosis. World psychiatry : official journal of the World Psychiatric Association 12:187-197.

Heinz A (2002) Dopaminergic dysfunction in alcoholism and schizophrenia--psychopathological and behavioral correlates. Eur Psychiatry 17:9-16.

Heresco-Levy U, Ermilov M, Shimoni J, Shapira B, Silipo G, Javitt DC (2002) Placebo-controlled trial of D-cycloserine added to conventional neuroleptics, olanzapine, or risperidone in schizophrenia. Am J Psychiatry 159:480-482.

Hitch GJ (1984) Working memory. Psychol Med 14:265-271.

Hodges A, Byrne M, Grant E, Johnstone E (1999) People at risk of schizophrenia. Sample characteristics of the first 100 cases in the Edinburgh High-Risk Study. Br J Psychiatry 174:547-553.

Honey GD, Fletcher PC (2006) Investigating principles of human brain function underlying working memory: what insights from schizophrenia? Neuroscience 139:59-71.

Honey GD, Fu CH, Kim J, Brammer MJ, Croudace TJ, Suckling J, Pich EM, Williams SC, Bullmore ET (2002) Effects of verbal working memory load on corticocortical connectivity modeled by path analysis of functional magnetic resonance imaging data. NeuroImage 17:573-582.

Honey GD, Bullmore ET, Soni W, Varatheesan M, Williams SC, Sharma T (1999) Differences in frontal cortical activation by a working memory task after substitution of risperidone for typical antipsychotic drugs in patients with schizophrenia. Proc Natl Acad Sci U S A 96:13432-13437.

Howes OD, Kambeitz J, Kim E, Stahl D, Slifstein M, Abi-Dargham A, Kapur S (2012) The nature of dopamine dysfunction in schizophrenia and what this means for treatment. Arch Gen Psychiatry 69:776-786.

Howes OD, Kapur S (2009) The dopamine hypothesis of schizophrenia: version III--the final common pathway. Schizophr Bull 35:549-562.

Huang LY, She HC, Chou WC, Chuang MH, Duann JR, Jung TP (2013) Brain oscillation and connectivity during a chemistry visual working memory task. International journal of psychophysiology : official journal of the International Organization of Psychophysiology 90:172-179.

Huys QJ, Moutoussis M, Williams J (2011) Are computational models of any use to psychiatry? Neural Netw 24:544-551.

Jackson ME, Frost AS, Moghaddam B (2001) Stimulation of prefrontal cortex at physiologically relevant frequencies inhibits dopamine release in the nucleus accumbens. Journal of neurochemistry 78:920-923.

Javitt DC, Zukin SR, Heresco-Levy U, Umbricht D (2012) Has an angel shown the way? Etiological and therapeutic implications of the PCP/NMDA model of schizophrenia. Schizophr Bull 38:958-966.

Javitt DC (2010) Glutamatergic theories of schizophrenia. Isr J Psychiatry Relat Sci 47:4-16.

Javitt DC (2007) Glutamate and schizophrenia: phencyclidine, N-methyl-D-aspartate receptors, and dopamine-glutamate interactions. Int Rev Neurobiol 78:69-108.

Javitt DC, Frusciante MJ, Zukin SR (1994) Activation-related and activation-independent effects of polyamines on phencyclidine receptor binding within the N-methyl-D-aspartate receptor complex. The Journal of pharmacology and experimental therapeutics 270:604-613.

Johnstone EC, Russell KD, Harrison LK, Lawrie SM (2003) The Edinburgh High Risk Study: current status and future prospects. World psychiatry : official journal of the World Psychiatric Association 2:45-49.

Johnstone EC, Abukmeil SS, Byrne M, Clafferty R, Grant E, Hodges A, Lawrie SM, Owens DG (2000) Edinburgh high risk study--findings after four years: demographic, attainment and psychopathological issues. Schizophr Res 46:1-15.

Jones EG (1997) Cortical development and thalamic pathology in schizophrenia. Schizophr Bull 23:483-501.

Kantrowitz JT, Javitt DC (2010) Thinking glutamatergically: changing concepts of schizophrenia based upon changing neurochemical models. Clin Schizophr Relat Psychoses 4:189-200.

Kapur S (2003) Psychosis as a state of aberrant salience: a framework linking biology, phenomenology, and pharmacology in schizophrenia. Am J Psychiatry 160:13-23.

Kapur S, Seeman P (2001) Does fast dissociation from the dopamine d(2) receptor explain the action of atypical antipsychotics?: A new hypothesis. Am J Psychiatry 158:360-369.

Kay SR, Sevy S (1990) Pyramidical model of schizophrenia. Schizophr Bull 16:537-545.

Kay SR, Fiszbein A, Opler LA (1987) The positive and negative syndrome scale (PANSS) for schizophrenia. Schizophr Bull 13:261-276.

Kerns JG, Cohen JD, MacDonald AW, 3rd, Cho RY, Stenger VA, Carter CS (2004) Anterior cingulate conflict monitoring and adjustments in control. Science 303:1023-1026.

Kiebel SJ (2012) Dynamic Causal Modelling for magneto- and electroencephalography. Biomedizinische Technik Biomedical engineering.

Kiebel SJ, Kloppel S, Weiskopf N, Friston KJ (2007) Dynamic causal modeling: a generative model of slice timing in fMRI. Neuroimage 34:1487-1496.

Kiebel SJ, David O, Friston KJ (2006) Dynamic causal modelling of evoked responses in EEG/MEG with lead field parameterization. Neuroimage 30:1273-1284.

Kim HS, Shin NY, Jang JH, Kim E, Shim G, Park HY, Hong KS, Kwon JS (2011) Social cognition and neurocognition as predictors of conversion to psychosis in individuals at ultra-high risk. Schizophr Res 130:170-175.

Kim SY, Lee H, Kim HJ, Bang E, Lee SH, Lee DW, Woo DC, Choi CB, Hong KS, Lee C, Choe BY (2011) In vivo and ex vivo evidence for ketamine-induced hyperglutamatergic activity in the cerebral cortex of the rat: Potential relevance to schizophrenia. NMR in biomedicine 24:1235-1242.

Kim JJ, Kwon JS, Park HJ, Youn T, Kang DH, Kim MS, Lee DS, Lee MC (2003) Functional disconnection between the prefrontal and parietal cortices during working memory processing in schizophrenia: a[15(O)]H2O PET study. Am J Psychiatry 160:919-923.

Kirchner WK (1958) Age differences in short-term retention of rapidly changing information. Journal of experimental psychology 55:352-358.

Kiss T, Hoffmann WE, Scott L, Kawabe TT, Milici AJ, Nilsen EA, Hajos M (2011) Role of Thalamic Projection in NMDA Receptor-Induced Disruption of Cortical Slow Oscillation and Short-Term Plasticity. Front Psychiatry 2:14.

Kolluri N, Sun Z, Sampson AR, Lewis DA (2005) Lamina-specific reductions in dendritic spine density in the prefrontal cortex of subjects with schizophrenia. Am J Psychiatry 162:1200-1202.

Krawitz A, Braver TS, Barch DM, Brown JW (2011) Impaired error-likelihood prediction in medial prefrontal cortex in schizophrenia. Neuroimage 54:1506-1517.

Kremen WS, Seidman LJ, Faraone SV, Toomey R, Tsuang MT (2000) The paradox of normal neuropsychological function in schizophrenia. Journal of abnormal psychology 109:743-752.

Krystal JH, D'Souza DC, Mathalon D, Perry E, Belger A, Hoffman R (2003) NMDA receptor antagonist effects, cortical glutamatergic function, and

schizophrenia: toward a paradigm shift in medication development. Psychopharmacology (Berl) 169:215-233.

Krystal JH, D'Souza DC, Karper LP, Bennett A, Abi-Dargham A, Abi-Saab D, Cassello K, Bowers MB, Jr., Vegso S, Heninger GR, Charney DS (1999) Interactive effects of subanesthetic ketamine and haloperidol in healthy humans. Psychopharmacology (Berl) 145:193-204.

Krystal JH, Karper LP, Seibyl JP, Freeman GK, Delaney R, Bremner JD, Heninger GR, Bowers MB, Jr., Charney DS (1994) Subanesthetic effects of the noncompetitive NMDA antagonist, ketamine, in humans. Psychotomimetic, perceptual, cognitive, and neuroendocrine responses. Arch Gen Psychiatry 51:199-214.

Kukla M, Davis LW, Lysaker PH (2013) Cognitive Behavioral Therapy and Work Outcomes: Correlates of Treatment Engagement and Full and Partial Success in Schizophrenia. Behavioural and cognitive psychotherapy 1-16.

Kumra S, Shaw M, Merka P, Nakayama E, Augustin R (2001) Childhood-onset schizophrenia: research update. Can J Psychiatry 46(10):923–930.

Lancaster JL, Woldorff MG, Parsons LM, Liotti M, Freitas CS, Rainey L, Kochunov PV, Nickerson D, Mikiten SA, Fox PT (2000) Automated Talairach atlas labels for functional brain mapping. Hum Brain Mapp 10:120-131.

Lancaster JL, Rainey LH, Summerlin JL, Freitas CS, Fox PT, Evans AC, Toga AW, Mazziotta JC (1997) Automated labeling of the human brain: a preliminary report on the development and evaluation of a forward-transform method. Hum Brain Mapp 5:238-242.

Lane HY, Chang YC, Liu YC, Chiu CC, Tsai GE (2005) Sarcosine or D-serine add-on treatment for acute exacerbation of schizophrenia: a randomized, double-blind, placebo-controlled study. Arch Gen Psychiatry 62:1196-1204.

Laruelle M, Frankle WG, Narendran R, Kegeles LS, Abi-Dargham A (2005) Mechanism of action of antipsychotic drugs: from dopamine D(2) receptor antagonism to glutamate NMDA facilitation. Clin Ther 27 Suppl A:S16-24.

Lawrie SM, Buechel C, Whalley HC, Frith CD, Friston KJ, Johnstone EC (2002) Reduced frontotemporal functional connectivity in schizophrenia associated with auditory hallucinations. Biol Psychiatry 51:1008-1011.

Lee CM, Chang WC, Chang KB, Shyu BC (2007) Synaptic organization and input-specific short-term plasticity in anterior cingulate cortical neurons with intact thalamic inputs. The European journal of neuroscience 25:2847-2861.

Lenartowicz A, McIntosh AR (2005) The role of anterior cingulate cortex in working memory is shaped by functional connectivity. J Cogn Neurosci 17:1026-1042.

Lenroot RK, Giedd JN (2008) The changing impact of genes and environment on brain development during childhood and adolescence: initial findings from a neuroimaging study of pediatric twins. Dev Psychopathol 20:1161-1175.

Leonard CM (1969) The prefrontal cortex of the rat. I. Cortical projection of the mediodorsal nucleus. II. Efferent connections. Brain Res 12:321-343.

Levin ED, Briggs SJ, Christopher NC, Auman JT (1994) Working memory performance and cholinergic effects in the ventral tegmental area and substantia nigra. Brain Res 657:165-170.

Lewis DA, Gonzalez-Burgos G (2008) Neuroplasticity of neocortical circuits in schizophrenia. Neuropsychopharmacology 33:141-165.

Lewis DA, Gonzalez-Burgos G (2006) Pathophysiologically based treatment interventions in schizophrenia. Nat Med 12:1016-1022.

Lewis DA, Moghaddam B (2006) Cognitive dysfunction in schizophrenia: convergence of gamma-aminobutyric acid and glutamate alterations. Arch Neurol 63:1372-1376.

Lewis DA, Lieberman JA (2000) Catching up on schizophrenia: natural history and neurobiology. Neuron 28:325-334.

Li B, Daunizeau J, Stephan KE, Penny W, Hu D, Friston K (2011) Generalised filtering and stochastic DCM for fMRI. Neuroimage 58:442-457.

Lieberman AN, Goldstein M, Gopinathan G, Neophytides A (1987) D-1 and D-2 agonists in Parkinson's disease. Can J Neurol Sci 14:466-473.

Liemburg EJ, Knegtering H, Klein HC, Kortekaas R, Aleman A (2012) Antipsychotic medication and prefrontal cortex activation: a review of neuroimaging findings. Eur Neuropsychopharmacol 22:387-400.

Lijffijt M, Lane SD, Meier SL, Boutros NN, Burroughs S, Steinberg JL, Moeller FG, Swann AC (2009) P50, N100, and P200 sensory gating: relationships with behavioral inhibition, attention, and working memory. Psychophysiology 46:1059-1068.

Lisman JE, Coyle JT, Green RW, Javitt DC, Benes FM, Heckers S, Grace AA (2008) Circuit-based framework for understanding neurotransmitter and risk gene interactions in schizophrenia. Trends Neurosci 31:234-242.

Luby ED, Cohen BD, Rosenbaum G, Gottlieb JS, Kelley R (1959) Study of a new schizophrenomimetic drug; sernyl. AMA Arch Neurol Psychiatry 81:363-369.

Lutkenhoff ES, van Erp TG, Thomas MA, Therman S, Manninen M, Huttunen MO, Kaprio J, Lonnqvist J, O'Neill J, Cannon TD (2010) Proton MRS in twin pairs discordant for schizophrenia. Molecular psychiatry 15:308-318.

MacDonald AW, Schulz SC (2009) What we know: findings that every theory of schizophrenia should explain. Schizophr Bull 35:493-508.

Macmillan NA, Creelman, C.D. (1991) Detection Theory: A User's Guide. Cambridge: Cambridge University.

Macmillan NA, Kaplan HL (1985) Detection theory analysis of group data: estimating sensitivity from average hit and false-alarm rates. Psychological bulletin 98:185-199.

Manoach DS (2003) Prefrontal cortex dysfunction during working memory performance in schizophrenia: reconciling discrepant findings. Schizophr Res 60:285-298.

Mantz J, Godbout R, Tassin JP, Glowinski J, Thierry AM (1990) Inhibition of spontaneous and evoked unit activity in the rat medial prefrontal cortex by mesencephalic raphe nuclei. Brain Res 524:22-30.

Marinazzo D, Liao W, Chen H, Stramaglia S (2011) Nonlinear connectivity by Granger causality. NeuroImage 58:330-338.

Marr D (1976) Analyzing natural images: a computational theory of texture vision. Cold Spring Harbor symposia on quantitative biology 40:647-662.

Marreiros AC, Kiebel SJ, Friston KJ (2008) Dynamic causal modelling for fMRI: a two-state model. Neuroimage 39:269-278.

McCormick DA, Bal T (1997) Sleep and arousal: thalamocortical mechanisms. Annual review of neuroscience 20:185-215.

McDonald C, Murray RM (2000) Early and late environmental risk factors for schizophrenia. Brain Res Brain Res Rev 31:130-137.

McGuffin P, Farmer A, Harvey I (1991) A polydiagnostic application of operational criteria in studies of psychotic illness. Development and reliability of the OPCRIT system. Arch Gen Psychiatry 48:764-770.

McIntosh AR (2000) Towards a network theory of cognition. Neural Netw 13:861-870.

McIntosh AR, Grady CL, Ungerleider LG, Haxby JV, Rapoport SI, Horwitz B (1994) Network analysis of cortical visual pathways mapped with PET. The Journal of neuroscience : the official journal of the Society for Neuroscience 14:655-666.

Meador-Woodruff JH, Clinton SM, Beneyto M, McCullumsmith RE (2003) Molecular abnormalities of the glutamate synapse in the thalamus in schizophrenia. Annals of the New York Academy of Sciences 1003:75-93.

Mehta MA, Montgomery AJ, Kitamura Y, Grasby PM (2008) Dopamine D2 receptor occupancy levels of acute sulpiride challenges that produce working memory and learning impairments in healthy volunteers. Psychopharmacology (Berl) 196(1):157-165.

Menzies L, Ooi C, Kamath S, Suckling J, McKenna P, Fletcher P, Bullmore E, Stephenson C (2007) Effects of gamma-aminobutyric acid-modulating drugs on working memory and brain function in patients with schizophrenia. Arch Gen Psychiatry 64:156-167.

Meyer-Lindenberg A, Poline JB, Kohn PD, Holt JL, Egan MF, Weinberger DR, Berman KF (2001) Evidence for abnormal cortical functional connectivity during working memory in schizophrenia. Am J Psychiatry 158:1809-1817.

Meyer-Lindenberg AS, Olsen RK, Kohn PD, Brown T, Egan MF, Weinberger DR, Berman KF (2005) Regionally specific disturbance of dorsolateral prefrontal-hippocampal functional connectivity in schizophrenia. Arch Gen Psychiatry 62:379-386.

Miller P, Wang XJ (2006) Inhibitory control by an integral feedback signal in prefrontal cortex: a model of discrimination between sequential stimuli. Proc Natl Acad Sci U S A 103:201-206.

Mirnics K, Lewis DA (2001) Genes and subtypes of schizophrenia. Trends in molecular medicine 7:281-283.

Mitelman SA, Brickman AM, Shihabuddin L, Newmark R, Chu KW, Buchsbaum MS (2005) Correlations between MRI-assessed volumes of the thalamus and cortical Brodmann's areas in schizophrenia. Schizophr Res 75:265-281.

Moghaddam B, Krystal JH (2012) Capturing the angel in "angel dust": twenty years of translational neuroscience studies of NMDA receptor antagonists in animals and humans. Schizophr Bull 38:942-949.

Moghaddam B, Adams B, Verma A, Daly D (1997) Activation of glutamatergic neurotransmission by ketamine: a novel step in the pathway from NMDA receptor blockade to dopaminergic and cognitive disruptions associated with the prefrontal cortex. J Neurosci 17:2921-2927.

Mongillo G, Barak O, Tsodyks M (2008) Synaptic theory of working memory. Science 319:1543-1546.

Montague PR, Dolan RJ, Friston KJ, Dayan P (2012) Computational psychiatry. Trends Cogn Sci 16:72-80.

Moran RJ, Jung F, Kumagai T, Endepols H, Graf R, Dolan RJ, Friston KJ, Stephan KE, Tittgemeyer M (2011) Dynamic causal models and physiological inference: a validation study using isoflurane anaesthesia in rodents. PloS one 6:e22790.

Murphy BK, Miller KD (2003) Multiplicative gain changes are induced by excitation or inhibition alone. J Neurosci 23:10040-10051.

Murray JD, Anticevic A, Gancsos M, Ichinose M, Corlett PR, Krystal JH, Wang XJ (2014) Linking microcircuit dysfunction to cognitive impairment: effects of disinhibition associated with schizophrenia in a cortical working memory model. Cereb Cortex 24:859-872.

Murty VP, Sambataro F, Radulescu E, Altamura M, Iudicello J, Zoltick B, Weinberger DR, Goldberg TE, Mattay VS (2011) Selective updating of working memory content modulates meso-cortico-striatal activity. Neuroimage 57:1264-1272.

Nathaniel-James DA, Frith CD (2002) The role of the dorsolateral prefrontal cortex: evidence from the effects of contextual constraint in a sentence completion task. Neuroimage 16:1094-1102.

Nathaniel-James DA, Fletcher P, Frith CD (1997) The functional anatomy of verbal initiation and suppression using the Hayling Test. Neuropsychologia 35:559-566.

Negyessy L, Goldman-Rakic PS (2005) Morphometric characterization of synapses in the primate prefrontal cortex formed by afferents from the mediodorsal thalamic nucleus. Experimental brain research 164:148-154.

Neher E, Sakaba T (2008) Multiple roles of calcium ions in the regulation of neurotransmitter release. Neuron 59:861-872.

Nejad AB, Ebdrup BH, Glenthoj BY, Siebner HR (2012) Brain connectivity studies in schizophrenia: unravelling the effects of antipsychotics. Current neuropharmacology 10:219-230.

Neurobehavioural Systems [online]. Available from: http://www.neurobs.com/ [Accessed 01/07/2013].

Newpher TM, Ehlers MD (2008) Glutamate receptor dynamics in dendritic microdomains. Neuron 58:472-497.

Ogawa S, Lee TM, Kay AR, Tank DW (1990) Brain magnetic resonance imaging with contrast dependent on blood oxygenation. Proc Natl Acad Sci U S A 87:9868-9872.

Oh JS, Kubicki M, Rosenberger G, Bouix S, Levitt JJ, McCarley RW, Westin CF, Shenton ME (2009) Thalamo-frontal white matter alterations in chronic schizophrenia: a quantitative diffusion tractography study. Hum Brain Mapp 30:3812-3825.

Onn SP, Wang XB (2005) Differential modulation of anterior cingulate cortical activity by afferents from ventral tegmental area and mediodorsal thalamus. The European journal of neuroscience 21:2975-2992.

Overton PG, Richards CD, Berry MS, Clark D (1999) Long-term potentiation at excitatory amino acid synapses on midbrain dopamine neurons. Neuroreport 10:221-226.

Pakkenberg B, Scheel-Kruger J, Kristiansen LV (2009) Schizophrenia; from structure to function with special focus on the mediodorsal thalamic prefrontal loop. Acta psychiatrica Scandinavica 120:345-354.

Pan B, Zucker RS (2009) A general model of synaptic transmission and short-term plasticity. Neuron 62:539-554.

Penny WD, Stephan KE, Daunizeau J, Rosa MJ, Friston KJ, Schofield TM, Leff AP (2010) Comparing families of dynamic causal models. PLoS computational biology 6:e1000709.

Penny WD, Stephan KE, Mechelli A, Friston KJ (2004) Comparing dynamic causal models. Neuroimage 22:1157-1172.

Perlstein WM, Carter CS, Noll DC, Cohen JD (2001) Relation of prefrontal cortex dysfunction to working memory and symptoms in schizophrenia. Am J Psychiatry 158:1105-1113.

Pettersson-Yeo W, Allen P, Benetti S, McGuire P, Mechelli A (2011) Dysconnectivity in schizophrenia: where are we now? Neurosci Biobehav Rev 35:1110-1124.

Pfister JP, Dayan P, Lengyel M (2010) Synapses with short-term plasticity are optimal estimators of presynaptic membrane potentials. Nature neuroscience 13:1271-1275.

Pinault D (2011) Dysfunctional thalamus-related networks in schizophrenia. Schizophr Bull 37:238-243.

Potkin SG, Turner JA, Brown GG, McCarthy G, Greve DN, Glover GH, Manoach DS, Belger A, Diaz M, Wible CG, Ford JM, Mathalon DH, Gollub R, Lauriello J, O'Leary D, van Erp TG, Toga AW, Preda A, Lim KO (2009) Working memory and DLPFC inefficiency in schizophrenia: the FBIRN study. Schizophr Bull 35:19-31.

Pycock CJ, Kerwin RW, Carter CJ (1980) Effect of lesion of cortical dopamine terminals on subcortical dopamine receptors in rats. Nature 286:74-76.

Qi Z, Miller GW, Voit EO (2010) Computational modeling of synaptic neurotransmission as a tool for assessing dopamine hypotheses of schizophrenia. Pharmacopsychiatry 43 Suppl 1:S50-60.

Quide Y, Morris RW, Shepherd AM, Rowland JE, Green MJ (2013) Task-related fronto-striatal functional connectivity during working memory performance in schizophrenia. Schizophr Res 150:468-475.

Ramsey AJ, Milenkovic M, Oliveira AF, Escobedo-Lozoya Y, Seshadri S, Salahpour A, Sawa A, Yasuda R, Caron MG (2011) Impaired NMDA receptor transmission alters striatal synapses and DISC1 protein in an age-dependent manner. Proc Natl Acad Sci U S A 108:5795-5800.

Rasetti R, Sambataro F, Chen Q, Callicott JH, Mattay VS, Weinberger DR (2011) Altered cortical network dynamics: a potential intermediate phenotype for schizophrenia and association with ZNF804A. Arch Gen Psychiatry 68:1207-1217.

Raz S, Raz N (1990) Structural brain abnormalities in the major psychoses: a quantitative review of the evidence from computerized imaging. Psychological bulletin 108:93-108.

Roebroeck A, Formisano E, Goebel R (2005) Mapping directed influence over the brain using Granger causality and fMRI. NeuroImage 25:230-242.

Roiser JP, Wigton R, Kilner JM, Mendez MA, Hon N, Friston KJ, Joyce EM (2013) Dysconnectivity in the frontoparietal attention network in schizophrenia. Front Psychiatry 4:176.

Romanides AJ, Duffy P, Kalivas PW (1999) Glutamatergic and dopaminergic afferents to the prefrontal cortex regulate spatial working memory in rats. Neuroscience 92:97-106.

Rothman JS, Cathala L, Steuber V, Silver RA (2009) Synaptic depression enables neuronal gain control. Nature 457:1015-1018.

Saarinen A, Linne ML, Yli-Harja O (2008) Stochastic differential equation model for cerebellar granule cell excitability. PLoS computational biology 4:e1000004.

Salinas E, Sejnowski TJ (2001) Gain modulation in the central nervous system: where behavior, neurophysiology, and computation meet. The Neuroscientist : a review journal bringing neurobiology, neurology and psychiatry 7:430-440.

Salinas E, Sejnowski TJ (2000) Impact of correlated synaptic input on output firing rate and variability in simple neuronal models. J Neurosci 20:6193-6209.

Salinas E, Abbott LF (1996) A model of multiplicative neural responses in parietal cortex. Proc Natl Acad Sci U S A 93:11956-11961.

Santana N, Mengod G, Artigas F (2009) Quantitative analysis of the expression of dopamine D1 and D2 receptors in pyramidal and GABAergic neurons of the rat prefrontal cortex. Cereb Cortex 19:849-860.

Scatton B, Worms P, Lloyd KG, Bartholini G (1982) Cortical modulation of striatal function. Brain Res 232:331-343.

Schizophrenia Working Group of the Psychiatric Genomics Consortium (2014) Biological insights from 108 schizophrenia-associated genetic loci. Nature 511:421-427.

Schlösser RG, Koch K, Wagner G, Nenadic I, Roebel M, Schachtzabel C, Axer M, Schultz C, Reichenbach JR, Sauer H (2008) Inefficient executive cognitive control in schizophrenia is preceded by altered functional activation during information encoding: an fMRI study. Neuropsychologia 46:336-347.

Schlösser RG, Wagner G, Sauer H (2006) Assessing the working memory network: studies with functional magnetic resonance imaging and structural equation modeling. Neuroscience 139:91-103.

Schlösser R, Gesierich T, Kaufmann B, Vucurevic G, Hunsche S, Gawehn J, Stoeter P (2003a) Altered effective connectivity during working memory performance in schizophrenia: a study with fMRI and structural equation modeling. Neuroimage 19:751-763.

Schlösser R, Gesierich T, Kaufmann B, Vucurevic G, Stoeter P (2003b) Altered effective connectivity in drug free schizophrenic patients. Neuroreport 14:2233-2237.

Schmidt A, Smieskova R, Aston J, Simon A, Allen P, Fusar-Poli P, McGuire PK, Riecher-Rossler A, Stephan KE, Borgwardt S (2013) Brain connectivity abnormalities predating the onset of psychosis: correlation with the effect of medication. JAMA psychiatry 70:903-912.

Scottish Mental Health Research Register [online]. Scottish Mental Health Research Network, Royal Edinburgh Hospital. Available from: http://www.smhrn.org.uk/register/default.asp [Accessed 01/07/2013].

Seeman P, Lee T, Chau-Wong M, Wong K (1976) Antipsychotic drug doses and neuroleptic/dopamine receptors. Nature 261:717-719.

Seeman P, Lee T (1975) Antipsychotic drugs: direct correlation between clinical potency and presynaptic action on dopamine neurons. Science 188:1217-1219.

Seghier ML, Josse G, Leff AP, Price CJ (2011) Lateralization is predicted by reduced coupling from the left to right prefrontal cortex during semantic decisions on written words. Cereb Cortex 21:1519-1531.

Seidman LJ, Giuliano AJ, Meyer EC, Addington J, Cadenhead KS, Cannon TD, McGlashan TH, Perkins DO, Tsuang MT, Walker EF, Woods SW, Bearden CE, Christensen BK, Hawkins K, Heaton R, Keefe RS, Heinssen R, Cornblatt BA, North American Prodrome Longitudinal Study G (2010) Neuropsychology of the prodrome to psychosis in the NAPLS consortium: relationship to family history and conversion to psychosis. Arch Gen Psychiatry 67:578-588.

Sequeira LS, Scherer LC, Reppold CT, Fonseca RP (2010) Hayling test – adult version: applicability in the assessment of executive functions in children. Psych & Neuroscie 3(2):189-194.

Sesack SR, Carr DB (2002) Selective prefrontal cortex inputs to dopamine cells: implications for schizophrenia. Physiol Behav 77:513-517.

Seshadri S, Zeledon M, Sawa A (2013) Synapse-specific contributions in the cortical pathology of schizophrenia. Neurobiology of disease 53:26-35.

Seth AK (2005) Causal connectivity of evolved neural networks during behavior. Network 16:35-54.

Shields J, Gottesman, II (1972) Cross-national diagnosis of schizophrenia in twins. The heritability and specificity of schizophrenia. Arch Gen Psychiatry 27:725-730.

Shimi A, Astle DE (2013) The strength of attentional biases reduces as visual short-term memory load increases. Journal of neurophysiology 110:12-18.

Shu Y, Hasenstaub A, Badoual M, Bal T, McCormick DA (2003) Barrages of synaptic activity control the gain and sensitivity of cortical neurons. J Neurosci 23:10388-10401.

Simpson MD, Slater P, Deakin JF, Royston MC, Skan WJ (1989) Reduced GABA uptake sites in the temporal lobe in schizophrenia. Neuroscience letters 107:211-215.

Smith EE, Jonides J (1999) Storage and executive processes in the frontal lobes. Science 283:1657-1661.

Smith EE, Jonides J (1998) Neuroimaging analyses of human working memory. Proc Natl Acad Sci U S A 95:12061-12068.

Snyder SH (1976) The dopamine hypothesis of schizophrenia: focus on the dopamine receptor. Am J Psychiatry 133:197-202.

Sodhi MS, Simmons M, McCullumsmith R, Haroutunian V, Meador-Woodruff JH (2011) Glutamatergic gene expression is specifically reduced in thalamocortical projecting relay neurons in schizophrenia. Biol Psychiatry 70:646-654.

Stephan KE, Mathys C (2014) Computational approaches to psychiatry. Curr Opin Neurobiol 25:85-92.

Stephan KE, Roebroeck A (2012) A short history of causal modeling of fMRI data. NeuroImage 62:856-863.

Stephan KE, Friston KJ (2010) Analyzing effective connectivity with fMRI. Wiley Interdiscip Rev Cogn Sci 1:446-459.

Stephan KE, Friston KJ, Frith CD (2009a) Dysconnection in schizophrenia: from abnormal synaptic plasticity to failures of self-monitoring. Schizophr Bull 35:509-527.

Stephan KE, Penny WD, Daunizeau J, Moran RJ, Friston KJ (2009b) Bayesian model selection for group studies. Neuroimage 46:1004-1017.

Stephan KE, Kasper L, Harrison LM, Daunizeau J, den Ouden HE, Breakspear M, Friston KJ (2008) Nonlinear dynamic causal models for fMRI. Neuroimage 42:649-662.

Stephan KE, Weiskopf N, Drysdale PM, Robinson PA, Friston KJ (2007) Comparing hemodynamic models with DCM. Neuroimage 38:387-401.

Stephan KE, Baldeweg T, Friston KJ (2006) Synaptic plasticity and dysconnection in schizophrenia. Biol Psychiatry 59:929-939.

Sun YG, Beierlein M (2011) Receptor saturation controls short-term synaptic plasticity at corticothalamic synapses. J Neurophysiol 105:2319-2329.

Sun X, Zhao Y, Wolf ME (2005) Dopamine receptor stimulation modulates AMPA receptor synaptic insertion in prefrontal cortex neurons. J Neurosci 25:7342-7351.

Susser M (1985) Separating heredity and environment. American journal of preventive medicine 1:5-23.

Takahata R, Moghaddam B (1998) Glutamatergic regulation of basal and stimulus-activated dopamine release in the prefrontal cortex. Journal of neurochemistry 71:1443-1449.

Talairach J, Tournoux, PA (1988) A Coplanar Stereotaxis Atlas of a Human Brain. Three-dimensional Proportional System: An Approach to Cerebral Imaging. Stuttgart: Thieme.

Tan HY, Chen AG, Kolachana B, Apud JA, Mattay VS, Callicott JH, Chen Q, Weinberger DR (2012) Effective connectivity of AKT1-mediated dopaminergic working memory networks and pharmacogenetics of anti-dopaminergic treatment. Brain : a journal of neurology 135:1436-1445.

Tan HY, Callicott JH, Weinberger DR (2007) Dysfunctional and compensatory prefrontal cortical systems, genes and the pathogenesis of schizophrenia. Cereb Cortex 17 Suppl 1:i171-181.

Tan HY, Sust S, Buckholtz JW, Mattay VS, Meyer-Lindenberg A, Egan MF, Weinberger DR, Callicott JH (2006) Dysfunctional prefrontal regional specialization and compensation in schizophrenia. Am J Psychiatry 163:1969-1977.

Tana MG, Montin E, Cerutti S, Bianchi AM (2010) Exploring cortical attentional system by using fMRI during a Continuous Perfomance Test. Computational intelligence and neuroscience 329213.

Tanaka S (2006) Dopaminergic control of working memory and its relevance to schizophrenia: a circuit dynamics perspective. Neuroscience 139:153-171.

Tang J, Liao Y, Zhou B, Tan C, Liu W, Wang D, Liu T, Hao W, Tan L, Chen X (2012) Decrease in temporal gyrus gray matter volume in first-episode, early onset schizophrenia: an MRI study. PloS one 7:e40247.

The Wellcome Department of Cognitive Neurology and collaborators. Statistical Parametric Mapping [online]. Institute of Neurology, University College London. Available from: http://www.fil.ion.ucl.ac.uk/spm/ [Accessed 02/02.2010].

Thermenos HW, Keshavan MS, Juelich RJ, Molokotos E, Whitfield-Gabrieli S, Brent BK, Makris N, Seidman LJ (2013) A review of neuroimaging studies of young relatives of individuals with schizophrenia: a developmental perspective from schizotaxia to schizophrenia. American journal of medical genetics Part B, Neuropsychiatric genetics : the official publication of the International Society of Psychiatric Genetics 162B:604-635.

Thermenos HW, Goldstein JM, Buka SL, Poldrack RA, Koch JK, Tsuang MT, Seidman LJ (2005) The effect of working memory performance on functional MRI in schizophrenia. Schizophr Res 74:179-194.

Thermenos HW, Seidman LJ, Breiter H, Goldstein JM, Goodman JM, Poldrack R, Faraone SV, Tsuang MT (2004) Functional magnetic resonance imaging during auditory verbal working memory in nonpsychotic relatives of persons with schizophrenia: a pilot study. Biol Psychiatry 55:490-500.

Thierry AM, Mantz J, Milla C, Glowinski J (1988) Influence of the mesocortical/prefrontal dopamine neurons on their target cells. Annals of the New York Academy of Sciences 537:101-111.

Tibbo P, Hanstock C, Valiakalayil A, Allen P (2004) 3-T proton MRS investigation of glutamate and glutamine in adolescents at high genetic risk for schizophrenia. The American journal of psychiatry 161:1116-1118.

Timofeeva OA, Levin ED (2011) Glutamate and nicotinic receptor interactions in working memory: importance for the cognitive impairment of schizophrenia. Neuroscience 195:21-36.

Tomasi D, Goldstein RZ, Telang F, Maloney T, Alia-Klein N, Caparelli EC, Volkow MD (2007) Widespread disruption in brain activation patterns to a working memory task during cocaine abstinence. Brain Res 1171:83-92.

Tseng KY, O'Donnell P (2004) Dopamine-glutamate interactions controlling prefrontal cortical pyramidal cell excitability involve multiple signaling mechanisms. J Neurosci 24:5131-5139.

Tzschentke TM (2001) Pharmacology and behavioral pharmacology of the mesocortical dopamine system. Prog Neurobiol 63:241-320.

Van Os J, Kapur S (2009) Schizophrenia. Lancet 374(9690):635–645.

Van Snellenberg JX, Torres IJ, Thornton AE (2006) Functional neuroimaging of working memory in schizophrenia: task performance as a moderating variable. Neuropsychology 20:497-510.

Volk DW, Eggan SM, Lewis DA (2010) Alterations in metabotropic glutamate receptor 1alpha and regulator of G protein signaling 4 in the prefrontal cortex in schizophrenia. Am J Psychiatry 167:1489-1498.

Volman V, Levine H, Sejnowski TJ (2010) Shunting inhibition controls the gain modulation mediated by asynchronous neurotransmitter release in early development. PLoS computational biology 6:e1000973.

Wager TD, Smith EE (2003) Neuroimaging studies of working memory: a meta-analysis. Cogn Affect Behav Neurosci 3:255-274.

Wagner G, Koch K, Schachtzabel C, Schultz CC, Gaser C, Reichenbach JR, Sauer H, Bar KJ, Schlosser RG (2013) Structural basis of the fronto-thalamic dysconnectivity in schizophrenia: A combined DCM-VBM study. Neuroimage Clin 3:95-105.

Wang L, Liu X, Guise KG, Knight RT, Ghajar J, Fan J (2010) Effective connectivity of the fronto-parietal network during attentional control. J Cogn Neurosci 22:543-553.

Wang XJ (2010) Neurophysiological and computational principles of cortical rhythms in cognition. Physiol Rev 90:1195-1268.

Watis L, Chen SH, Chua HC, Chong SA, Sim K (2008) Glutamatergic abnormalities of the thalamus in schizophrenia: a systematic review. Journal of neural transmission 115:493-511.

Welsh RC, Chen AC, Taylor SF (2010) Low-frequency BOLD fluctuations demonstrate altered thalamocortical connectivity in schizophrenia. Schizophr Bull 36:713-722.

Whalley HC, Gountouna VE, Hall J, McIntosh A, Whyte MC, Simonotto E, Job DE, Owens DG, Johnstone EC, Lawrie SM (2007) Correlations between fMRI activation and individual psychotic symptoms in un-medicated subjects at high genetic risk of schizophrenia. BMC psychiatry 7:61.

Whalley HC, Simonotto E, Moorhead W, McIntosh A, Marshall I, Ebmeier KP, Owens DG, Goddard NH, Johnstone EC, Lawrie SM (2006) Functional imaging as a predictor of schizophrenia. Biological psychiatry 60:454-462.

Whalley HC, Simonotto E, Flett S, Marshall I, Ebmeier KP, Owens DG, Goddard NH, Johnstone EC, Lawrie SM (2004) fMRI correlates of state and trait effects in subjects at genetically enhanced risk of schizophrenia. Brain : a journal of neurology 127:478-490.

Whalley HC, Simonotto E, Marshall I, Owens DG, Goddard NH, Johnstone EC, Lawrie SM (2005) Functional disconnectivity in subjects at high genetic risk of schizophrenia. Brain : a journal of neurology 128:2097-2108.

Wing JK, Cooper, J.E., Sartorius, N. (1974) The Description and Classification of Psychiatric Symptoms. An Instruction Manual for the PSE and Catego Systems. Cambridge: Cambridge University Press.

Woodward TS, Cairo TA, Ruff CC, Takane Y, Hunter MA, Ngan ET (2006) Functional connectivity reveals load dependent neural systems underlying

encoding and maintenance in verbal working memory. Neuroscience 139:317-325.

Xu J, Zhang S, Calhoun VD, Monterosso J, Li CS, Worhunsky PD, Stevens M, Pearlson GD, Potenza MN (2013) Task-related concurrent but opposite modulations of overlapping functional networks as revealed by spatial ICA. Neuroimage 79:62-71.

Yoo SY, Yeon S, Choi CH, Kang DH, Lee JM, Shin NY, Jung WH, Choi JS, Jang DP, Kwon JS (2009) Proton magnetic resonance spectroscopy in subjects with high genetic risk of schizophrenia: investigation of anterior cingulate, dorsolateral prefrontal cortex and thalamus. Schizophrenia research 111:86-93.

Yu Y, FitzGerald THB, Friston KJ (2013) Working memory and anticipated set modulate midbrain and putamen activity. J Neurosci 33(35):14040-14047.

Zhang H, Wei X, Tao H, Mwansisya TE, Pu W, He Z, Hu A, Xu L, Liu Z, Shan B, Xue Z (2013) Opposite effective connectivity in the posterior cingulate and medial prefrontal cortex between first-episode schizophrenic patients with suicide risk and healthy controls. PloS one 8:e63477.

Appendix

Relevant publications based on the two introductory chapters and the Hayling Sentence Completion Task fMRI data of the Edinburgh High Risk Study contained within this thesis are presented.

Dauvermann MR, Whalley HC, Schmidt A, Lee GL, Romaniuk L, Roberts N, Johnstone EC, Lawrie SM, Moorhead TW (2014) Computational Neuropsychiatry - Schizophrenia as a Cognitive Brain Network Disorder. Front Psychiatry 5:30.

Dauvermann MR, Whalley HC, Romaniuk L, Valton V, Owens DG, Johnstone EC, Lawrie SM, Moorhead TW (2013) The application of nonlinear Dynamic Causal Modelling for fMRI in subjects at high genetic risk of schizophrenia. Neuroimage 73:16-29.

Dauvermann MR, Mukherjee P, Moorhead WT, Stanfield AC, Fusar-Poli P, Lawrie SM, Whalley HC (2012) Relationship between gyrification and functional connectivity of the prefrontal cortex in subjects at high genetic risk of schizophrenia. Current pharmaceutical design 18:434-442.

frontiers in PSYCHIATRY

REVIEW ARTICLE
published: 25 March 2014
doi: 10.3389/fpsyt.2014.00030

Computational neuropsychiatry – schizophrenia as a cognitive brain network disorder

Maria R. Dauvermann[1]*, Heather C. Whalley[1], André Schmidt[2,3], Graham L. Lee[4], Liana Romaniuk[1], Neil Roberts[5], Eve C. Johnstone[1], Stephen M. Lawrie[1] and Thomas W. J. Moorhead[1]

[1] *Division of Psychiatry, Royal Edinburgh Hospital, University of Edinburgh, Edinburgh, UK*
[2] *Department of Psychiatry, University of Basel, Basel, Switzerland*
[3] *Medical Image Analysis Center, University Hospital Basel, Basel, Switzerland*
[4] *McGovern Institute for Brain Research, Massachusetts Institute of Technology, Cambridge, MA, USA*
[5] *Clinical Research Imaging Centre, QMRI, University of Edinburgh, Edinburgh, UK*

Edited by:
Stefan Borgwardt, University of Basel, Switzerland

Reviewed by:
Philip R. Corlett, Yale School of Medicine, USA
Lorenz Deserno, Max-Planck-Institute for Human Cognitive and Brain Sciences, Germany

****Correspondence:***
Maria R. Dauvermann, Division of Psychiatry, Royal Edinburgh Hospital, University of Edinburgh, Kennedy Tower, Morningside Park, Edinburgh EH10 5HF, UK
e-mail: m.r.dauvermann@sms.ed.ac.uk, maria.dauvermann@childrens.harvard.edu

Computational modeling of functional brain networks in fMRI data has advanced the understanding of higher cognitive function. It is hypothesized that functional networks mediating higher cognitive processes are disrupted in people with schizophrenia. In this article, we review studies that applied measures of functional and effective connectivity to fMRI data during cognitive tasks, in particular working memory fMRI studies. We provide a conceptual summary of the main findings in fMRI data and their relationship with neurotransmitter systems, which are known to be altered in individuals with schizophrenia. We consider possible developments in computational neuropsychiatry, which are likely to further our understanding of how key functional networks are altered in schizophrenia.

Keywords: computational neuropsychiatry, schizophrenia, fMRI, dynamic causal modeling, cognition, neurotransmitter, dopamine, glutamate

INTRODUCTION

Schizophrenia is a severe psychiatric disorder, which is initially manifested through positive symptoms including delusions, hallucinations, and disorganized thoughts. As the illness progresses negative symptoms such as avolition, alogia, and apathy may occur. Prior to diagnosis of illness, cognitive deficits can occur and illness progression can also be associated with cognitive deficits (1, 2). It is widely established that such cognitive deficits are considered a core symptom of schizophrenia (3) and are associated with reductions in working memory performance. Working memory deficits are one of the main neurocognitive impairments found in subjects with first episode schizophrenia (FES) (4, 5) and in people with established schizophrenia (EST) (6). Similar deficits also occur in individuals at high risk of schizophrenia [HR; Ref. (2)]. Furthermore, recent evidence has been presented, which indicates a relationship between severity of working memory deficits and the severity of negative symptoms (7). The severity of working memory deficits that is evident at the first episode of schizophrenia can predict the quality of life at the established stage of the illness (8, 9).

Two major neurotransmitter circuits have been implicated in clinical and cognitive symptoms in subjects with schizophrenia: these are the dopamine and glutamate neurotransmitter circuits. Evidence has been presented for separate alterations/disruptions of dopamine and glutamate as well as an interactive role between both neurotransmitters[1]. The two main neurobiological hypotheses in schizophrenia are based on the theories of altered dopaminergic transmission ("dopamine hypothesis of schizophrenia") and altered glutamatergic transmission ("glutamate hypothesis of schizophrenia"). It is thought that both dopamine and glutamate modulate the dorsolateral prefrontal cortex (DLPFC) and in schizophrenia alter the performance in cognitive processes such as in working memory (10–13). Such work supports the notion of schizophrenia as a brain disorder. FMRI and positron emission tomography (PET) findings of altered functional activation and functional connectivity (FC) during working memory have been

Abbreviations: AC/ACC, anterior cingulate/anterior cingulate cortex; ARMS, at-risk mental state; BMS, Bayesian model selection; BOLD response, blood-oxygen-level dependent response; D_1 receptor, D_1 subtype of the dopamine receptor; D_2 receptor, D_2 subtype of the dopamine receptor; $D_{2/3}$ receptors, $D_{2/3}$ subtype of the dopamine receptor; DCM, Dynamic Causal Modeling; DMN, default-mode network; DLPFC, dorsolateral prefrontal cortex; EC, effective connectivity; EST, subjects with EST; FC, functional connectivity; FEP, subjects with first episode psychosis; FES, subjects with first episode schizophrenia; GABA, γ-aminobutyric acid; GBC, global-based connectivity; HR, subjects at high risk of schizophrenia; HR+, subjects at high familial risk of schizophrenia with transient psychotic symptoms; HR−, subjects at high familial risk of schizophrenia without transient psychotic symptoms; HRill, subjects at high familial risk of schizophrenia who subsequent to scanning developed schizophrenia; HSCT, Hayling sentence completion task IFG inferior frontal gyrus; MFG, middle frontal gyrus; MRS, magnetic resonance spectroscopy; NMDA, *N*-Methyl-D-aspartate acid; PC, parietal cortex; PET, positron emission tomography; rCBF, regional cerebral blood flow; SPECT, single-photon emission computed tomography; SPL, superior parietal lobe; STG, superior temporal gyrus.

[1]It is noted that other neurotransmitter circuits are interacting with dopaminergic and/or glutamatergic circuits such as serotonin and GABA (24, 29, 149).

reported in people with schizophrenia when they are compared to healthy controls (14, 15). Furthermore, PET studies have presented evidence for indirect markers of altered dopamine transmission, which was correlated with working memory performance (2, 16). Alterations of indirect measures of glutamate concentrations have been reported by proton magnetic resonance spectroscopy (MRS) studies (17).

One subfield within the emerging field of computational neuropsychiatry is based on modeling fMRI networks and the evidence of (i) altered dopaminergic and/or glutamatergic transmission in (ii) cognitive function (i.e., working memory) in people with schizophrenia. Therefore, the objectives are the investigation of impaired cognitive function mediated by large-scale networks in combination with underlying neurobiological circuits such as dopamine and glutamate. Researchers in computational neuropsychiatry examine and model altered cognitive brain function in terms of functionally integrated regions [i.e., effective connectivity (EC)] (18), which may be mediated by genetic factors and neurotransmitter circuits (19–21). Mechanistic responses can be inferred from the computational modeling of cognitive brain function where the localized brain function is monitored through the BOLD response (22). This modeling approach allows computational neuropsychiatry to further our understanding of the neurobiological processes, which underlie altered cognitive brain function in individuals with schizophrenia. Thus, advancing our knowledge of schizophrenia as a cognitive brain network disorder.

In this review, we summarize fMRI findings in verbal/numeric working memory[2] in context of (i) the understanding of schizophrenia as a cognitive brain disorder (from clinical and cognitive neurosciences) and (ii) the understanding of schizophrenia as a cognitive brain network disorder (from computational neuropsychiatry). We discuss these sets of findings in context of the dopamine and the glutamate hypotheses of schizophrenia. We consider two key research questions for the discussion of each set of findings:

(i) To what extent do these sets of findings support the dopamine hypothesis and/or the glutamate hypothesis in subjects with schizophrenia?
(ii) Do the findings from computational neuropsychiatry lead to a better understanding of schizophrenia than that obtained from clinical and cognitive neurosciences?

The review is structured as followed: first, the dopamine and glutamate hypotheses of schizophrenia are summarized (Section Schizophrenia as a Brain Disorder). Second, exemplary findings of verbal/numeric working memory deficits from fMRI studies in subjects with schizophrenia are summarized. These findings are discussed in context of the dopamine hypothesis and the glutamate hypothesis of schizophrenia (Section Schizophrenia as a Cognitive Brain Disorder). Third, we present a brief introduction to computational neuropsychiatry. We provide examples from computational neuropsychiatry and the application to the investigation of cognitive brain large-scale networks in people with schizophrenia[3]. Finally, we consider current methodological limitations of the methods (Section From Computational Neuropsychiatry Towards Schizophrenia as a Cognitive Brain Network Disorder). We outline potential future influences of computational advances in schizophrenia that may shape our understanding of schizophrenia with the aim of developing more effective treatments for the disorder (Section Understanding of Schizophrenia).

SCHIZOPHRENIA AS A BRAIN DISORDER

Neurobiological research into alterations of dopaminergic and/or glutamatergic neurotransmission has paved the way for the understanding of schizophrenia as a disorder of the brain. The dopamine hypothesis posits that dopamine function is altered in schizophrenia and that this dysfunction may be the pathophysiological pathway leading to clinical and cognitive symptoms (23, 24). The glutamate hypothesis proposes that the altered dopaminergic dysfunction may be secondary to aberrant glutamatergic dysregulation, which may contribute to clinical and cognitive symptoms in schizophrenia (25–27).

DOPAMINE HYPOTHESIS OF SCHIZOPHRENIA

The origin of the dopamine hypothesis of schizophrenia is based on the discovery of antipsychotic drugs by Delay et al. (28) in 1952. Carlsson and Lindqvit reported the first findings of an effect of antipsychotic drugs on the metabolism of dopamine (29). The dopamine hypothesis posits that alterations of dopaminergic receptors may underlie the clinical symptoms of schizophrenia (30). Over last three decades, the dopamine hypothesis of schizophrenia has undergone reformulations in light of newly available preclinical and clinical findings. Here, we consider the three main hypotheses: (i) the "dopamine receptor hypothesis," (ii) the "modified dopamine hypothesis of schizophrenia," and (iii) the "dopamine hypothesis: version III."

The dopamine receptor hypothesis goes back to studies reporting antipsychotics affecting the affinity of dopamine receptors (31–33). Further evidence for the hypothesis was presented with increased synaptic monoamine levels during the induction of psychotic symptoms (34). The focus of this hypothesis rests on the excess of dopamine receptors. Thus, the clinical treatment is aimed at blocking the dopamine D_2 subtype of the dopamine receptors (35).

The modified dopamine hypothesis of schizophrenia has been formulated to integrate new findings (36). Preclinical and clinical studies (i.e., post-mortem, metabolite, and dopamine receptor neuroimaging studies) have advanced the understanding of relationships between affinity and occupancy of D_2 and D_1 subtypes of the dopamine receptors and regional specificity (37). Furthermore, it was assumed that findings of altered regional dopaminergic receptor function from preclinical and indirect clinical studies could be linked to clinical symptomatology in schizophrenia (36). The hypothesis suggests that "hypofrontality," as measured with reduced regional cerebral blood flow (rCBF) in the PFC may indicate low dopamine levels in the PFC (36). Findings from preclinical

[2]In this review, we focus on the "2-back" task [verbal "2-back", (104); numeric "2-back", (97)] to review/discuss brain function and PET findings of comparable experimental paradigms, psychological/ cognitive domains/components and activated brain regions.

[3]Exemplary studies on verbal fluency findings are presented.

lesion studies proposed that prefrontal "hypodopaminergia" lead to striatal "hyperdopaminergia" (38, 39). In addition, it is hypothesized that prefrontal "hypodopaminergia" could cause negative symptoms, whereas striatal "hyperdopaminergia" could lead to positive symptoms (36).

The dopamine hypothesis: version III synthesizes published findings on dopamine and its potential role in schizophrenia from the main fields into one unifying hypothesis. The hypothesis aims to provide a framework for findings from developments in clinical research into genetic (risk) factors, environmental risk factors, neurochemical and neuroimaging studies, and preclinical studies, which may be related to increased presynaptic striatal dopaminergic function in schizophrenia (23). The hypothesis is comprised of four components: (i) The interaction of "hits" such as frontotemporal dysfunction, genes, stress, and drugs may lead to striatal dopamine dysregulation (i.e., increased presynaptic dopamine synthesis capacity) and therefore to psychosis. (ii) It is hypothesized that the primary dopaminergic dysfunction is located at the presynaptic dopaminergic level instead of the D_2 receptor level. (iii) The hypothesis assumes that the dopamine dysregulation combined with cultural and societal factors could lead to future clinical diagnosis of "psychosis" rather than schizophrenia. (iv) It is proposed that the dopamine dysfunction could change the perception and judgment of stimuli (possibly through aberrant salience), which could result in cognitive deficits (40, 41).

Recent meta-analyses, which examined markers of striatal dopamine alterations in schizophrenia, reported evidence of different types of elevated dopamine dysfunction. Supporting evidence for the dopamine hypothesis has been shown by increased striatal presynaptic dopaminergic function in medication-free or medication-naïve patients with schizophrenia contrasted to healthy controls (42) and increased striatal dopamine synthesis capacity (43). Contradictory findings have however been reported by Fusar-Poli and Meyer-Lindenberg (44), who found no difference in striatal dopamine active transporter density between patients with schizophrenia and healthy controls.

In summary, while both the dopamine receptor hypothesis and the modified dopamine hypothesis of schizophrenia have their origins in the neurobiological investigation of the mode of action of antipsychotics, the dopamine hypothesis: version III aims at integrating advances in research of schizophrenia into one unifying dopamine hypothesis. The scope of understanding of dopaminergic dysregulation has become more defined, ranging from the whole brain perspective, through the perspective of regional specificity between (DL)PFC and striatum, to the current perspective of elevated presynaptic striatal dopaminergic function. The development of the dopamine hypothesis over the three versions has helped shape the understanding of schizophrenia as a brain disorder.

GLUTAMATE HYPOTHESIS OF SCHIZOPHRENIA

The origin of the glutamate hypothesis of schizophrenia was based on the discovery of psychotomimetic effects of ketamine and phencyclidine, which elicited psychotic symptoms in healthy people. Symptoms such as delusions and hallucinations experienced by healthy individuals were compared to positive symptoms seen in FES (45, 46). The glutamate hypothesis postulates a mechanistic process of altered interacting glutamatergic and/or dopaminergic neurotransmitter circuitries implicated in the pathophysiology of clinical and cognitive symptoms in schizophrenia (47–50). In this review, we consider three models of the glutamate hypothesis with relevance to the investigation of altered working memory function in people with schizophrenia: (i) the "*N*-Methyl-D-aspartate acid (NMDA) receptor hypofunction model" of schizophrenia, (ii) the "acute ketamine model," and (iii) the "dysconnection hypothesis" of schizophrenia.

The NMDA receptor hypofunction model of schizophrenia posits that the subtype of the glutamate receptor is implicated in multiple pathological brain mechanisms of schizophrenia ranging across cellular, chemical, and neuronal levels (51–54). It has been proposed that NMDA receptor hypofunction could underlie the pathophysiology of negative and cognitive symptoms in schizophrenia (29, 51, 55, 56). Clinical trials with agents modulating NMDA receptor in addition to treatment with first-generation antipsychotics (FGA; such as chlorpromazine, haloperidol, perphenazine) and second-generation antipsychotics (SGA; such as clozapine and olanzapine) presented supporting evidence for amelioration of negative and cognitive symptoms (51, 57, 58). Evidence for the involvement of NMDA receptor hypofunction through interactions among different neurotransmitters such as γ-aminobutyric acid (GABAergic) interneurons (51) and dopamine (59, 60) has also been reported.

Evidence for the glutamate hypothesis in humans is based on clinical studies with ketamine in healthy subjects. Results suggest that glutamatergic alterations could explain the pathophysiological mechanisms resulting in positive symptoms predominantly experienced by FES and those with first episode psychosis (FEP) (45, 61). While findings from ketamine injection studies have aided the understanding of glutamatergic signaling in the development of delusions and hallucinations, evidence for altered glutamatergic transmission in negative and cognitive symptoms is scarce. FMRI findings from ketamine studies in healthy subjects propose that altered glutamatergic signaling could be implicated in working memory (12, 45, 62). These findings are in keeping with evidence from glutamatergic animal models, which report aberrant working memory function after the inhibition of glutamatergic receptors (63–66).

The dysconnection hypothesis of schizophrenia posits that altered NMDA receptor-mediated synaptic plasticity may be the underlying pathophysiological mechanism in individuals with schizophrenia (20, 21, 67). The authors propose that altered synaptic plasticity may explain both clinical symptoms and cognitive deficits in people with schizophrenia neurobiologically by altered NMDA receptor neuromodulation. Therefore, the dysconnection hypothesis synthesizes neurobiological findings (i.e., dopamine as one of the main neuromodulators leading to aberrant NMDA receptor function) with clinical and cognitive neuroscientific findings (i.e., cognitive impairment) in individuals with schizophrenia. One of the main objectives of the dysconnection hypothesis is to offer a new approach and therefore new interpretation of neurophysiological and neuroimaging data. This may be used to assist in the understanding of altered cognitive function in people with schizophrenia. For functional neuroimaging data, the biophysical modeling approach of dynamic causal modeling [DCM; Ref.

(18)] has been proposed to infer biophysical processes (namely, NMDA receptor-dependent synaptic plasticity) underlying the blood-oxygen-level-dependent (BOLD) responses. In addition, the authors provide arguments that the development of positive symptoms such as delusions can be explained by a "failure of self-monitoring mechanism" or "corollary discharge" (20). Abnormal EC findings from EEG and fMRI studies across a range of cognitive tasks in subjects with schizophrenia in contrast to healthy controls have been reported (68–70). These lead to a new insight into altered connectivity above those provided by FC studies, which are formulated under different theoretical frameworks, specifically DCM findings enable the inference of biophysical processes underlying neural responses (18, 19, 71).

In summary, the three hypotheses, the NMDA receptor hypofunction model, the acute ketamine model, and the dysconnection hypothesis, have motivated researchers to investigate biophysical circuit processes implicated in glutamatergic and dopaminergic interaction in negative symptoms and cognitive function in schizophrenia. These circuit mechanisms are thought to underlie altered working memory function in schizophrenia. Research on the NMDA receptor hypofunction model has its roots in the pharmacological examination of antipsychotics, the development of new agents, and its effects on clinical and cognitive symptoms in preclinical and clinical research in schizophrenia. The focus of researchers examining the acute ketamine model and the dysconnection hypothesis lies on elucidating proposed neurobiological processes of blockade of NMDA receptor underlying altered cognitive brain function in schizophrenia. The study designs of both versions differ in the investigation of (i) the pharmacological effect of ketamine on altered cognitive brain function and clinical symptomatology in healthy controls (the acute ketamine model) and (ii) altered synaptic plasticity during altered cognitive brain function in subjects with schizophrenia. Despite the different approaches, researchers of both versions of the glutamate hypothesis share the common aim of increasing our insight into schizophrenia by the translation of neurobiological knowledge from basic research to clinical research in schizophrenia. Furthermore, researchers share the common methodological approach of large-scale network analysis of fMRI data. Taken together, development over the three versions of the glutamate hypothesis of schizophrenia have presented promising evidence for shaping the understanding of schizophrenia as a cognitive brain network disorder.

SCHIZOPHRENIA AS A COGNITIVE BRAIN DISORDER

Clinical and cognitive neuroscience studies have applied *in vivo* neuroimaging techniques of fMRI, PET, and single-photon emission computed tomography (SPECT) to assess neurobiological processes that underlie working memory function in people with schizophrenia. Techniques such as PET and SPECT use injections of positron-emitting radionuclide as tracer (for PET) or gamma-emitting radionuclide as tracer (for SPECT) in the living brain. Although these nuclear medical imaging techniques are non-invasive they require the administration of tracers. FMRI provides non-invasive *in vivo* imaging, which measures brain function by means of the BOLD response (72).

In the last two decades, the fields of clinical and cognitive neurosciences merged to provide a multidisciplinary approach to research into schizophrenia. This approach has created the notion of schizophrenia as a cognitive brain disorder (15, 73, 74).

EXAMPLES OF fMRI AND PET STUDIES INVESTIGATING ALTERED WORKING MEMORY FUNCTION IN SUBJECTS WITH SCHIZOPHRENIA

Working memory tasks were initially investigated with fMRI in healthy subjects (75–78). These initial findings led to the use of fMRI as a tool for examining neurobiological markers that could be related to working memory performance. The examination of working memory function was extended to individuals with schizophrenia.

Reported findings of brain function during working memory (among several domains and components of working memory tasks) in healthy controls have led to the understanding that dopamine modulates working memory in healthy controls (79–81). This evidence of dopaminergic involvement in working memory was extended by the findings of altered dopaminergic modulation in schizophrenia (74, 82). Subsequently, converging findings were reported that regions such as DLPFC, anterior cingulate cortex (ACC), and parietal cortex (PC) are activated in working memory in both healthy controls and in subjects with schizophrenia (83–86). However, in those with schizophrenia, these regions exhibit increased or reduced functional activations and FC between prefrontal and parietal regions as well as between prefrontal and temporal regions in contrast to healthy controls. Alterations in FC occur at all stages of the illness (87, 88): (i) in HR subjects (89); (ii) in FES and FEP (90), and (iii) in subjects with EST (91).

Systematic reviews and meta-analyses of working memory fMRI studies in people with schizophrenia do not report consistent findings (92–95). Some studies report increased activation of the DLPFC, commonly referred to as "hyperfrontality," however, others report decreased activation or "hypofrontality." This picture of differing functional activation in terms of the direction, extent, and/or pattern of BOLD responses was attributed to the variation of domains and components of working memory tasks (92–95). Also it was considered that methodological factors in the applied analyses would contribute to these variations in functional activation (93, 95, 96). In addition, differences in medication could contribute to variation in the reported functional activation between studies.

Here, we review exemplary fMRI studies using the numeric or verbal "N-back" task in subjects with EST and healthy controls, which reported functional activation and FC findings (**Table 1**). The reviewed studies present group differences between subjects with schizophrenia and healthy controls. In functional activation studies, evidence was reported for increased activation in DLPFC, PFC, ventral PFC, medial frontal gyrus, and AC during high working memory load in subjects with EST (89, 97–101). However, reduced activation in prefrontal regions, such as ventral PFC, DLPFC, AC, and parietal regions was found during high working memory load in subjects with EST (97, 98, 102). One study in FES found a reduction of activation in inferior frontal gyrus (IFG), superior frontal gyrus, and AC during high working memory load (103). We note three factors, which contributed to difficulties in comparing the findings across the reviewed studies: (i) missing information of phase of schizophrenia (100), (ii)

Table 1 | Understanding of schizophrenia as a cognitive brain disorder – I summary of main findings in verbal/numeric working memory.

Study	Subjects – phase of schizophrenia: HC – HR, FES, EST	Medication	Experimental paradigm	Functional connectivity method; seed regions/ROIs/VOIs; seed regions/ ROIs/VOIs; definition; sphere size	Main finding(s)
fMRI STUDIES – FA					
(97)	18 HC; 13 EST[a]	Not reported	Numeric "2-back"	N/A	↑ With increasing WM load in right DLPFC, left PFC, left AC; ↓ with increasing WM load includ. right AC, right PC, left vPFC
(102)	16 HC; 17 EST	17 EST, stable injectable FGA for 2 months	Verbal "2-back"	N/A	Main effect of group: ↑ subgenual AC gyrus; group × WM load interaction for high WM load: ↓ in right DLPFC
(98)	14 HC; 14 Patients[b] subdivided into HP: 8 HC, 7 patients; LP: 6 HC, 7 patients	14 Patients, 476.3 (291.7)[c]; 7 Patients, 556.0 (157.0)[c]; 6 Patients, 237.7 (96.4)[c]	Numeric "2-back"	N/A	↑ and ↓ for high WM load in different subdivisions of the right and left DLPFC in 14 patients; bilateral prefrontal areas of ↑ and ↓ for high WM load in HP patients; bilateral prefrontal areas of ↓ for high WM load in LP patients
(99)	22 HC; 14 EST	Not reported	Verbal "2-back"	N/A	↑ For high WM load in right medial FG; ↑ for hits during for high WM load in right medial FG
fMRI STUDIES – FC					
(100)	26 HC; 15 Patients[b], subdivided into HP: 14 HC, 8 patients; LP: 12 HC, 7 patients	15 Patients, 501 (337.0)[c]	Numeric "2-back"	Seed-based cross-correlation; seed regions: right dPFC and left vPFC; functional ROIs 10 mm sphere size	↑ FA with increasing WM load in bilateral vPFC in 15 patients; ↑ FC between left vPFC and left SPL in 15 patients; ↓ FC between right dPFC and bilateral IPL in 15 patients
(89)	153 HC; 78 EST[b]	75 EST, FGA, and SGA; 3 EST, data missing	Numeric "2-back"	Seed-based cross-correlation[d]; Seed regions: right DLPFC; functional ROIs 6 mm sphere size	↑ FA for high WM load in right DLPFC; ↓ FC between right DLPFC and bilateral HF; ↓ FC between right DLPFC and right IPL
(103)	28 HC; 30 FES[a]	Not reported	Numeric "2-back"	Seed-based cross-correlation; seed regions: left gyrus rectus, left IFG, left SFG, left AC, right PHG, right amygdala; functional ROIs sphere size not reported	↑ FA for high WM load in left gyrus rectus, left IFG, left SFG, left AC, right PHG, right amygdala; ↓ FC between medial FG and right precuneus; between medial FG and left OFG; between medial frontal gyrus and right precentral gyrus
(101)	28 HC; 28 EST[a,b]	24 EST, 294.45 (316.36)[c]	Numeric "2-back"	ROI-to-ROI FC; ROIs: bilateral DLPFC, vlPFC, putamen, caudate nuclei, IPL; functional ROIs sphere size not reported	↑ FA for high WM load in bilateral putamen, left DLPFC, OFC, cuneus, and PC; ↓ FC between left putamen and right vlPFC; ↓ FC between left putamen and left vlPFC; between right IPL and right vlPFC

↑ Increased in subjects with schizophrenia in contrast to HC.

↓ Decreased in subjects with schizophrenia in contrast to HC.

AC, anterior cingulate; DLPFC, dorsolateral prefrontal cortex; dPFC, dorsal prefrontal cortex; EST, subjects with established schizophrenia; FA, functional activation; FC, Functional connectivity; FES, subjects with first episode schizophrenia; FG, frontal gyrus; FGA, First-generation antipsychotics; HC, healthy controls; HF, hippocampal formation; HP, high-performers; HR, subjects at high risk of schizophrenia; IFG, inferior frontal gyrus; IPL, inferior parietal lobe; LP, low-performers; OFG, orbitofrontal gyrus; PC, posterior cingulate; PHG, parahippocampal gyrus; ROI, region of interest; SGA, second-generation antipsychotics; SFG, superior frontal gyrus; SPL, superior parietal lobule; vPFC, ventral prefrontal cortex; vlPFC, ventrolateral PFC; WM, working memory.

[a] Patients with different schizophrenia subtypes, such as paranoid subtype, schizoaffective subtype, undifferentiated subtype.

[b] Phase of illness, illness onset, and illness duration not reported. Phase of illness based on symptoms scores.

[c] Chlorpromazine equivalents in milligrams per day.

[d] Seed-based connectivity only reported here.

heterogeneous groups of subjects with EST (97, 101, 103), and (iii) limited information on antipsychotic treatment (89, 97–101, 103). Fundamentally, none of the functional activation findings was interpreted in context of the dopamine or glutamate hypothesis. The lack of a clear understanding in terms of neural activation and pathophysiological mechanism suggests there is a need for studies examining wider prefrontal circuitry underlying working memory deficits in schizophrenia (93, 95).

Functional connectivity studies applied voxel-based seed approaches to the BOLD response (89, 100, 103), with the exception of one study, which applied an ROI-to-ROI approach (101). Despite equivalent methodological approaches, the FC findings are not entirely comparable due to the use of different seed locations. Findings of reduced connectivity involving subregions of the PFC were found in FES and EST. Reduced FC findings in subjects with schizophrenia and EST were reported in the majority of studies: (i) Reduced prefrontal–parietal[4] FC in subjects with schizophrenia (100); (ii) Reduced prefrontal–hippocampal, prefrontal–striatal, and within-PFC FC in EST (89); and (iii) Reduced parieto-prefrontal FC and between putamen and ventrolateral PFC in EST (101). Further evidence for reduced FC between medial frontal gyrus and putamen was found in FES (103). In contrast to most studies that report reduced FC in the early and late phases of the illness, increased FC between the ventral PFC and posterior PC was shown in subjects with schizophrenia (100). The findings of both reduced and increased FC between subregions of the PFC and the posterior PC may be related to variations in behavioral response to task load for subjects with schizophrenia (100). Similar difficulties in comparing the FC findings among the studies are present as in the comparison of the functional activation studies due to unclear and missing information regarding the illness phase, diagnosis, and medication treatment. Similarly, no reference is made to the dopamine or glutamate hypothesis in interpreting the FC findings.

In summary, findings presented by FC studies during the "N-back" task have paved the way for the understanding of large-scale functional networks in working memory. Furthermore, the insight of brain alterations in subjects with schizophrenia has advanced with FC from individually activated regions to connectivity between brain regions. The perspective of circuit-based neurobiology and cognitive brain function opens the doors for translational research from preclinical and clinical research in schizophrenia. However, FC is limited as the connection assessments are based upon regional correlations and this approach does not allow inferences of directions or causality between connected regions (18).

Positron emission tomography and SPECT imaging in schizophrenia research are used to investigate indirect markers of dopamine measures such as D2/3 receptors, presynaptic dopaminergic function, dopamine synthesis capacity, dopamine release, and dopamine transporters. Three [H215O] PET studies consistently reported reduced rCBF in DLPFC and PC in verbal/numeric "2-back" in subjects with EST in contrast to healthy controls (104–106). Reduced prefrontal–hippocampal FC findings in subjects with schizophrenia in contrast to healthy controls (105, 106) confirmed the hypothesis of reduced functional connections in working memory. Correlational PET studies provided support for dopaminergic alterations and measures of the "2-back" task in subjects with schizophrenia (2, 16).

In summary, fMRI and PET studies in the field of clinical and cognitive neurosciences have been used to investigate brain function during working memory in people with schizophrenia (**Figure 1**). Both fMRI and PET findings have advanced the understanding of altered working memory performance and brain function in subjects with schizophrenia. This has led to better insight into the interaction between altered working memory function and experimental/clinical factors (such as cognitive domains of working memory function, performance level, phases of illness, clinical symptomatology, and effects of antipsychotic medication) in individuals with schizophrenia.

EXAMPLES OF fMRI STUDIES INVESTIGATING ALTERED SPATIAL WORKING MEMORY FUNCTION – GLUTAMATE HYPOTHESIS OF SCHIZOPHRENIA

The role of the DLPFC in working memory deficits has been associated with glutamatergic alterations and more specifically in dopamine–glutamate interactions (10, 50, 51). Furthermore, it has been reported that ketamine, a NMDA receptor antagonist, can induce psychosis-like symptoms in healthy subjects (45). Here, we briefly summarize the main functional activation and FC findings of fMRI studies on the spatial "N-back" task in the context of the glutamate hypothesis of schizophrenia (**Table 2**).

Anticevic et al. (12) presented ketamine-induced reduced functional activation in task-activated regions (such as the DLPFC and the precuneus) and task-deactivated regions of the default-mode network (DMN). In addition, the combination of a spiking local-circuit model of performance during the spatial "N-back" task and the functional activation findings revealed that the modulation of

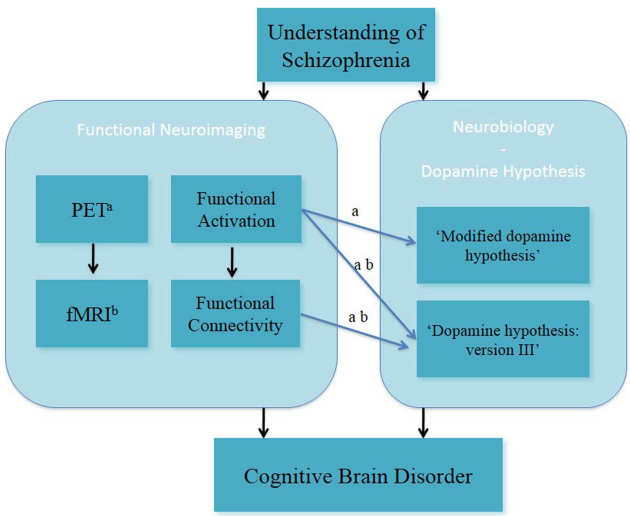

FIGURE 1 | Understanding of schizophrenia as a cognitive brain disorder – verbal/numeric "N-back" task. [a]fMRI; [b]PET, positron emission tomography.

[4]Reduced FC between the dorsal PFC and posterior PC.

Table 2 | Schizophrenia as a cognitive brain disorder II – summary of main findings in spatial working memory.

Study	Subjects HC	Medication/ketamine injection	Experimental paradigm	Functional connectivity method Seed regions/ROIs Seed regions/ROIs definition Sphere size	Computational modeling	Main finding(s)
fMRI + KETAMINE STUDIES						
(12)	19 HC	One saline injection; initial ketamine bolus 0.23 mg/kg for I min; subsequent ketamine bolus 0.58 mg/kg for 1 h	Spatial "2-back" and "4-back"	Seed-based cross-correlation Seeds: FP–DMN pair; CO–DMN pair; anatomical ROIs 15 mm sphere size	Modeling of the acute ketamine effect of local and long-range E–I connections Spiking E and I cell local-circuit models: task-activated module and task-deactivated module	Ketamine attenuated task-activated regions (i.e., DLPFC and precuneus) Ketamine attenuated task-deactivated regions overlapping the DMN; ↓ E–I conductance led to attenuation in task-activated regions; modulation of task-activated FC between FP–DMN networks during delay of WM
(62)	22 HC	One saline injection; one initial ketamine bolus 0.23 mg/kg for 1 min; one subsequent ketamine bolus 0.58 mg/kg for 1 h	Spatial "2-back" and "4-back"	(1) Seed-based cross-correlation; seed regions: bilateral MFG, IFG, SFG, and Heschl's gyrus; anatomical ROIs 10 mm sphere size (2) Global-based connectivity; see details as in (1)	N/A	Ketamine effect using (1): ↓ FC between right DLPFC and MFG, IFG, frontal OC, insula, medial FG; angular gyrus; ketamine effect using (2): ↓ FC within left DLPFC

↓*Reduced.*

CO, cingulo-occipital; DLPFC, dorsolateral prefrontal cortex; DMN, default-mode network; E cells, excitatory cells; FC, functional connectivity; FG, frontal gyrus; FP, fronto-parietal; HC, healthy controls; I cells, inhibitory cells; IFG, inferior frontal gyrus; MFG, middle frontal gyrus; NMDA, N-Methyl-d-aspartate acid; OC, orbital cortex; ROI, region of interest; SFG, superior frontal gyrus; WM, working memory.

ketamine alters the association between the task-activated and the task-deactivated networks. Finally, it was shown that ketamine modulates FC between the fronto-parietal and DMN networks. In a recent study, Driesen et al. (62) provided further support for ketamine-induced reduced prefrontal FC during the spatial "N-back" task. Two FC approaches with the same seed regions were employed, seed-based FC and global-based connectivity (GBC), which revealed both decreased FC within the DLPFC. The seed-based analysis resulted in reduced FC between DLPFC and middle frontal gyrus [MFG, IFG, and insula (among other regions) under ketamine in contrast to saline]. The GBC analysis showed decreased FC of the DLPFC under ketamine.

In summary, these studies on altered spatial working memory function inform on the glutamate hypothesis, through the acute ketamine model (**Figure 2**). In this, they have advanced the understanding of NMDA receptor-modulated brain function in healthy subjects.

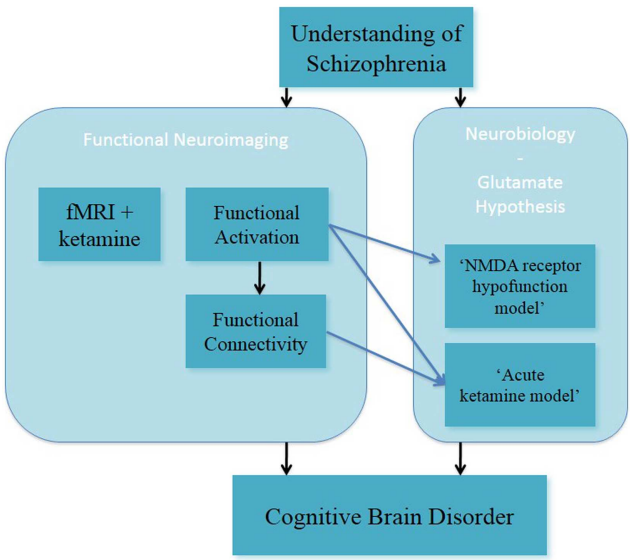

FIGURE 2 | Understanding of schizophrenia as a cognitive brain disorder – spatial "N-back" task.

FROM COMPUTATIONAL NEUROPSYCHIATRY TOWARD SCHIZOPHRENIA AS A COGNITIVE BRAIN NETWORK DISORDER

Clinical and cognitive neurosciences have advanced the understanding of altered working memory function in subjects with schizophrenia. FMRI studies in working memory among other neuroimaging and electrophysiological techniques, have reported on functional activation and FC findings in subjects with schizophrenia. Both findings of functional activation and FC revealed methodological, cognitive, and clinical factors related to our understanding of altered working memory function in patients with schizophrenia. In particular, FC findings mark the beginning of the notion of "disconnection" and "dysconnection" (20, 21, 67, 107) in working with people with schizophrenia. FC is defined as the statistical association or dependency among two or more anatomically distinct time-series (107). FC findings cannot be interpreted in terms of causal effects between connected regions and thus, does not allow for a mechanistic inference of the BOLD responses.

The modeling of functional large-scale networks[5] during working memory function in schizophrenia could provide mechanistic explanations for altered brain function in individuals with schizophrenia. The advantage of modeling functional large-scale networks in terms of EC over FC is that inferences can be drawn on mechanistic processes, which are not directly observable in the BOLD response.

COMPUTATIONAL NEUROSCIENCE AND COMPUTATIONAL NEUROPSYCHIATRY

Marr proposes a theoretical framework for computational research on the brain on three levels (1976). At the first level, researchers should aim to gain knowledge of the high-level computations of the brain such as working memory ("computational level"). At the next level, the testing of the brain's methods and algorithms for the high-level working memory function is led by hypotheses derived from the acquired knowledge and testing how appropriate an algorithm such as Bayesian inference is for modeling the working memory brain function ("algorithmic level"). Finally, when an algorithm is found, which is valid and more likely than alternative algorithms to predict known brain function/behavior, then the investigation of the biological implementation can be pursued ("physical level").

Computational neuropsychiatry is an emerging field within computational neuroscience. Computational neuropsychiatry aims to provide an explanatory bridge between altered cognitive function and neurobiological mechanisms associated with the development of mental illness (108, 109, Huys, unreferred preprint). Computational neuropsychiatry in humans has been defined by outlining a set of components, which include biophysical modeling and computational modeling (109). Different types of computational models at different neural levels are used dependent on the study hypothesis (108, Huys, unreferred preprint).

COMPUTATIONAL NEUROPSYCHIATRY AND MODELING OF FUNCTIONAL LARGE-SCALE NETWORKS IN SUBJECTS WITH SCHIZOPHRENIA

Connectionist and neural network models in working memory/cognitive control in subjects with schizophrenia have added to our understanding of both the brain function and the neurobiological mechanism underlying working memory (74, 76). The strength of these models is based on the translational link between human brain function (i.e., functional activation) and preclinical neurobiological evidence (namely, dopaminergic modulation) during working memory.

Following on from the work of Cohen and Braver, evidence for the understanding of schizophrenia as a cognitive network disorder has been presented by both preclinical studies (8, 10, 110–113) and human FC studies in working memory (89, 100, 101, 103). Recent studies examining biophysical mechanisms underlying

[5]As one subfield within computational psychiatry.

altered functional large-scale networks aim to bridge the gap between the human functional network used in working memory and the preclinical neurobiological processes. Examples of such computational neuropsychiatric studies, including EC during working memory in subjects with schizophrenia, are reviewed. In this, we focus on DCM studies investigating the numeric/verbal "N-back" task in subjects with schizophrenia and healthy controls. This is considered in the context of the dopamine and glutamate hypotheses of schizophrenia. Both neurobiological hypotheses have contributed to the formulation of research objectives in computational neuropsychiatry (114) and the development of computational modeling techniques of fMRI data in subjects with schizophrenia (20).

Dynamic causal modeling for fMRI – examples of modeling functional large-scale networks

Dynamic causal modeling for fMRI has been introduced as a method to provide insight into the notion of "functional integration" during cognitive performance. "Functional integration" has been advanced from the historic notion of "functional specialization" (115), which is defined by context-dependent interactions among different brain regions (18, 116–118).

Dynamic causal modeling has been described as a biophysical modeling of neuronal dynamic processes (18, 19)[6], which can be used as a method for the computation of synaptic plasticity from fMRI task-based studies (20, 21). Together biophysical modeling and Bayesian inference analysis form the framework for DCM (71, 117, 118). Thus, DCM is a modeling approach, which combines defined network models (i.e., hypotheses) with Bayesian inversion methods (19, 117). Specifically, DCM assesses inter-regional EC through assessment of experimentally induced changes (18) and therefore allows for mechanistic inferences from neuronal function.

Bilinear DCM infers dynamics at the neuronal level by translating modeled neuronal responses into predicted BOLD measurements (18). Non-linear DCM for fMRI (71, 119) is an advanced approach for increasing the biological plausibility of DCMs by the means of modeling "gain modulation" (i.e., non-linear modulation of neuronal connections) (19, 117, 118). In non-linear DCM, the modulation of connection strengths by experimental inputs is supplemented by direct modulation of neural activity in one or more network regions (18, 119). The computations for gating in neural networks use the multiplicative computation of non-linear modulation (120, 121). Accordingly, non-linear DCM can be used for inferring that the strength of a connection is modulated by activity of other neuronal populations (119, 122).

Findings of altered effective connectivity during working memory in subjects with schizophrenia. The first DCM studies in healthy controls described large-scale networks in working memory and a similar task [continuous performance test; (123–125)]. A recent study in healthy controls built the linkage between EC results and underlying dopaminergic modulation of large-scale networks comprising of the DLPFC and PC during verbal memory performance (126).

To date four DCM studies have examined the verbal/numeric "N-back" task in subjects with schizophrenia using bilinear DCM (127–130) (**Table 3**). These provide novel insights into reduced task-dependent EC and increased task-independent EC measures through modeling large-scale networks in schizophrenia.

In the first study, increased fronto-temporal intrinsic connectivity was found to be associated with increased functional activation of the superior temporal gyrus (STG) during the numeric "N-back" task in the subjects at the prodromal and at the acutely psychotic stage of schizophrenia in contrast to the healthy controls. This suggests a potential marker for vulnerability to the disorder (127). Furthermore, progressively decreased intrinsic connectivity between the STG and the MFG in subjects at-risk mental state (ARMS) and FES subjects in contrast to the healthy controls was reported. This finding suggested that functional activation may resemble increased task-independent EC between the PFC and the STG. However, the results of the study are not comparable to other DCM studies because (i) only one model was examined and (ii) the biological plausibility of the EC measures is not clearly accessible. No reference to the dopamine or glutamate hypotheses was made.

The second study investigated the working memory-dependent modulatory effect for the prefrontal–parietal connectivity in subjects with EST and healthy subjects during the numeric "N-back" task (128). The large-scale networks included the right DLPFC, the PC, and the visual cortex with bidirectional connection between all regions. The main finding was decreased task-dependent EC from the DLPFC to the PC in the subjects with EST. Thus, this finding could resemble evidence for the glutamate hypothesis of schizophrenia, specifically the NMDA receptor hypofunction model and the dysconnection hypothesis.

The third study examined possible vulnerability markers for psychosis from the verbal "N-back" task in ARMS subjects, FES subjects, and healthy subjects (129). This study examined reduced task-dependent EC measures as well as relationships between connectivity parameters and antipsychotic medication received by subjects. In this study, EC in interhemispheric large-scale networks between the bilateral superior parietal lobes (SPL) and the bilateral MFG was assessed. This study reported novel findings of progressively decreased working memory and induced modulation of connectivity between the MFG and the SPL (from healthy subjects to ARMS). Additionally, further decreased EC of modulatory effects were observed in non-medicated subjects with FEP contrasted to healthy controls. Evidence for amelioration of reduced EC between the MFG and the SPL in subjects with FES, who received SGA medication, could reflect alterations of dopaminergic regulation of NMDA receptor-dependent synaptic plasticity of fronto-parietal connections. However, this interpretation is limited by the lack of a control group of FES who are treated with different types of antipsychotic medication. These findings across different subpopulations of schizophrenia together with the effect of antipsychotic medication may reflect support for the NMDA receptor hypofunction model and the dysconnection hypothesis.

[6]We consider DCM as the generative model approach as introduced in the seminal article by Friston et al. (18).

Table 3 | Schizophrenia as a cognitive brain network disorder II – summary of main findings in verbal/numeric working memory – neuroimaging and biophysical modeling.

Study	Subjects – phase of schizophrenia; HC – HR, FES/FEP, EST	Medication	Experimental paradigm	Networks – model space; number of models; regions	DCM settings – DCM version; sphere size; inference technique(s)	Main finding(s)
(127)	13 HC; 16 HR[a]; 10 FES	HR, not medicated; 7 FES, risperidone or quetiapine, 3 FES, not medicated	Numeric "2-back"	1 Left hemispheric model; STG, SMA, MFG, INS, PPC	DCM in SPM5; Sphere sizes not reported; BMS not performed	Progressively ↑ IC of the prefrontal–temporal connection in HR and FES
(128)	42 HC; 41 EST	35 EST, FGA; 5 EST, SGA; 1 EST, not medicated	Numeric "2-back"	48 Intrahemispheric models; 3 model families; DLPFC, PC, VC	DCM10 in SPM8; 4 mm spheres; random-effects BMS[e,f]; BMA	↓ EC (effect of task-modulation) from DLPFC to PC
(129)	20 HC; 17 HR[a]; 21 FEP	HR, not medicated; 7 FEP, completely antipsychotic naïve; 6 FEP, antipsychotic naïve at the time of scanning; 8 FEP, SGA	Verbal "2-back"	12 Intrahemispheric models; bilateral SPL, bilateral MFG	DCM10 in SPM8; 12 mm spheres; random-effects BMS[e]; BMA	Progressively ↓ EC (effect of task-modulation) between MFG and SPL in HC, HR, and FES. Ameliorated EC correlated with antipsychotic treatment.
(130)	15 HC; 14 FES[b]; 19 FES[c]	FES[b], 254.76 (192.09)[d]; FES[c], 325.88 (185.19)[d]	Verbal "2-back"	5 Left hemispheric models; medial PFC, PCC	DCM version not reported; SPM8; 6 mm spheres; BMS[e]; BMA	↑ IC from PCC to medial PFC in both FES[e] and FES[f]

↑Increased in subjects with schizophrenia in contrast to HC.

↓Decreased in subjects with schizophrenia in contrast to HC.

BMA, Bayesian model averaging; BMS, Bayesian model selection; DLPFC, dorsolateral prefrontal cortex; EC, effective connectivity; EST, subjects with established schizophrenia; FES, subjects with first episode schizophrenia; FEP, subjects with first episode psychosis; FGA, first-generation antipsychotics; HC, healthy controls; HR, subjects at high risk of schizophrenia; IC, intrinsic connectivity; IFG, inferior frontal gyrus; INS, insula; MFG, middle frontal gyrus; PC, parietal cortex; PCC, posterior parietal cortex; PFC, prefrontal cortex; SGA, second-generation antipsychotics; SMA, supramarginal area; SPL, superior parietal lobe; STG, superior temporal gyrus; VC, visual cortex.

[a]Subjects at high clinical risk of schizophrenia.

[b]With high suicidal risk.

[c]With low suicidal risk.

[d]Chlorpromazine equivalents in mg/day.

[e]BMS at the group-level.

[f]BMS at the model family level.

In the fourth study, Zhang et al. (130) explored EC measures in terms of possible neurobiological markers in groups of subjects with schizophrenia with high or low suicide risk and contrasted these with healthy controls during the verbal "N-back" task. The large-scale networks were defined by unidirectional and bidirectional connections between the two regions of the medial PFC and PC as well as working memory effects on these regions. This pilot study presented novel findings in subjects with schizophrenia at suicidal risk in terms of increased intrinsic connectivity from the PC to the MFG in both groups with FES (in comparison to healthy controls). This finding was interpreted as a possible association to schizophrenia, in which increased intrinsic connectivity from the MFG to the PC in the subjects with high risk of suicide could reflect vulnerability of suicide. However, the results are not directly comparable to the other DCM studies because of the study population, which focused on the issue of suicide. The findings were also not interpreted in context of the dopamine or glutamate hypotheses.

We highlight main experimental and methodological limitations in the four DCM studies, which impede the comparability of findings (please see **Table 3** for details). The main experimental limitation focuses on the discrepancies between the different patient subpopulations. Two studies analyzed working memory fMRI data of subjects with ARMS and FES in comparison to healthy controls (127, 129), whereas one study modeled scans from subjects with EST (128). Zhang et al. (130) reported findings of a unique patient population of FES with high and low suicidal risk. In terms of methodological issues, one limitation lies in different definitions of model spaces for the large-scale networks, despite equivalence in the experimental tasks. Another limitation is that the reviewed DCM studies employed deterministic DCM for the comparison of the models. Deterministic models can predict processes perfectly if all inputs are known (131). However, at this early stage of employing biophysical modeling approaches to human brain function, we do not have a full understanding of the brain responses to working memory. Future studies may employ stochastic DCM as an extension (117, 118, 132). A further limitation is that different DCM versions were applied across the four studies, which impede the comparability of the findings. The priors are differently defined in the used DCM versions, which give rise to a variation in model evidence between the studies (117). Thus, it is possible that discrepancies in EC findings could be due to the prior definition and may not be solely due to differences in performance, brain function, or clinical aspects of subjects with schizophrenia. Lastly, a general limitation of DCM for fMRI is that maximally 10 regions within a large-scale network can be modeled. This simplification results in difficulties of biophysical modeling of tasks, which are likely to encompass more than ten regions. Furthermore, not only the definition of different regions and different numbers of regions but also different modulatory inputs result in further extensions to the model space. Such model spaces are difficult to validate and analyze.

The four DCM studies presented evidence for increased task-dependent EC and increased task-independent EC findings during verbal/numeric working memory in subjects with schizophrenia. We discuss these EC findings in context of (i) the dopamine and glutamate hypothesis and (ii) FC findings during verbal/numeric working memory in subjects with schizophrenia.

The four studies modeled large-scale networks during the "N-back" task in subjects with schizophrenia. However, only two out of these four studies consider their DCM results in the light of biophysical processes (128, 129). The findings of reduced EC (namely, the effect of task-modulation) of the prefrontal–parietal connection in subjects with schizophrenia in contrast to healthy controls were interpreted biophysically and linked to the NMDA receptor hypofunction model and the dysconnection hypothesis (128, 129). Both studies reported reduced EC findings of the prefrontal–parietal connection during working memory, however, these findings need to be considered carefully due to different experimental designs (i.e., patient subpopulations, antipsychotic medication treatment of FGA and SGA) and methodological implementation (i.e., model space, DCM settings, and inference techniques).

Three of the DCM studies reported altered EC findings of the prefrontal–parietal and parieto-prefrontal connections during the "N-back" task in subjects with schizophrenia in contrast to healthy controls. Deserno et al. (128) and Schmidt et al. (129) presented reduced EC (effect of task-modulation) of the prefrontal–parietal connection in subjects with schizophrenia in contrast to healthy controls, whereas Zhang et al. (130) found increased EC (intrinsic connectivity) of the parietal–prefrontal connection. The reduced task-dependent EC findings are in keeping with reduced FC findings of these connections, although increased FC between a different prefrontal subregion and the PC was reported (100).

The study by Crossley et al. (127) reported increased EC (intrinsic connectivity) of the prefrontal–temporal connection in subjects at HR and FES (in contrast to healthy controls). Reduced FC of the prefrontal–temporal connection during the "N-back" task in subjects with schizophrenia has been previously reported in PET studies (105, 106). However, the regions within the PFC and temporal region differ between the studies.

Findings of altered effective connectivity during verbal fluency in subjects with schizophrenia. Here, we discuss bilinear and non-linear DCM studies, which have assessed large-scale networks during verbal fluency [namely, the Hayling sentence completion task (HSCT)] in subjects with schizophrenia and healthy controls (**Table 4**). One bilinear DCM study in healthy controls investigated the task-dependent modulation of response initiation and response suppression in EC between left hemispheric temporal and prefrontal regions (133). The main finding was a difference in connection strength of the modulatory effect in response initiation and response suppression.

Two clinical bilinear DCM studies have investigated EC measures during the HSCT in HR subjects and healthy controls: (i) Subjects at high clinical risk of schizophrenia [ARMS; Ref. (134)] and (ii) subjects at high familial risk of schizophrenia (135). Allen et al. (134) investigated increased fronto-temporal EC (intrinsic connectivity) as a potential measure of vulnerability of developing schizophrenia. Two main findings were reported: firstly, no significant effect of task-dependent modulation on the fronto-temporal connection between ARMS subjects and healthy controls was revealed. Secondly, ARMS subjects displayed increased intrinsic connectivity between the ACC and the MTG in comparison to healthy controls. Furthermore, the Bayesian model selection (BMS) approach revealed that the same network was equally likely

Table 4 | Schizophrenia as a cognitive brain network disorder II – summary of main findings in verbal fluency – neuroimaging and biophysical modeling.

Study	Subjects – phase of schizophrenia; HC – HR, FES/FEP, EST	Medication	Experimental paradigm	Networks – model space; number of models; regions	DCM settings – DCM version; sphere size; inference technique(s)	Main finding(s)
(134)	15 HC; 15 HR[a]	2 HR risperidone and quetiapine[c]	HCST	14 Left hemispheric models; MFG, ACC, MTG	DCM in SPM5; 12 mm spheres; random-effects BMS4	↑ IC between ACC and MTG; same winning model in both groups
(135)	19 HC; 26 HR[b] – 20 HR+, 4 HRill	Not medicated	HCST	8 Left hemispheric models; 3 model families; IPS, IFG, ACC, MTG, MD thalamus	DCM8 in SPM8; 8 mm spheres (IPS, DLPFC, MTG); 6 mm spheres (ACC, MD thalamus); Random-effects BMS[d,e]; BMA	Progressively ↓ connection strength with non-linear modulation of the thalamo-cortical connection in HR+ and HRill in contrast to HC

↑Increased in subjects with schizophrenia in contrast to HC.

↓Decreased in subjects with schizophrenia in contrast to HC.

ACC, anterior cingulate cortex; ARMS, subjects with at-risk mental state; BMA, Bayesian model averaging; BMS, Bayesian model selection; EC, effective connectivity; FEP, subjects with first episode psychosis; FES, subjects with first episode schizophrenia; HC, healthy controls; HR−, subjects at high familial risk of schizophrenia without transient psychotic symptoms; HR+, subjects at high familial risk of schizophrenia with transient psychotic symptoms; HRill, subjects at familial risk of schizophrenia who subsequent to the scanning developed schizophrenia; HSCT, Hayling sentence completion task; IC, intrinsic connectivity; IFG, inferior frontal gyrus; IPS, intraparietal sulcus; MD mediodorsal; MFG, middle frontal gyrus; MTG, middle temporal gyrus;

[a] *Subjects at high clinical risk of schizophrenia.*

[b] *Subjects at high familial risk of schizophrenia.*

[c] *At the time of scanning.*

[d] *BMS at the group-level.*

[e] *BMS at the model family level.*

to explain the given HSCT fMRI data in both the ARMS subjects and the healthy controls. No reference to the glutamate hypothesis was made.

Dauvermann et al. (135) modeled EC measures in a similar version of the HSCT that was used by Allen et al. (134). This study was conducted in subjects at high familial risk of schizophrenia and healthy subjects. The results reported by Allen et al. (134) of a similar large-scale network in both HR subjects and healthy controls was replicated[7]. This finding was also confirmed by Dauvermann et al. (135), when the group of HR subjects was subdivided into high risk subjects without transient psychotic symptoms (referred to as HR−), high risk subjects with transient psychotic symptoms (referred to as HR+) and high risk subjects who subsequent to scanning developed schizophrenia [referred to as HRill; please see Ref. (136, 137)]. Comparability between these two studies is limited due to differences in the model space. The model space in Dauvermann et al. (135) includes the IPS and the mediodorsal thalamus, which are not incorporated in the model space by Allen et al. (134). In addition, endogenous connections and task-dependent modulations were accordingly changed [Ref. (135); **Table 4**]. There was no reference to the glutamate hypothesis of schizophrenia.

Limitations of bilinear DCM have been addressed through the development of non-linear DCM for fMRI (119). This method was applied in the genetic high risk study reported by Dauvermann et al. (135). The progress from the bilinear DCM to the non-linear DCM as reported by Dauvermann is based on the biophysical modeling of connection strength with non-linear modulation during the HSCT response. The authors show that relative to healthy controls there is reduced connection strength with non-linear modulation of the thalamo-cortical connection during the HSCT in HR+ subjects and a further reduction in this connection strength in HRill subjects (135). The authors suggest that reduced gain control may underlie the reduced strength in the thalamo-cortical connection. Furthermore, the findings of reduced connection strength with non-linear modulation of the thalamo-cortical connection could reflect altered glutamatergic neurotransmission, which may underlie a disruption of synaptic plasticity in this thalamo-cortical connection [Ref. (135); **Table 4**]. Thus, the findings were interpreted in context of the NMDA receptor hypofunction model and the dysconnection hypothesis.

Summary of studies modeling functional large-scale networks – dynamic causal modeling for fMRI

Evidence from brain function in working memory in subjects with schizophrenia at the level of functional large-scale networks (i.e., clinical and cognitive neurosciences) and neurobiological mechanisms in working memory in animal models of schizophrenia (preclinical neurobiological research) in combination with computational neuroscientific approaches has informed and enabled research in computational neuropsychiatry.

Exemplary DCM studies in subjects with schizophrenia have reported both increased and reduced EC findings during cognition in subjects with schizophrenia in contrast to healthy controls. These studies applied DCM as a biophysical modeling approach to functional large-scale networks, which enabled the interpretation of EC findings on the basis of the glutamate hypothesis of schizophrenia, namely the NMDA receptor hypofunction model and the dysconnection hypothesis (128, 129, 135). We emphasize that the findings support not only the glutamate hypothesis but also the dopamine hypothesis. Dopamine is a neuromodulator that may crucially affect glutamate-induced synaptic plasticity. Synaptic plasticity may be involved in a regulation of dopamine synthesis and release via other neurotransmitter systems. Specifically for non-linear effects, it has been shown that dopamine acts as a neuromodulator mediating postsynaptic gain (74, 138).

In a recent study, it has been reported that the combination of the DCM analysis of numerical "N-back" task in EST (128) and generative embedding resulted in the dissection of three subgroups of EST based on the mechanistically inferred DCM findings (139). This exemplary study showed that DCM can be applied as a generative model of large-scale networks in individuals with schizophrenia. In summary, DCM is a promising approach for modeling synaptic plasticity; nevertheless in its current form it cannot reflect the full complexity in the processing required for the implementation of tasks such as working memory (**Figure 3**).

UNDERSTANDING OF SCHIZOPHRENIA IN DEVELOPMENT

Our understanding of schizophrenia is in continuous development and with more preclinical and clinical findings being published this understanding will advance further. A critical aspect of this understanding is the facilitation of multidisciplinary approach between preclinical and clinical research in schizophrenia.

The original understanding of schizophrenia as a brain disorder stems from observational clinical work, which led onto preclinical

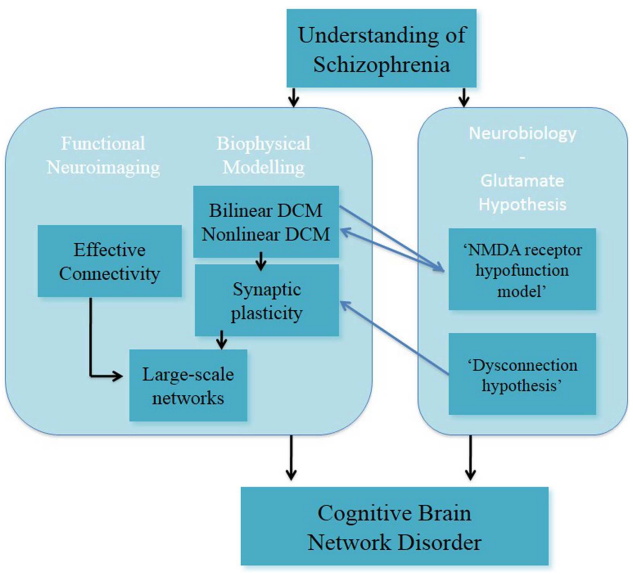

FIGURE 3 | Understanding of schizophrenia as a cognitive brain network disorder – verbal/numeric "N-back" task.

[7]It is noted, however, that the large-scale networks differed slightly from the previous study.

investigation. Over time, the knowledge of alterations of cellular, chemical, and molecular mechanisms has increased: (i) findings of dopaminergic and glutamatergic modulation of working memory (and clinical features) in animal models of schizophrenia contributed to form the understanding of schizophrenia as a cognitive brain disorder; (ii) findings of neurotransmitter circuit systems, mainly dopaminergic and glutamatergic systems, were found to modulate working memory in animal models of schizophrenia in combination with computational studies (140), which plays a role in shaping the understanding of schizophrenia as a cognitive network disorder.

Understanding of schizophrenia has not only been shaped by preclinical research but also by clinical research in subjects with schizophrenia, which has been and continues to be illuminated by preclinical neurobiological and computational work. The field of clinical and cognitive neurosciences has contributed to forming our understanding of schizophrenia as a cognitive brain disorder. Importantly, the multidisciplinary field of computational neuropsychiatry (preclinical neurobiology, clinical and cognitive neurosciences, and computational psychiatry) has allowed for progress in our understanding of schizophrenia as a cognitive brain network disorder.

SCHIZOPHRENIA AS COGNITIVE BRAIN NETWORK DISORDER

The use of computational neuropsychiatric research in developing our understanding of schizophrenia as a cognitive brain network disorder is at an early stage. Here, we focused on FC and EC studies (DCM studies) during the verbal/numeric "N-back" task in subjects with schizophrenia and healthy controls. We discuss these FC and EC findings in context of two key research questions. Consideration of these questions was seen as a means to inform future schizophrenia research in the fields of clinical and cognitive neurosciences and/or computational neuropsychiatry:

To what extent do these sets of findings support the dopamine hypothesis and/or the glutamate hypothesis in subjects with schizophrenia?

Studies reported both increased and reduced FC during the "N-back" task in subjects with schizophrenia in contrast to healthy controls. These findings have introduced the notion of human large-scale networks underlying brain function during working memory. The FC correlational analyses do not allow for the inference of directions or weights of in functional connections. Thus, from FC findings it is not practical to draw inferences on neurobiological causal processing.

Studies, which applied DCM as a biophysical modeling approach to functional large-scale networks, showed that reduced EC findings could be interpreted in context of the NMDA receptor hypofunction model and the dysconnection hypothesis.

In summary, FC findings cannot be interpreted in context of the dopamine or glutamate hypothesis. For EC findings, the computational neuropsychiatric approach of modeling large-scale networks requires biophysically plausible networks, which are hypothesis-driven from neurobiological and cognitive neuroscience in subjects with schizophrenia. EC findings have been interpreted in the context of the glutamate hypothesis and the dopamine hypothesis.

Do the findings from computational neuropsychiatry lead to a gain in understanding of schizophrenia in comparison to the findings from clinical and cognitive neurosciences?

Functional connectivity findings from cognitive and clinical neuroscience have contributed to the understanding of schizophrenia as a cognitive brain disorder. The analysis of altered working memory at the level of large-scale networks has advanced our knowledge of cognitive function in humans. However, it is not wholly understood what altered FC during cognition neurobiologically means in schizophrenia. EC findings from computational neuropsychiatry, here specifically modeling functional large-scale networks with DCM, have shown indications of linkage between clinical network-based working memory (large-scale networks) and preclinical neurotransmitter modulation of cognitive function. Altered synaptic plasticity during working memory can be interpreted with dopaminergic and glutamatergic mechanisms. We emphasize that the interpretation of altered neurotransmitter circuits should be considered carefully because the DCM method is likely to underestimate the processing complexity in neurobiological circuits. Nonetheless, a strength of DCM lies in interpretation of altered synaptic plasticity based on the inference of mechanistic information.

The consideration of schizophrenia as a cognitive brain network disorder from computational neuropsychiatry offers a holistic view of schizophrenia. Computational neuropsychiatry seeks to bridge the gap between neurobiology and cognitive and clinical neurosciences in subjects with schizophrenia. It is hoped that this research will enhance our understanding of schizophrenia, clinical treatment, and improve outcome in people with schizophrenia.

FUTURE OUTLOOK AND OPEN QUESTIONS

The reviewed findings in biophysical modeling of functional large-scale networks are promising. In order to reach the objective of predicting and improving clinical treatment in subjects with schizophrenia, longitudinal study designs, and the combination of subfields within computational neuropsychiatry should be pursued.

We consider computational neuropsychiatric research areas for the combination of biophysical modeling of functional large-scale networks and other computational (neuro)psychiatric approaches, which are of clinical relevance for subjects with schizophrenia, for example:

- Neurotransmitter systems
- Behavior
- Clinical symptoms
- Effects of antipsychotic medication
- Clinical outcome.

We suggest specific study designs, which may increase our understanding for developing clinical treatment for subjects with schizophrenia:

(i) Combination of biophysical modeling of functional large-scale networks with computation, for example:
   (a) Brain function and brain circuit model (12);
   (b) Brain function and behavior (141);
   (c) Brain function and effect of antipsychotic medication:

(ii) Combination of biophysical modeling of functional large-scale networks with multimodal neuroimaging study designs, for example:
  (a) FMRI and EEG/magnetoencephalography study designs;
  (b) FMRI and transcranial magnetic stimulation study designs (142);
  (c) FMRI and MRS study designs;
  (d) FMRI and PET study designs;
(iii) Combination of biophysical modeling of functional large-scale networks and computational modeling for the investigation of clinical (sub)groups, for example:
  (a) Associative learning (143, 144);
  (b) Machine learning approach (139, 145);
  (c) Reinforcement learning (109).

Findings of modeling functional large-scale networks contribute to shaping the understanding of schizophrenia as a cognitive brain network disorder. The combination of computational neuropsychiatric areas may bring researchers closer to the common long-term objectives of developing a diagnostic tool for schizophrenia along with the development of more effective treatments.

ACKNOWLEDGMENTS

We acknowledge Vincent Valton for his help. Maria R. Dauvermann and Thomas W. J. Moorhead are supported by Dr Mortimer and Theresa Sackler Foundation. Heather C. Whalley is supported by Royal Society Dorothy Hodgkin Fellowship.

REFERENCES

1. MacDonald AW, Schulz SC. What we know: findings that every theory of schizophrenia should explain. *Schizophr Bull* (2009) **35**:493–508. doi:10.1093/schbul/sbp017
2. Fusar-Poli P, Howes OD, Allen P, Broome M, Valli I, Asselin MC, et al. Abnormal frontostriatal interactions in people with prodromal signs of psychosis: a multimodal imaging study. *Arch Gen Psychiatry* (2010) **67**(7):683–91. doi:10.1001/archgenpsychiatry.2010.77
3. Gold JM. Cognitive deficits as treatment targets in Schizophrenia. *Schizophr Res* (2004) **72**(1):21–8. doi:10.1016/j.schres.2004.09.008
4. Seidman LJ, Giuliano AJ, Meyer EC, Addington J, Cadenhead KS, Cannon TD, et al. Neuropsychology of the prodrome to psychosis in the NAPLS consortium: relationship to family history and conversion to psychosis. *Arch Gen Psychiatry* (2010) **67**:578–88. doi:10.1001/archgenpsychiatry.2010.66
5. Kim HS, Shin NY, Jang JH, Kim E, Shim G, Park HY, et al. Social cognition and neurocognition as predictors of conversion to psychosis in individuals at ultra-high risk. *Schizophr Res* (2011) **130**:170–5. doi:10.1016/j.schres.2011.04.023
6. Genevsky A, Garrett CT, Alexander PP, Vinogradov S. Cognitive training in schizophrenia: a neuroscience-based approach. *Dialogues Clin Neurosci* (2010) **12**(3):416–21.
7. Bora E, Murray RM. Meta-analysis of cognitive deficits in ultra-high risk to psychosis and first-episode psychosis: do the cognitive deficits progress over, or after the onset of psychosis? *Schizophr Bull* (2013). doi:10.1093/schbul/sbt085
8. Seshadri S, Zeledon M, Sawa A. Synapse-specific contributions in the cortical pathology of schizophrenia. *Neurobiol Dis* (2013) **53**:26–35. doi:10.1016/j.nbd.2013.01.009
9. Kukla M, Davis LW, Lysaker PH. Cognitive behavioral therapy and work outcomes: correlates of treatment engagement and full and partial success in schizophrenia. *Behav Cogn Psychother* (2013). doi:10.1017/S1352465813000428
10. Tanaka S. Dopaminergic control of working memory and its relevance to schizophrenia: a circuit dynamics perspective. *Neuroscience* (2006) **139**:153–71. doi:10.1016/j.neuroscience.2005.08.070
11. Tan HY, Callicott JH, Weinberger DR. Dysfunctional and compensatory prefrontal cortical systems, genes and the pathogenesis of schizophrenia. *Cereb Cortex* (2007) **17**:i171–81. doi:10.1093/cercor/bhm069
12. Anticevic A, Gancsos M, Murray JD, Repovs G, Driesen NR, Ennis DJ, et al. NMDA receptor function in large-scale anticorrelated neural systems with implications for cognition and schizophrenia. *Proc Natl Acad Sci U S A* (2012) **109**:16720–5. doi:10.1073/pnas.1208494109
13. Volk DW, Lewis DA. Prefrontal cortical circuits in schizophrenia. *Curr Top Behav Neurosci* (2010) **4**:485–508. doi:10.1007/7854_2010_44
14. Kim JJ, Kwon JS, Park HJ, Youn DH, Kang MS, Kim MS, et al. Functional disconnection between the prefrontal and parietal cortices during working memory processing in schizophrenia: a [15(O)]H20 PET study. *Am J Psychiatry* (2003) **160**(5):919–23. doi:10.1176/appi.ajp.160.5.919
15. Honey GD, Fletcher PC. Investigating principles of human brain function underlying working memory: what insights from schizophrenia? *Neuroscience* (2006) **139**:59–71. doi:10.1016/j.neuroscience.2005.05.036
16. Abi-Dargham A, Mawlawi O, Lombardo I, Gil R, Martinez D, Huang Y, et al. Prefrontal dopamine D1 receptors and working memory in schizophrenia. *J Neurosci* (2002) **22**(9):3708–19.
17. Poels EM, Kegeles LS, Kantrowitz JT, Javitt DC, Lieberman JA, Abi-Dargham A, et al. Glutamatergic abnormalities in schizophrenia: a review of proton MRS findings. *Schizophr Res* (2014) **152**(2–3):325–32. doi:10.1016/j.schres.2013.12.013
18. Friston KJ, Harrison L, Penny W. Dynamic causal modelling. *Neuroimage* (2003) **19**:1273–302. doi:10.1016/S1053-8119(03)00202-7
19. Friston KJ, Dolan RJ. Computational and dynamic models in neuroimaging. *Neuroimage* (2010) **52**:752–65. doi:10.1016/j.neuroimage.2009.12.068
20. Stephan KE, Friston KJ, Frith CD. Dysconnection in schizophrenia: from abnormal synaptic plasticity to failures of self-monitoring. *Schizophr Bull* (2009) **35**:509–27. doi:10.1093/schbul/sbn176
21. Stephan KE, Baldeweg T, Friston KJ. Synaptic plasticity and dysconnection in schizophrenia. *Biol Psychiatry* (2006) **59**:929–39. doi:10.1016/j.biopsych.2005.10.005
22. Stephan KE, Mathys C. Computational approaches to psychiatry. *Curr Opin Neurobiol* (2014) **25**:85–92. doi:10.1016/j.conb.2013.12.007
23. Howes OD, Kapur S. The dopamine hypothesis of schizophrenia: version III – the final common pathway. *Schizophr Bull* (2009) **35**:549–62. doi:10.1093/schbul/sbp006
24. Qi Z, Miller GW, Voit EO. Computational modeling of synaptic neurotransmission as a tool for assessing dopamine hypotheses of schizophrenia. *Pharmacopsychiatry* (2010) **43**(Suppl 1):S50–60. doi:10.1055/s-0030-1248317
25. Coyle JT. NMDA receptor and schizophrenia: a brief history. *Schizophr Bull* (2012) **38**(5):920–6. doi:10.1093/schbul/sbs076
26. Coyle JT, Basu A, Benneyworth M, Balu D, Konopaske G. Glutamatergic synaptic dysregulation in schizophrenia: therapeutic implications. *Handb Exp Pharmacol* (2012) **2012**:267–95. doi:10.1007/978-3-642-25758-2_10
27. Kantrowitz JT, Javitt DC. *N*-methyl-D-aspartate (NMDA) receptor dysfunction or dysregulation: the final common pathway on the road to schizophrenia? *Brain Res Bull* (2010) **83**:108–21. doi:10.1016/j.brainresbull.2010.04.006
28. Delay J, Deniker P, Harl JM. Therapeutic use in psychiatry of phenothiazine of central elective action (4560 RP). *Ann Med Psychol (Paris)* (1952) **110**(2):112–7.
29. Carlsson A. Does dopamine have a role in schizophrenia? *Biol Psychiatry* (1978) **13**(1):3–21.
30. Emilien G, Maloteaux JM, Geurts M, Owen MJ. Dopamine receptors and schizophrenia: contribution of molecular genetics and clinical neuropsychology. *Int J Neuropsychpharmacol* (1999) **2**(3):197–227. doi:10.1017/S1461145799001479
31. Seeman P, Lee T. Antipsychotic drugs: direct correlation between clinical potency and presynaptic action on dopamine neurons. *Science* (1975) **188**:1217–9. doi:10.1126/science.1145194
32. Creese I, Burt DR, Snyder SH. Dopamine receptor binding predicts clinical and pharmacological potencies of antischizophrenic drugs. *Science* (1976) **192**:481–3. doi:10.1126/science.3854
33. Seeman P, Lee T, Chau-Wong M, Wong K. Antipsychotic drug doses and neuroleptic/dopamine receptors. *Nature* (1976) **261**:77–9. doi:10.1038/261717a0
34. Lieberman AN, Goldstein M, Gopinathan G, Nophytides A. D-1 and D-2 agonists in Parkinson's disease. *Can J Neurol Sci* (1987) **14**(3 Suppl):466–73.
35. Snyder SH. The dopamine hypothesis of schizophrenia: focus on the dopamine receptor. *Am J Psychiatry* (1976) **133**(2):197–202.

36. Davis KL, Kahn RS, Ko G, Davidson M. Dopamine in schizophrenia: a review and reconceptualization. *Am J Psychiatry* (1991) **148**:1474–86.
37. Kapur S, Seeman P. Does fast dissociation from the dopamine D(2) receptor explain the action of atypical antipsychotics? A new hypothesis. *Am J Psychiatry* (2001) **158**:360–9. doi:10.1176/appi.ajp.158.3.360
38. Pycock CJ, Kerwin RW, Carter CJ. Effect of lesion of cortical dopamine terminals on subcortical dopamine receptors in rats. *Nature* (1980) **286**:74–6. doi:10.1038/286074a0
39. Scatton B, Worms P, Lloyd KG, Bartholini G. Cortical modulation of striatal function. *Brain Res* (1982) **232**(2):331–43. doi:10.1016/0006-8993(82)90277-3
40. Heinz A. Dopaminergic dysfunction in alcoholism and schizophrenia – psychopathological and behavioral correlates. *Eur Psychiatry* (2002) **17**(1):9–16. doi:10.1016/S0924-9338(02)00628-4
41. Kapur S. Psychosis as a state of aberrant salience: a framework linking biology, phenomenology, and pharmacology in schizophrenia. *Am J Psychiatry* (2003) **160**(1):13–23. doi:10.1176/appi.ajp.160.1.13
42. Howes OD, Kambeitz J, Kim E, Stahl D, Slifstein M, Abi-Dargham A, et al. The nature of dopamine dysfunction in schizophrenia and what this means for treatment. *Arch Gen Psychiatry* (2012) **69**(8):776–86. doi:10.1001/archgenpsychiatry.2012.169
43. Fusar-Poli P, Meyer-Lindenberg A. Striatal presynaptic dopamine in schizophrenia, part I: meta-analysis of dopamine active transporter (DAT) density. *Schizophr Bull* (2013) **39**(1):22–32. doi:10.1093/schbul/sbr111
44. Fusar-Poli P, Meyer-Lindenberg A. Striatal presynaptic dopamine in schizophrenia, part II: meta-analysis of [(18)F/(11)C]-DOPA PET studies. *Schizophr Bull* (2013) **39**(1):33–42. doi:10.1093/schbul/sbr180
45. Krystal JH, Karper LP, Seibyl JP, Freeman GK, Delaney R, Bremner JD, et al. Subanesthetic effects of the noncompetitive NMDA antagonist, ketamine, in humans. Psychotomimetic, perceptual, cognitive, and neuroendocrine responses. *Arch Gen Psychiatry* (1994) **51**(3):199–214. doi:10.1001/archpsyc.1994.03950030035004
46. Abi-Saab WM, D'Souza DC, Moghaddam B, Krystal JH. The NMDA antagonist model for schizophrenia: promise and pitfalls. *Pharmacopsychiatry* (1998) **31**(Suppl 2):104–9. doi:10.1055/s-2007-979354
47. Luby E, Cohen B, Rosenbaum G, Gottlieb J, Kelley J. Study of a new schizophrenomimetic drugs. *AMA Arch Neurol Psychiatry* (1959) **81**:363–9. doi:10.1001/archneurpsyc.1959.02340150095011
48. Carlsson A, Waters N, Waters S, Carlsson ML. Network interactions in schizophrenia – therapeutic implications. *Brain Res Brain Res Rev* (2000) **31**(2–3):342–9. doi:10.1016/S0165-0173(99)00050-8
49. Farber NB, Kim SH, Dikranian K, Jiang XP, Heinkel C. Receptor mechanisms and circuitry underlying NMDA antagonist neurotoxicity. *Mol Psychiatry* (2002) **7**:32–43. doi:10.1038/sj.mp.4000912
50. Javitt DC. Glutamate and schizophrenia: phencyclidine, *N*-methyl-D-aspartate receptors, and dopamine-glutamate interactions. *Int Rev Neurobiol* (2007) **78**:69–108. doi:10.1016/S0074-7742(06)78003-5
51. Coyle JT. Glutamate and schizophrenia: beyond the dopamine hypothesis. *Cell Mol Neurobiol* (2006) **26**:365–84. doi:10.1007/s10571-006-9062-8
52. Coyle JT, Balu D, Benneyworth M, Basu A, Roseman A. Beyond the dopamine receptor: novel therapeutic targets for treating schizophrenia. *Dialogues Clin Neurosci* (2010) **12**(3):359–82.
53. Moghaddam B, Krystal JH. Capturing the angel in "angel dust": twenty years of translational neuroscience studies of NMDA receptor antagonists in animals and humans. *Schizophr Bull* (2012) **38**:942–9. doi:10.1093/schbul/sbs075
54. Javitt DC, Zukin SR, Heresco-Levy U, Umbricht D. Has an angel shown the way? Etiological and therapeutic implications of the PCP/NMDA model of schizophrenia. *Schizophr Bull* (2012) **38**:958–66. doi:10.1093/schbul/sbs069
55. Javitt DC. Glutamatergic theories of schizophrenia. *Isr J Psychiatry Relat Sci* (2010) **47**(1):4–16.
56. Goff DC, Coyle JT. The emerging role of glutamate in the pathophysiology and treatment of schizophrenia. *Am J Psychiatry* (2001) **158**:1367–77. doi:10.1176/appi.ajp.158.9.1367
57. Heresco-Levy U, Ermilov M, Shimoni J, Shapira B, Silipo G, Javitt DC. Placebo-controlled trial of D-cycloserine added to conventional neuroleptics, olanzapine, or risperidone in schizophrenia. *Am J Psychiatry* (2002) **159**(3):480–2. doi:10.1176/appi.ajp.159.3.480
58. Lane HY, Chang YC, Liu YC, Chiu CC, Tsai GE. Sarcosine or D-serine add-on treatment for acute exacerbation of schizophrenia: a randomized, double-blind, placebo-controlled study. *Arch Gen Psychiatry* (2005) **62**(11):1196–204. doi:10.1001/archpsyc.62.11.1196
59. Tzschentke TM. Pharmacology and behavioral pharmacology of the mesocortical dopamine system. *Prog Neurobiol* (2001) **63**(3):241–320. doi:10.1016/S0301-0082(00)00033-2
60. Sesack SR, Carr DB. Selective prefrontal cortex inputs to dopamine cells: implications for schizophrenia. *Physiol Behav* (2002) **77**(4–5):513–7. doi:10.1016/S0031-9384(02)00931-9
61. Krystal JH, D'Souza DC, Karper LP, Bennett A, Abi-Dargham A, Abi-Saab D, et al. Interactive effects of subanesthetic ketamine and haloperidol in healthy humans. *Psychopharmacology* (1999) **145**(2):193–204. doi:10.1007/s002130051049
62. Driesen NR, McCarthy G, Bhagwagar Z, Bloch MH, Calhoun VD, D'Souza DC, et al. The impact of NMDA receptor blockade on human working memory-related prefrontal function and connectivity. *Neuropsychopharmacology* (2013) **38**(13):2613–22. doi:10.1038/npp.2013.170
63. Moghaddam B, Adams B, Verma A, Daly D. Activation of glutamatergic neurotransmission by ketamine: a novel step in the pathway from NMDA receptor blockade to dopaminergic and cognitive disruptions associated with the prefrontal cortex. *J Neurosci* (1997) **17**:2921–7.
64. Timofeeva OA, Levin ED. Glutamate and nicotinic receptor interactions in working memory: importance for the cognitive impairment of schizophrenia. *Neuroscience* (2011) **195**:21–36. doi:10.1016/j.neuroscience.2011.08.038
65. Fitzgerald PJ. The NMDA receptor may participate in widespread suppression of circuit level neural activity, in addition to a similarly prominent role in circuit level activation. *Behav Brain Res* (2012) **230**:291–8. doi:10.1016/j.bbr.2012.01.057
66. Arnsten AF, Wang MJ, Paspalas CD. Neuromodulation of thought: flexibilities and vulnerabilities in prefrontal cortical network synapses. *Neuron* (2012) **76**:223–39. doi:10.1016/j.neuron.2012.08.038
67. Stephan KE, Penny WD, Daunizeau J, Moran RJ, Friston KJ. Bayesian model selection for group studies. *Neuroimage* (2009) **46**:1004–17. doi:10.1016/j.neuroimage.2009.03.025
68. Dima D, Roiser JP, Dietrich DE, Bonnemann C, Lanfermann H, Emrich HM, et al. Understanding why patients with schizophrenia do not perceive the hollow-mask illusion using dynamic causal modelling. *Neuroimage* (2009) **46**(4):1180–6. doi:10.1016/j.neuroimage.2009.03.033
69. Dima D, Dietrich DE, Dillo W, Emrich HM. Impaired top-down processes in schizophrenia: a DCM study of ERPs. *Neuroimage* (2010) **52**(3):824–32. doi:10.1016/j.neuroimage.2009.12.086
70. Wagner G, Koch K, Schachtzabel C, Schultz CC, Gaser C, Reichenbach JR, et al. Structural basis of the fronto-thalamic dysconnectivity in schizophrenia: a combined DCM-VBM study. *Neuroimage Clin* (2013) **3**:95–105. doi:10.1016/j.nicl.2013.07.010
71. Stephan KE, Friston KJ. Analyzing effective connectivity with fMRI. *Wiley Interdiscip Rev Cogn Sci* (2010) **1**:446–59. doi:10.1002/wcs.58
72. Ogawa S, Lee TM, Kay AR, Tank DW. Brain magnetic resonance imaging with contrast dependent on blood oxygenation. *Proc Natl Acad Sci U S A* (1990) **87**:9868–72. doi:10.1073/pnas.87.24.9868
73. Cohen JD, Servan-Schreiber D. A theory of dopamine function and its role in cognitive deficits in schizophrenia. *Schizophr Bull* (1993) **19**:85–104. doi:10.1093/schbul/19.1.85
74. Braver TS, Barch DM, Cohen JD. Cognition and control in schizophrenia: a computational model of dopamine and prefrontal function. *Biol Psychiatry* (1999) **46**:312–28. doi:10.1016/S0006-3223(99)00116-X
75. Cohen JD, Servan-Schreiber D. Context, cortex, and dopamine: a connectionist approach to behavior and biology in schizophrenia. *Psychol Rev* (1992) **99**:45–77. doi:10.1037/0033-295X.99.1.45
76. Cohen JD, Braver TS, O'Reilly RC. A computational approach to prefrontal cortex, cognitive control and schizophrenia: recent developments and current challenges. *Philos Trans R Soc Lond B Biol Sci* (1996) **351**:1515–27. doi:10.1098/rstb.1996.0138
77. Smith EE, Jonides J. Storage and executive processes in the frontal lobes. *Science* (1999) **283**:1657–61. doi:10.1126/science.283.5408.1657

78. Collette F, Van der Linden M. Brain imaging of the central executive component of working memory. *Neurosci Biobehav Rev* (2002) **26**:105–25. doi:10.1016/S0149-7634(01)00063-X
79. Braver TS, Cohen JD, Nystrom LE, Jonides J, Smith EE, Noll DC. A parametric study of prefrontal cortex involvement in human working memory. *Neuroimage* (1997) **5**:49–62. doi:10.1006/nimg.1996.0247
80. Cohen JD, Braver TS, Brown JW. Computational perspectives on dopamine function in prefrontal cortex. *Curr Opin Neurobiol* (2002) **12**:223–9. doi:10.1016/S0959-4388(02)00314-8
81. Cools R, Gibbs SE, Miyakawa A, Jagust W, D'Esposito M. Working memory capacity predicts dopamine synthesis capacity in the human striatum. *J Neurosci* (2008) **28**(5):1208–12. doi:10.1523/JNEUROSCI.4475-07.2008
82. Hazy TE, Frank MJ, O'Reilly RC. Banishing the homunculus: making working memory work. *Neuroscience* (2006) **139**:105–18. doi:10.1016/j.neuroscience.2005.04.067
83. Cole MW, Schneider W. The cognitive control network: integrated cortical regions with dissociable functions. *Neuroimage* (2007) **37**:343–60. doi:10.1016/j.neuroimage.2007.03.071
84. Lenartowicz A, McIntosh AR. The role of anterior cingulate cortex in working memory is shaped by functional connectivity. *J Cogn Neurosci* (2005) **17**(7):1026–42. doi:10.1162/0898929054475127
85. Woodward TS, Cairo TA, Ruff CC, Takane Y, Hunter MA, Ngan ET. Functional connectivity reveals load dependent neural systems underlying encoding and maintenance in verbal working memory. *Neuroscience* (2006) **139**:317–25. doi:10.1016/j.neuroscience.2005.05.043
86. Gazzaley A, Nobre AC. Top-down modulation: bridging selective attention and working memory. *Trends Cogn Sci* (2012) **16**:129–35. doi:10.1016/j.tics.2011.11.014
87. Broome MR, Matthiasson P, Fusar-Poli P, Woolley JB, Johns LC, Tabraham P, et al. Neural correlates of executive function and working memory in the 'at-risk mental state'. *Br J Psychiatry* (2009) **194**:25–33. doi:10.1192/bjp.bp.107.046789
88. Liemburg EJ, Knegtering H, Klein HC, Kortekaas R, Aleman A. Antipsychotic medication and prefrontal cortex activation: a review of neuroimaging findings. *Eur Neuropsychopharmacol* (2012) **22**:387–400. doi:10.1016/j.euroneuro.2011.12.008
89. Rasetti R, Sambataro F, Chen Q, Callicott JH, Mattay VS, Weinberger DR. Altered cortical network dynamics: a potential intermediate phenotype for schizophrenia and association with ZNF804A. *Arch Gen Psychiatry* (2011) **68**:1207–17. doi:10.1001/archgenpsychiatry.2011.103
90. Barch DM, Carter CS, Braver TS, Sabb FW, MacDonald A III, Noll DC, et al. Selective deficits in prefrontal cortex function in medication-naive patients with schizophrenia. *Arch Gen Psychiatry* (2001) **58**:280–8. doi:10.1001/archpsyc.58.3.280
91. Potkin SG, Turner JA, Brown GG, McCarthy G, Greve DN, Glover GH, et al. Working memory and DLPFC inefficiency in schizophrenia: the FBIRN study. *Schizophr Bull* (2009) **35**:19–31. doi:10.1093/schbul/sbn162
92. Brown GG, Thompson WK. Functional brain imaging in schizophrenia: selected results and methods. *Curr Top Behav Neurosci* (2010) **4**:181–214. doi:10.1007/7854_2010_54
93. Manoach DS. Prefrontal cortex dysfunction during working memory performance in schizophrenia: reconciling discrepant findings. *Schizophr Res* (2003) **60**:285–98. doi:10.1016/S0920-9964(02)00294-3
94. Wager TD, Smith EE. Neuroimaging studies of working memory: a meta-analysis. *Cogn Affect Behav Neurosci* (2003) **3**:255–74. doi:10.3758/CABN.3.4.255
95. Glahn DC, Ragland JD, Abramoff A, Barrett J, Laird AR, Bearden CE, et al. Beyond hypofrontality: a quantitative meta-analysis of functional neuroimaging studies of working memory in schizophrenia. *Hum Brain Mapp* (2005) **25**(1):60–9. doi:10.1002/hbm.20138
96. van Snellenberg JX, Torres IJ, Thornton AE. Functional neuroimaging of working memory in schizophrenia: task performance as a moderating variable. *Neuropsychology* (2006) **20**(5):497–510. doi:10.1037/0894-4105.20.5.497
97. Callicott JH, Bertolino A, Mattay VS, Langheim FJ, Duyn J, Coppola R, et al. Physiological dysfunction of the dorsolateral prefrontal cortex in schizophrenia revisited. *Cereb Cortex* (2000) **10**:1078–92. doi:10.1093/cercor/10.11.1078
98. Callicott JH, Mattay VS, Verchinski BA, Marenco S, Egan MF, Weinberger DR. Complexity of prefrontal cortical dysfunction in schizophrenia: more than up or down. *Am J Psychiatry* (2003) **160**:2209–15. doi:10.1176/appi.ajp.160.12.2209
99. Thermenos HW, Goldstein JM, Buka SL, Poldrack RA, Koch JK, Tsuang MT, et al. The effect of working memory performance on functional MRI in schizophrenia. *Schizophr Res* (2005) **74**(2–3):19–94. doi:10.1016/j.schres.2004.07.021
100. Tan HY, Sust S, Buckholtz JW, Mattay VS, Meyer-Lindenberg A, Egan MF, et al. Dysfunctional prefrontal regional specialization and compensation in schizophrenia. *Am J Psychiatry* (2006) **163**(11):1969–77. doi:10.1176/appi.ajp.163.11.1969
101. Quidé Y, Morris RW, Shepherd AM, Rowland JE, Green MJ. Task-related fronto-striatal functional connectivity during working memory performance in schizophrenia. *Schiozphr Res* (2013) **150**(2–3):468–75. doi:10.1016/j.schres.2013.08.009
102. Perlstein WM, Carter CS, Noll DC, Cohen JD. Relation of prefrontal cortex dysfunction to working memory and symptoms in schizophrenia. *Am J Psychiatry* (2001) **158**(7):1105–13. doi:10.1176/appi.ajp.158.7.1105
103. Guerrero-Pedraza A, McKenna PJ, Gomar JJ, Sarró S, Salvador R, Amann B, et al. First-episode psychosis is characterized by failure of deactivation but not by hypo- or hyperfrontality. *Psychol Med* (2012) **42**(1):73–84. doi:10.1017/S0033291711001073
104. Carter CS, Perlstein W, Ganguli R, Brar J, Mintun M, Cohen JD. Functional hypofrontality and working memory dysfunction in schizophrenia. *Am J Psychiatry* (1998) **155**(9):1285–7.
105. Meyer-Lindenberg A, Poline JB, Kohn PD, Holt JL, Egan MF, Weinberger DR, et al. Evidence for abnormal cortical functional connectivity during working memory in schizophrenia. *Am J Psychiatry* (2001) **158**(11):1809–17. doi:10.1176/appi.ajp.158.11.1809
106. Meyer-Lindenberg AS, Olsen RK, Kohn PD, Brown T, Egan MF, Weinberger DR, et al. Regionally specific disturbance of dorsolateral prefrontal-hippocampal functional connectivity in schizophrenia. *Arch Gen Psychiatry* (2005) **62**(4):379–86. doi:10.1001/archpsyc.62.4.379
107. Friston KJ, Frith CD. Schizophrenia: a disconnection syndrome? *Clin Neurosci* (1995) **3**(2):89–97.
108. Huys QJ, Moutoussis M, Williams J. Are computational models of any use to psychiatry? *Neural Netw* (2011) **24**:544–51. doi:10.1016/j.neunet.2011.03.001
109. Montague PR, Dolan RJ, Friston KJ, Dayan P. Computational psychiatry. *Trends Cogn Sci* (2012) **16**:72–80. doi:10.1016/j.tics.2011.11.018
110. Lewis DA, Moghaddam B. Cognitive dysfunction in schizophrenia: convergence of gamma-aminobutyric acid and glutamate alterations. *Arch Neurol* (2006) **63**:1372–6. doi:10.1001/archneur.63.10.1372
111. Lewis DA, Gonzalez-Burgos G. Neuroplasticity of neocortical circuits in schizophrenia. *Neuropsychopharmacology* (2008) **33**:141–65. doi:10.1038/sj.npp.1301563
112. Gonzalez-Burgos G, Hashimoto T, Lewis DA. Alterations of cortical GABA neurons and network oscillations in schizophrenia. *Curr Psychiatry Rep* (2010) **12**:335–44. doi:10.1007/s11920-010-0124-8
113. Volk DW, Eggan SM, Lewis DA. Alterations in metabotropic glutamate receptor 1 alpha and regulator of G protein signaling 4 in the prefrontal cortex in schizophrenia. *Am J Psychiatry* (2010) **167**:1489–98. doi:10.1176/appi.ajp.2010.10030318
114. Schwartz TL, Sachdeva S, Stahl SM. Glutamate neurocircuitry: theoretical underpinnings in schizophrenia. *Front Pharmacol* (2012) **3**:195. doi:10.3389/fphar.2012.00195
115. Friston K. Beyond phrenology: what can neuroimaging tell us about distributed circuitry? *Annu Rev Neurosci* (2002) **25**:221–50. doi:10.1146/annurev.neuro.25.112701.142846
116. McIntosh AR. Towards a network theory of cognition. *Neural Netw* (2000) **13**:861–70. doi:10.1016/S0893-6080(00)00059-9
117. Daunizeau J, David O, Stephan KE. Dynamic causal modelling: a critical review of the biophysical and statistical foundations. *Neuroimage* (2011) **58**:312–22. doi:10.1016/j.neuroimage.2009.11.062
118. Daunizeau J, Preuschoff K, Friston KJ, Stephan KE. Optimizing experimental d esign for comparing models of brain function. *PLoS Comput Biol* (2011) **7**:e1002280. doi:10.1371/journal.pcbi.1002280
119. Stephan KE, Kasper L, Harrison LM, Daunizeau J, den Ouden HE, Breakspear M, et al. Nonlinear dynamic causal models for fMRI. *Neuroimage* (2008) **42**:649–62. doi:10.1016/j.neuroimage.2008.04.262

120. Salinas E, Sejnowski TJ. Gain modulation in the central nervous system: where behavior, neurophysiology, and computation meet. *Neuroscientist* (2001) **7**:430–40. doi:10.1177/107385840100700512
121. Volman V, Levine H, Sejnowski TJ. Shunting inhibition controls the gain modulation mediated by asynchronous neurotransmitter release in early development. *PLoS Comput Biol* (2010) **6**:e1000973. doi:10.1371/journal.pcbi.1000973
122. Stephan KE, Harrison LM, Kiebel SJ, David O, Penny WD, Friston KJ. Dynamic causal models of neural system dynamics: current state and future extensions. *J Biosci* (2007) **32**:129–44. doi:10.1007/s12038-007-0012-5
123. Tana MG, Montin E, Cerutti S, Bianchi AM. Exploring cortical attentional system by using fMRI during a continuous performance test. *Comput Intell Neurosci* (2010) **2010**:329213. doi:10.1155/2010/329213
124. Wang L, Liu X, Guise KG, Knight RT, Ghajar J, Fan J. Effective connectivity of the fronto-parietal network during attentional control. *J Cogn Neurosci* (2010) **22**:543–53. doi:10.1162/jocn.2009.21210
125. Brazdil M, Mikl M, Marecek R, Krupa P, Rektor I. Effective connectivity in target stimulus processing: a dynamic causal modeling study of visual oddball task. *Neuroimage* (2007) **35**:827–35. doi:10.1016/j.neuroimage.2006.12.020
126. Tan HY, Chen AG, Kolachana B, Apud JA, Mattay VS, Callicott JH, et al. Effective connectivity of AKT1-mediated dopaminergic working memory networks and pharmacogenetics of anti-dopaminergic treatment. *Brain* (2012) **135**:1436–45. doi:10.1093/brain/aws068
127. Crossley NA, Mechelli A, Fusar-Poli P, Broome MR, Matthiasson P, Johns LC, et al. Superior temporal lobe dysfunction and frontotemporal dysconnectivity in subjects at risk of psychosis and in first-episode psychosis. *Hum Brain Mapp* (2009) **30**:4129–37. doi:10.1002/hbm.20834
128. Deserno L, Sterzer P, Wustenberg T, Heinz A, Schlagenhauf F. Reduced prefrontal-parietal effective connectivity and working memory deficits in schizophrenia. *J Neurosci* (2012) **32**:12–20. doi:10.1523/JNEUROSCI.3405-11.2012
129. Schmidt A, Smieskova R, Aston J, Simon A, Allen P, Fusar-Poli P, et al. Brain connectivity abnormalities predating the onset of psychosis: correlation with the effect of medication. *JAMA Psychiatry* (2013) **70**(9):903–12. doi:10.1001/jamapsychiatry.2013.117
130. Zhang H, Wei X, Tao H, Mwansisya TE, Pu W, He Z, et al. Opposite effective connectivity in the posterior cingulate and medial prefrontal cortex between first-episode schizophrenic patients with suicide risk and healthy controls. *PLoS One* (2013) **8**:e63477. doi:10.1371/journal.pone.0063477
131. Dayan P, Abbot LF. *Theoretical Neuroscience: Computational and Mathematical Modeling of Neural Systems.* Cambridge, MA: The MIT Press (2000).
132. Li B, Daunizeau J, Stephan KE, Penny W, Hu D, Friston K. Generalised filtering and stochastic DCM for fMRI. *Neuroimage* (2011) **58**:442–57. doi:10.1016/j.neuroimage.2011.01.085
133. Allen P, Mechelli A, Stephan KE, Day F, Dalton J, Williams S, et al. Fronto-temporal interactions during overt verbal initiation and suppression. *J Cogn Neurosci* (2008) **20**:1656–69. doi:10.1162/jocn.2008.20107
134. Allen P, Stephan KE, Mechelli A, Day F, Ward N, Dalton J, et al. Cingulate activity and fronto-temporal connectivity in people with prodromal signs of psychosis. *Neuroimage* (2010) **49**:947–55. doi:10.1016/j.neuroimage.2009.08.038
135. Dauvermann MR, Whalley HC, Romaniuk L, Valton V, Owens DG, Johnstone EC, et al. The application of nonlinear dynamic causal modelling for fMRI in subjects at high genetic risk of schizophrenia. *Neuroimage* (2013) **73**:16–29. doi:10.1016/j.neuroimage.2013.01.063
136. Whalley HC, Simonotto E, Flett S, Marshall I, Ebmeier KP, Owens DG, et al. FMRI correlates of state and trait effects in subjects at genetically enhanced risk of schizophrenia. *Brain* (2004) **127**:478–90. doi:10.1093/brain/awh070
137. Whalley HC, Simonotto E, Marshall I, Owens DG, Goddard NH, Johnstone EC, et al. Functional disconnectivity in subjects at high genetic risk of schizophrenia. *Brain* (2005) **128**:2097–108. doi:10.1093/brain/awh556
138. Friston KJ, Shiner T, FitzGerald T, Galea JM, Adams R, Brown H, et al. Dopamine, affordance and active inference. *PLoS Comput Biol* (2012) **8**(1):e1002327. doi:10.1371/journal.pcbi.1002327
139. Brodersen KJ, Deserno L, Schlagenhauf F, Lin Z, Penny WD, Buhmann JM, et al. Dissecting psychiatric spectrum disorders. *Neuroimage Clin* (2013) **4**:98–111. doi:10.1016/j.nicl.2013.11.002
140. Durstewitz D, Seamans JK. The computational role of dopamine D1 receptors in working memory. *Neural Netw* (2002) **15**(4–6):561–72. doi:10.1016/S0893-6080(02)00049-7
141. Murray JD, Anticevic A, Gancsos M, Ichinose M, Corlett PR, Krystal JH, et al. Linking microcircuit dysfunction to cognitive impairment: effects of disinhibition associated with schizophrenia in a cortical working memory model. *Cereb Cortex* (2012) **24**(4):859–72. doi:10.1093/cercor/bhs370
142. D'Ardenne K, Eshel N, Luka J, Lenartowicz A, Nystrom LE, Cohen JD. Role of prefrontal cortex and the midbrain dopamine system in working memory updating. *Proc Natl Acad Sci U S A* (2012) **109**:19900–9. doi:10.1073/pnas.1116727109
143. den Ouden HE, Friston KJ, Daw ND, McIntosh AR, Stephan KE. A dual role for prediction error in associative learning. *Cereb Cortex* (2009) **19**(5):1175–85. doi:10.1093/cercor/bhn161
144. den Ouden HE, Daunizeau J, Roiser J, Friston KJ, Stephan KE. Striatal prediction error modulates cortical coupling. *J Neurosci* (2010) **30**(9):3210–9. doi:10.1523/JNEUROSCI.4458-09.2010
145. Brodersen KH, Schofield TM, Leff AP, Ong CS, Lomakina EI, Buhmann JM, et al. Generative embedding for model-based classification of fMRI data. *PLoS Comput Biol* (2011) **7**(6):e1002079. doi:10.1371/journal.pcbi.1002079
146. Stephan KE, Penny WD, Moran RJ, den Ouden HE, Daunizeau J, Friston KJ. Ten simple rules for dynamic causal modeling. *Neuroimage* (2010) **49**(4):3099–109. doi:10.1016/j.neuroimage.2009.11.015
147. Penny WD, Stephan KE, Mechelli A, Friston KJ. Comparing dynamic causal models. *Neuroimage* (2004) **22**(3):1157–72. doi:10.1016/j.neuroimage.2004.03.026
148. Penny WD, Stephan KE, Daunizeau J, Rosa MJ, Friston KJ, Schofield TM, et al. Comparing families of dynamic causal models. *PLoS Comput Biol* (2010) **6**(3):e1000709. doi:10.1371/journal.pcbi.1000709
149. Lisman JE, Coyle JT, Green RW, Javitt DC, Benes FM, Heckers S, et al. Circuit-based framework for understanding neurotransmitter and risk gene interactions in schizophrenia. *Trends Neurosci* (2008) **31**:234–42. doi:10.1016/j.tins.2008.02.005

Conflict of Interest Statement: Maria R. Dauvermann, Neil Roberts, Stephen M. Lawrie, and Thomas W. J. Moorhead have received financial support from Pfizer (formerly Wyeth) in relation to imaging studies of people with schizophrenia. Stephen M. Lawrie has done consultancy work for Roche Pharmaceuticals in connection with a possible new treatment for schizophrenia. Stephen M. Lawrie has also received honoraria for lectures, chairing meetings, and consultancy work from Janssen in connection with brain imaging and therapeutic initiatives for psychosis.

Received: 04 September 2013; accepted: 10 March 2014; published online: 25 March 2014.

*Citation: Dauvermann MR, Whalley HC, Schmidt A, Lee GL, Romaniuk L, Roberts N, Johnstone EC, Lawrie SM and Moorhead TWJ (2014) Computational neuropsychiatry – schizophrenia as a cognitive brain network disorder. Front. Psychiatry **5**:30. doi: 10.3389/fpsyt.2014.00030*

This article was submitted to Schizophrenia, a section of the journal Frontiers in Psychiatry.

APPENDIX

DYNAMIC CAUSAL MODELING

Dynamic causal modeling is general framework for model-based assessment of competing theories about neuronal circuits (18, 146). In particular, DCM is a generic Bayesian system identification technique, which allows for inference on "hidden" neurophysiological mechanisms that generated observed measures, such as blood-oxygen-level-dependent signal in functional magnetic resonance imaging (fMRI) or evoked responses measured with electroencephalography (EEG). The principle idea thereby is to formulate a simplified model of neuronal population responses (z) and combine this with a modality-specific forward model (λ) such that one can predict the measurement (y) that would arise from any particular neuronal circuit (18).

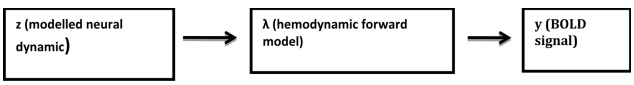

In DCM for fMRI, the dynamics of the neural states underlying regional BOLD response are modeled by a bilinear differential equation that describes how the neural states (x) change over time (t) as a function of endogenous inter-regional connections (matrix A), modulatory effects on these connections (matrix B), and direct (driving) inputs (matrix C) (Eq. A1) (18, 122). The endogenous connections represent coupling strengths in the absence of input u_j to the system, whereas the modulatory effects represent task-specific alterations in this connectivity.

$$f(x,u) = \frac{dx}{xt} = \left(A + \sum_{i=1}^{m} uB^{(j)}\right) x + Cu \qquad \text{(A1)}$$

The bilinear state equation has subsequently been extended by a non-linear term, where the modulation of connection strengths by experimental inputs is supplemented by direct modulation with neural activity in one or more regions (119). In other words, non-linear DCMs allow addressing how the connection between two neuronal units is gated by activity in other units. This is of particular interest as gating processes represent a key mechanism for many neurobiological processes and thus increasing the biological realism of non-linear compared to bilinear DCMs. To this end, compared with the bilinear state equation, the new term in the non-linear equations are the D matrices (Eq. A2), which encode how the n regions gate connections in the system.

$$f(x,u) = \frac{dx}{dt} = \left(A + \sum_{i=1}^{m} uB^{(j)} + \sum_{j=1}^{n} x_j D^{(j)}\right) x + Cu \qquad \text{(A2)}$$

BAYESIAN MODEL SELECTION AND BAYESIAN MODEL AVERAGING

Bayesian model selection is an essential procedure of DCM studies as it can be used to test competing hypotheses (different DCMs) about the neural mechanisms generating the data. BMS rests on comparing the evidence of a predefined set of models (the model space). The model evidence is the probability of observing the empirical data, given a model, and represents a principled measure of model quality, derived from probability theory (147, 148). Concretely, it represents the mean predicted data under random sampling from the model's priors or, alternatively, a principled measure of the balance between model fit and model complexity. A random-effects BMS approach has been suggested for group studies, which is capable of quantifying the degree of heterogeneity in a population while being extremely robust to potential outliers (20, 67). The probability that one model is more likely than any other model, given the group data, can be expressed by the exceedance probability (φ_k) of each model:

$$\exists k \in \{1 \ldots k\}, \forall j \in \{1 \ldots k | j \neq k\}:$$
$$\varphi_k = p(r_k > r_j | y; a)$$

After inference on the most likely network architecture underlying a specific neural process, one can compare the parameter estimates of the most likely model obtained from BMS (winning model) for between-group inferences. However, statistical comparison of model parameter estimates across groups is only valid if those estimates stem from the same model. Given that different models may be found to be optimal across groups, Bayesian model averaging (BMA) has been recommended as standard approach for clinical DCM studies (146). BMA averages posterior parameter estimates over models, weighted by the posterior model probabilities (148). Thus, models with a low posterior probability contribute little to the estimation of the marginal posterior. In brief, BMS and BMA are central components of DCM studies to infer on neural mechanisms at the neural system level and on specific model parameters across groups, respectively (146).

In non-linear DCM analysis, the connection strengths between selected nodes are assessed for activity-dependent modulation of the reciprocal neuronal projections by the introduction of gating mechanisms. Non-linear DCM is applied to the models identified as winning models from the application of bilinear state equation. The bilinear model and the non-linear models differ only in the introduction of gating mechanisms such as a parametric response in the tested functional task. Such gating mechanisms are applied to nodal connections, which are expected to explain the variation in subject response to the functional task. The appropriate placement of the gating input is assessed through the application of model space partitioning and family inference. The exceedance probabilities of the models are compared and the non-linear models, which provide higher exceedance probabilities than the bilinear models are identified as winning models.

NeuroImage 73 (2013) 16–29

Contents lists available at SciVerse ScienceDirect

NeuroImage

journal homepage: www.elsevier.com/locate/ynimg

The application of nonlinear Dynamic Causal Modelling for fMRI in subjects at high genetic risk of schizophrenia

Maria R. Dauvermann [a,*], Heather C. Whalley [a], Liana Romaniuk [a], Vincent Valton [b], David G.C. Owens [a], Eve C. Johnstone [a], Stephen M. Lawrie [a], Thomas W.J. Moorhead [a]

[a] Division of Psychiatry, Royal Edinburgh Hospital, University of Edinburgh, UK
[b] Institute for Adaptive and Neural Computation (IANC), Department of Informatics, University of Edinburgh, UK

ARTICLE INFO

Article history:
Accepted 22 January 2013
Available online 4 February 2013

Keywords:
Nonlinear Dynamic Causal Modelling for fMRI
Connection strength with nonlinear modulation
Synaptic plasticity
Mediodorsal thalamus
High genetic risk of schizophrenia

ABSTRACT

Nonlinear Dynamic Causal Modelling (DCM) for fMRI provides computational modelling of gating mechanisms at the neuronal population level. It allows for estimations of connection strengths with nonlinear modulation within task-dependent networks.

This paper presents an application of nonlinear DCM in subjects at high familial risk of schizophrenia performing the Hayling Sentence Completion Task (HSCT). We analysed scans of 19 healthy controls and 46 subjects at high familial risk of schizophrenia, which included 26 high risk subjects without psychotic symptoms and 20 subjects with psychotic symptoms. The activity-dependent network consists of the intra parietal cortex (IPS), inferior frontal gyrus (IFG), middle temporal gyrus (MTG), anterior cingulate cortex (ACC) and the mediodorsal (MD) thalamus. The connections between the MD thalamus and the IFG were gated by the MD thalamus. We used DCM to investigate altered connection strength of these connections. Bayesian Model Selection (BMS) at the group and family level was used to compare the optimal bilinear and nonlinear models. Bayesian Model Averaging (BMA) was used to assess the connection strengths with the gating from the MD thalamus and the IFG.

The nonlinear models provided the better explanation of the data. Furthermore, the BMA analysis showed significantly lower connection strength of the thalamocortical connection with nonlinear modulation from the MD thalamus in high risk subjects with psychotic symptoms and those who subsequently developed schizophrenia.

These findings demonstrate that nonlinear DCM provides a method to investigate altered connectivity at the level of neural circuits. The reduced connection strength with thalamic gating may be a neurobiomarker implicated in the development of psychotic symptoms. This study suggests that nonlinear DCM could lead to new insights into functional and effective dysconnection at the network level in subjects at high familial risk.

Introduction

Dynamic Causal Modelling is an established method for the computation of synaptic plasticity from fMRI data (Stephan et al., 2006, 2009a). Bilinear DCM provides for the inference of causal mechanisms, which at the regional neuronal level give estimations of how the rate of change of neuronal activity in one region influences neuronal activity in other regions (Friston, 2009; Friston et al., 2003; Stephan et al., 2008). Nonlinear DCM is an extension of bilinear DCM, which assesses inhibitions of a neuronal connection and provides a means to model nonlinearities in fMRI data (Stephan et al., 2008). It is assumed that these nonlinear effects originate from activity-dependent synaptic plasticity processes (Abbott et al., 1997; Rothman et al., 2009; Salinas and Sejnowski, 2001; Shu et al., 2003). Furthermore, it has been suggested that altered gain control (i.e. nonlinear modulation of neuronal connections) of the thalamocortical connection could be the underlying factor for altered synaptic plasticity and cortical dysconnectivity in schizophrenia (Andreasen et al., 1997; Negyessy and Goldman-Rakic, 2005).

We know from neurophysiological studies that nonlinear mechanisms are integral to short-term synaptic plasticity. Nonlinear modulation has been shown to regulate synaptic plasticity modulated by neurotransmitters (Berends et al., 2005; Neher and Sakaba, 2008; Pan and Zucker, 2009; Sun and Beierlein, 2011). Also thalamocortical

Abbreviations: ACC, Anterior cingulate cortex; BMA, Bayesian Model Averaging; BMS, Bayesian Model Selection; DCM, Dynamic Causal Modelling; EHRS, Edinburgh High Risk Study; IFG, Inferior frontal gyrus; IPS, Intra parietal sulcus; HR+, High risk subjects with psychotic symptoms; HR−, High risk subjects without psychotic symptoms; HRall, All high risk subjects (high risk subjects with psychotic symptoms and without psychotic symptoms); HSCT, Hayling Sentence Completion Task; MD thalamus, Mediodorsal thalamus; mGluR, Metabotropic glutamate receptors; MTG, Middle temporal gyrus; NART, National Adult Reading Test; NMDA, N-methyl-D-aspartate; PSE, Present State Examination; Xp, Exceedance probability.

* Corresponding author at: Division of Psychiatry, University of Edinburgh, Kennedy Tower, Royal Edinburgh Hospital, Edinburgh, EH10 5HF, UK. Fax: +44 1315376691.
E-mail address: M.R.Dauvermann@sms.ed.ac.uk (M.R. Dauvermann).

1053-8119/$ – see front matter © 2013 Elsevier Inc. All rights reserved.
http://dx.doi.org/10.1016/j.neuroimage.2013.01.063

synapses underlie nonlinear dynamic modulation which indicates gating of these connections (Alelú-Paz and Giménez-Amaya, 2008; Chance et al., 2002; Deng and Klyachko, 2011; Destexhe, 2009; Kolluri et al., 2005; Negyessy and Goldman-Rakic, 2005). Thus, we have indications that nonlinear DCM is a means of modelling nonlinear mechanisms of short-term modulatory processes between neuronal groups.

The 'Disconnection Hypothesis' of schizophrenia proposes that altered modulation of synaptic efficacy may lead to a disruption of learning processes, which underlie cognitive deficits in schizophrenia (Friston, 1999). FMRI studies analysing verbal fluency tasks using a variety of connectivity techniques consistently report cortical dysconnection in the established illness (Alelú-Paz and Giménez-Amaya, 2008; Boksman et al., 2005; Curtis et al., 1998; Fu et al., 2002; Lawrie et al., 2002), which support the 'Disconnection Hypothesis'. Also, deficits in cortical connectivity have been reported in the prodromal stage of the illness, suggesting possible trait-related neurobiological markers of the disorder (Fusar-Poli et al., 2011; Lencz et al., 2006; Simon et al., 2007). It has been proposed that cortical dysfunction in verbal fluency tasks could be mediated by thalamic disruption (Fusar-Poli et al., 2011) and/or alterations of the thalamocortical neuronal projection (Byne et al., 2009; Lewis and Lieberman, 2000; Pakkenberg et al., 2009; Sodhi et al., 2011; Watis et al., 2008). We are however unaware of any fMRI studies of effective connectivity addressing thalamic dysconnectivity in unaffected individuals at high familial risk.

Previous fMRI findings using the Hayling Sentence Completion Task (HSCT), a test considered to be an extension of verbal fluency paradigms, demonstrated significantly reduced activation of the mediodorsal (MD) thalamus in the Edinburgh High Risk Study (EHRS) (Whalley et al., 2004). In this study, subjects at high familial risk of schizophrenia are compared to healthy controls (Johnstone et al., 2003). This finding of reduced activation in the high risk (HR) subjects was further supported by reduced functional connectivity measures between the inferior frontal gyrus (IFG) and the MD thalamus only in the HR group (Whalley et al., 2005). A recent study of functional connectivity in the EHRS cohort suggested that the reduced functional connectivity between the IFG and the MD thalamus, which was associated with increased PFC folding, was predictive of subsequent schizophrenia and may be a trait characteristic of vulnerability of the illness (Dauvermann et al., 2012; Harris et al., 2007).

We use nonlinear DCM to investigate the causal factors of reduced thalamocortical connectivity for the HR subjects in the EHRS data. To ensure that we followed a structured approach, we developed a heuristic search protocol for the application of nonlinear DCM. In this protocol we test the fitness of both bilinear and nonlinear models and consider how these models perform across the clinical groupings in the EHRS study. We analyse the connection strengths with nonlinear modulation of the thalamocortical connectivity in the healthy controls subjects, the HR subjects who remained well and the HR subjects who subsequently developed schizophrenia. We consider whether reduced thalamocortical connection strength with nonlinear modulation may be a neurobiomarker implicated in the development of psychotic symptoms.

Material and methods

Subjects

The EHRS examined young healthy adults at enhanced genetic risk of schizophrenia over the period at which they were at greatest risk of becoming ill. The subjects recruited for the EHRS were aged between 16 and 25 and had at least two first or second degree relatives with schizophrenia (Hodges et al., 1999; Johnstone et al., 2000). The control group had no family history of the illness or a serious mental disorder. All subjects were well at time of scanning and were antipsychotic naïve throughout the study. The study was approved by the Psychiatry and Clinical Psychology subcommittee of the Lothian research ethics committee.

Functional imaging of the HSCT was added to the EHRS study in 1999 and full details of the sample and the respective functional localisation results for the HSCT have been presented previously (Whalley et al., 2004).

On detailed interview (the Present State Examination, PSE; Wing et al., 1974) at the time of the scans none of the subjects met diagnostic criteria for any psychotic disorder. Twenty six high risk subjects reported isolated transient or partial psychotic symptoms (all subclinical) at the time of the functional scan (referred to as HR+), the other subjects of the high risk group reported no psychotic symptoms (referred to as HR−). HR+ and HR− are referred to as HRall. In addition to the PSE, the PANSS interview was administered at the time of the functional scan. The rescaled PANSS scoring system was used (Kay et al., 1987). Four HR subjects subsequently developed schizophrenia (referred to as four ill subjects) (Whalley et al., 2004).

Functional experimental details

Experimental details of the HSCT have been presented previously (Whalley et al., 2004, 2005). Briefly, subjects were shown sentences with the last word missing and were asked to think of an appropriate word to complete the sentence (without speaking the word), and press a button when they had done so. Our experimental design was a block design alternating rest conditions with task conditions, where the task conditions had four levels of difficulty, which characterised the differences in activation over parametric manipulations of task difficulty in sentence completion blocks. Immediately after scanning, subjects were presented with the same sequence of sentences on paper and requested to complete each sentence with the word they first thought of in the scanner. 'Word appropriateness' scores were determined from the word frequency list of sentence completion norms (Bloom and Fischler, 1980).

Functional scanning procedure

Functional imaging was carried out at the Brain Imaging Research Centre for Scotland (Edinburgh, Scotland, UK) on a GE 1.5 T Signa scanner (GE Medical, Milwaukee, USA). Functional data was acquired using an EPI sequence. The HSCT was acquired using the following parameters: axial orientation TR/TE = 4000/40 ms; matrix 64×128; FOV 22×44 cm^2; 38 slices; 5 mm slice thickness; no gap. A total of 204 volumes were acquired. Visual stimuli were presented using a screen (IFIS, MRI Devices, Waukesha, WI, USA) placed in the bore of the magnet; corrective lenses were used where necessary.

FMRI data analysis

Data processing and statistical analyses for the current analysis were performed with the Statistical Parametric Mapping SPM8 software package (Wellcome Trust Centre for Neuroimaging; http://www.fil.ion.ucl.ac.uk/spm/). All functional volumes were spatially realigned, unwarped, normalized to MNI space and spatially smoothed with an isotropic 8 mm full-width at half-maximum Gaussian kernel to compensate for residual variability in functional anatomy after spatial normalization and to facilitate application of Gaussian random field theory for adjusted statistical inference. The voxel size generated from the above acquisition parameters was oversampled to $1 \times 1 \times 1$ mm^3.

We applied established SPM first and second-level analyses employing the settings used in our previous analyses (Whalley et al., 2004). From this second-level analysis we generated statistical parametric maps of the *T* statistic and *F* statistic at each voxel SPM {*t*} and SPM {*F*}, which characterised differences in activation for the parametric modulation.

Subject and ROI selection

DCM has stringent requirements for the subject and region selection. In addition to the selection of the fMRI scans (Whalley et al., 2004), the condition of activation in each ROI must be met.

The second-level analysis in the initial sample of 21 healthy controls and 69 HR subjects identified robust left-lateralized activations in the inferior parietal sulcus (IPS), inferior frontal gyrus (IFG), middle temporal gyrus (MTG), anterior cingulate cortex (ACC) and the MD thalamus as previously reported (Whalley et al., 2004). ROIs located in all five regions were selected for the DCM analyses. The selection of the IPS, IFG, MTG and the ACC ROIs is consistent with other functional imaging studies of the HSCT (studies in healthy controls: Allen et al., 2008; Collette et al., 2001; Frith et al., 1991, 1995; Nathaniel-James and Frith, 2002; Nathaniel-James et al., 1997; studies in HR subjects of schizophrenia and healthy controls: Allen et al., 2010). Our previous reports demonstrated deficits in functional connectivity between the MD thalamus and the IFG in HR subjects when they were compared to healthy controls (Dauvermann et al., 2012; Whalley et al., 2005). Thus we included the MD thalamus in the network used for our DCM study. Also it has been established that altered synaptic plasticity of the connection from the MD thalamus to the PFC may underlie cortical dysfunction in schizophrenia (Negyessy and Goldman-Rakic, 2005).

The ROIs for DCM were defined by extracting the eigenvectors (i.e. time series) from each subject's individual activation map thresholded at $p<0.05$ uncorrected at the closest maxima within a distance of 8 mm of the group peak voxel (for the IPS, IFG and MTG) and within 6 mm of the group peak voxel respectively (for the ACC and MD thalamus). This rationale ensured that the functional regions included in the DCM models were consistent across subjects (Stephan et al., 2007). In cases where the subject did not show activation in all five ROIs that satisfied the criteria, data from these subjects were excluded (2 healthy controls and 23 HR subjects). The final subject selection included 19 healthy controls and 46 high risk subjects. This selection included the four subjects who subsequently developed schizophrenia. Demographic details are presented in Table 1.

Contrast images of parameter estimates encoding condition-specific effects were created for each subject and entered separately into voxel-wise one-sample t-tests, to implement a second-level random effects analysis. We report regions that survive cluster-level correction for multiple comparisons across the whole brain at $p<0.05$. The ROI locations detailed in Table 2 are given in accordance with the standard Talairach and Tournoux atlas (Talairach and Tournoux, 1988).

DCM analyses

It has been assumed that the thalamocortical projections can be gated by neuronal regions in the MD thalamus or the IFG in schizophrenia (Andreasen et al., 1997; Negyessy and Goldman-Rakic, 2005). Thus, we adopted an approach that would allow us to model nonlinear biological responses expected for the HCST by the means of nonlinear DCMs.

Application of DCM to the EHRS data

In order to follow the established DCM methods for determining whether bilinear or nonlinear modelling would be the most appropriate and would hold for the experimental groupings that had been previously employed in our analyses of the EHRS data, we developed a heuristic search protocol to optimise the DCM architecture and evaluate group differences. Specifically, there are three phases in this DCM protocol: (i) In phase 1, bilinear DCM was used in order to test the structure for the HSCT across all subjects; (ii) in phase 2, nonlinear DCM was applied to model the nonlinear mechanisms and (iii) in phase 3, connection strengths with nonlinear modulation within the winning models were assessed. A flow diagram for our DCM protocol is given in Fig. 1.

In order to ensure that the DCM based analyses were consistent across the contrast groupings we ran the phased protocol on three separate groupings of the EHRS data. In the first grouping, the DCM analyses were applied to healthy controls (n = 19) and HRall subjects (n = 46). In the second grouping, the DCM analyses were applied to healthy controls (n = 19), HR− (n = 26) and HR+ (n = 20). In the third grouping, the DCM analyses were applied to healthy controls (n = 19), HR− (n = 25), HR+ (n = 17) and the four ill HR subjects (n = 4) who subsequently developed schizophrenia.

Overview of phased approach as laid out in Fig. 1.

1) In phase 1, bilinear DCM was used in order to select the structure for the HSCT network across all subjects. This analysis contained modulations for the activity-dependent neuronal interactions between the five regions. The analysis steps are depicted in the protocol (column 1; Fig. 1). The optimal model of this analysis was entered into phase 2.
2) In phase 2, nonlinear DCM was applied to model the connection strengths with activity-dependent modulation of the reciprocal neuronal projection between the MD thalamus and the IFG. In order to ensure the modelling of the gating (i.e. nonlinear models), two preconditions were met:
   (i) The specification of the nonlinear models was based on the optimal bilinear model. Therefore, the bilinear model and the nonlinear models differed only in the single parameter of nonlinearity from each other.
   (ii) The implementation of Model Space Partitioning and Family Inference was applied to compare between the bilinear and nonlinear models which ensured the advantage of the nonlinear models over the bilinear model.

Table 2
Coordinates of the five ROIs.

	Coordinates in Talairach space
IPS BA40	−42, −48, 48
IFG BA47	−50, 18, −4
MTG BA21	−50, −37, −5
ACC BA32	0, 22, 34
MD Thal	−8, −13, 6

ACC, anterior cingulate cortex; IFG, inferior frontal gyrus; IPS, intra parietal sulcus; MD Thal, mediodorsal thalamus; MTG, middle temporal gyrus.

Table 1
Demographic details.

	Healthy controls	HR−	HR+	Four ill	Test	*p*-Value
Number	19	26	20	4	–	–
Mean age (SD)	26.9 (3.5)	25.8 (3.2)	26.1 (3.1)	22.8 (4.50)	$F=.518$[a]	.598
Gender (M:F)	12:7	12:14	9:11	3:1	$x^2=2.56$[b]	.345
Mean NART IQ (SD)	99.94 (9.50)	96.74 (8.90)	98.58 (10.00)	97.95 (16.33)	$F=1.175$	.211
Handedness (R:L)	16:3	23:3	18:2	4:0	$x^2=4.36$[c]	.099
PSE score[d] (0/1:2:3)	19:0:0	26:0:0	0:16:4	0:0:4	–	–

HR−, high risk subjects without psychotic symptoms; HR+, high risk subjects with psychotic symptoms, four ill subjects, four HR subjects who became subsequently ill; NART, National Adult Reading Test; IQ, intelligence quotient; ANOVA, analysis of variance; PANSS, Positive and Negative Syndrome Scale; PSE, Present State Examination; SD, Standard Deviation.

[a] ANOVA.
[b] Pearsons chi-square.
[c] Kruskal–Wallis test.
[d] Simplified PSE scoring system, see text. No subject received a score of 4 at the baseline interview.

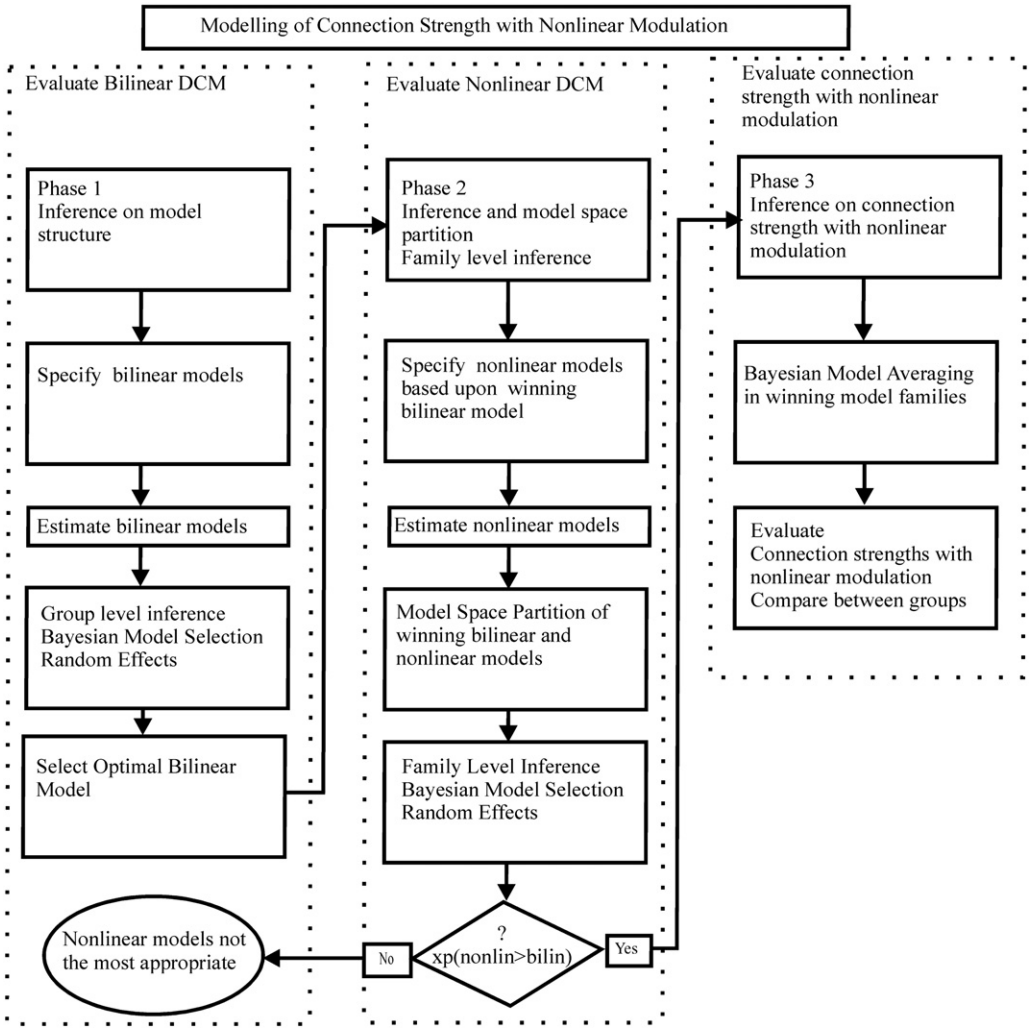

Fig. 1. Protocol for the Application of Nonlinear DCM. This protocol is subdivided into three phases which allow the modelling of connection strength with nonlinear modulation. The protocol was run for each grouping: (i) Healthy controls and all high risk subjects, (ii) healthy controls, high risk subjects without psychotic symptoms and high risk subjects with psychotic symptoms, (iii) healthy controls, high risk subjects without psychotic symptoms, high risk subjects with psychotic symptoms and four ill subjects who subsequently developed schizophrenia.

The analysis steps are depicted in the protocol (column 2, Fig. 1). The winning models of this analysis entered the third phase.

3) In phase 3, the connection strengths with the gating of the nonlinear models within the winning model family were assessed using the posterior densities over connection strengths as assessed with Bayesian Model Averaging (BMA). This step allowed inference of the connection strengths with nonlinear modulation of the bidirectional thalamocortical projection. The analysis steps are depicted in the protocol (column 3, Fig. 1).

The theoretical implementations of bilinear DCM (Friston et al., 2003), nonlinear DCM (Stephan et al., 2008) and Family Level Inference (e.g. Model Space Partitioning, Bayesian Model Selection (BMS) at the model family level and BMA; Penny et al., 2010) have been reported previously. The application of bilinear DCM, Model Space Partitioning, Family Inference and BMA has been shown to produce reliable results (Seghier et al., 2011).

Theoretically, the inference computations (i.e. Inference on Nonlinear DCM, Inference Level on Family Level with BMS on the family level allow to test an infinite number of models (Penny et al., 2010)). However, we considered a limited but plausible model space that comprised of eight bilinear models and four nonlinear variants of the winning bilinear model.

Phase 1 — detailed description — bilinear DCM

Theoretical background. DCM is a tool for assessing inter-regional effective connectivity by its experimentally induced changes (Friston et al., 2003). DCM allows one to infer neuronal function mechanistically by the means of estimation of how the neural activity changes the neural activity in another region. The ensuing responses are then entered into a biophysical model of haemodynamic responses at each region or voxel (Friston, 2009; Friston et al., 2003). Hidden neural dynamics are described by coupled differential equations and linked to predicted BOLD responses. The bilinear neuronal state equation (Eq. (1)) describes the timing and the place of the onset of the inputs as well as the modulation of the neuronal states and endogenous connectivity changes, given m known inputs (Friston et al., 2003; Stephan et al., 2007):

$$f(x,u) = f(0,0) + \frac{\partial f}{\partial x}x + \frac{\partial f}{\partial u}u + \frac{\partial^2 f}{\partial x \partial u}xu : \\ f(x,u) = \frac{dx}{dt} = \left(A + \sum_{i=1}^{m} uB^{(i)}\right)x + Cu \quad (1)$$

x	neuronal state
m	number of inputs
u_i	ith input
A	matrix A
B	matrix B
C	matrix C

The neuronal states, which represent the neuronal population activity of the modelled brain regions, change accordingly to the system's connectivity and experimentally controlled inputs. In this equation, matrix A represents the endogenous strength with the connections in the absence of experimental manipulations; matrix B denotes the modulation of those connections by the experimental manipulation (here, the measured changes in effective connectivity induced by the four difficulty levels of the HSCT); matrix C reflects driving inputs, which represent extrinsic parameters that change the neuronal state of brain regions within the model (here, visual presentation of the sentences with the last word missing). The bilinear effects were driven by box car stimulus functions encoding task difficulty, whereas the driving inputs were driven by box car stimulus functions encoding the main effect of task.

Model space of bilinear models. We derived our biophysical DCMs from neurobiological and neurocellular studies. Evidence for the bidirectional connections between the MD thalamus and IFG (matrix A) was based on (Abitz et al., 2007; Kolluri et al., 2005; Lewis and Lieberman, 2000; Onn and Wang, 2005), and for the bidirectional connections between the MD thalamus and the ACC (matrix A) we considered findings from (Lee et al., 2007; Lewis and Lieberman, 2000; Onn and Wang, 2005; Welsh et al., 2010). For modelling the experimental manipulations, well established PET studies and fMRI in healthy subjects performing the HSCT were used (Collette et al., 2001; Frith et al., 1991, 1995; Nathaniel-James and Frith, 2002; Nathaniel-James et al., 1997) as well as functional connectivity results in HR subjects of schizophrenia (Whalley et al., 2005). Specifically, two previous DCM studies on the task in healthy subjects (Allen et al., 2008) and HR subjects of schizophrenia (Allen et al., 2010) enabled the modelling of the matrices B and C.

For each subject, eight bilinear DCMs were modelled. Firstly, the models differed in their unidirectional and bidirectional connections between the five regions (matrix A). Specifically, the eight models are subdivided into two groups: (i) Endogenous connection from the IPS to the IFG (Models 1–4; Figs. 2(a–d)) and (ii) endogenous connection from the IPS to the MTG (Models 5–8; Figs. 2(e–h)). This subdivision was based on findings, which suggest that either neuronal connections between the IPS and the IFG or between the IPS and the MTG can underlie the processing of verbal fluency (Allen et al., 2008, 2010). Secondly, the models are specified in terms of the bilinear effect of the parametric (difficulty) of the task. Thirdly, the processing of visual stimuli was modelled by the driving input that corresponded to the main effect of task (relative to rest).

Random-effects Bayesian Model Selection. The aim of this step within phase 1 was to identify the most likely model to explain the fMRI data using the random-effects BMS process as implemented in SPM8. We estimated the model evidence with the negative free energy (Stephan et al., 2009b). This measure takes into account not only the relative fit of competing models but also their relative complexity (cf. number of free parameters) (Stephan et al., 2009b). After the estimation of the model evidence, we computed the model evidence at the group level (Penny et al., 2004) by applying a hierarchical Bayesian approach (Stephan et al., 2009b) in order to correct for outliers. The application of the posterior exceedance probability estimates the criterion for the conditional likelihood of the model given the data at random (Stephan et al., 2009b). In Eq. (2), the exceedance probability (φ_k) is the likelihood that model k is more likely than any other model (of the K models tested), given the group data.

$$\exists k \in \{1 \ldots k\}, \forall j \in \{1 \ldots k | j \neq k\} : \varphi_k = p\left(r_k > r_j \middle| y; a\right)$$

$$\varphi_k = \text{exceedance probabilities (sum to one over all models tested)} \tag{2}$$

Phase 2 — detailed description — nonlinear DCM

Theoretical background. The advantage of bilinear DCM lies in the possibility of inferring the dynamics of biophysical processes at the neuronal level that translates neuronal activity of regions into predicted BOLD measurements (Stephan et al., 2008).

Nonlinear DCM represents a straightforward extension of bilinear DCM, where the modulation of connection strengths by experimental inputs is supplemented by direct modulation with neural activity in one or more regions (Friston et al., 2003; Stephan et al., 2008). This corresponds to an activity-dependent modulation of synaptic efficacy, which models the short-term plasticity we are interested in.

The well-established computations for gating in neural networks is the multiplicative computation of nonlinear modulation (Salinas and Sejnowski, 2001; Volman et al., 2010). In order to infer gating within the assumed network, we used nonlinear DCM as implemented in DCM8 in SPM8 (http://www.fil.ion.ucl.ac.uk/spm/spm8) software (Stephan et al., 2008). Nonlinear DCM (Stephan et al., 2007, 2008) can be used to examine whether the connection strength of a connection is modulated by activity of other neuronal populations. To model nonlinear interactions within the network, the bilinear state equation (Eq. (1)) extends the Taylor series to set matrix D to be second order in the neuronal states (Stephan et al., 2008; Eq. (3)).

$$\begin{aligned} f(x,u) &= f(0,0) + \frac{\partial f}{\partial x}x + \frac{\partial f}{\partial u}u + \frac{\partial^2 f}{\partial x \partial u}xu + \frac{1}{2}\frac{\partial^2 f}{\partial x^2}\frac{x^2}{2} \\ D^{(j)} &= \Theta\left|\frac{1}{2}\frac{\partial^2 f}{\partial x_j^2}\right| u = 0 (1 \leq j \leq n) : \\ f(x,u) &= \frac{dx}{dt} = \left(A + \sum_{i=1}^{m} uB^{(i)} + \sum_{j=1}^{n} x_j D^{(j)}\right)x + Cu \end{aligned} \tag{3}$$

x_j	jth neuronal state
u_i	ith input
A	matrix A
B	matrix B
C	matrix C
D	matrix D

The matrices A, B and C were modelled as described in bilinear DCM (see section on Model space of bilinear models). Matrix D resembles the gating of a connection between two regions by the activity of a third region. Therefore, nonlinear DCM enables to infer whether the strength of a connection (here, the connections of interest are the connection from the IFG to the MD thalamus and the connection from the MD thalamus to the IFG) depends on the activity of other neuronal populations (here, the focus of the study was on the MD thalamus and the IFG; Alelú-Paz and Giménez-Amaya, 2008; Kolluri et al., 2005). Thus, the nonlinear modulation of the network interactions can be allocated to an explicit neuronal population (Stephan et al., 2007, 2008).

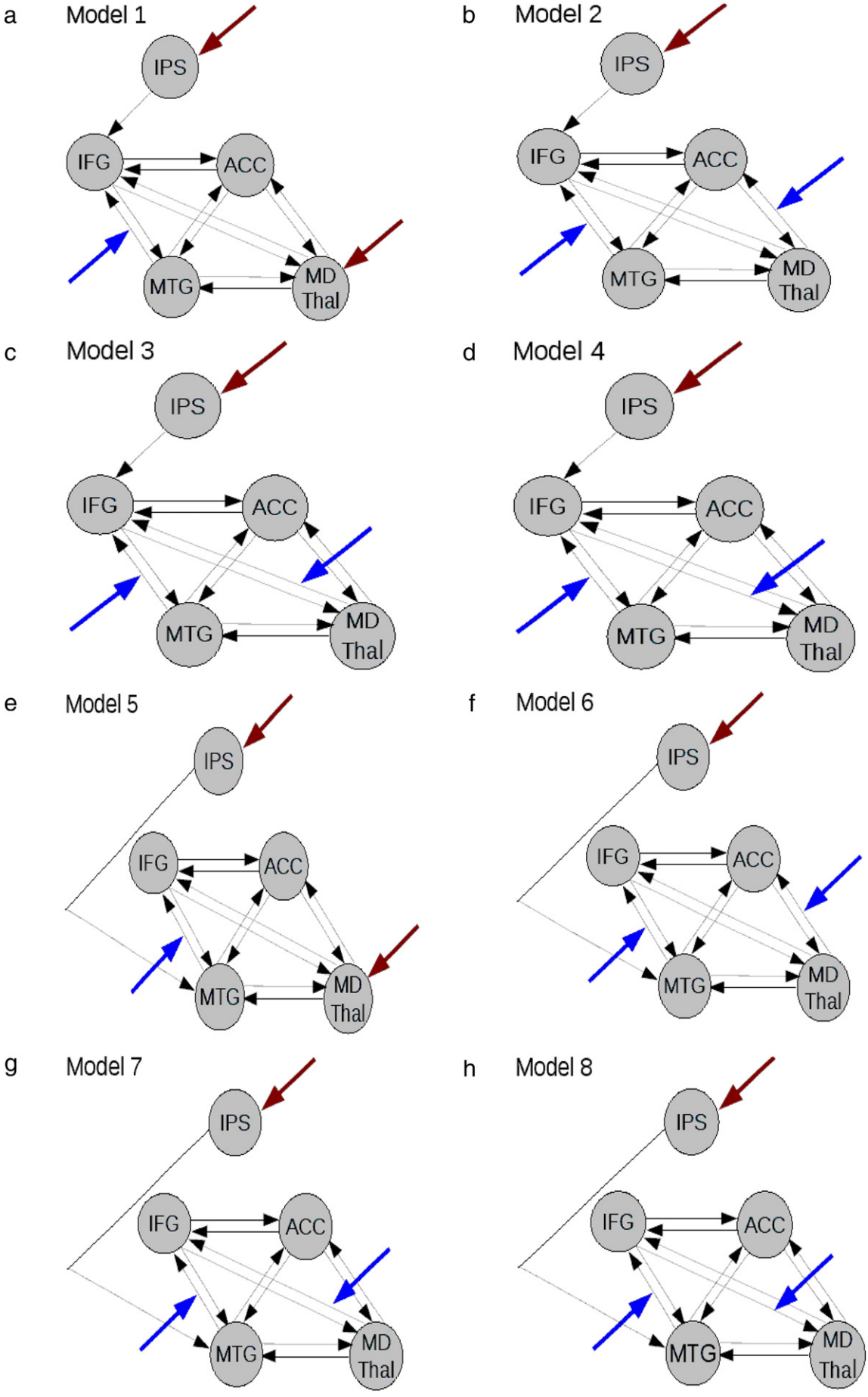
a
Model 1
IPS
IFG
ACC
MTG
MD Thal
b
Model 2
IPS
IFG
ACC
MTG
MD Thal
c
Model 3
IPS
IFG
ACC
MTG
MD Thal
d
Model 4
IPS
IFG
ACC
MTG
MD Thal
e
Model 5
IPS
IFG
ACC
MTG
MD Thal
f
Model 6
IPS
IFG
ACC
MTG
MD Thal
g
Model 7
IPS
IFG
ACC
MTG
MD Thal
h
Model 8
IPS
IFG
ACC
MTG
MD Thal

Model Space of Nonlinear Models. The bilinear modelling in phase 1 specified the constraints on the *A*, *B* and *C* matrices. Thus, the optimal Model 7 from the bilinear DCM analyses serves as the "basic" structure of the nonlinear models. In phase 2, our primary aim was to model the connectivity with the nonlinear modulation of the reciprocal neuronal projection between the MD thalamus and the IFG. The nonlinear DCMs were specified on the basis of neurobiological evidence for nonlinear mechanisms in neuronal functions, including cognitive tasks for evidence on altered corticothalamic and thalamocortical connections (Alelú-Paz and Giménez-Amaya, 2008; Kolluri et al., 2005) in schizophrenia. Fig. 3 shows the four different nonlinear models that were used to identify the gating of the bidirectional endogenous connection between the IFG and the MD thalamus. Two nonlinear models were specified by the nonlinear modulation from the MD thalamus onto both endogenous connections between the IFG and the MD thalamus (i.e. nonlinear models — MD thalamus; Figs. 3a and b).

Two further models were specified by the nonlinear modulation from the IFG onto both endogenous connections between the IFG and the MD thalamus (i.e. nonlinear models — IFG; Figs. 3c and d).

Model Space Partitioning — Family Level Inference — Bayesian Model Averaging. The well-established Bayesian inference approach of Family Level Inference and BMA (Penny et al., 2010) was applied. Family Level Inference allows the comparison of models of different characteristics (i.e. bilinear and nonlinear models) at the family level. Family Level Inference removes uncertainty about aspects of model characteristics by focusing on the criterion of interest (Penny et al., 2010). To this end, the models differed from each other in the nonlinear aspect.

Here, the model space was partitioned into three model families:

i) Model Family 1: bilinear model
   Model Family 1 contained the optimal bilinear model (Fig. 2(g)).
ii) Model Family 2: nonlinear models — MD thalamus
   Model Family 2 contained the two nonlinear models with nonlinear modulation from the MD thalamus (see Figs. 3a and b).
iii) Model Family 3: nonlinear models — IFG
   Model Family 3 contained the two nonlinear models with nonlinear modulation from the IFG (see Figs. 3c and d).

Family Level Inference provides an approach for random-effects analyses (Penny et al., 2010) for this schizophrenia study. This inference is hypothesised in this study since it is very likely that different subject groups use different coping strategies to solve the HSCT. Additionally, this inference method deals with model families that contain different number of models (Penny et al., 2010). Random-effect BMS at the family level uses a Gibbs sampling method (with 1,000,000 samples) and a Dirichlet distribution to compute the family frequencies of each model family in the population and defining a prior over these likelihoods and the exceedance probabilities. In Eq. (4), the exceedance probability (φ_k) is the likelihood that a model family k is more likely than any other model family (of K families compared), given the fMRI data (Penny et al., 2010). It has been previously shown that this approach is reliable (Seghier et al., 2011).

Phase 3 — detailed description — Bayesian Model Averaging

Theoretical background. We applied BMA over the winning models resulting from the BMS at the family level. BMA assesses the full posterior density on parameters by weighting the evidence to the contribution of each model to the mean effect (Penny et al., 2010). Posterior density means that models with the highest evidence maximize their contribution to the evidence, while models with weak evidence minimize their contribution to the evidence. These results can be computed for posterior means of connectivity on single subject level.

The significance of connection strength with the nonlinear modulation for the four nonlinear models was computed by the fraction of samples in the posterior density different from zero. Significant effects are reported at a posterior probability level of 0.95. This approach has been shown to produce reliable results (Seghier et al., 2011). In short, we used BMA to assess the posterior density over the bidirectional connections between the MD thalamus and the IFG by pooling evidence from different groups of subjects, in a way that accounts for uncertainty about the particular model generating the data.

Correlation between the connection strength with the nonlinear modulation and the PANSS symptoms severity delusions and hallucinations

Finally, the individual posterior densities of the connection strengths with the nonlinear modulation entered the following statistical analyses for within-group correlations between the connection strengths with the nonlinear modulation and the clinical symptoms assessed using PANSS scores. In order to estimate the sampling error of the original subpopulations, bivariate Pearson correlation with Bootstrapping and Confidence Intervals of 95% were constructed (Cohen, 1988; Efron and Tibshirani, 1993). These analyses were run in the healthy controls, HRall and HR + but not in the four ill subjects because of the small number of this group. The statistical analyses were conducted in SPSS (SPSS BMI 19.0).

Results

Demographic and behavioural results

Demographic and behavioural performance measures have been previously presented (Whalley et al., 2004, 2005). Briefly, there were no significant differences in mean age, gender, mean intelligence quotient (NART IQ) or handedness between the groups. Subjects performed the task appropriately during scanning. Behavioural performance between the groups was not significantly different.

DCM analyses

Results summary

The results are summarised for the grouped analyses by following the protocol given in Fig. 1 and the phased approach detailed in the methods section. In the first phase, the optimal model for the HSCT identified the general structure of the network. In the second phase, this structure was further interrogated to reveal the model families that best explain the expected group separation in our cohort. In the

Fig. 2. Model space of bilinear models. Models 1 to 4 are characterised by the endogenous connections from IPS to IFG. a. Model 1 is specified by driving inputs into the IFG and the MD Thal and modulatory input onto the connection from the MTG to the IFG. b. Model 2 is specified by driving input into the IFG and modulatory inputs onto the connection from the MTG to the IFG and from the MD Thal to the ACC. c. Model 3 is specified by driving input into the IFG and modulatory inputs onto the connection from the MTG to the IFG and from the MD Thal to the IFG. d. Model 4 is specified by driving input into the IFG and modulatory inputs onto the connection from the MTG to the IFG and from the IFG to the MD Thal. Models 5 to 8 are denoted by the endogenous connection from IFG to MTG. e. Model 5 is specified by driving inputs into the IFG and the MD Thal and modulatory input onto the connection from the MTG to the IFG. f. Model 6 is specified by driving input into the IFG and modulatory inputs onto the connection from the MTG to the IFG and from the MD Thal to the ACC. g. Model 7 is specified by driving input into the IFG and modulatory inputs onto the connection from the MTG to the IFG and from the MD Thal to the IFG. h. Model 8 is specified by driving input into the IFG and modulatory inputs onto the connection from the MTG to the IFG and from the IFG to the MD Thal. ACC, anterior cingulate cortex; IFG, inferior frontal gyrus; IPS, inferior parietal sulcus; MTG, middle temporal gyrus; MD Thal, mediodorsal thalamus. Black arrows denote endogenous connections. Blue arrows denote modulatory inputs. Red arrows denote driving inputs.

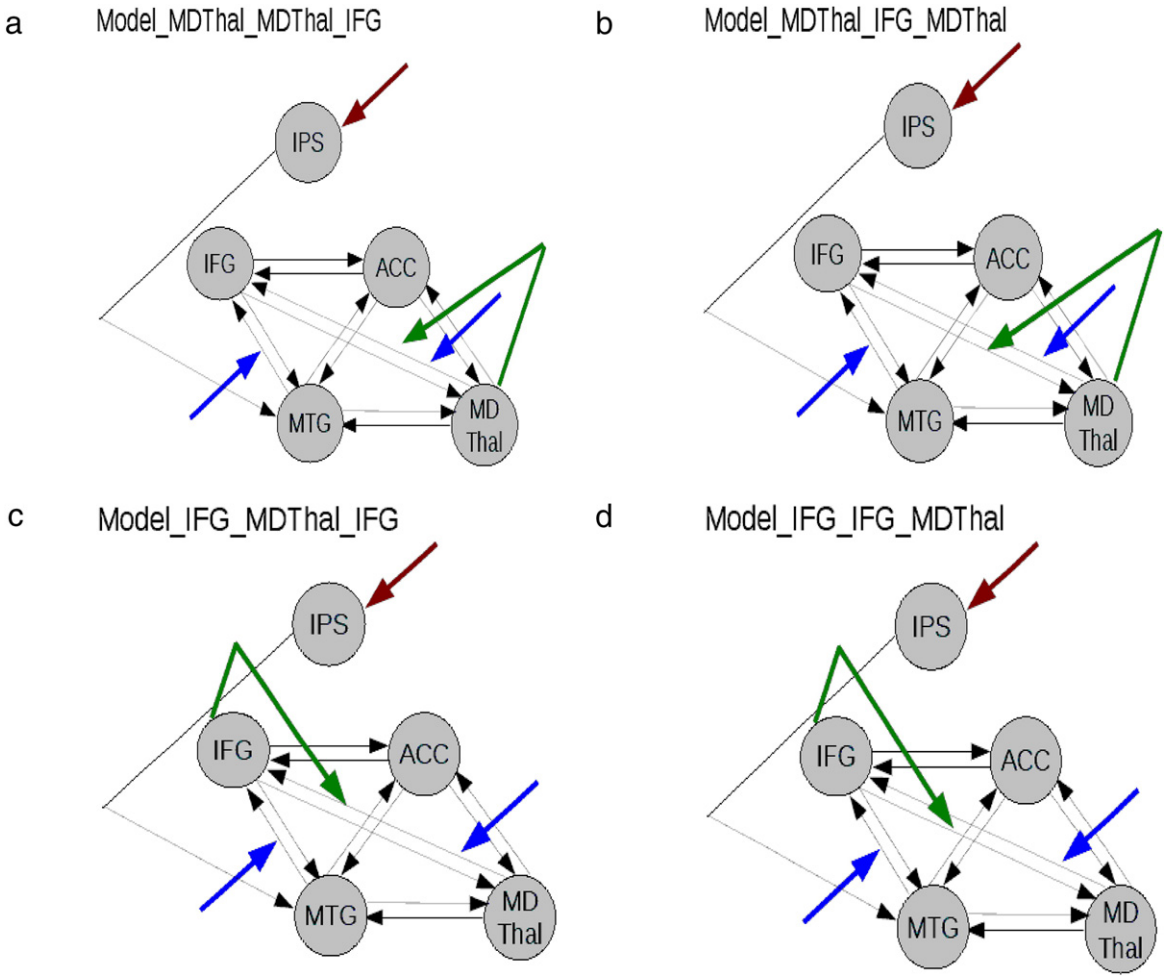

Fig. 3. Model space of nonlinear models. Model_MDThal_MDThal_IFG and Model_MDThal_IFG_MDThal are characterised by the nonlinear modulation from the MD Thal onto the bidirectional connection between the MD Thal and the IFG. Both models are specified upon the winning bilinear model and form Model Family 2. a. Model_MDThal_MDThal_IFG is specified by the nonlinear modulation from the MD Thal onto the connection from the MD Thal to the IFG. b. Model_MDThal_IFG_MDThal is specified by the nonlinear modulation from the MD Thal onto the connection from the IFG to the MD Thal. Model_IFG_MDThal_IFG and Model_IFG_IFG_MDThal are characterised by the nonlinear modulation from the IFG onto the bidirectional connection between the MD Thal and the IFG. Both models are specified upon the winning bilinear model and form Model Family 3. c. Model_IFG_MDThal_IFG is specified by the nonlinear modulation from the IFG onto the connection from the MD Thal to the IFG. d. Model_IFG_IFG_MDThal is specified by the nonlinear modulation from the IFG onto the connection from the IFG to the MD Thal. ACC, anterior cingulate cortex; IFG, inferior frontal gyrus; IPS, inferior parietal sulcus; MTG, middle temporal gyrus; MD Thal, mediodorsal thalamus. Black arrows denote endogenous connections. Blue arrows denote modulatory inputs. Red arrows denote driving inputs. Green arrows denote nonlinear modulations. All nonlinear models are specified on the basis of Model 7 (Fig. 2g).

third phase, the nonlinear modulation was assessed within the two winning model families resulting from the analyses in phase 2. The findings of each phase are compared between the three groupings.

Phase 1 — bilinear DCM — optimal model

In Fig. 4, the exceedance probabilities of the eight bilinear models labelled M1 to M8 across the three subject groupings are presented. In Fig. 4a, the BMS results are shown for the first grouping of healthy controls and all HR. In Fig. 4b, the BMS results are shown for the second grouping of healthy controls, HR− and HR+. In Fig. 4c, the BMS results are shown for the third grouping of healthy controls, HR−, HR+ and the four ill subjects who subsequently developed schizophrenia. This random-effects BMS analyses showed that Model 7 (M7) outperformed all other models for the tested groupings. Model 7 demonstrated exceedance probability (Xp) of 0.63 in healthy controls and Xp = 0.52 in HRall (Fig. 4a); Xp = 0.59 in HR− and Xp = 0.63 in HR+ (Fig. 4b); and Xp = 0.63 in the four ill subjects (Fig. 4c). The likelihood of Model 7 is three times the probability of the closest likely Model 6 and Model 8.

Model 7 is illustrated in Fig. 2(g). It contains one unidirectional connection from the IPS to the MTG and reciprocal endogenous connections between all the other regions. The BMS results from Model 5 to Model 8 demonstrate that the unidirectional connection from the IPS to the MTG is more likely than the connection from the IPS to the IFG. Furthermore, the exceedance probabilities from Model 3 and particularly Model 7 show that the task-dependent modulation was optimal for the forward connection between the MTG and the IFG and the forward connection between the MD thalamus and the IFG. Model 7 is similarly structured to the optimal model found in the HSCT study reported by Allen et al. (2010) although this study did not include the (MD) thalamus.

We note that the exceedance probability in the implementation of Model 7 is consistent across the tested groups. The exceedance probabilities for Model 7 vary from a minimum of 0.58 to a maximum of 0.63 across all subjects and three groupings. We also note similar consistency in exceedance probabilities for the other tested bilinear models. This consistency in BMS exceedance probabilities in healthy controls and HR subjects was also reported by Allen et al. (2010).

Phase 2 — nonlinear DCM — winning model families

The results of this phase are presented for the repeated grouping analyses. Three model families were compared against each other. The partitioning of the model space was the same for each grouping (see section on Model Space Partitioning – Family Level Inference – Bayesian Model Averaging).

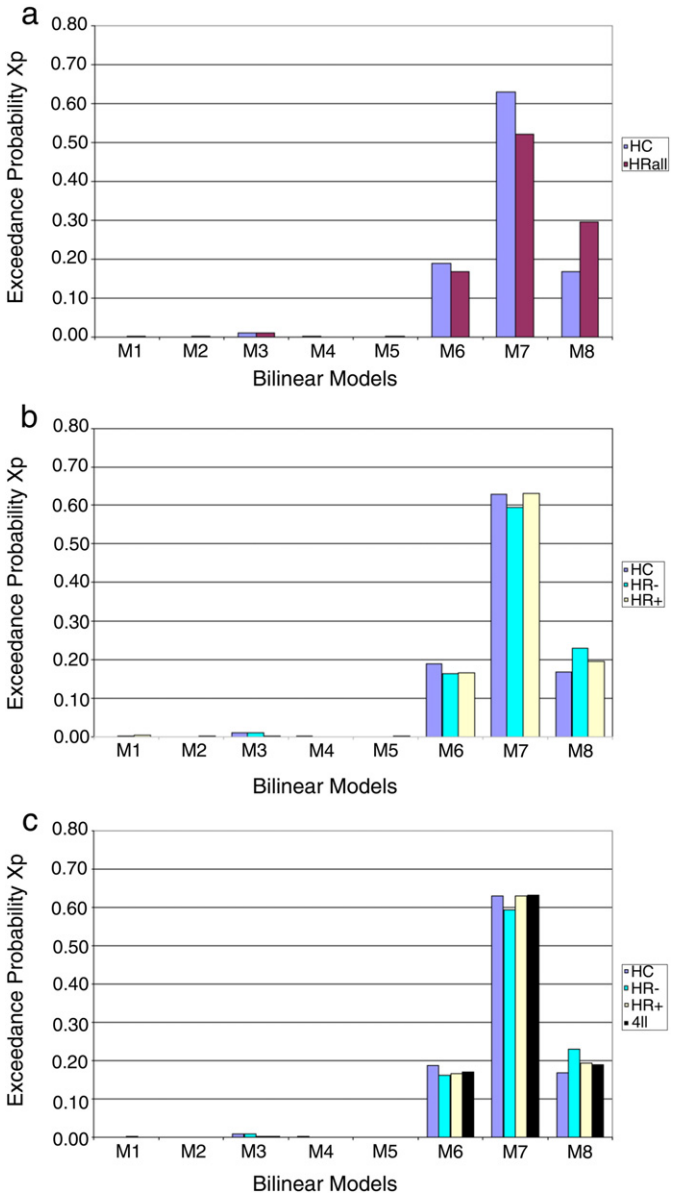

Fig. 4. Bayesian Model Selection at the group level for bilinear models. a. Bayesian Model Selection at the group level for healthy controls and all high risk subjects. First grouping of the BMS analysis for healthy controls and HRall. Model 7 is the optimal model in both healthy controls and HRall. b. Bayesian Model Selection at the group level for healthy controls, high risk subjects without psychotic symptoms and high risk subjects with psychotic symptoms. Second grouping of the BMS analysis for healthy controls, HR− and HR+. Model 7 is the optimal model in healthy controls, HR− and HR+. c. Bayesian Model Selection at the group level for healthy controls, high risk subjects without psychotic symptoms, high risk subjects with psychotic symptoms and the four ill subjects. Third grouping of BMS analysis for healthy controls, HR−, HR+ and four ill subjects. Model 7 is the optimal model in healthy controls, HR−, HR+ and the four ill subjects. BMS, Bayesian Model Selection; HC, healthy controls; HRall, all HR subjects; HR−, high risk subjects without psychotic symptoms; HR+, high risk subjects with psychotic symptoms; Four ill subjects, four HR subjects who subsequently became ill; eight bilinear models (Fig. 2) are labelled M1 to M8; M7, Model 7 (Fig. 2g); Xp, exceedance probability.

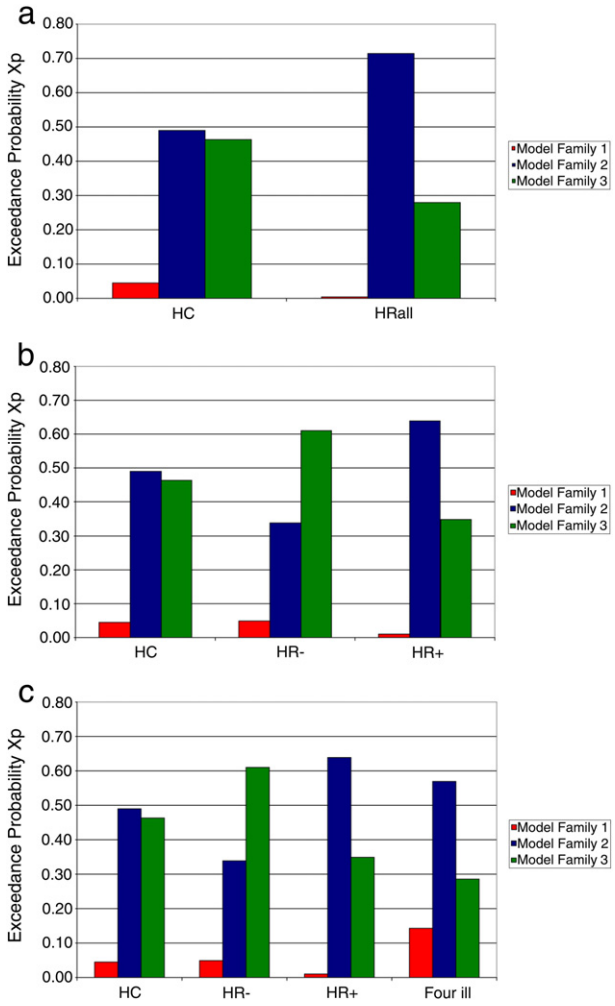

Fig. 5. Bayesian Model Selection at the model family level. a. Bayesian Model Selection at the model family level for healthy controls and all high risk subjects. First grouping of the BMS analysis for healthy controls and HRall. The winning model families are Model Families 2 and 3 in both healthy controls and HRall. b. Bayesian Model Selection at the level for healthy controls, high risk subjects without psychotic symptoms and high risk subjects with psychotic symptoms. Second grouping of the BMS analysis for healthy controls, HR− and HR+. The winning model families are Model Families 2 and 3 in healthy controls, HR− and HR+. c. Bayesian Model Selection at the level for healthy controls, high risk subjects without psychotic symptoms, high risk subjects with psychotic symptoms and the four ill subjects. Third grouping of the BMS analysis for healthy controls, HR−, HR+ and four ill subjects. The winning model families are Model Families 2 and 3 healthy controls, HR−, HR+ and the four ill subjects. BMS, Bayesian Model Selection; HC, healthy controls; HRall, all HR subjects; HR−, high risk subjects without psychotic symptoms; HR+, high risk subjects with psychotic symptoms; Four ill subjects, four HR subjects who subsequently became ill; Xp, exceedance probability. Red column: Model Family 1 — bilinear Model 7; Blue Column: Model Family 2 — Nonlinear Models with nonlinear modulation from MD Thalamus: Green Column: Model Family 3 — Nonlinear Models with nonlinear modulations from IFG.

We compared the different model families using the random-effects BMS approach at the family level to reveal the optimal model family across the three groupings in healthy controls and the high risk subjects. The BMS analysis over the model families resulted in different exceedance probabilities (Xp) between the healthy controls and the HR subjects (Fig. 5). The main findings of this phase are structured following the structure of Figs. 5a, b and c, which summarises and compares the three groupings. The exceedance probabilities for the two winning Model Families 2 and 3 were summarised (for a similar approach see Penny et al., 2010; Seghier et al., 2011).

i) The two winning model families 2 and 3 outperform the model family 1 in every group. In other words, both model families 2 and 3 are more likely than model family 1 to explain the HSCT fMRI data.
ii) Model families 2 and 3 accounted for a total of Xp = 0.95 in healthy controls and Xp = 0.99 in HRall in the first run (Fig. 5a).
iii) Model families 2 and 3 accounted for a total of Xp = 0.95 in healthy controls, Xp = 0.99 in HR− and Xp = 0.99 in HR+ in the second run (Fig. 5b).

iv) Model families 2 and 3 accounted for a total of Xp = 0.95 in healthy controls, Xp = 0.95 in HR−, Xp = 0.99 in HR+ and Xp = 0.86 in the four ill subjects in the third run (Fig. 5c).

In both model families 2 and 3, the nonlinear modulations onto both reciprocal connections between the MD thalamus and the IFG reveal the optimal modelling.

The results of the three groupings demonstrated that the distribution of likelihoods of the model families 2 and 3 differentiated between the groupings of HR subjects. In the first grouping, the HRall showed a different distribution of exceedance probabilities to healthy controls. In the second run, the finding revealed that the distribution of the HR+ seemed to resemble the distribution of the HRall. In the third run, the additional subgroup of four ill subjects demonstrated that the pattern of the HR+ was repeated in the four ill subjects.

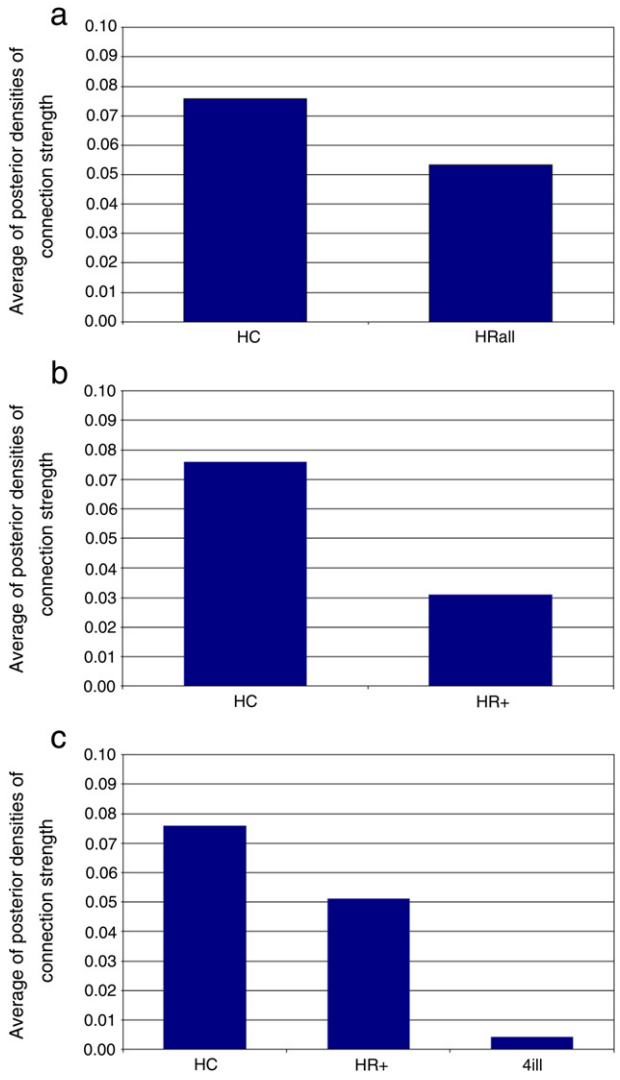

Fig. 6. Bayesian Model Averaging Results for the Thalamocortical Connection with nonlinear modulation from the MD thalamus — Model_MDThal_MDThal_IFG. a. Average of posterior densities of connection strength with nonlinear modulation for healthy controls and all high risk subjects. First grouping of the BMA analysis for healthy controls and HRall. The connection strength with the nonlinear modulation was not significantly different. b. Average of posterior densities of connection strength with nonlinear modulation for healthy controls and high risk subjects with psychotic symptoms. Second grouping of the BMA analysis for healthy controls and HR+. The connection strength with the nonlinear modulation was significantly reduced in HR+ in contrast to healthy controls. c. Average of posterior densities of connection strength with nonlinear modulation for healthy controls, high risk subjects with psychotic symptoms and the four ill subjects. Third grouping of the BMA analysis for healthy controls, HR+ and four ill subjects. The connection strength with the nonlinear modulation was significantly reduced in HR+ in contrast to healthy controls and the four ill subjects in contrast to the healthy controls. Average of posterior densities of connection strength with nonlinear modulation (in Hertz), (all significant at posterior probability threshold $p > 0.95$). BMA, Bayesian Model Averaging; HC, healthy controls; HRall, all high risk subjects; HR+, high risk subjects with psychotic symptoms; four ill subjects, 4 subjects who subsequently became ill.

Phase 3 — significant connection strength with the nonlinear modulation

The results of this phase are presented for the repeated grouping analyses. In order to investigate the posterior probabilities of the connectivity with the nonlinear modulation, we assessed the connection strengths from model family 2, nonlinear models — MD thalamus in every grouping. The BMA analysis within the two winning models resulted in different posterior probabilities of the nonlinear modulation in the Model MDThal_MDThal_IFG (Fig. 3a; Fig. 6). The main findings of this phase are structured following the structure of Figs. 6a, b and c, which summarises and compares the three groupings.

i) The connection strength with the nonlinear modulation was reduced in HRall, HR+ and the four ill subjects across the three groups; this parameter was significantly lower in the HR+ and the four ill subjects who subsequently developed schizophrenia in contrast to the healthy controls (posterior probability 0.95).
ii) The connection strength with nonlinear modulation was not significantly different between the healthy controls and the HRall (Fig. 6a).
iii) The connection strength with nonlinear modulation was significantly reduced in the HR+ in contrast to healthy controls (posterior probability 0.95; Fig. 6b).
iv) The connection strength with nonlinear modulation was significantly reduced in the HR+ in contrast to healthy controls (posterior probability 0.95; Fig. 6c). Furthermore, this parameter was significantly lower in the four ill subjects in comparison to healthy controls (posterior probability 0.95; Fig. 6c).

The connection strengths with the nonlinear modulation from the other nonlinear model (model family 2, Model MDThal_IFG_MDThal) were not significantly different between the groups.

Correlation between the connection strength with the nonlinear modulation and the PANSS symptoms severity for delusions and hallucinations

The result of the significant connection strength with the nonlinear modulation for the Model MDThal_MDThal_IFG demonstrated reduced connection strengths with the nonlinear modulation in HR+ and the four ill subjects but not in HRall. In the next step we examined whether the finding of effective dysconnectivity could underlie the clinical symptoms in the HR+. A significant correlation was found between the individual connection strength with the nonlinear modulation of Model_MDThal_MDThal_IFG and the symptom 'delusion' in HR+ ($r = -.246$; $p = 0.041$; 95% CI (-0.543; -0.024)). The significant association in HR+ supported the more pronounced reduction of this connection strength with nonlinear modulation in the four ill subjects (Fig. 6c), who showed delusions at the time of transition to the illness. Furthermore, the correlation in HR+ in addition to the significant relationship in HRall ($r = -.201$; $p = 0.05$; 95% CI (-0.446; 0.02)) confirms the BMS results on the model family level (Figs. 5a in HRall and b in HR+). The distribution of the likelihood of the model families 2 and 3 between HRall, HR− and HR+ (Figs. 5a and b) can therefore be explained by the lower connection strength with the nonlinear modulation (in the Model MDThal_MDThal_IFG) as a state-marker in the HRall and HR+ groups. There was no significant association between the symptom 'hallucination' and the connection strength with the gating.

Discussion

We have reported the application of nonlinear DCM to fMRI data for the HSCT in subjects at high genetic risk of schizophrenia. For the HSCT, nonlinear DCM allowed us to effectively model connection strength with the nonlinear modulation and the interactions between neuronal populations in the MD thalamus and the IFG. Our results demonstrate that the connection strength with nonlinear modulation of the thalamocortical connection is reduced in HR+. This could result in reduced prefrontal-thalamic functional connectivity and cortical dysconnectivity and both is in keeping with and extends our previous findings of functional connectivity on this cohort (Whalley et al., 2005). In addition, we see further reductions of connection strength with the nonlinear modulation in the four ill subjects in our HR cohort although this should be considered preliminary given the small subject number in this group. Furthermore, we found significantly negative correlations between lower connection strength with nonlinear modulation and the PANSS symptom severity of delusion in HR+ and the HRall. This indicates that the presence of active symptomatology in HR+ (and to a lesser extent in the HRall) may be a factor for the state-related differences between HR− and HR+. All subjects disavowed the presence of psychotic symptoms at more than a subclinical level at the time of scanning and indeed regarded themselves as well. None were on antipsychotic medication. Thus our findings are not confounded by the effect of medication.

The altered connection strength with the gating of the thalamocortical neuronal projection may represent the neurobiophysiological cause for cortical functional and effective dysconnectivity found in the HR stage and the established illness of schizophrenia. Alterations of the MD thalamus have been associated with the pathology of schizophrenia (Clinton and Meador-Woodruff, 2004; Meador-Woodruff et al., 2003; Oh et al., 2009) because of its cortio-thalamo-cortico network (Briggs and Usray, 2008; Kantrowitz and Javitt, 2012; Oh et al., 2009). Further evidence for such alterations is seen in fMRI studies, which report cortical dysfunction and cognitive deficits in schizophrenia for verbal fluency tasks (Curtis et al., 1998; Fu et al., 2002; Fusar-Poli et al., 2011). Other studies have also demonstrated that the disrupted connection between the left MD thalamus and the dorsolateral prefrontal cortex plays a crucial role in schizophrenia (Hazlett et al., 2004; Krystal et al., 2003; Mitelman et al., 2005; Thermenos et al., 2004), which could result in cognitive deficits (Clinton and Meador-Woodruff, 2004; Jones, 1997; Meador-Woodruff et al., 2003). These alterations of the thalamocortical connection may contribute to cortical dysfunction observed in schizophrenia (Balu and Coyle, 2012; Byne et al., 2009; Lewis and Lieberman, 2000; Pakkenberg et al., 2009; Sodhi et al., 2011; Watis et al., 2008).

Our results of lower connection strength with the nonlinear modulation are in keeping with those studies proposing that nonlinear models can resemble reduced gating and provide a better explanation to the fMRI data than linear models. The finding of reduced connection strength with the thalamocortical projection via the MD thalamus in the HR+ and the four ill subjects supports the hypothesis of disrupted synaptic plasticity, which is gated by nonlinear biophysical processes. Short-term synaptic modulation encompasses biophysical processes which are known to be highly relevant for cognitive tasks (Abbott and Regehr, 2004; Deng and Klyachko, 2011; Neher and Sakaba, 2008; Pan and Zucker, 2009). It has been reported that probabilistic computational modelling of short-term depression processes resembles gating mechanisms at the synaptic level (Pfister et al., 2010). The thalamocortical synapses underlie nonlinear dynamic modulation (Chance et al., 2002; Deng and Klyachko, 2011; Destexhe, 2009; Negyessy and Goldman-Rakic, 2005), which has also been shown for the corticothalamic connection (Freyer et al., 2011; Shu et al., 2003). Gating processes show comparable nonlinear mechanisms (Abbott et al., 1997; Ardid et al., 2007; Berends et al., 2005; Chance et al., 2002; Freyer et al., 2011; Murphy and Miller, 2003; Rothman et al., 2009; Salinas and Sejnowski, 2001; Shu et al., 2003), which gate cognitive functions (Salinas and Sejnowski, 2001; Stephan et al., 2008) in a multiplicative nonlinear way. That means that neurons from two or more sources integrate information for cognitive performance (Salinas and Sejnowski, 2001; Stephan et al., 2008). Our results support previous findings of disrupted synaptic plasticity of the thalamocortical connection (Krystal et al., 2003; Negyessy and Goldman-Rakic, 2005) resulting in cortical dysconnectivity in schizophrenia (Balu and Coyle, 2012; Byne et al., 2009; Goff and Coyle, 2001; Lewis and Lieberman, 2000; Pakkenberg et al., 2009; Sodhi et al., 2011; Watis et al., 2008).

We consider that our indications of lower connection strengths with the nonlinear modulation of the thalamocortical connection during the HSCT suggest that altered glutamatergic transmission of the MD thalamus could underlie the reduced gating of the task. We acknowledge the lack of a measure of glutamate concentration in the MD thalamus in this study. However, the translation of the neurobiophysical dynamic system of the connection strength with the gating of a neuronal region is valid because of the computational framework of DCM, specifically nonlinear DCM (Friston et al., 2003; Stephan et al., 2008), which employs second-order nonlinear computations. Studies applying these second-order nonlinear computations have demonstrated that gating at the neuronal region modulates glutamatergic neurotransmission (Berends et al., 2005; Sun and Beierlein, 2011; Volman et al., 2010). Also, nonlinear DCM assesses selective changes in each region, which can be used to indirectly estimate excitatory glutamatergic subpopulations (Stephan et al., 2008). Our findings of the reduced connection strength with the nonlinear modulation of the thalamocortical projection offer a mechanistic interpretation for cortical dysconnection in schizophrenia.

There is extensive evidence that alterations of glutamatergic neurotransmission may contribute to disrupted synaptic plasticity in schizophrenia (Balu and Coyle, 2012; Coyle, 2006). The N-methyl-D-aspartate (NMDA) receptor hypofunction model for schizophrenia proposes that altered glutamatergic modulation may underlie the pathophysiology of the disorder (Coyle, 2006; Coyle et al., 2011; Javitt, 2010). This suggests that glutamate neurotransmission, specifically NMDA receptor-mediated transmission, may be disrupted in schizophrenia (Goff and Coyle, 2001; Goff et al., 1995; Javitt et al., 1994; Moghaddam et al., 1997). Several studies have shown that the modulation of the thalamocortical projection is primarily altered by excitatory glutamatergic neurotransmission (Balu and Coyle, 2012; Gray and Roth, 2007; McCormick and Bal, 1997; Romanides et al., 1999; Watis et al., 2008), which could be attributed to NMDA receptor dysfunctions (Kiss et al., 2011; Santana et al., 2009), but also to thalamic inhibitory interneurons (Augustinaite and Heggelund, 2007; Crandall and Cox, 2012; Errington et al., 2010; Lewis and González-Burgos, 2008; Neher and Sakaba, 2008; Pan and Zucker, 2009), interneurons in the DLPFC (Wang, 2010); metabotropic Glutamate receptors (mGluR) (Jones, 1997; Newpher and Ehlers, 2008; Pinault, 2011; Sodhi et al., 2011) and ionotropic receptors (Meador-Woodruff et al., 2003). Importantly, it has been shown that gating at the synaptic level is mediated by glutamatergic neurotransmission (Berends et al., 2005; Neher and Sakaba, 2008; Pan and Zucker, 2009; Sun and Beierlein, 2011; Volman et al., 2010), which is modulated by excitatory (mainly glutamatergic) and inhibitory (inhibitory interneurons) inputs (Murphy and Miller, 2003; Salinas and Sejnowski, 2001; Salinas and Sejnowski, 2000; Wang, 2010). These known processes of glutamatergic neuromodulation have also been reported for the corticothalamic connection via NMDA receptors and mGluR (McCormick, 1992). Despite the evidence for glutamatergic neurotransmission, it is assumed that altered interactions between glutamatergic and dopaminergic neurotransmission may lead to the cortical dysconnectivity (Alelú-Paz and Giménez-Amaya, 2008; Coyle, 2006; Javitt, 2010; Moghaddam et al., 1997).

DCM is a translational brain modelling framework with physiologically interpretable dynamic system models, which are combined with dynamic causal models fitted to the fMRI data to provide estimates of pathophysiological mechanisms of a neuronal group. The

main advantage of DCM is the inference of causal mechanisms (for example gating) at the neuronal level that provides a more precise estimation of how the rate of change of activity in one region influences the rate of change in other regions (Friston, 2009; Friston et al., 2003; Stephan et al., 2008). The main advantage of nonlinear DCM over bilinear DCM is anchored in the differentiation between nonlinearities in the BOLD signal at the level of neuronal or haemodynamic mechanisms (Friston et al., 2003; Stephan et al., 2007, 2008) by combining neuronal state equations with a haemodynamic feedforward network. Specifically, in nonlinear DCM (Stephan et al., 2008) inhibitions of a neuronal group or neuronal connection can be modelled. In addition, nonlinear DCM assesses selective changes in each region, which can be used to model effects exerted by neurotransmitters like glutamate. In other words, the modelling of activity-dependent gating of connections allows indirect estimations of excitatory glutamatergic subpopulations.

There are general limitations of bilinear and nonlinear DCM and specific limitations of this study. The temporal resolution of fMRI is limited, which leads to an inability to consider conduction delays in inputs and interregional interactions (Friston et al., 2003). DCM requires strict subject and ROI inclusion criteria (Stephan et al., 2007), which results in exclusion of more subjects compared to the usual fMRI analyses, leading to a smaller sample size for this study than for our previous analyses (Whalley et al., 2004, 2005). Also DCM8 does not allow a direct assessment of alterations of excitatory glutamatergic subpopulations in the models (Marreiros et al., 2008) or an explicit neuronal population (Daunizeau et al., 2009). Thus, we cannot definitely state that glutamatergic neurotransmission is implicated in the lower connection strength with the gating in the high risk subjects. The nonlinear dynamical systems were estimated by deterministic inference methods, and these do not fully represent the random or stochastic noise of neuronal activity (Saarinen et al., 2008) and hidden neuronal and physiological processes (Li et al., 2011). Our DCM analyses of subjects who subsequently develop schizophrenia were limited to four individuals. Because of the small size in this group in the DCM analysis it is not possible to consider the DCM results to have predictive validity although the four individuals can be treated as single-subject results (Stephan et al., 2007). For predictive studies using DCM results, the DCM-based generative embedding approach using support vector machines (Brodersen et al., 2011) is an additional approach. Finally, the DCM analyses in this study were run in DCM8 limiting us to deterministic and one-state DCM.

Conclusion

This is the first study to report on the clinical application of nonlinear DCM to fMRI data. Our results show that gating mechanism at the neuronal population level of the MD thalamus is altered and may contribute to or be an underlying cause for the development of psychotic symptoms. This study suggests that nonlinear DCM may further our understanding of altered connectivity in subjects at high familial risk stage of schizophrenia.

Acknowledgments

MRD is supported by Dr Mortimer and Theresa Sackler Foundation. HCW is supported by a Dorothy Hodgkin Fellowship from the Royal Society (DH080018). VV is supported by the EPSRC, BBSRC and MRC. TWJM is supported by Dr Mortimer and Sackler Foundation and TMRC. The Edinburgh High Risk Study was funded by two MRC programme grants. Scanning was conducted at the Scottish Brain Imaging Research Centre which is supported by SINAPSE (Scottish Imaging Network, a Platform for Scientific Excellence, www.sinapse.ac.uk). All imaging aspects also received financial support from the Dr Mortimer and Theresa Sackler Foundation.

Conflict of interest

MRD, HCW, LR, SML and TWJM have received financial support from Pfizer (formerly Wyeth) in relation to imaging studies of people with schizophrenia. ECJ and SML have done consultancy work for Roche Pharmaceuticals in connection with a possible new treatment for schizophrenia. ECJ has also done consultancy work for Novartis. SML has also received honoraria for lectures, chairing meetings, and consultancy work from Janssen in connection with brain imaging and therapeutic initiatives for psychosis. The authors VV and DGCO have no competing interests to declare.

References

Abbott, L.F., Regehr, W.G., 2004. Synaptic computation. Nature 431 (7010), 796–803 (14).
Abbott, L.F., Varela, J.A., Sen, K., Nelson, S.B., 1997. Synaptic depression and cortical gain control. Science 275 (5297), 220–224.
Abitz, M., Nielsen, R.D., Jones, E.G., Laursen, H., Graem, N., Pakkenberg, B., 2007. Excess of neurons in the human newborn mediodorsal thalamus compared with that of the adult. Cereb. Cortex 17 (11), 2573–2578.
Alelú-Paz, R., Giménez-Amaya, J.M., 2008. The mediodorsal thalamic nucleus and schizophrenia. J. Psychiatry Neurosci. 33 (6), 489–498.
Allen, P., Mechelli, A., Stephan, K.E., Day, F., Dalton, J., Williams, S., McGuire, P.K., 2008. Fronto-temporal interactions during overt verbal initiation and suppression. J. Cogn. Neurosci. 20 (9), 1656–1669.
Allen, P., Stephan, K.E., Mechelli, A., Day, F., Ward, N., Dalton, J., Williams, S.C., McGuire, P., 2010. Cingulate activity and fronto-temporal connectivity in people with prodromal signs of psychosis. NeuroImage 49 (1), 947–955.
Andreasen, N.C., O'Leary, D.S., Flaum, M., Nopoulos, P., Watkins, G.L., Boles Ponto, L.L., Hichwa, R.D., 1997. Hypofrontality in schizophrenia: distributed dysfunctional circuits in neuroleptic-naïve patients. Lancet 349, 1730–1734.
Ardid, S., Wang, X.J., Compte, A., 2007. An integrated microcircuit model of attentional processing in the neocortex. J. Neurosci. 27 (32), 8486–8495.
Augustinaite, S., Heggelund, P., 2007. Changes in firing pattern of lateral geniculate neurons caused by membrane potential dependent modulation of retinal input through NMDA receptors. J. Physiol. 582 (1), 297–315.
Balu, D.T., Coyle, J.T., 2012. Neuroplasticity signaling pathways linked to the pathophysiology of schizophrenia. Neurosci. Biobehav. Rev. 35 (3), 848–870.
Berends, M., Maex, R., De Schutter, E., 2005. The effect of NMDA receptors on gain modulation. Neural Comput. 17 (12), 2531–2547.
Bloom, P.A., Fischler, I., 1980. Completion norms for 329 sentence contexts. Mem. Cognit. 8 (6), 631–642.
Boksman, K., Théberge, J., Williamson, P., Drost, D.J., Malla, A., Densmore, M., Takhar, J., Pavlosky, W., Menon, R.S., Neufeld, R.W.J., 2005. A 4.0-T fMRI study of brain connectivity during word fluency in first-episode schizophrenia. Schizophr. Res. 75 (2–3), 247–263.
Briggs, F., Usray, W.M., 2008. Emerging views of corticothalamic function. Curr. Opin. Neurobiol. 18 (4), 403–407.
Brodersen, K.H., Schofield, T.M., Leff, A.P., Ong, C.S., Lomakina, E.I., Buhmann, J.M., Stephan, K.E., 2011. Generative embedding for model-based classification of fMRI data. PLoS Comput. Biol. 7 (6), e1002079.
Byne, W., Hazlett, E.A., Buchsbaum, M.S., Kemether, E., 2009. The thalamus and schizophrenia: current status of research. Acta Neuropathol. 117 (4), 347–368.
Chance, F.S., Abbott, L.F., Reyes, A.D., 2002. Gain modulation from background synaptic input. Neuron 35 (4), 773–782.
Clinton, S.M., Meador-Woodruff, J.H., 2004. Thalamic dysfunction in schizophrenia: neurochemical, neuropathological, and in vivo imaging abnormalities. Schizophr. Res. 69 (2003), 237–253.
Cohen, J., 1988. Statistical Power Analysis for the Behavioral Sciences. Lawrence Erlbaum Associates, Hillsdale, New Jersey.
Collette, F., Van der Linden, M., Delfiore, G., Degueldre, C., Luxen, A., Salmon, E., 2001. The functional anatomy of inhibition processes investigated with the Hayling task. NeuroImage 14 (2), 258–267.
Coyle, J.T., 2006. Glutamate and schizophrenia: beyond the dopamine hypothesis. Cell. Mol. Neurobiol. 26 (4–6), 365–384.
Coyle, J.T., Balu, D., Benneyworth, M., Basu, A., Roseman, A., 2011. Beyond the dopamine receptor: novel therapeutic targets for treating schizophrenia. Dialogues Clin. Neurosci. 12 (3), 359–382.
Crandall, S.R., Cox, C.L., 2012. Local dendrodendritic inhibition regulates fast synaptic transmission in visual thalamus. J. Neurosci. 32 (7), 2513–2522.
Curtis, V.A., Bullmore, E.T., Brammer, M.J., Wright, I.C., Williams, S.C., Morris, R.G., Sharma, T.S., Murray, R.M., McGuire, P.K., 1998. Attenuated frontal activation during a verbal fluency task in patients with schizophrenia. Am. J. Psychiatry 155 (8), 1056–1063.
Daunizeau, J., Friston, K.J., Kiebel, S.J., 2009. Variational Bayesian identification and prediction of stochastic nonlinear dynamic causal models. Physica D 238 (21), 2089–2118.
Dauvermann, M.R., Mukherjee, P., Moorhead, W.T., Stanfield, A.C., Fusar-Poli, P., Lawrie, S.M., Whalley, H.C., 2012. Relationship between gyrification and functional connectivity of

the prefrontal cortex in subjects at high genetic risk of schizophrenia. Curr. Pharm. Des. 18 (4), 434–442.
Deng, P.Y., Klyachko, V.A., 2011. The diverse functions of short-term plasticity components in synaptic computations. Commun. Integr. Biol. 4 (5), 543–548.
Destexhe, A., 2009. Self-sustained asynchronous irregular states and Up–Down states in thalamic, cortical and thalamocortical networks of nonlinear integrate-and-fire neurons. J. Comput. Neurosci. 27 (3), 493–506.
Efron, B., Tibshirani, R.J., 1993. An Introduction to the Bootstrap. Chapman and Hall, New York.
Errington, A.C., Renger, J.J., Uebele, V.N., Crunelli, V., 2010. State-dependent firing determines intrinsic dendritic Ca^{2+} signalling in thalamocortical neurons. J. Neurosci. 30 (44), 14843–14853.
Freyer, F., Roberts, J.A., Becker, R., Robinson, P.A., Ritter, P., Breakspear, M., 2011. Biophysical mechanisms of multistability in resting-state cortical rhythms. J. Neurosci. 31 (17), 6353–6361.
Friston, K.J., 1999. Schizophrenia and the disconnection hypothesis. Acta Psychiatr. Scand. Suppl. 395, 68–79.
Friston, K., 2009. Causal modelling and brain connectivity in functional magnetic resonance imaging. PLoS Biol. 7 (2), e33 (17).
Friston, K.J., Harrison, L., Penny, W., 2003. Dynamic causal modelling. NeuroImage 19 (4), 1273–1302.
Frith, C.D., Friston, K.J., Liddle, P.F., Frackowiak, R.S., 1991. A PET study of word finding. Neuropsychologia 29 (12), 1137–1148.
Frith, C.D., Friston, K.J., Herold, S., Silbersweig, D., Fletcher, P., Cahill, C., Dolan, R.J., Frackowiak, R.S., Liddle, P.F., 1995. Regional brain activity in chronic schizophrenic patients during the performance of a verbal fluency task. Br. J. Psychiatry 167 (3), 343–349.
Fu, C.H.Y., Morgan, K., Suckling, J., Williams, S.C.R., Andrew, C., Vythelingum, G.N., McGuire, P.K., 2002. A functional magnetic resonance imaging study of overt letter verbal fluency using a clustered acquisition sequence: greater anterior cingulate activation with increased task demand. NeuroImage 17 (2), 871–879.
Fusar-Poli, P., Stone, J.M., Broome, M.R., Valli, I., Mechelli, A., McLean, M.A., Lythgoe, D.J., O'Gorman, R.L., Barker, G.J., McGuire, P.K., 2011. Thalamic glutamate levels as a predictor of cortical response during executive functioning in subjects at high risk for psychosis. Arch. Gen. Psychiatry 68 (9), 881–890.
Goff, D.C., Coyle, J.T., 2001. The emerging role of glutamate in the pathophysiology and treatment of schizophrenia. Am. J. Psychiatry 16, 1367–1377.
Goff, D.C., Tsai, G., Manoach, D.S., Coyle, J.T., 1995. Dose-finding trial of D-cycloserine added to neuroleptics for negative symptoms in schizophrenia. Am. J. Psychiatry 152 (8), 1213–1215.
Gray, J.A., Roth, B.L., 2007. Molecular targets for treating cognitive dysfunction in schizophrenia. Schizophr. Bull. 33 (5), 1100–1119.
Harris, J.M., Moorhead, T.W.J., Miller, P., McIntosh, A.M., Bonnici, H.M., Owens, D.G.C., Johnstone, E.C., Lawrie, S.M., 2007. Increased prefrontal gyrification in a large high-risk cohort characterizes those who develop schizophrenia and reflects abnormal prefrontal development. Biol. Psychiatry 62 (7), 722–729.
Hazlett, E.A., Buchsbaum, M.S., Kemether, E., Bloom, R., Platholi, J., Brickman, A.M., Shihabuddin, L., Tang, C., Byne, W., 2004. Abnormal glucose metabolism in the mediodorsal nucleus of the thalamus in schizophrenia. Am. J. Psychiatry 161 (2), 305–314.
Hodges, A., Byrne, M., Grant, E., Johnstone, E.C., 1999. People at risk of schizophrenia. Sample characteristics of the first 100 cases in the Edinburgh High-Risk Study. Br. J. Psychiatry 174, 547–553.
Javitt, D.C., 2010. Glutamatergic theories of schizophrenia. Isr. J. Psychiatry Relat. Sci. 47 (1), 4–16.
Javitt, D.C., Frusciante, M.J., Zukin, S.R., 1994. Activation-related and activation-independent effects of polyamines on phencyclidine receptor binding within the N-methyl-D-aspartate receptor complex. J. Pharmacol. Exp. Ther. 604–613.
Johnstone, E.C., Abukmeil, S.S., Byrne, M., Clafferty, R., Grant, E., Hodges, A., Lawrie, S.M., Owens, D.G., 2000. Edinburgh high risk study — findings after four years: demographic, attainment and psychopathological issues. Schizophr. Res. 46 (1), 1–15.
Johnstone, E.C., Russell, K.D., Harrison, L.K., Lawrie, S.M., 2003. The Edinburgh High Risk Study: current status and future prospects. World Psychiatry 2 (1), 45–49.
Jones, E.G., 1997. Cortical development and thalamic pathology in schizophrenia. Schizophr. Bull. 483–501.
Kantrowitz, J., Javitt, D.C., 2012. Glutamatergic transmission in schizophrenia: from basic research to clinical practice. Curr. Opin. Psychiatry 25 (2), 96–102.
Kay, S.R., Fiszbein, A., Opler, L.A., 1987. The positive and negative syndrome scale (PANSS) for schizophrenia. Schizophr. Bull. 13 (2), 261–276.
Kiss, T., Hoffmann, W.E., Scott, L., Kawabe, T.T., Milici, A.J., Nilsen, E.A., Hajós, M., 2011. Role of thalamic projection in NMDA receptor-induced disruption of cortical slow oscillation and short-term plasticity. Front. Psychiatry 2, 14.
Kolluri, N., Sun, Z., Sampson, A.R., Lewis, D.A., 2005. Lamina-specific reductions in dendritic spine density in the prefrontal cortex of subjects with schizophrenia. Am. J. Psychiatry 162 (6), 1200–1202.
Krystal, J.H., D'Souza, D.C., Mathalon, D., Perry, E., Belger, A., Hoffman, R., 2003. NMDA receptor antagonist effects, cortical glutamatergic function, and schizophrenia: toward a paradigm shift in medication development. Psychopharmacology 169 (3–4), 215–233.
Lawrie, S.M., Buechel, C., Whalley, H.C., Frith, C.D., Friston, K.J., Johnstone, E.C., 2002. Reduced frontotemporal functional connectivity in schizophrenia associated with auditory hallucinations. Biol. Psychiatry 51 (12), 1008–1011.
Lee, C.M., Chang, W.C., Chang, K.B., Shyu, B.C., 2007. Synaptic organization and input-specific short-term plasticity in anterior cingulate cortical neurons with intact thalamic inputs. Eur. J. Neurosci. 25 (9), 2847–2861.
Lencz, T., Smith, C.W., McLaughlin, D., Auther, A., Nakayama, E., Hovey, L., Cornblatt, B.A., 2006. Generalized and specific neurocognitive deficits in prodromal schizophrenia. Biol. Psychiatry 59 (9), 863–871.
Lewis, D.A., González-Burgos, G., 2008. Neuroplasticity of neocortical circuits in schizophrenia. Neuropsychopharmacology 33 (1), 141–165.
Lewis, D.A., Lieberman, J.A., 2000. Catching up on schizophrenia: natural history and neurobiology. Neuron 28 (2), 325–334.
Li, B., Daunizeau, J., Stephan, K.E., Penny, W., Hu, D., Friston, K., 2011. Generalised filtering and stochastic DCM for fMRI. NeuroImage 58 (2), 442–457.
Marreiros, A.C., Kiebel, S.J., Friston, K.J., 2008. Dynamic causal modelling for fMRI: a two-state model. NeuroImage 39 (1), 269–278.
McCormick, D.A., 1992. Neurotransmitter actions in the thalamus and cerebral cortex and their role in neuromodulation of thalamocortical activity. Prog. Neurobiol. 39 (4), 337–388.
McCormick, D.A., Bal, T., 1997. Sleep and arousal: thalamocortical mechanisms. Annu. Rev. Neurosci. 20, 185–215.
Meador-Woodruff, J.H., Clinton, S.M., Beneyto, M., McCullumsmith, R.E., 2003. Molecular abnormalities of the glutamate synapse in the thalamus in schizophrenia. Ann. N. Y. Acad. Sci. 1003, 75–93.
Mitelman, S.A., Brickman, A.M., Shihabuddin, L., Newmark, R., Chu, K.W., Buchsbaum, M.S., 2005. Correlations between MRI-assessed volumes of the thalamus and cortical Brodmann's areas in schizophrenia. Schizophr. Res. 75 (2–3), 265–281.
Moghaddam, B., Adams, B., Verma, A., Daly, D., 1997. Activation of glutamatergic neurotransmission by ketamine: a novel step in the pathway from NMDA receptor blockade to dopaminergic and cognitive disruptions associated with the prefrontal cortex. J. Neurosci. 17 (8), 2921–2927.
Murphy, B.K., Miller, K.D., 2003. Multiplicative gain changes are induced by excitation or inhibition alone. J. Neurosci. 23 (31), 10040–10051.
Nathaniel-James, D., Frith, C.D., 2002. The role of the dorsolateral prefrontal cortex: evidence from the effects of contextual constraint in a sentence completion task. NeuroImage 16 (4), 1094–1102.
Nathaniel-James, D.A., Fletcher, P., Frith, C.D., 1997. The functional anatomy of verbal initiation and suppression using the Hayling Test. Neuropsychologia 35 (4), 559–566.
Negyessy, L., Goldman-Rakic, P.S., 2005. Morphometric characterization of synapses in the primate prefrontal cortex formed by afferents from the mediodorsal thalamic nucleus. Exp. Brain Res. 164 (2), 148–154.
Neher, E., Sakaba, T., 2008. Multiple roles of calcium ions in the regulation of neurotransmitter release. Neuron 59 (6), 861–872.
Newpher, T.M., Ehlers, M.D., 2008. Glutamate receptor dynamics in dendritic microdomains. Neuron 58 (4), 472–497.
Oh, J.S., Kubicki, M., Rosenberger, G., Boiux, F., Levitt, J., McCarley, R.W., Westin, C.-F., Shenton, M.E., 2009. Thalamo-frontal white matter alterations in chronic schizophrenia: a quantitative diffusion tractography study. Hum. Brain Mapp. 30 (11), 3812–3825.
Onn, S.P., Wang, X.B., 2005. Differential modulation of anterior cingulate cortical activity by afferents from ventral tegmental area and mediodorsal thalamus. Eur. J. Neurosci. 21 (11), 2975–2992.
Pakkenberg, B., Scheel-Krüger, J., Kristiansen, L.V., 2009. Schizophrenia; from structure to function with special focus on the mediodorsal thalamic prefrontal loop. Acta Psychiatr. Scand. 120 (5), 345–354.
Pan, B., Zucker, R.S., 2009. A general model of synaptic plasticity transmission and short-term plasticity. Neuron 62 (4), 539–554.
Penny, W.D., Stephan, K.E., Mechelli, A., Friston, K.J., 2004. Comparing dynamic causal models. NeuroImage 22 (3), 1157–1172.
Penny, W.D., Stephan, K.E., Daunizeau, J., Rosa, M.J., Friston, K.J., Schofield, T.M., Leff, A.P., 2010. Comparing families of dynamic causal models. PLoS Comput. Biol. 6 (3), e1000709.
Pfister, J.P., Dayan, P., Lengyel, M., 2010. Synapses with short-term plasticity are optimal estimators of presynaptic membrane potentials. Nat. Neurosci. 13 (10), 1271–1275.
Pinault, D., 2011. Dysfunctional thalamus-related networks in schizophrenia. Schizophr. Bull. 37 (2), 238–243.
Romanides, A.J., Duffy, P., Kalivas, P.W., 1999. Glutamatergic and dopaminergic afferents to the prefrontal cortex regulate spatial working memory in rats. Neuroscience 92 (1), 97–106.
Rothman, J.S., Cathala, L., Steuber, V., Silver, R.A., 2009. Synaptic depression enables neuronal gain control. Nature 457 (7232), 1015–1018.
Saarinen, A., Linne, M.-L., Yli-Harja, O., 2008. Stochastic differential equation model for cerebellar granule cell excitability. PLoS Comput. Biol. 4 (2), e1000004.
Salinas, E., Sejnowski, T.J., 2001. Gain modulation in the central nervous system: where behavior, neurophysiology, and computation meet. Neuroscientist 7 (5), 430–440.
Salinas, E., Sejnowski, T.J., 2000. Impact of correlated synaptic input on output firing rate and variability in simple neuronal models. J. Neurosci. 20 (16), 6193–6209.
Santana, N., Mengod, G., Artigas, F., 2009. Quantitative analysis of the expression of dopamine D1 and D2 receptors in pyramidal and GABAergic neurons of the rat prefrontal cortex. Cereb. Cortex 19 (4), 849–860.
Seghier, M.L., Josse, G., Leff, A.P., Price, C.J., 2011. Lateralization is predicted by reduced coupling from the left to right prefrontal cortex during semantic decisions on written words. Cereb. Cortex 21 (7), 1519–1531.
Shu, Y., Hasenstaub, A., Badoual, M., Bal, T., McCormick, D.A., 2003. Barrages of synaptic activity control the gain and sensitivity of cortical neurons. J. Neurosci. 23 (32), 10388–10401.
Simon, A.E., Cattapan-Ludewig, K., Zmilacher, S., Arbach, D., Gruber, K., Dvorsky, D.N., Roth, B., Isler, E., Zimmer, A., Umbricht, D., 2007. Cognitive functioning in the schizophrenia prodrome. Schizophr. Bull. 33 (3), 761–771.
Sodhi, M.S., Simmons, M., McCullumsmith, R., Haroutunian, V., Meador-Woodruff, J.H., 2011. Glutamatergic gene expression is specifically reduced in thalamocortical projecting relay neurons in schizophrenia. Biol. Psychiatry 70 (7), 646–654.
Stephan, K.E., Baldeweg, T., Friston, K.J., 2006. Synaptic plasticity and dysconnection in schizophrenia. Biol. Psychiatry 59 (10), 929–939.

Stephan, K.E., Harrison, L.M., Kiebel, S.J., David, O., Penny, W.D., Friston, K.J., 2007. Dynamic causal models of neural system dynamics: current state and future extensions. J. Biosci. 32 (1), 129–144.
Stephan, K.E., Kasper, L., Harrison, L.M., Daunizeau, J., Hanneke Ouden, E.M., Breakspear, M., Friston, K.J., 2008. Nonlinear dynamic causal models for fMRI. NeuroImage 42 (2), 649–662.
Stephan, K.E., Friston, K.J., Frith, C.D., 2009a. Dysconnection in schizophrenia: from abnormal synaptic plasticity to failures of self-monitoring. Schizophr. Bull. 35 (3), 509–527.
Stephan, K.E., Penny, W.D., Daunizeau, J., Moran, R.J., Karl, J., 2009b. Bayesian model selection for group studies. NeuroImage 46 (4), 1004–1017.
Sun, Y.G., Beierlein, M., 2011. Receptor saturation controls short-term synaptic plasticity at corticothalamic synapses. J. Neurophysiol. 105 (5), 2319–2329.
Talairach, J., Tournoux, P.A., 1988. A Coplanar Stereotaxic Atlas of a Human Brain. Three-dimensional Proportional System: An Approach to Cerebral Imaging. Thieme, Stuttgart.
Thermenos, H.W., Seidman, L.J., Breiter, H., Goldstein, J.M., Goodman, J.M., Poldrack, R., Faraone, S.V., Tsuang, M.T., 2004. Functional magnetic resonance imaging during auditory verbal working memory in nonpsychotic relatives of persons with schizophrenia: a pilot study. Biol. Psychiatry 55 (5), 490–500.
Volman, V., Levine, H., Sejnowski, T.J., 2010. Shunting inhibition controls the gain modulation mediated by asynchronous neurotransmitter release in early development. PLoS Comput. Biol. 6 (11), e1000973.
Wang, X.J., 2010. Neurophysiological and computational principles of rhythms in cognition. Physiol. Rev. 90 (3), 1195–1268.
Watis, L., Chen, S.H., Chua, H.C., Chong, S.A., Sim, K., 2008. Glutamatergic abnormalities of the thalamus in schizophrenia: a systematic review. J. Neural Transm. 115 (3), 493–511.
Welsh, R.C., Chen, A.C., Taylor, S.F., 2010. Low-frequency BOLD fluctuations demonstrate altered thalamocortical connectivity in schizophrenia. Schizophr. Bull. 36 (4), 713–722.
Whalley, H.C., Simonotto, E., Flett, S., Marshall, I., Ebmeier, K.P., Owens, D.G.C., Goddard, N.H., Johnstone, E.C., Lawrie, S.M., 2004. fMRI correlates of state and trait effects in subjects at genetically enhanced risk of schizophrenia. Brain 127 (Pt 3), 478–490.
Whalley, H.C., Simonotto, E., Marshall, I., Owens, D.G.C., Goddard, N.H., Johnstone, E.C., Lawrie, S.M., 2005. Functional disconnectivity in subjects at high genetic risk of schizophrenia. Brain 128 (9), 2097–2108.
Wing, J.K., Cooper, J.E., Sartorius, N., 1974. The Description and Classification of Psychiatric Symptoms. An Instruction Manual for the PSE and Catego Systems. Cambridge University Press, Cambridge.

Relationship Between Gyrification and Functional Connectivity of the Prefrontal Cortex in Subjects at High Genetic Risk of Schizophrenia

Maria R. Dauvermann, Prerona Mukherjee, William T. Moorhead, Andrew C. Stanfield, Paolo Fusar-Poli, Stephen M. Lawrie and Heather C. Whalley*

Division of Psychiatry, School of Molecular and Clinical Medicine, University of Edinburgh, Edinburgh, Scotland, UK

Abstract: Measures of cortical folding ('gyrification') and connectivity are both reported to be disrupted in schizophrenia. There are also reports that increases in prefrontal gyrification may be predictive of subsequent illness in individuals at familial risk of the disorder. Such measures therefore have important potential clinical relevance. The nature of the relationship between cortical morphology and underlying connectivity is however unclear. In the current study we sought to explore the relationship between measures of gyrification and functional connectivity in a cohort of individuals at high genetic risk for the disorder. The theoretical background is based on the hypothesis that increased gyrification index (GI) in the prefrontal cortex may reflect increased short range regional connectivity. The cohort comprised 68 young unaffected relatives of schizophrenia patients and 21 healthy controls. Cortical folding was assessed using an automated Gyrification Index method (A-GI). Participants performed the Hayling sentence completion paradigm in the scanner and measures of functional connectivity were assessed using a correlation based approach. In the high risk subjects significant positive associations were found between prefrontal GI and prefrontal lateral-medial connectivity, while a negative correlation was found between prefrontal GI and prefrontal-thalamic connectivity. These associations indicate that measures describing morphological features of the brain surface relate to measures of underlying functional connectivity in the high risk subjects. Correlations in high risk people were more pronounced than in control subjects. We suggest our previous finding of increased prefrontal gyrification may therefore relate to increased local short range prefrontal connectivity and reduced long range connectivity.

Keywords: Gyrification, Functional Connectivity, Prefrontal Cortex, Thalamus, Short Distance Connection, Long Distance Connection, Schizophrenia, High Risk.